

Synthesis of Novel High-Affinity FimH Antagonists with Improved Pharmacokinetic Properties

Inauguraldissertation

zur Erlangung der Würde eines Doktors der Philosophie
vorgelegt der Philosophisch-Naturwissenschaftlichen Fakultät
der Universität Basel

von

Wojciech Schönemann
aus Krakow, Poland

Basel, 2017

Originaldokument gespeichert auf dem Dokumentenserver der Universität Basel
edoc.unibas.ch

Genehmigt von der Philosophisch-Naturwissenschaftlichen Fakultät auf Antrag von:

Prof. Dr. Beat Ernst

Institut für Molekulare Pharmazie

Departement Pharmazeutische Wissenschaften

Universität Basel

Klingelbergstrasse 50/70, CH-4055 Basel

Prof. Olivier R. Martin

Institut de Chimie Organique et Analytique

Université d'Orléans

Rue de Chartres, F-45067 Orléans, France

Basel, 08 December 2015

Prof. Dr. Jörg Schibler

Dekan

Acknowledgements

Most of all, I would like to express my deepest gratitude to Prof. Dr. Beat Ernst for giving me the opportunity to perform PhD research in his group. I am thankful for his mentoring, trust and patience. It was a pleasure to be a part of his group.

I would also like to thank Prof. Olivier R. Martin for accepting to be the co-referee of this doctoral dissertation.

Special thanks go to Bea Wagner, Claudia Huber and Gabi Lichtenhahn for their technical and administrative support and help with day-to-day problems.

This work would not be possible without people directly involved in this research project. I am very grateful to Dr. Simon Kleeb, Dr. Said Rabbani, Dr. Jacqueline Bezençon and Deniz Eris for numerous preformed assays and countless discussions. I would also like to thank Dr. Lijuan Pang, Dr. Xiaohua Jiang, Dr. Meike Scharenberg, Dr. Roland Preston, Dr. Daniela Abgottspon, Dr. Anja Sigl, Dr. Brigitte Fiege, Marleen Silbermann, Priska Frei and Pascal Zihlmann for a fruitful collaboration. Many thanks go to Prof. Dr. Angelo Vedani and his team, especially Dr. Adam Zalewski and Dr. Martin Smieško. All those conversations provided so much needed food for thought and the pictures they generated made the manuscripts more visually appealing. I would also like to thank my master students, Philipp Dätwyler, Marcel Lindegger and Sophie Boschung for their contribution and a great time I had with them in the lab.

I would particularly like to thank the members of my lab who I had pleasure to work with: Giulio Navarra for his friendship and support, Dr. Rachel Hevey for her kindness and plenty of reasons to laugh, Dr. Fan Yang for our interesting discussions on broad scientific topics, Dr. Arjan Oedra for a helping hand during the first few months of my PhD and Dr. Oliver Schwardt for his time and expertise. I had a great time working with all of you.

I would also like to thank all the other current and former members of the Institute of Molecular Pharmacy, especially Norbert, Blijke, Oya, Christoph, Tobias, Mirko, Kathi and Gianluca for providing a stimulating research environment and relaxing atmosphere after work.

Finally, I would like to thank my family for their love, constant support and encouragement when it was needed the most. I would not be where I am today without them.

Abstract

Urinary tract infections (UTIs) belong to the most common bacterial infections worldwide. Uropathogenic *Escherichia coli* (UPEC) are held accountable for majority of the cases. Millions of people suffer from UTI each year, with the highest incidence rate reported among women. Moreover, woman once affected will most likely experience a recurrent infection. High prevalence and recurrence of UTI lead to considerable medical costs. The current treatment generally involves antibiotics. However, choosing a proper antibiotic therapy becomes more difficult as resistant strains rapidly proliferate. Therefore, the need to develop alternative, non-antibiotic strategies is more pressing than ever.

UPEC express filamentous organelles called type 1 pili (fimbriae), which protrude from the bacterial surface and mediate the adhesion to the bladder-epithelial cells. The mannose-specific adhesin FimH is located on the distal end of the pili. It contains the mannose-specific carbohydrate recognition domain (CRD), which binds to highly mannosylated uroplakin 1a (UP1a) expressed by urothelial cells leading to the infection. The compounds capable of blocking the interaction between FimH and surface-exposed glycans pave the way for a novel anti-adhesive strategy to treat and prevent UTI.

The *first part* of the thesis addresses the problem of poor oral bioavailability arising from high polarity of the FimH antagonists. The strategy involves a prodrug approach, in which lipophilic esters are introduced to the parent compounds either on the aglycone's carboxylic acid or the mannose moiety. The absorption potential as well as propensity to hydrolysis by esterases of liver or plasma was evaluated. The *second part* of the thesis emphasizes the optimization of the pharmacodynamic properties of FimH antagonists. In the first approach, the mannose moiety was modified in order to explore a cavity located at the entrance to binding pocket. The obtained antagonists were evaluated in competitive binding assay and by isothermal titration calorimetry (ITC) to reveal their thermodynamic binding profile. The second approach involved an elongation of the aglycone to allow additional interactions with the guanidinium side chain of Arg98. For the evaluation of these antagonists, competitive binding assays with the wild type FimH and the R98A mutant was established.

Abbreviations

Å	Angstrom
Ac ₂ O	Acetic anhydride
AcOH	Acetic acid
ADME	Absorption, distribution, metabolism, excretion, toxicity
AgOTf	Silver trifluoromethanesulfonate
Ar	Aryl
BChE	Butyrylcholinesterase
BF ₃ ·Et ₂ O	Boron trifluoride diethyl etherate
Bn	Benzyl
BNPP	Bis(4-nitrophenyl) phosphate
Bu	Butyl
BuOH	Butanol
BzCl	Benzoyl chloride
Caco-2 cells	Colorectal adenocarcinoma cells
CES	Carboxylesterase
COMU	(1-Cyano-2-ethoxy-2-oxoethylidenaminoxy)dimethylamino-morpholino-carbenium hexafluorophosphate
COSY	Correlation Spectroscopy
CRD	Carbohydrate recognition domain
<i>D</i>	Octanol-water distribution coefficient
DCM	Dichloromethane
DIC	<i>N,N'</i> -Diisopropylcarbodiimide
DIPEA	<i>N,N</i> -Diisopropylethylamine
DMAP	4-Dimethylaminopyridine
DMF	<i>N,N</i> -Dimethylformamide
DMSO	Dimethylsulfoxide
dppf	1,1'-Bis(diphenylphosphino)ferrocene
ER	Endoplasmic reticulum
ESI-MS	Electrospray mass spectrometry
Et	Ethyl
EtOAc	Ethyl acetate
EtOH	Ethanol
hCE1	Human carboxylesterase isotype 1
hCE2	Human carboxylesterase isotype 2
HLM	Human liver microsomes
HMBC	Heteronuclear multiple-bond correlation spectroscopy
HPLC	High performance liquid chromatography
HRMS	High resolution mass spectrometry
HSQC	Heteronuclear Single Quantum Coherence
Hz	Hertz
IC ₅₀	Half maximal inhibitory concentration
iPrOH	Isopropyl alcohol

ITC	Isothermal titration calorimetry
K_d	Dissociation constant
LC-MS	Liquid chromatography-mass spectrometry
MD	Molecular dynamic
Me	Methyl
MeCN	Acetonitrile
MeOH	Methanol
MeONa	Sodium methoxide
MPLC	Medium pressure liquid chromatography
MS	Molecular sieves
NIS	<i>N</i> -Iodosuccinimide
NMR	Nuclear magnetic resonance
P	Octanol-water partition coefficient
p -NO ₂ PhSCl	<i>p</i> -Nitrobenzenesulfenyl chloride
PAMPA	Parallel artificial membrane permeability assay
P_{app}	Apparent permeability
PD	Pharmacodynamics
PDB	Protein data bank
P_e	Effective permeability
PhSH	Thiophenol
PivOH	Pivalic acid
PK	Pharmacokinetics
PPB	Plasma protein binding
ppm	Parts per million
Pr	Propyl
PrOH	Propanol
rIC ₅₀	Relative IC ₅₀
RLM	Rat liver microsomes
RP	Reversed phase
rt	Room temperature
<i>t</i> -BuOH	<i>tert</i> -Butyl alcohol
$t_{1/2}$	Half-life
TBAB	Tetrabutylammonium bromide
TBAI	Tetrabutylammonium iodide
TBDMS	<i>tert</i> -Butyldimethylsilyl
TEA	Triethylamine
TFA	Trifluoroacetic acid
TLC	Thin-layer chromatography
TMSOTf	Trimethylsilyl trifluoromethanesulfonate
TRIS	Tris(hydroxymethyl)aminomethane
UPEC	Uropathogenic <i>Escherichia coli</i>
UTI	Urinary tract infection
UV	Ultraviolet

Table of contents

1. Introduction.....	1
1.1 Urinary tract infection.....	1
1.1.1 The etiology and the infection cycle.....	1
1.1.2 Structure and biogenesis of type 1 pilus (fimbria).....	3
1.2 The uropathogenic virulence factor FimH.....	4
1.2.1 Allosteric catch bond in FimH adhesion.....	4
1.2.2 The carbohydrate recognition domain (CRD).....	7
1.3 FimH antagonists.....	8
1.3.1 Development of high-affinity ligands.....	8
1.3.2 Development of orally available anti-adhesives for the treatment of UTI.....	11
1.4 The aim of the thesis.....	12
2. Results and Discussion.....	24
2.1 <i>Manuscript 1: FimH Antagonists: Ester Prodrugs for Achieving Oral Bioavailability</i> ..	24
2.2 <i>Paper 2: Prodruggability of Carbohydrates – Oral FimH Antagonists</i>	66
2.3 <i>Chapter 3: Antagonists Targeting the Arg98 Residue of FimH Adhesin</i>	78
2.4 <i>Paper 4: 2-C-Branched Mannosides as a Novel Family of FimH Antagonists – Synthesis and Biological Evaluation</i>	118
3. Summary and Outlook.....	128
4. Formula Index.....	130
5. Curriculum Vitae.....	134

1. Introduction

1.1 Urinary tract infection

Urinary tract infections (UTIs) belong to the most widespread infectious diseases, affecting millions of people every year.^{1,2} The high incidence rate results in substantial associated costs estimated for US\$ 3.5 billion every year in the United States alone.³ The highest morbidity is observed among women with 40-50% risk of the onset of the disease at one point in their life.^{4,5} Approximately 25% of the afflicted women will experience a second UTI episode within six months after the prior infection.⁶ However, the elderly, infants and patients with diabetes, catheter or spinal cord injuries are even more prone to UTI.⁷ When UTI is confined to the bladder it is referred to as cystitis, whereas an infection located in the kidneys is called pyelonephritis.⁸ UTIs can be further differentiated into uncomplicated and complicated. Uncomplicated UTIs involve individuals, who are otherwise healthy with no structural or functional abnormalities. However, when urinary tract or host defense is compromised (e.g. urinary obstruction, renal transplantation, immunosuppression, catheters) UTIs are classified as complicated.⁹ Symptoms elicited by uncomplicated lower urinary tract infections include dysuria, bacteriuria, frequent urination, pyuria and haematuria.^{3,10} The first-line treatment involves 3-to-7-day regimen with nitrofurantoin, trimethoprim-sulfamethoxazole, fosfomycin or the β -lactam pivmecillinam. Fluoroquinolones (e.g. ciprofloxacin, levofloxacin) and additional β -lactams (e.g. amoxicillin-clavulanate, cefdinir) belong to the second-line treatment.¹¹ However, the choice of the proper treatment becomes increasingly complicated, due to antimicrobial resistance.¹² It is believed that trimethoprim-sulfamethoxazole may no longer be recommended for the treatment of acute uncomplicated cystitis.¹³ Therefore, novel non-antibiotic approaches to treat UTI are urgently needed.

1.1.1 The etiology and the infection cycle

The etiology of UTIs is attributed to uropathogenic *Escherichia coli* (UPEC) in 80-85% of the cases. The second most prevalent uropathogen is *Staphylococcus saprophyticus*, accounting for 5-15% of the diagnosed UTIs. Other less frequent bacterial pathogens include

Klebsiella pneumoniae and *Proteus mirabilis*.^{10,14,15} The colonization of the host by UPEC follows a well-described infection cycle (Figure 1.1).¹⁶⁻¹⁹

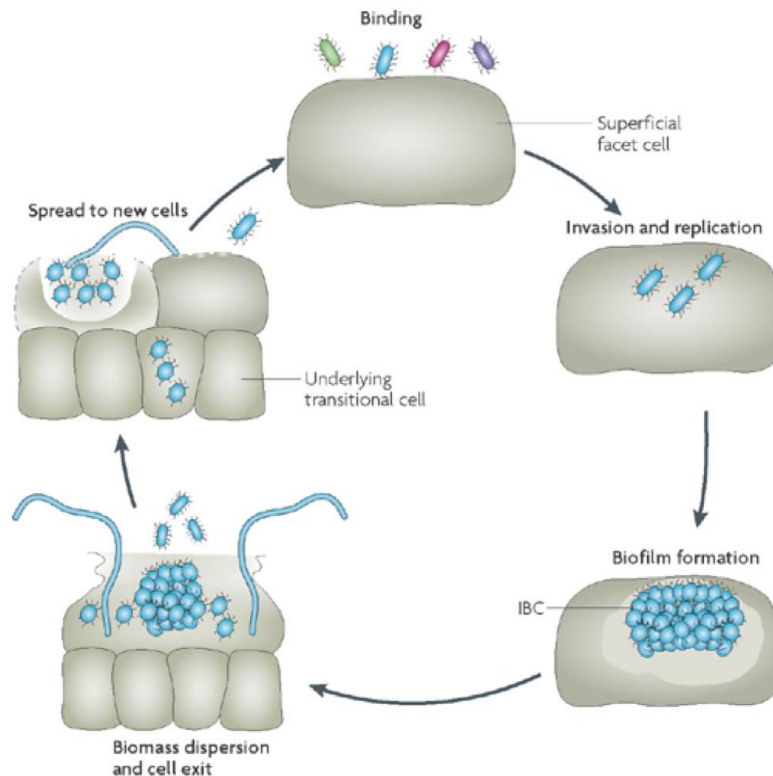


Figure 1.1. Infection cycle of uropathogenic *Escherichia coli* (UPEC) in the bladder (adopted from ref. 28). In the first step, UPEC bind to the superficial cells of the bladder. Bacteria thereupon invade the cells and rapidly replicate in the cytosol to form protective biofilm-like intracellular bacterial communities (IBCs). Mature bacteria then escape from the cell to the bladder lumen and spread to another superficial or underlying cells.

The whole process begins with the bacterial adhesion to bladder-epithelial cells (urothelial cells), which prevents UPEC from being washed out by micturition. The adhesion results from the interaction of the mannose-specific adhesin FimH located at the tip of bacterial type 1 pili with highly-mannosylated glycoprotein uroplakin 1a (UP1a) expressed on urothelial cells.^{20,21} Attached to the cell surface, UPEC can enter the superficial umbrella cells and start to replicate in the cytosol.^{17,22} This leads to the formation of biofilm-like intracellular bacterial communities (IBCs), which protect UPEC from the host immune system or exposure to antibiotics.^{23,24} After IBCs reach a mature state, bacteria is released to the bladder in order to reinitiate the infection cycle.¹⁸ Moreover, some of these bacteria re-emerge in the form of filamentous structures, allowing them to evade neutrophil phagocytosis.²⁵ In response to the infection, the superficial cells of the bladder are exfoliated.²⁶ However, that results in spreading of UPEC in the environment, since the bacteria is able to escape from dying cells. Moreover, exfoliation exposes underlying layer of immature cells, which then can also be

infected.^{18,26} In these cells, bacteria form quiescent intracellular reservoirs (QIRs), which are insensitive to antibiotics and can persist for weeks. These reservoirs are therefore the source of the pathogen initiating recurrent infections.^{27,28}

1.1.2 Structure and biogenesis of type 1 pilus (fimbria)

Type 1 pili (fimbriae) are expressed by essentially all UPEC isolates and a large number of other bacteria of *Enterobacteriaceae* family.^{29,30} *E. coli* express between 100 and 400 of these filamentous organelles per each cell.³¹ The pilus rod is the proximal part of the fimbria. It is 7 nm-wide helical structure composed of 500 to 3000 copies of protein FimA, which is anchored to the bacterial outer membrane by means of the usher FimD.^{32,33} The tip fibrillum is the most distal 3 nm-wide fragment containing two adaptor subunits FimF and FimG followed by a single copy of mannose-binding adhesin FimH. Upon assembly, the type 1 pili can protrude up to 3 μm from the surface of the bacterium.³⁴⁻³⁶

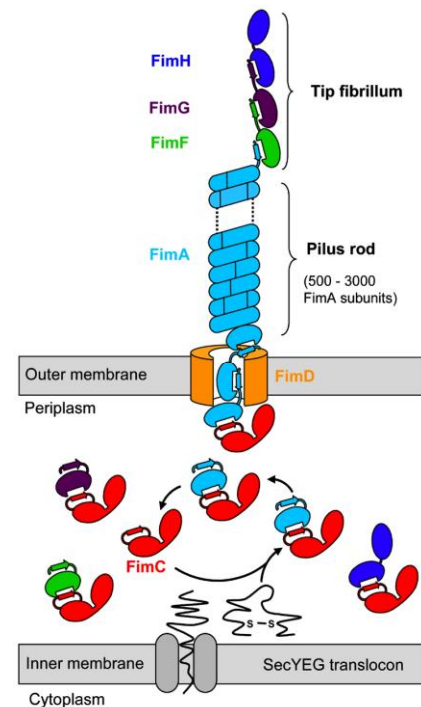


Figure 1.2. Schematic representation of type 1 pilus biogenesis via chaperone-usher pathway (adopted from ref. 42). The periplasmic chaperone FimC transports the subunits to the FimD usher, which assembles and translocates them through the outer membrane.

The biogenesis of the type 1 pili begins in the periplasm via the chaperone/usher pathway (Figure 1.2).³⁷⁻³⁹ It requires the assistance of proteins FimC and FimD. The first one serves as a chaperone, whereas the latter forms a channel in the bacterial outer membrane and translocates the subunits out of the cell. All fimbrial subunits represent an incomplete immunoglobuline (Ig)-like fold devoid of a C-terminal β -strand. The chaperone FimC donates the missing β -strand to the subunits in a process called donor-strand complementation (DSC).⁴⁰⁻⁴² The chaperone-subunit complex diffuses to FimD, where FimC is replaced by amino-terminal extension of the subunit already embedded in a growing pilus. This mechanism is known as donor-strand exchange (DSE).⁴³ It was proposed that the correct order of the subunits during the assembly of the pili is governed by periplasmic

concentrations of a given subunit, affinity of different chaperone-subunit complexes for FimD and reaction kinetics of DSE different for each subunit.^{44,45} Apart from the highest affinity of FimC-FimH for the usher, it is also the only complex capable of transforming FimD into highly efficient assembly catalyst by inducing its proper conformation.⁴⁶

1.2 The uropathogenic virulence factor FimH

The adhesin FimH is located at the tip of type 1 pili. It consists of the N-terminal lectin domain containing residues 1-156 and the C-terminal pilin domain composed of residues 160-279, both linked together by a short peptide chain. The lectin domain is folded into a jelly roll-like, elongated β barrel, which contains the mannose-binding carbohydrate recognition domain (CRD) on its distal end. Similar to other subunits, the pilin domain has Ig-like topology with a missing C-terminal β -strand. It is connected to FimG, which donates the missing strand thereby stabilizing the structure of the pilin domain.^{35,40,47}

In 1999, the first crystal structure of the chaperone-adhesin complex co-crystallized with cyclohexylbutanoyl-*N*-hydroxyethyl-D-glucamide (C-HEGA) was reported.⁴⁰ Over the course of the following years, the X-ray structures were determined only for the purified lectin domain or FimH in the complex with FimC.^{35,40,48,49} In all of these examples, the lectin domain adopted a narrow, elongated high-affinity state. In 2010, Le Trong and co-workers solved the first crystal structure of FimH in wide and more compressed low-affinity state.⁴⁷ The published research showed also the involvement of the pilin domain in switching between high- and low-affinity state.

1.2.1 Allosteric catch bond in FimH adhesion

Adhesive molecular interactions are constantly exposed to a shear stress due cytoskeletal contraction or the flow of the biological fluids. Most interactions become weaker and short-lived under tensile force. This type of interaction is referred to as a slip bond. By contrast, an interaction enhanced by mechanical force is called a catch bond (Figure 1.3).^{50,51} Although less common, catch bonds are involved in selectin-mediated adhesion of leukocytes,^{52,53} interaction of actin with myosin⁵⁴ and FimH-mediated bacterial adhesion.⁵⁵⁻⁵⁷

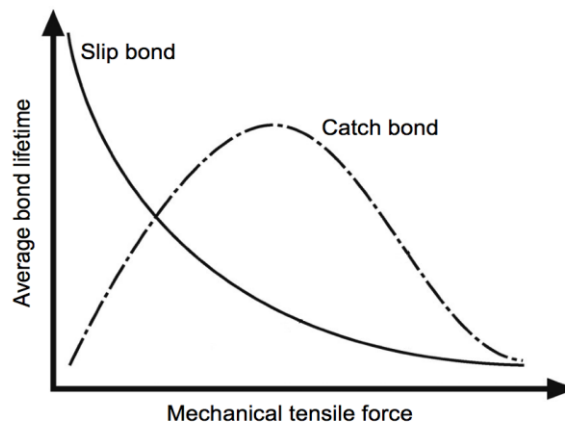


Figure 1.3. Schematic plots illustrating the difference between slip and catch bonds. The catch bond is the weakest and the slip bond is the strongest when tensile force is weak. Upon the increase of tensile force, the slip bond loses its strength, while the catch bond becomes stronger until the point where it is overpowered by force.

Over a decade ago, Thomas and co-workers provided the first experimental data supporting a catch bond mechanism for FimH adhesion.⁵⁵ Under static conditions, the red blood cells did not agglutinate despite the presence of *E. coli*. By contrast, the same cells subjected to rocking formed tight aggregates.⁵⁵ The following studies reporting on shear force-induced differences in cell adhesion and the bond strength between FimH and mannose further supported the involvement of the catch bond mechanism in the FimH adhesion.^{58,59} It was also proposed that FimH could adopt two distinct conformations, a high- and a low-affinity state conformation.⁵⁵ An interdomain interaction was shown to regulate the force-induced change between these two conformations by an allosteric mechanism.^{55,60,61}

The crystal structure of the full-length FimH protein in the low-affinity state obtained a few years later provided a structural basis for a force regulated conformational change (Figure 1.4).⁴⁷ When compared to the high-affinity conformation,⁴⁸ the adhesin in the low-affinity state has a wider and more compressed lectin domain leading to a looser binding site. Moreover, the pilin domain interacting with the lectin domain forces a large β sheet to twist and thereby opens the binding pocket. This allosteric auto-inhibition can be abolished by force-induced separation of the two domains. This results in untwisting of the β sheet and closing the binding pocket around the ligand. Since the conformational change of the β sheet resembles the process of sliding the page in the book before turning it, this process is referred to as a “page-turning” mechanism (Figure 1.5).⁴⁷

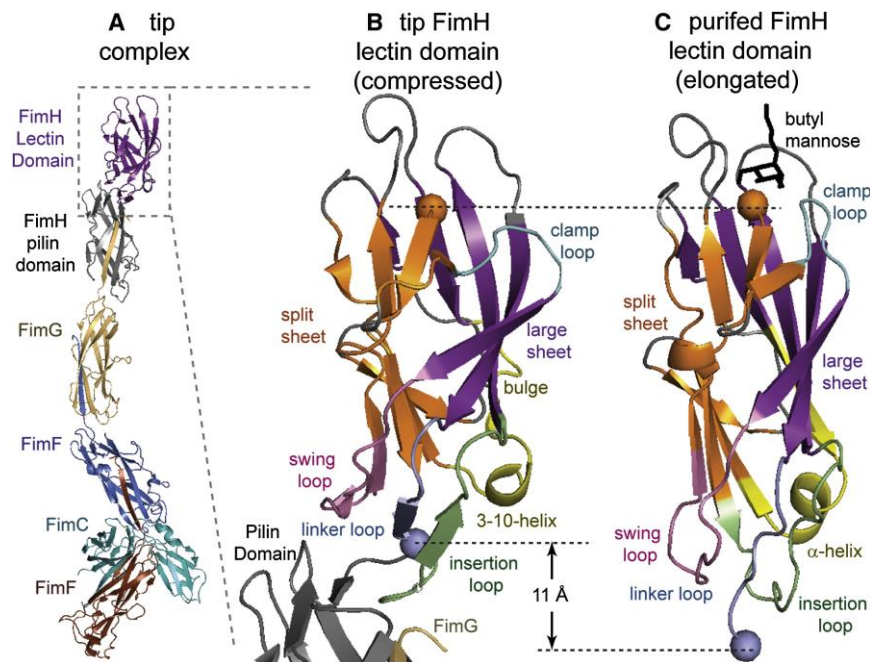


Figure 1.4. (A) The crystal structure of the tip fibrillum in the complex with the chaperone FimC (PDB ID: 3JWN). (B) A compressed and wide lectin FimH in the low-affinity state. (C) The crystal structure of the purified lectin domain in the high-affinity state with *n*-butyl α -D-mannoside bound to the FimH-CRD (PDB ID: 1UWF). The structure is longer than the lectin domain in the low-affinity state by 11 Å and contains the binding pocket tightly clamped around the ligand (adopted from ref. 47).

The shear-force enhanced bacterial adhesion has several advantages. Since soluble oligosaccharides or natural defense proteins (e.g. Tamm-Horsfall glycoprotein) cannot exert any force on the adhesin, they are worse ligands for FimH than surface-exposed glycans.⁶² Moreover, short-lived interactions lead to weak rolling adhesion responsible for rapid colonization of the surface, whereas a subsequently adopted high-affinity conformation allows to establish tight microcolonies.⁶³ Furthermore, a recently proposed kinetic-selection model of binding suggests that a higher association rate for the low-affinity state facilitates an initiation of binding at high flow.⁶⁴ By contrast, a slower dissociation rate for the high-affinity state induced upon binding prevents the detachment of the adhesin. This combination of association/dissociation rates for different conformations allows bacteria to reach higher effective affinity than the one achieved by each separate state.⁶⁴

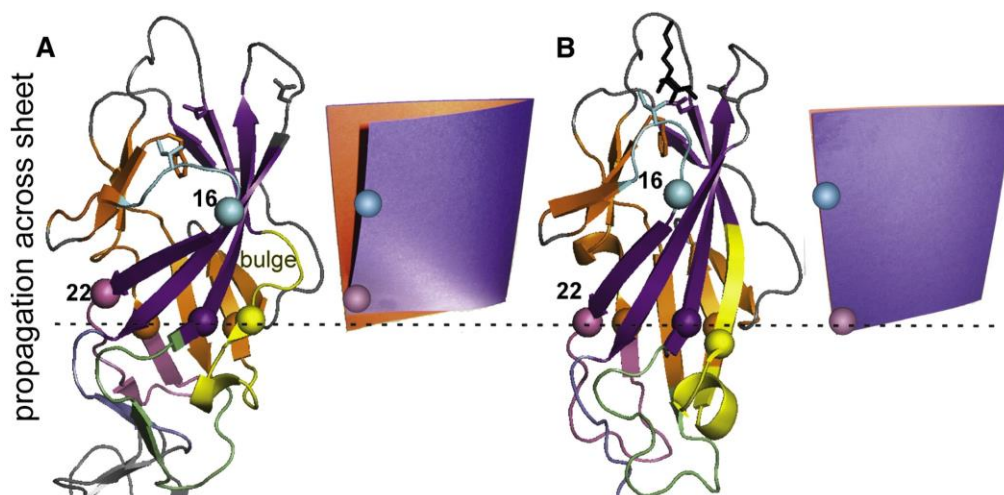


Figure 1.5. The illustration of a “page-turning” mechanism (adopted from ref. 47). (A) The bottom left corner of the β sheet is pushed upward opening the FimH-CRD in the low-affinity state. (B) The same corner is pushed downward tightening the FimH-CRD in the high-affinity state.

1.2.2 The carbohydrate recognition domain (CRD)

The first crystal structure of FimH was very important for understanding the assembly mechanism, however it did not reveal the binding mode of natural ligands to FimH.⁴⁰ Few years later, Hung and co-workers resolved the crystal structure of the FimC-FimH complex co-crystallized with α -D-mannose providing an invaluable insight into the binding mode of a physiologically important ligand (PDB ID: 1KLF).³⁵ The carbohydrate recognition

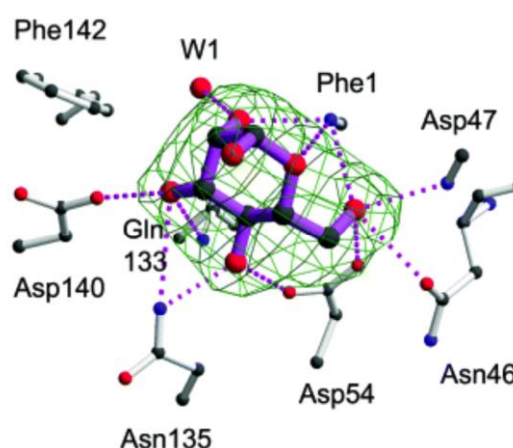


Figure 1.6. The complex hydrogen bond network between the FimH-CRD and α -D-mannose (adopted from ref. 35).

domain is a deep and negatively charged pocket, which envelops the mannose exposing only the anomeric hydroxyl group of the sugar. The other hydroxyl groups interact with Phe1, Asn46, Asp47, Asp54, Gln133, Asn135 and Asp140 forming ten direct hydrogen bonds and indirect hydrogen bonds via the water molecule located in the binding site (Figure 1.6).³⁵ The entrance to the pocket forms a hydrophobic rim composed of Tyr48, Ile52 and Tyr137, also known as the tyrosine gate. Bouckaert *et al.* further explored hydrophobic interactions between aliphatic aglycone and the tyrosine gate showing the significance of these three

amino acids for binding.⁴⁸ The crystal structures obtained within the next few years enabled a rational design of highly potent monovalent FimH antagonists.^{49,65-71}

1.3 FimH antagonists

An emerging antimicrobial resistance in UPEC poses a serious threat to patients. Moreover, it accounts for healthcare expenditure reaching billions of dollars each year.^{3,12,72} Therefore, different treatment strategies for UTI are urgently needed. A molecule capable of preventing the bacterial adhesion would enable the clearance of the pathogen by the bulk flow of urine. Since FimH antagonists do not kill the bacteria, the imposed selection pressure is markedly reduced resulting in a low risk of developing resistance.^{73,74} Moreover, these mannose-based molecules show high selectivity for FimH reducing the risk of side effects.⁷⁵ Therefore, an anti-adhesive therapy based on FimH antagonists is a promising alternative to antibiotics.⁷⁶⁻⁷⁸ Until now, this strategy has been tested *in vivo* in several studies.^{49,70,79-84}

1.3.1 Development of high-affinity ligands

More than three decades ago, Sharon and co-workers reported several monosaccharides (i.e. D-mannose, methyl α -D-mannoside, aryl α -D-mannosides) and mannose-containing oligosaccharides capable of preventing the type 1 pili-mediated yeast agglutination in the presence of UPEC.⁸⁵⁻⁸⁹ Since activity of aromatic α -D-mannoside **4** was superior to affinity of oligosaccharides,^{85,86} a library of aryl monosaccharides was prepared and tested.⁸⁸ Based on the results, a model of a mannose-binding site surrounded by hydrophobic region was proposed without any crystal structure available at that time.⁸⁹ Over the next years, various oligosaccharides were also investigated, which ultimately led to identification of a low nanomolar ligand oligomannose-3 ($K_d = 20$ nM).^{88,90} The adhesin FimH was later co-crystallized with oligomannose-3 to reveal the docking mode of this natural glycan ligand.⁴⁹ Nevertheless, the big size and high polarity of oligosaccharides preclude their oral administration.^{91,92}

In 2005, Bouckaert *et al.* made a serendipitous discovery of butyl α -D-mannoside (**2**) co-crystallized with FimH despite no deliberate addition of that ligand to the protein.⁴⁸ It was postulated, that the Luria-Bertani medium used for growing bacteria during expression of

FimH had been the source of alkyl mannoside. The crystal structure revealed that the alkyl aglycone forms van der Waals contacts with the tyrosine gate. Further optimization of the alkyl aglycone resulted in identification of 30-fold more potent *n*-heptyl α -D-mannoside (**3**, $K_d = 5$ nM).⁴⁸

Over the following decade, a great effort has been made to understand and optimize the interactions with the tyrosine gate. Numerous studies focused on mannose-based ligands containing aromatic aglycones led to a discovery of low nanomolar FimH antagonists,^{69,71,93-95} including biphenyl (e.g. **6-10**),^{65,70,81-83} indolinyphenyl (e.g. **11**)⁸⁴ and squaric acid (e.g. **5**)⁹⁶ derivatives (Figure 1.7).

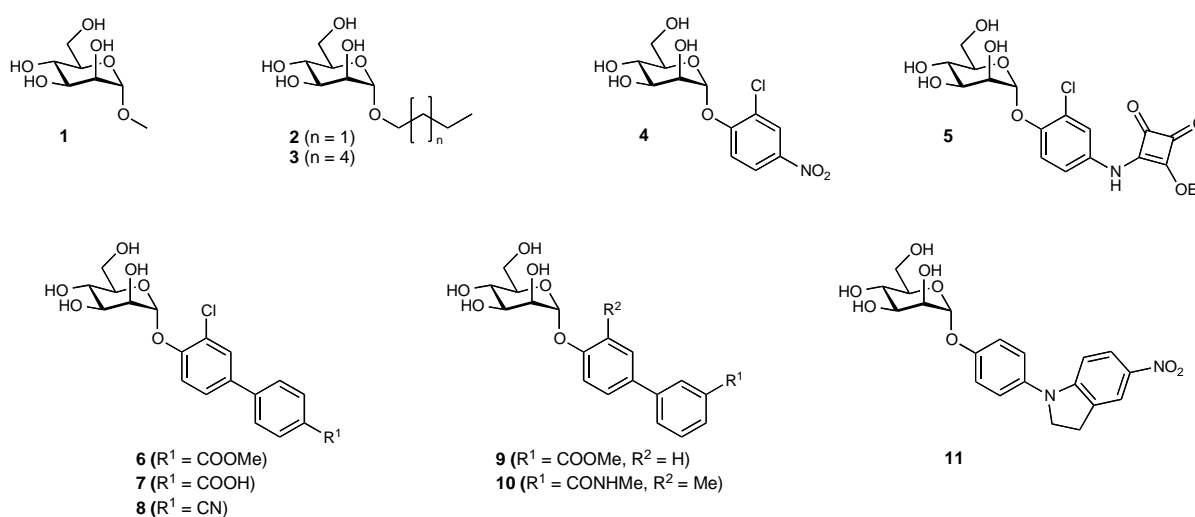


Figure 1.7. The most prominent examples of FimH antagonists. The structures of each FimH antagonist contain a crucial for binding mannose moiety and an aliphatic (**1-3**) or an aromatic (**4-11**) aglycone.

In order to explain the improved activity, several aryl mannosides were co-crystallized with the FimH protein. It was found that the tyrosine gate could adopt two distinct conformations ensuring an optimal π - π stacking with the aglycone. In the *closed conformation*, the aglycone interacts mainly with the side chain of Tyr48, which is rotated towards Tyr137 (Figure 1.8A) precluding the aglycone from inserting into the gate.^{65,67,69-71} By contrast, the *open conformation* comprises the side chains of both tyrosines oriented parallel to each other leaving more space for the ligand (Figure 1.8B).⁶⁶ The π - π stacking with the electron-rich tyrosine gate could be further improved by the addition of electron-withdrawing groups to the terminal phenyl ring of biphenyl aglycones.^{65,70,81-83,93} It was also proposed that some of the

substituents in *meta*-position of the outer aromatic ring of the biphenyl aglycone contribute to binding by interacting with the nearby Arg98.⁶⁵ To date, only few molecules were designed to reach and establish a salt bridge with Arg98.^{65,93} However, these antagonists did not show the expected improvement in affinity. Apart from modifications on the distal part of the aglycone, different hydrophobic substituents in *ortho*-position of the proximal phenyl ring proved to be also beneficial for binding.^{82,89,93} A prominent example of a highly active compound combining this substituent with optimal electron-withdrawing *p*-cyano group on the terminal phenyl ring (\rightarrow **8**) was recently published by Kleeb *et al.*⁷⁰

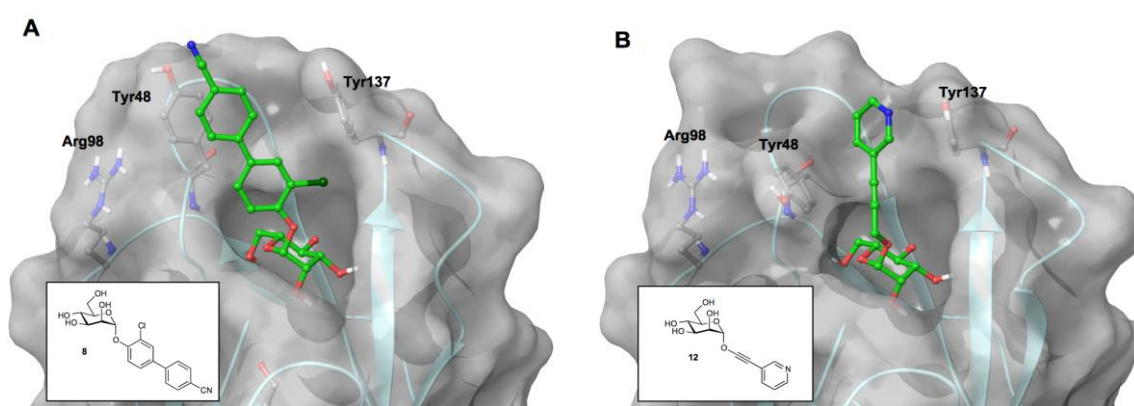


Figure 1.8. The crystal structure of **8** (PDB ID: 4CST) and **12** (PDB ID: 4AVK) bound to FimH-CRD with tyrosine gate adopting open (A) and close (B) conformation.

Since the mannose moiety forms an optimal hydrogen bond network within the binding site, any replacement of the mannose moiety by other hexoses (e.g. fucose, glucose, galactose) or removal/substitution of hydroxyl groups weakened the interaction with the binding site.^{48,65,71,97} Moreover, recently published 1-*C*-branched mannose derivatives showed a reduced activity upon addition of bulky groups at anomeric carbon.⁹⁸ It was proposed that the steric clash caused by these groups induced an unfavorable tilted binding mode. However, mannoside derivatives containing carbon or nitrogen in place of anomeric oxygen have been reported to reach nanomolar affinity.^{69,94}

Multivalent mannosides, which capitalize on the cluster effect improving affinity, form another class of nanomolar FimH antagonists.⁹⁹ To date, numerous multivalent antagonists have been described in the literature.¹⁰⁰⁻¹⁰⁶ Furthermore, the first *in vivo* study evaluating heptavalent glycoconjugates of heptyl α -D-mannoside tethered to β -cyclodextrin showed a preventive effect in UTI mouse model.¹⁰⁶ Despite high affinity reached by the multivalent

ligands, these molecules are too big and too polar to be absorbed in the gastrointestinal tract and therefore have to be applied directly to the bladder.^{91,92} Hence, these antagonists do not have a therapeutic potential to treat UTI.

1.3.2 Development of orally available anti-adhesives for the treatment of UTI

The anti-adhesive therapy may require a daily intake of the drug for an extended period of time. Therefore, oral administration of FimH antagonists is the most suitable route of application. High bioavailability of FimH antagonists can be attained only with FimH antagonists exhibiting solubility, lipophilicity and permeability allowing efficient intestinal absorption.^{107,108} Moreover, the renal excretion should be the main route of elimination since the target, uropathogenic *E. coli*, is located in the bladder. Therefore, metabolic stability is a further required property.

The main impediment precluding carbohydrate-based drugs from crossing the intestinal membrane is the intrinsically high polarity of the sugar moiety, conferred by many hydroxyl groups. Reducing polarity by removal of these groups or replacing them by lipophilic substituents is not a suitable strategy for FimH antagonists due to a loss of affinity.^{48,65,71,97} The lipophilic aglycone can counterbalance high polarity of the sugar moiety, however in most of FimH antagonists, the aglycone comprises of lipophilic biphenyl decorated with additional polar groups (e.g. carboxylic acid).

These issues were addressed with an ester prodrug approach.¹⁰⁹ In general, prodrugs designed to enhance the intestinal absorption enclose lipophilic promoiety masking the polarity of the parent compound. Upon absorption, the promoiety is cleaved by hepatic or plasma-borne esterases to release the active principle.¹¹⁰ Several carbohydrate derivatives with lipophilic promoieties incorporated into the sugar core have been reported to show enhanced cellular uptake.¹¹¹⁻¹¹⁷ By contrast, Klein *et al.* implemented the ester prodrug approach to mask polar group located on the aglycone (\rightarrow **6**, Figure 1.9).⁸¹ The methyl ester **6** was the first reported orally available FimH antagonist, which showed preventive effect in the UTI mouse model. Nevertheless, low solubility of **6** limits the application of this prodrug.

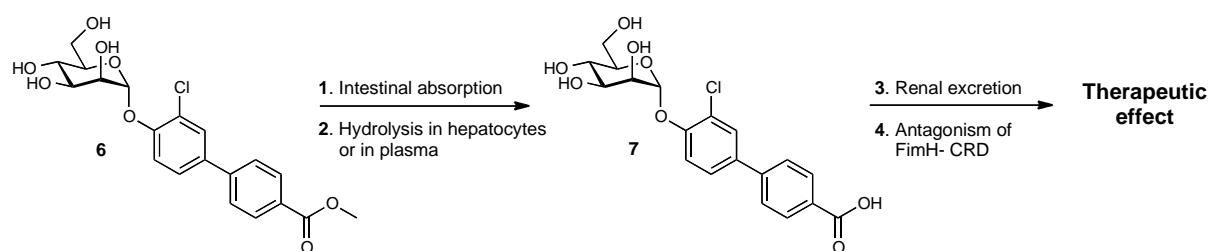


Figure 1.9. The concept of an ester prodrug approach implemented by Klein *et al.*⁸¹ The lipophilic methyl promoiety allows efficient intestinal absorption of **6**. Upon hydrolysis of the methyl ester in the liver, the active principle **7** is excreted to the bladder, where it reaches the target.

The next *in vivo* study of FimH antagonists included methyl amide-substituted biphenyl mannosides (e.g. **10**).⁸² Although the invasion to the bladder was prevented upon an oral application of **10**, a high oral dose of the antagonist was required. By contrast, Jiang *et al.* reported indolinyphenyl **11** capable of reducing bacterial load in the bladder by 3.7 log units after an intravenously injected dose of 1 mg/kg.⁸⁴ However, the solubility of **11** is too low for the oral application. Recently, Kleeb *et al.* published a series of compounds with bioisosteric groups replacing carboxylic acid in antagonist **7**.⁷⁰ Apart from high affinity for FimH, the most prominent antagonist **8** showed an excellent PK profile *in vivo*. Moreover, it reduced the bacterial load in the bladder by 2.7 log units 3 h after infection in UTI mouse model.

1.4 The aim of the thesis

The first goal of this thesis was to optimize physicochemical and pharmacokinetic properties of lead FimH antagonists. The strategy involved prodrug approaches, with promoieties located either on the carboxylic acid of the aglycone or on the sugar moiety. The second goal was to establish new interactions with previously unexplored regions of the FimH protein in order to improve affinity. The new FimH antagonists targeted either Arg98 or a hydrophobic pocket located close to the 2-C position of the mannose moiety.

REFERENCES

1. Foxman, B.; Barlow, R.; D'Arcy, H.; Gillespie, B.; Sobel, J. D. Urinary tract infection: Self reported incidence and associated costs. *Ann. Epidemiol.* **2000**, *10*, 509-515.

2. Roland, A. The etiology of urinary tract infection: Traditional and emerging pathogens. *Am. J. Med.* **2002**, *113* (Suppl 1A), 14S-19S.
3. Flores-Mireles, A. L.; Walker, J. N.; Caparon, M.; Hultgren, S. J. Urinary tract infections: epidemiology, mechanisms of infection and treatment options. *Nat. Rev. Microbiol.* **2015**, *13*, 269-285.
4. Foxman, B.; Somsel, P.; Tallman, P.; Gillespie, B.; Raz, R.; Colodner, R.; Kandula, D.; Sobel, J. D. Urinary tract infection among women aged 40 to 65: Behavioral and sexual risk factors. *J. Clin. Epidemiol.* **2001**, *54*, 710-718.
5. Foxman, B. Epidemiology of urinary tract infections: Incidence, morbidity, and economic costs. *Am. J. Med.* **2002**, *113* (Suppl 1A), 5S-13S.
6. Foxman, B. Recurring urinary tract infection: incidence and risk factors. *Am. J. Public Health* **1990**, *80*, 331-333.
7. Foxman, B. Epidemiology of urinary tract infections: Incidence, morbidity, and economic costs. *Dis Mon.* **2003**, *49*, 53-70.
8. Foxman, B. The epidemiology of urinary tract infection. *Nat. Rev. Urol.* **2010**, *7*, 653-660.
9. Lichtenberger, P.; Hooton, T. M. Complicated urinary tract infections. *Curr Infect Dis Rep* **2008**, *10*, 499-504.
10. Hooton, T. M.; Besser, R.; Foxman, B.; Fritsche, T. R.; Nicolle, L. E. Acute uncomplicated cystitis in an era of increasing antibiotic resistance: a proposed approach to empirical therapy. *Clin. Infect. Dis.* **2004**, *39*, 75-80.
11. Hooton, T. M. Uncomplicated urinary tract infection. *N. Engl. J. Med.* **2012**, *366*, 1028-1037.
12. Sanchez, G. V.; Master, R. N.; Karlowsky, J. A.; Bordon, J. M. In vitro antimicrobial resistance of urinary *Escherichia coli* isolates among U.S. outpatients from 2000 to 2010. *Antimicrob. Agents Chemother.* **2012**, *56*, 2181-2183.
13. Sanchez, G. V.; Master, R. N.; Bordon, J. M. Trimethoprim-sulfamethoxazole may no longer be acceptable for the treatment of acute uncomplicated cystitis in the United States. *Clin. Infect. Dis.* **2011**, *53*, 316-317.
14. Stamm, W. E.; Hooton, T. M. Management of urinary tract infections in adults. *N. Engl. J. Med.* **1993**, *329*, 1328-1334.

15. Ikäheimo, R.; Siitonen, A.; Heiskanen, T.; Kärkkäinen, U.; Kuosmanen, P.; Lipponen, P.; Mäkelä, P. H. Recurrence of urinary tract infection in a primary care setting: analysis of a 1-year follow-up of 179 women. *Clin. Infect. Dis.* **1996**, *22*, 91–99.
16. Anderson, G. G.; Dodson, K. W.; Hooton, T. M.; Hultgren, S. J. Intracellular bacterial communities of uropathogenic *Escherichia coli* in urinary tract pathogenesis. *Trends Microbiol.* **2004**, *12*, 424–430.
17. Martinez, J. J.; Mulvey, M. A.; Schilling, J. D.; Pinkner, J. S.; Hultgren, S. J. Type 1 pilus-mediated bacterial invasion of bladder epithelial cells. *EMBO J.* **2000**, *19*, 2803–2812.
18. Mulvey, M. A.; Schilling, J. D.; Martinez, J. J.; Hultgren, S. J. Bad bugs and beleaguered bladders: interplay between uropathogenic *Escherichia coli* and innate host defenses. *Proc. Natl. Acad. Sci. U.S.A.* **2000**, *97*, 8829–8835.
19. Wiles, T. J.; Kulesus, R. R.; Mulvey, M. A. Origins and virulence mechanisms of uropathogenic *Escherichia coli*. *Exp. Mol. Pathol.* **2008**, *85*, 11–19.
20. Zhou, G.; Mo, W. J.; Sebbel, P.; Min, G.; Neubert, T. A.; Glockshuber, R.; Wu, X. R.; Sun, T. T.; Kong, X. P. Uroplakin Ia is the urothelial receptor for uropathogenic *Escherichia coli*: evidence from in vitro FimH binding. *J. Cell Sci.* **2001**, *114*, 4095–4103.
21. Xie, B.; Zhou, G.; Chan, S. Y.; Shapiro, E.; Kong, X. P.; Wu, X. R.; Sun, T. T.; Costello, C. E. Distinct glycan structures of uroplakins Ia and Ib: structural basis for the selective binding of FimH adhesin to uroplakin Ia. *J. Biol. Chem.* **2006**, *281*, 14644–14653.
22. Mulvey, M. A. Adhesion and entry of uropathogenic *Escherichia coli*. *Cell Microbiol.* **2002**, *4*, 257–271.
23. Anderson, G. G.; Palermo, J. J.; Schilling, J. D.; Roth, R.; Heuser, J.; Hultgren, S. J. Intracellular bacterial biofilm-like pods in urinary tract infections. *Science* **2003**, *301*, 105–107.
24. Mulvey, M. A.; Lopez-Boado, Y. S.; Wilson, C. L.; Roth, R.; Parks, W. C.; Heuser, J.; Hultgren, S. J. Induction and evasion of host defenses by type 1-piliated uropathogenic *Escherichia coli*. *Science* **1998**, *282*, 1494–1497.
25. Justice, S. S.; Hunstad, D. A.; Seed, P. C.; Hultgren, S. J. Filamentation by *Escherichia coli* subverts innate defenses during urinary tract infection. *Proc. Natl. Acad. Sci. U.S.A.* **2006**, *103*, 19884–19889.

26. McTaggart, L. A.; Rigby, R. C.; Elliott, T. S. The pathogenesis of urinary tract infections associated with *Escherichia coli*, *Staphylococcus saprophyticus* and *S. epidermidis*. *J. Med. Microbiol.* **1990**, *32*, 135–141.
27. Blango, M. G.; Mulvey, M. A. Persistence of uropathogenic *Escherichia coli* in the face of multiple antibiotics. *Antimicrob. Agents Chemother.* **2010**, *54*, 1855-1863.
28. Cegelski, L.; Marshall, G. R.; Eldridge, G. R.; Hultgren, S. J. The biology and future prospects of antivirulence therapies. *Nat. Rev. Microbiol.* **2008**, *6*, 17-27.
29. Garofalo, C. K.; Hooton, T. M.; Martin, S. M.; Stamm, W. E.; Palermo, J. J.; Gordon, J. I.; Hultgren, S. J. *Escherichia coli* from urine of female patients with urinary tract infections is competent for intracellular bacterial community formation. *Infect. Immun.* **2007**, *75*, 52-60.
30. Soto, G. E.; Hultgren, S. J. Bacterial adhesins: common themes and variations in architecture and assembly. *J. Bacteriol.* **1999**, *181*, 1059-1071.
31. Lindhorst, T. K.; Kieburg, C.; Krallmann-Wenzel, U. Inhibition of the type 1 fimbriae-mediated adhesion of *Escherichia coli* to erythrocytes by multiantennary alpha-mannosyl clusters: the effect of multivalency. *Glycoconj. J.* **1998**, *15*, 605-613.
32. Capitani, G.; Eidam, O.; Glockshuber, R.; Grütter, M. G. Structural and functional insights into the assembly of type 1 pili from *Escherichia coli*. *Microbes Infect.* **2006**, *8*, 2284-2290.
33. Hahn, E.; Wild, P.; Hermanns, U.; Sebbel, P.; Glockshuber, R.; Häner, M.; Taschner, N.; Burkhard, P.; Aebi, U.; Müller, S. A. Exploring the 3D molecular architecture of *Escherichia coli* type 1 pili. *J. Mol. Biol.* **2002**, *323*, 845-857.
34. Jones, C. H.; Pinkner, J. S.; Roth, R.; Heuser, J.; Nicholes, A. V.; Abraham, S. N.; Hultgren, J. S. FimH adhesin of type 1 pili is assembled into a fibrillar tip structure in the Enterobacteriaceae. *Proc. Natl. Acad. Sci. U.S.A.* **1995**, *92*, 2081–2085.
35. Hung, C. S.; Bouckaert, J.; Hung, D.; Pinkner, J.; Widberg, C.; DeFusco, A.; Augustine, C. G.; Strouse, R.; Langermann, S.; Waksman, G.; Hultgren, S. J. Structural basis of tropism of *Escherichia coli* to the bladder during urinary tract infection. *Mol. Microbiol.* **2002**, *44*, 903-915.
36. Schilling, J. D.; Mulvey, M. A.; Hultgren, S. J. Structure and function of *Escherichia coli* type 1 pili: new insight into the pathogenesis of urinary tract infections. *J. Infect. Dis.* **2001**, *183* (Suppl 1), S36-S40.

37. Hung, D. L.; Hultgren, S. J. Pilus biogenesis via the chaperone/usher pathway: an integration of structure and function. *J. Struct. Biol.* **1998**, *124*, 201-220.
38. Sauer, F. G.; Barnhart, M.; Choudhury, D.; Knight, S. D.; Waksman, G.; Hultgren, S. J. Chaperone-assisted pilus assembly and bacterial attachment. *Curr. Opin. Struct. Biol.* **2000**, *10*, 548-556.
39. Waksman, G.; Hultgren, S. J. Structural biology of the chaperone-usher pathway of pilus biogenesis. *Nat. Rev. Microbiol.* **2009**, *7*, 765-774.
40. Choudhury, D.; Thompson, A.; Stojanoff, V.; Langermann, S.; Pinkner, J.; Hultgren, S. J.; Knight, S. D. X-ray structure of the FimC-FimH chaperone-adhesin complex from uropathogenic *Escherichia coli*. *Science* **1999**, *285*, 1061-1066.
41. Sauer, F. G.; Pinkner, J. S.; Waksman, G.; Hultgren, S. J. Chaperone priming of pilus subunits facilitates a topological transition that drives fiber formation. *Cell* **2002**, *111*, 543-551.
42. Puorger, C.; Eidam, O.; Capitani, G.; Erilov, D.; Grütter, M. G.; Glockshuber, R. Infinite kinetic stability against dissociation of supramolecular protein complexes through donor strand complementation. *Structure* **2008**, *16*, 631-642.
43. Le Trong, I.; Aprikian, P.; Kidd, B. A.; Thomas, W. E.; Sokurenko, E. V.; Stenkamp, R. E. Donor strand exchange and conformational changes during *E. coli* fimbrial formation. *J. Struct. Biol.* **2010**, *172*, 380-388.
44. Busch, A.; Waksman, G. Chaperone-usher pathways: diversity and pilus assembly mechanism. *Philos. Trans. R. Soc. Lond., B, Biol. Sci.* **2012**, *367*, 1112-1122.
45. Allen, W. J.; Phan, G.; Hultgren, S. J.; Waksman, G. Dissection of pilus tip assembly by the FimD usher monomer. *J. Mol. Biol.* **2013**, *425*, 958-967.
46. Nishiyama, M.; Ishikawa, T.; Rechsteiner, H.; Glockshuber, R. Reconstitution of pilus assembly reveals a bacterial outer membrane catalyst. *Science* **2008**, *320*, 376-379.
47. Le Trong, I.; Aprikian, P.; Kidd, B. A.; Forero-Shelton, M.; Tchesnokova, V.; Rajagopal, P.; Rodriguez, V.; Interlandi, G.; Klevit, R.; Vogel, V.; Stenkamp, R. E.; Sokurenko, E. V.; Thomas, W. E. Structural Basis for Mechanical Force Regulation of the Adhesin FimH via Finger Trap-like β Sheet Twisting. *Cell* **2010**, *141*, 645-655.
48. Bouckaert, J.; Berglund, J.; Schembri, M.; Genst, E. D.; Cools, L.; Wuhler, M.; Hung, C. S.; Pinkner, J.; Slättergard, R.; Zavialov, A.; Choudhury, D.; Langermann, S.; Hultgren, S. J.; Wyns, L.; Klemm, P.; Oscarson, S.; Knight, S. D.; Greve, H. D. Receptor binding studies disclose a novel class of high-affinity inhibitors of the *Escherichia coli* FimH adhesin. *Mol. Microbiol.* **2005**, *55*, 441-455.

49. Wellens, A.; Garofalo, C.; Nguyen, H.; Van Gerven, N.; Slättegård, R.; Hernalsteens, J. P.; Wyns, L.; Oscarson, S.; De Greve, H.; Hultgren, S.; Bouckaert, J. Intervening with urinary tract infections using anti-adhesives based on the crystal structure of the FimH-oligomannose-3 complex. *PLoS One* **2008**, *3*, e2040.
50. Dembo, M.; Torney, D. C.; Saxman, K.; Hammer, D. The reaction-limited kinetics of membrane-to-surface adhesion and detachment. *Proc. R. Soc. Lond., B, Biol. Sci.* **1988**, *234*, 55-83.
51. Thomas, W. E.; Vogel, V.; Sokurenko, E. Biophysics of catch bonds. *Annu. Rev. Biophys.* **2008**, *37*, 399-416.
52. Marshall, B. T.; Long, M.; Piper, J. W.; Yago, T.; McEver, R. P.; Zhu, C. Direct observation of catch bonds involving cell-adhesion molecules. *Nature* **2003**, *423*, 190-193.
53. Evans, E.; Leung, A.; Heinrich, V.; Zhu, C. Mechanical switching and coupling between two dissociation pathways in a P-selectin adhesion bond. *Proc. Natl. Acad. Sci. U.S.A.* **2004**, *101*, 11281-11286.
54. Guo, B.; Guilford, W. H. Mechanics of actomyosin bonds in different nucleotide states are tuned to muscle contraction. *Proc. Natl. Acad. Sci. U.S.A.* **2006**, *103*, 9844-9849.
55. Thomas, W. E.; Trintchina, E.; Forero, M.; Vogel, V.; Sokurenko, E. V. Bacterial adhesion to target cells enhanced by shear force. *Cell* **2002**, *109*, 913-923.
56. Thomas, W. E.; Nilsson, L. M.; Forero, M.; Sokurenko, E. V.; Vogel, V. Shear-dependent 'stick-and-roll' adhesion of type 1 fimbriated *Escherichia coli*. *Mol. Microbiol.* **2004**, *53*, 1545-1557.
57. Thomas, W. Catch bonds in adhesion. *Annu. Rev. Biomed. Eng.* **2008**, *10*, 39-57.
58. Yakovenko, O.; Sharma, S.; Forero, M.; Tchesnokova, V.; Aprikian, P.; Kidd, B.; Mach, A.; Vogel, V.; Sokurenko, E.; Thomas, W. E. FimH forms catch bonds that are enhanced by mechanical force due to allosteric regulation. *J. Biol. Chem.* **2008**, *283*, 11596-11605.
59. Nilsson, L. M.; Thomas, W. E.; Trintchina, E.; Vogel, V.; Sokurenko, E. V. Catch bond-mediated adhesion without a shear threshold: trimannose versus monomannose interactions with the FimH adhesin of *Escherichia coli*. *J. Biol. Chem.* **2006**, *281*, 16656-16663.
60. Aprikian, P.; Tchesnokova, V.; Kidd, B.; Yakovenko, O.; Yarov-Yarovoy, V.; Trinchina, E.; Vogel, V.; Thomas, W.; Sokurenko, E. Interdomain interaction in the

- FimH adhesin of *Escherichia coli* regulates the affinity to mannose. *J. Biol. Chem.* **2007**, *282*, 23437-23446.
61. Tchesnokova, V.; Aprikian, P.; Yakovenko, O.; Larock, C.; Kidd, B.; Vogel, V.; Thomas, W.; Sokurenko, E. Integrin-like allosteric properties of the catch bond-forming FimH adhesin of *Escherichia coli*. *J. Biol. Chem.* **2008**, *283*, 7823-7833.
62. Nilsson, L. M.; Thomas, W. E.; Sokurenko, E. V.; Vogel, V. Elevated shear stress protects *Escherichia coli* cells adhering to surfaces via catch bonds from detachment by soluble inhibitors. *Appl. Environ. Microbiol.* **2006**, *72*, 3005-3010.
63. Anderson, B. N.; Ding, A. M.; Nilsson, L. M.; Kusuma, K.; Tchesnokova, V.; Vogel, V.; Sokurenko, E. V.; Thomas, W. E. Weak rolling adhesion enhances bacterial surface colonization. *J. Bacteriol.* **2007**, *189*, 1794-1802.
64. Yakovenko, O.; Tchesnokova, V.; Sokurenko, E. V.; Thomas, W. E. Inactive conformation enhances binding function in physiological conditions. *Proc. Natl. Acad. Sci. U.S.A.* **2015**, *112*, 9884-9889.
65. Han, Z.; Pinkner, J. S.; Ford, B.; Obermann, R.; Nolan, W.; Wildman, S. A.; Hobbs, D.; Ellenberger, T.; Cusumano, C. K.; Hultgren, S. J.; Janetka, J. W. Structure-based drug design and optimization of mannoside bacterial FimH antagonists. *J. Med. Chem.* **2010**, *53*, 4779– 4792.
66. Wellens, A.; Lahmann, M.; Touaibia, M.; Vaucher, J.; Oscarson, S.; Roy, R.; Remaut, H.; Bouckaert, J. The tyrosine gate as a potential entropic lever in the receptor-binding site of the bacterial adhesin FimH. *Biochemistry* **2012**, *51*, 4790– 4799.
67. Roos, G.; Wellens, A.; Touaibia, M.; Yamakawa, N.; Geerlings, P.; Roy, R.; Wyns, L.; Bouckaert, J. Validation of Reactivity Descriptors to Assess the Aromatic Stacking within the Tyrosine Gate of FimH. *ACS Med. Chem. Lett.* **2013**, *4*, 1085-1090.
68. Vanwetswinkel, S.; Volkov, A. N.; Sterckx, Y. G.; Garcia-Pino, A.; Buts, L.; Vranken, W. F.; Bouckaert, J.; Roy, R.; Wyns, L.; Van Nuland, N. A. Study of the structural and dynamic effects in the FimH adhesin upon α -D-heptyl mannose binding. *J. Med. Chem.* **2014**, *57*, 1416-1427.
69. Brument, S.; Sivignon, A.; Dumych, T. I.; Moreau, N.; Roos, G.; Guérardel, Y.; Chalopin, T.; Deniaud, D.; Bilyy, R. O.; Darfeuille-Michaud, A.; Bouckaert, J.; Gouin, S. G. Thiazolylaminomannosides as potent antiadhesives of type 1 piliated *Escherichia coli* isolated from Crohn's disease patients. *J. Med. Chem.* **2013**, *56*, 5395– 5406.

70. Kleeb, S.; Pang, L.; Mayer, K.; Eris, D.; Sigl, A.; Preston, R. C.; Zihlmann, P.; Sharpe, T.; Roman, P. J.; Abgottspon, D.; Hutter, A.; Scharenberg, M.; Jiang, X.; Navarra, G.; Rabbani, S.; Smieško, M.; Lüdin, N.; Bezençon, J.; Schwardt, O.; Maier, T. Ernst, B. FimH antagonists: bioisosteres to improve the in vitro and in vivo PK/PD profile. *J. Med. Chem.* **2015**, *58*, 2221-2239.
71. Fiege, B.; Rabbani, S.; Preston, R. C.; Jakob, R. P.; Zihlmann, P.; Schwardt, O.; Jiang, X.; Maier, T.; Ernst, B. The tyrosine gate of the bacterial lectin FimH: a conformational analysis by NMR spectroscopy and X-ray crystallography. *ChemBioChem* **2015**, *16*, 1235-1246.
72. Levy, S. B. Antibiotic resistance-the problem intensifies. *Adv. Drug Deliv. Rev.* **2005**, *57*, 1446-1450.
73. Ofek, I.; Hasty, D. L.; Sharon, N. Anti-adhesion therapy of bacterial diseases: prospects and problems. *FEMS Immunol. Med. Microbiol.* **2003**, *38*, 181-191.
74. Pieters, R. J. Intervention with bacterial adhesion by multivalent carbohydrates. *Med. Res. Rev.* **2007**, *27*, 796-816.
75. Scharenberg, M.; Schwardt, O.; Rabbani, S.; Ernst, B. Target Selectivity of FimH Antagonists. *J. Med. Chem.* **2012**, *55*, 9810-9816.
76. Sharon, N. Carbohydrates as future anti-adhesion drugs for infectious diseases. *Biochim. Biophys. Acta.* **2006**, *1760*, 527-537.
77. Ofek, I.; Kahane, I.; Sharon, N. Toward anti-adhesion therapy for microbial diseases. *Trends Microbiol.* **1996**, *4*, 297-299.
78. Ofek, I.; Sharon, N. A bright future for anti-adhesion therapy of infectious diseases. *Cell. Mol. Life Sci.* **2002**, *59*, 1666-1667.
79. Aronson, M.; Medalia, O.; Schori, L.; Mirelman, D.; Sharon, N.; Ofek, I. Prevention of colonization of the urinary tract of mice with *Escherichia coli* by blocking of bacterial adherence with methyl α -D-mannopyranoside. *J. Infect. Dis.* **1979**, *139*, 329-332.
80. Edén, C. S.; Freter, R.; Hagberg, L.; Hull, R.; Hull, S.; Leffler, H.; Schoolnik, G. Inhibition of experimental ascending urinary tract infection by an epithelial cell-surface receptor analogue. *Nature* **1982**, *298*, 560-562.
81. Klein, T.; Abgottspon, D.; Wittwer, M.; Rabbani, S.; Herold, J.; Jiang, X.; Kleeb, S.; Lüthi, C.; Scharenberg, M.; Bezençon, J.; Gubler, E.; Pang, L.; Smieško, M.; Cutting, B.; Schwardt, O.; Ernst, B. FimH antagonists for the oral treatment of urinary tract infections: from design and synthesis to in vitro and in vivo evaluation. *J. Med.*

- Chem.* **2010**, *53*, 8627– 8641.
82. Cusumano, C. K.; Pinkner, J. S.; Han, Z.; Greene, S. E.; Ford, B. A.; Crowley, J. R.; Henderson, J. P.; Janetka, J. W.; Hultgren, S. J. Treatment and prevention of urinary tract infection with orally active FimH inhibitors. *Sci. Transl. Med.* **2011**, *3*, 109ra115.
 83. Han, Z.; Pinkner, J. S.; Ford, B.; Chorell, E.; Crowley, J. M.; Cusumano, C. K.; Campbell, S.; Henderson, J. P.; Hultgren, S. J.; Janetka, J. W. Lead optimization studies on FimH antagonists: discovery of potent and orally bioavailable ortho-substituted biphenyl mannosides. *J. Med. Chem.* **2012**, *55*, 3945– 3959.
 84. Jiang, X.; Abgottspon, D.; Kleeb, S.; Rabbani, S.; Scharenberg, M.; Wittwer, M.; Haug, M.; Schwardt, O.; Ernst, B. Antiadhesion therapy for urinary tract infections – A balanced PK/PD profile proved to be key for success. *J. Med. Chem.* **2012**, *55*, 4700– 4713.
 85. Eshdat, Y.; Ofek, I.; Yashouv-Gan, Y.; Sharon, N.; Mirelman, D. Isolation of a mannose-specific lectin from *Escherichia coli* and its role in the adherence of the bacteria to epithelial cells. *Biochem. Biophys. Res. Commun.* **1978**, *85*, 1551-1559.
 86. Firon, N.; Ofek, I.; Sharon, N. Interaction of mannose-containing oligosaccharides with the fimbrial lectin of *Escherichia coli*. *Biochem. Biophys. Res. Commun.* **1982**, *105*, 1426-1432.
 87. Firon, N.; Ofek, I.; Sharon, N. Carbohydrate specificity of the surface lectins of *Escherichia coli*, *Klebsiella pneumoniae*, and *Salmonella typhimurium*. *Carbohydr. Res.* **1983**, *120*, 235-249.
 88. Sharon, N. Bacterial lectins, cell-cell recognition and infectious disease. *FEBS Lett.* **1987**, *217*, 145-157.
 89. Firon, N.; Ashkenazi, S.; Mirelman, D.; Ofek, I.; Sharon, N. Aromatic alpha-glycosides of mannose are powerful inhibitors of the adherence of type 1 fimbriated *Escherichia coli* to yeast and intestinal epithelial cells. *Infect. Immun.* **1987**, *55*, 472-476.
 90. Bouckaert, J.; Mackenzie, J.; de Paz, J. L.; Chipwaza, B.; Choudhury, D.; Zavialov, A.; Mannerstedt, K.; Anderson, J.; Piérard, D.; Wyns, L.; Seeberger, P. H.; Oscarson, S.; De Greve, H.; Knight, S. D. The affinity of the FimH fimbrial adhesin is receptor-driven and quasi-independent of *Escherichia coli* pathotypes. *Mol. Microbiol.* **2006**, *61*, 1556-1568.
 91. Lipinski, C. A. Drug-like properties and the causes of poor solubility and poor permeability. *J. Pharmacol. Toxicol. Methods* **2000**, *44*, 235-249.
 92. Lipinski, C. A.; Lombardo, F.; Dominy, B. W.; Feeney, P. J. Experimental and

- computational approaches to estimate solubility and permeability in drug discovery and development settings. *Adv. Drug Deliv. Rev.* **2001**, *46*, 3-26.
93. Pang, L.; Kleeb, S.; Lemme, K.; Rabbani, S.; Scharenberg, M.; Zalewski, A.; Schädler, F.; Schwardt, O.; Ernst, B. FimH antagonists: structure-activity and structure-property relationships for biphenyl α -D-mannopyranosides. *ChemMedChem* **2012**, *7*, 1404–1422.
94. Schwardt, O.; Rabbani, S.; Hartmann, M.; Abgottspon, D.; Wittwer, M.; Kleeb, S.; Zalewski, A.; Smieško, M.; Cutting, B.; Ernst, B. Design, synthesis and biological evaluation of mannosyl triazoles as FimH antagonists. *Bioorg. Med. Chem.* **2011**, *19*, 6454-6473.
95. Scharenberg, M.; Jiang, X.; Pang, L.; Navarra, G.; Rabbani, S.; Binder, F.; Schwardt, O.; Ernst, B. Kinetic properties of carbohydrate-lectin interactions: FimH antagonists. *ChemMedChem* **2014**, *9*, 78-83.
96. Sperling, O.; Fuchs, A.; Lindhorst, T. K. Evaluation of the carbohydrate recognition domain of the bacterial adhesin FimH: Design, synthesis and binding properties of mannoside ligands. *Org. Biomol. Chem.* **2006**, *4*, 3913– 3922.
97. Old, D. C. Inhibition of the interaction between fimbrial haemagglutinins and erythrocytes by D-mannose and other carbohydrates. *J. Gen. Microbiol.* **1972**, *71*, 149–157.
98. Gloe, T. E.; Stamer, I.; Hojnik, C.; Wrodnigg, T. M.; Lindhorst, T. K. Are D-manno-configured Amadori products ligands of the bacterial lectin FimH? *Beilstein J. Org. Chem.* **2015**, *11*, 1096-1104.
99. Lundquist, J. J.; Toone, E. J. The cluster glycoside effect. *Chem. Rev.* **2002**, *102*, 555-578.
100. Lindhorst, T. K.; Kieburg, C.; Krallmann-Wenzel, U. Inhibition of the type 1 fimbriae-mediated adhesion of *Escherichia coli* to erythrocytes by multiantennary D-mannosyl clusters: the effect of multivalency. *Glycoconjugate J.* **1998**, *15*, 605– 613.
101. Nagahori, N.; Lee, R. T.; Nishimura, S.-L.; Pagé, S.; Roy, R.; Lee, Y. C. Inhibition of adhesion of type 1 fimbriated *Escherichia coli* to highly mannosylated ligands. *ChemBioChem* **2002**, *3*, 836– 844.
102. Appeldoorn, C. C. M.; Joosten, J. A. F.; Maate, F. A.; Dobrindt, U.; Hacker, J.; Liskamp, R. M. J.; Khan, A. S.; Pieters, R. J. Novel multivalent mannose compounds

- and their inhibition of the adhesion of type 1 fimbriated uropathogenic *E. coli*. *Tetrahedron: Asymmetry* **2005**, *16*, 361–372.
103. Patel, A.; Lindhorst, T. K. A modular approach for the synthesis of oligosaccharide mimetics. *Carbohydr. Res.* **2006**, *341*, 1657-1668.
104. Touaibia, M.; Wellens, A.; Shiao, T. C.; Wang, Q.; Sirois, S.; Bouckaert, J.; Roy, R. Mannosylated G(0) dendrimers with nanomolar affinities to *Escherichia coli* FimH. *ChemMedChem* **2007**, *2*, 1190-1201.
105. Durka, M.; Buffet, K.; Iehl, J.; Holler, M.; Nierengarten, J.-F.; Taganna, J.; Bouckaert, J.; Vincent, S. P. The functional valency of dodecamannosylated fullerenes with *Escherichia coli* FimH—towards novel bacterial antiadhesives. *Chem. Commun.* **2011**, *47*, 1321-1323.
106. Bouckaert, J.; Li, Z.; Xavier, C.; Almant, M.; Caveliers, V.; Lahoutte, T.; Weeks, S. D.; Kovensky, J.; Gouin, S. G. Heptyl α -D-mannosides grafted on a β -cyclodextrin core to interfere with *Escherichia coli* adhesion: an in vivo multivalent effect. *Chem. Eur. J.* **2013**, *19*, 7847– 7855.
107. van De Waterbeemd, H.; Smith, D. A.; Beaumont, K.; Walker, D. K. Property-based design: optimization of drug absorption and pharmacokinetics. *J. Med. Chem.* **2001**, *44*, 1313-1333.
108. Burton, P. S.; Goodwin, J. T.; Vidmar, T. J.; Amore, B. M. Predicting drug absorption: how nature made it a difficult problem. *J. Pharmacol. Exp. Ther.* **2002**, *303*, 889-895.
109. Rautio, J.; Kumpulainen, H.; Heimbach, T.; Oliyai, R.; Oh, D.; Järvinen, T.; Savolainen, J. Prodrugs: design and clinical applications. *Nat. Rev. Drug Discov.* **2008**, *7*, 255-270.
110. Beaumont, K.; Webster, R.; Gardner, I.; Dack, K. Design of ester prodrugs to enhance oral absorption of poorly permeable compounds: challenges to the discovery scientist. *Curr. Drug Metab.* **2003**, *4*, 461-485.
111. Saxon, E.; Bertozzi, C. R. Cell surface engineering by a modified Staudinger reaction. *Science* **2000**, *287*, 2007-2010.
112. Sarkar, A. K.; Fritz, T. A.; Taylor, W. H.; Esko, J. D. Disaccharide uptake and priming in animal cells: inhibition of sialyl Lewis X by acetylated Gal β 1 \rightarrow 4GlcNAc β -*O*-naphthalenemethanol. *Proc. Natl. Acad. Sci. U.S.A.* **1995**, *92*, 3323-3327.
113. Lavergne, T.; Baraguey, C.; Dupouy, C.; Parey, N.; Wuensche, W.; Sczakiel, G.; Vasseur, J.-J.; Debart, F. Synthesis and preliminary evaluation of pro-RNA 2'-*O*-

- masked with biolabile pivaloyloxymethyl groups in an RNA interference assay. *J. Org. Chem.* **2011**, *76*, 5719–5731.
114. Parey, N.; Baraguey, C.; Vasseur, J.-J.; Debart, F. First evaluation of acyloxymethyl or acylthiomethyl groups as biolabile 2'-O-protections of RNA. *Org. Lett.* **2006**, *8*, 3869–3872.
115. Martin, A. R.; Lavergne, T.; Vasseur, J.-J.; Debart, F. Assessment of new 2'-O-acetalester protecting groups for regular RNA synthesis and original 2'-modified proRNA. *Bioorg. Med. Chem. Lett.* **2009**, *19*, 4046-4049.
116. Ochi, Y.; Nakagawa, O.; Sakaguchi, K.; Wada, S-i.; Uarata, H. A post-synthetic approach for the synthesis of 2'-O-methyldithiomethyl-modified oligonucleotides responsive to a reducing environment. *Chem. Commun.* **2013**, *49*, 7620-7622.
117. Thillier, Y.; Stevens, S. K.; Moy, C.; Taylor, J.; Vasseur, J.-J.; Beigelman, L.; Debart, F. Solid-phase synthesis of 5'-triphosphate 2'-5'-oligoadenylates analogs with 3'-O-biolabile groups and their evaluation as RNase L activators and antiviral drugs. *Bioorg. Med. Chem.* **2013**, *21*, 5461–5469.

2. Results and Discussion

2.1 Manuscript 1: FimH Antagonists: Ester Prodrugs for Achieving Oral Bioavailability

This manuscript describes the optimization of the intestinal absorption potential of FimH antagonist by means of an ester prodrug approach. The ester promoieties employed in this strategy span from simple aliphatic chains to more complex oxygen- and nitrogen-containing heteroalkyl structures. Moreover, enzymatic hydrolysis of these esters via liver- and plasma-borne esterases is discussed in detail.

Contribution to the project:

Wojciech Schönemann was involved in the design of the ester promoieties as well as the chemical synthesis of all compounds described in this manuscript. Furthermore, he is responsible for writing the synthetic part.

This manuscript is in preparation for *ChemMedChem*.

FimH Antagonists: Ester Prodrugs for Achieving Oral Bioavailability

Simon Kleeb[†], Wojciech Schönemann[†], Oliver Schwardt, and Beat Ernst*

* *Institute of Molecular Pharmacy, Pharmacenter, University of Basel, Klingelbergstr. 50, 4056 Basel (Switzerland); E-mail: beat.ernst@unibas.ch*

[[†]] These authors equally contributed to this work.

Keywords: Enzyme-mediated bioactivation, ester prodrugs, FimH antagonists, oral bioavailability.

Abbreviations: BChE, butyrylcholinesterase; BNPP, bis(4-nitrophenyl) phosphate; Caco-2 cells, colorectal adenocarcinoma cells; CES, carboxylesterase; CRD, carbohydrate-recognition domain; *D*, octanol-water distribution coefficient; ER, endoplasmic reticulum; hCE1, human carboxylesterase isotype 1; hCE2, human carboxylesterase isotype 2; HLM, human liver microsomes; *P*, octanol-water partition coefficient; *P*_{app}, apparent permeability; *P*_e, effective permeability; PAMPA, parallel artificial membrane permeability assay; RLM, rat liver microsomes, UPEC, uropathogenic *Escherichia coli*; UTI, urinary tract infection.

Abstract

Urinary tract infections by uropathogenic *Escherichia coli* are among the most prevalent infectious diseases requiring antibiotic treatment. Since recurrent antibiotic exposure leads to the emergence of antimicrobial resistance, a novel prevention and treatment strategy is urgently required. The interaction of FimH, a lectin located at the tip of bacterial pili, with mannosylated glycoproteins on the urinary bladder mucosa is the initial step of the infection cycle. Biphenyl α -D-mannopyranosides with an electron-withdrawing carboxylic acid substituent on the terminal aromatic ring of the agylcone were identified as potent antagonists of this interaction.

The present report describes the synthesis and pharmacokinetic evaluation of various ester prodrugs that increase the intestinal absorption potential of the biphenyl α -D-mannopyranoside FimH antagonist. We identified two ester prodrugs with well-balanced pharmacokinetic profiles: the 2-(dimethylamino)ethyl ester derivative **5l** displaying high solubility, moderate membrane permeability, and rapid hydrolysis mediated by the plasma-borne cholinesterase as well as the 2-ethoxyethyl ester derivative **3g** exhibiting moderate solubility, high permeability, and prolonged bioactivation by the hepatic carboxylesterase. These two compounds will be selected for future *in vivo* pharmacokinetic studies.

Introduction

Urinary tract infections (UTIs), characterized by dysuria, frequent and urgent urination, bacteriuria, or pyuria, are among the most frequent bacterial infections. Around 60% of women have at least one UTI in their lifetime. Most episodes are caused by uropathogenic *Escherichia coli* (UPEC).^[1] UTI requires an antibiotic treatment to tackle the symptoms and to prevent potentially devastating complications like pyelonephritis and urosepsis.^[2] However, recurrent infections with subsequent antibiotic exposure result in antimicrobial resistance. This often leads to treatment failure and reduces the range of therapeutic options.^[3] Therefore, efficient non-antibiotic treatment strategies are urgently needed.

The pathogenesis of UTI relies on bacterial lectins which recognize carbohydrate ligands located on the endothelial cells of the urinary tract.^[4] P-piliated UPEC cause pyelonephritis by binding to galabiose-containing ligands on the kidney epithelium, while mannose-binding type 1 pili promote cystitis by targeting uroplakin 1a on the mucosal surface of the urothelial cells of the bladder.^[5] The bacterial adhesion prevents rapid clearance of UPEC from the urinary tract by the bulk flow of urine and enables the colonization of the host cells.^[6] The

lectin FimH expressed at the tip of bacterial type 1 pili encloses a carbohydrate recognition domain (CRD) which can interact with a mannosylated glycoprotein on the cell surface (uropod 1a), and a pilin domain regulating the switch between the low and high affinity states of the CRD.^[7,8]

The inhibition of the bacteria-cell interaction by FimH antagonists is not inducing a selection pressure and is therefore a promising approach to reduce or even avoid the resistance problem accompanying the current antibiotic treatment. More than two decades ago, Sharon and coworkers investigated various mannosides as antagonists for type 1 fimbriae-mediated bacterial adhesion.^[9-11] Since then, two different approaches have been explored for the further improvement of the anti-adhesive effects. First, multivalent mannosides^[12-14] were investigated and second, monovalent high-affinity antagonists^[15-21] were designed based on the structural information obtained from crystal structures of FimH co-crystallized with alkyl and aryl α -D-mannopyranosides.^[15,22-25] Only recently, the first *in vivo* studies performed in a mouse model were published, describing antibacterial effects in the bladder upon oral administration of biphenyl α -D-mannopyranosides.^[18,26] In either of the reported cases, high dose (≥ 50 mg/kg body weight) was however necessary to maintain the minimal therapeutic concentration in the urine over an extended period of time due to unfavorable physicochemical and pharmacokinetic properties of the orally applied antagonists.^[18,21]

In order to reach the urinary bladder, an orally applied FimH antagonist needs to be absorbed from the intestinal lumen into the portal vein, to be metabolically stable and survive the first liver passage and subsequently to be excreted via the kidneys. Permeability through the intestinal mucosa usually improves with increasing lipophilicity.^[27,28] By contrast, renal excretion is necessary to reach the target in the bladder. However after filtration at the glomerulus, hydrophilic compounds are not re-absorbed from the primary urine in the renal tubules and therefore they are quickly excreted.^[29,30] As a consequence, the minimal therapeutic concentration cannot be maintained in the bladder for an extended period of time. In this report we present an ester prodrug concept (Figure 1) combining lipophilicity, conferred by an alkyl moiety, and hydrophilicity, provided by the free carboxylate upon enzyme-mediated hydrolysis of the ester in hepatocytes or in plasma.^[31,32]

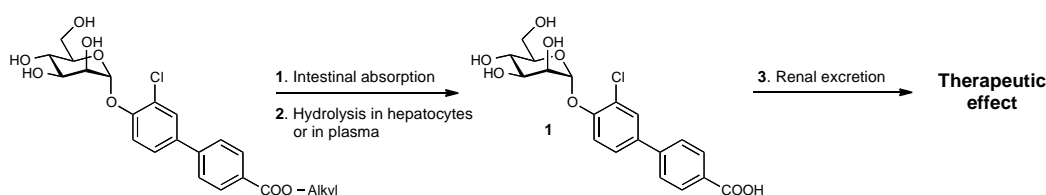
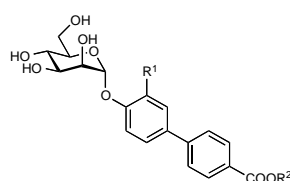


Figure 1. Ester prodrug concept enabling oral bioavailability and renal excretion for the biphenyl α -D-mannopyranoside FimH antagonist **1**.

Results and Discussion

In a previous publication, we described the biphenyl α -D-mannopyranoside **1** exhibiting nanomolar affinity towards the isolated FimH-CRD and treatment efficacy in a mouse disease model.^[18] Moreover, we showed that esterification of the polar carboxylate with a methyl promoiety (\rightarrow **2**) is a promising approach for achieving oral bioavailability. Nevertheless, the levels of the parent compound in plasma detected upon oral administration of the prodrug were moderate when compared to the concentrations reached by intravenous application. Therefore, we expanded the ester prodrug strategy in order to optimize the oral absorption potential. In a first step, we synthesized a set of simple alkyl esters (\rightarrow **3a-e**, Table 1) and characterized their intestinal absorption potential. Based on these findings we then optimized the prodrug by (a) introducing alkyl promoiety containing heteroatoms (\rightarrow **3f-i**, **k-n**) and by (b) replacing the *ortho*-chloro substituent of the biphenyl aglycone with a trifluoromethyl group (\rightarrow **4**, **5l**).

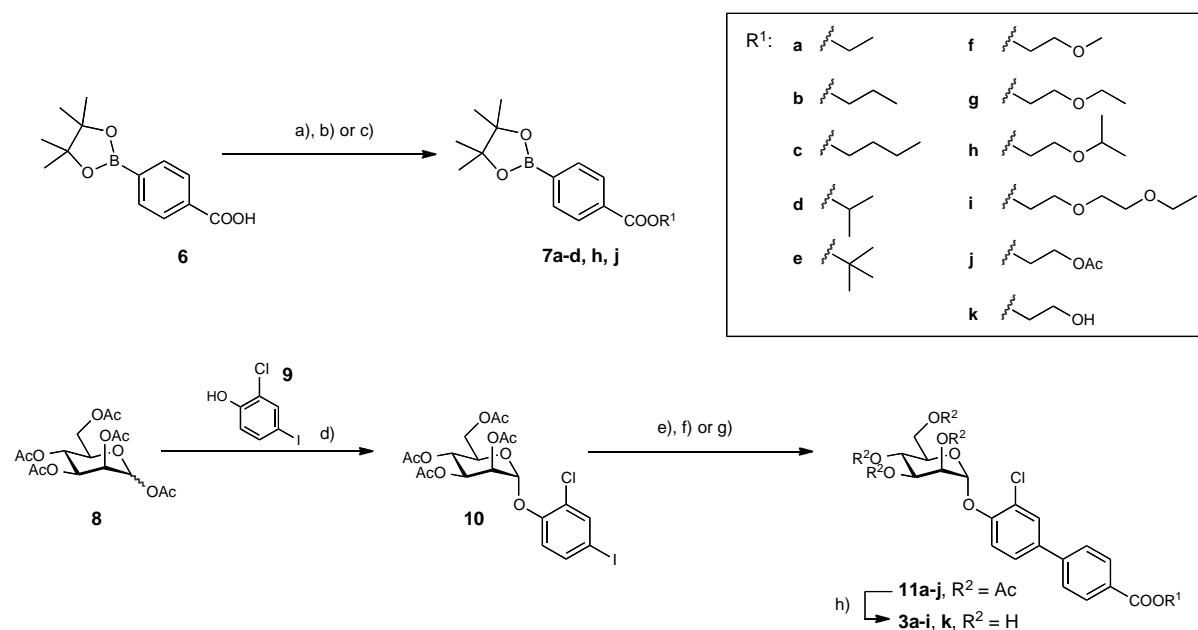
Table 1. Ester prodrugs for optimizing oral bioavailability of the biphenyl α -D-mannopyranosides **1** and **4**.



cpd	R ¹	R ²	cpd	R ¹	R ²	cpd	R ¹	R ²
1 ^[18]	Cl	H	3f	Cl	CH ₂ CH ₂ OCH ₃	4 ^[21]	CF ₃	H
2 ^[18]	Cl	CH ₃	3g	Cl	CH ₂ CH ₂ OCH ₂ CH ₃	5l	CF ₃	CH ₂ CH ₂ N(CH ₃) ₂
3a	Cl	CH ₂ CH ₃	3h	Cl	CH ₂ CH ₂ OCH(CH ₃) ₂			
3b	Cl	CH ₂ CH ₂ CH ₃	3i	Cl	CH ₂ CH ₂ OCH ₂ CH ₂ OCH ₂ CH ₃			
3c	Cl	(CH ₂) ₃ CH ₃	3k	Cl	CH ₂ CH ₂ OH			
3d	Cl	CH(CH ₃) ₂	3l	Cl	CH ₂ CH ₂ N(CH ₃) ₂			
3e	Cl	C(CH ₃) ₃	3m	Cl	CH ₂ CH ₂ -N			
			3n	Cl	CH ₂ CH ₂ -N			

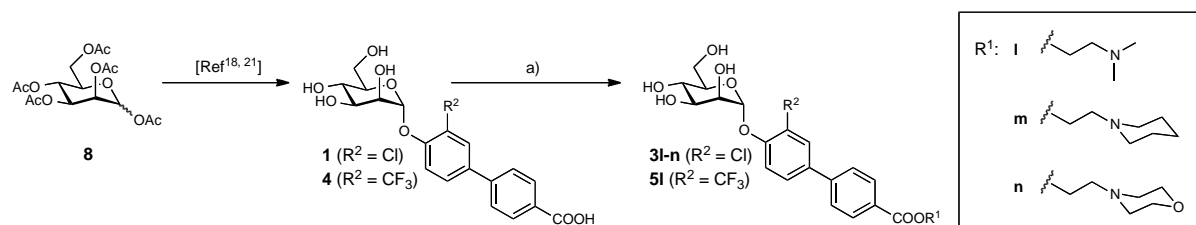
Synthesis

The synthesis of alkyl and oxygen-containing heteroalkyl esters is depicted in Scheme 1. The glycosylation between commercially available **8** and phenol **9** was performed in presence of Lewis acid affording α -D-mannoside **10** in 62% yield. The boronate ester intermediates **7a-d**, **f**, **g** were obtained by treating acid **6** with thionyl chloride and an excess of corresponding alcohol. The esters **7h-j** were obtained by Steglich esterification.^[33] All boronate ester intermediates were purified by MPLC on silica gel and characterized except **7f**, **7g** and **7i**, from which only major impurities were removed before using them in the next step. The compound **7e** was purchased from Frontier Scientific, Inc. Starting from **10**, palladium-mediated Suzuki coupling reactions^[34] with **7a-j** yielded the biphenyls **11a-j**. To avoid transesterification reactions, a mixture of chloroform and corresponding alcohol together with its alkoxide was used for deacetylation. In the case of more complex alcohols (\rightarrow **3e-j**), bulky *tert*-butanol with potassium *tert*-butoxide was applied.



Scheme 1. a) R¹-OH, SOCl₂, 60 °C, 2-6 h, 42-65% (**7a-c**); b) R¹-OH, DIC, DMAP, DCM, 0 °C → rt, 1-4 h, 43-69% (**7h, j**); c) *i*PrOH, SOCl₂, Et₃N, CHCl₃, 60 °C, 5 h, 32% (**7d**); d) BF₃·Et₂O, DCM, 4 Å MS, 40 °C, 50 h, 62%; e) **7a-e**, **7h** or **7j**, PdCl₂(dppf)·CH₂Cl₂, K₃PO₄, DMF, 80 °C, 2-6 h, 55-81% (**11a-e, h, j**); f) i. **6**, R¹-OH, SOCl₂, 60 °C, 4-6 h; ii. PdCl₂(dppf)·CH₂Cl₂, K₃PO₄, DMF, 80 °C, 4-5.5 h, 47-52% (**11f, g**); g) i. **6**, R¹-OH, DIC, DMAP, DCM, 0 °C → rt, 3.5 h; ii. PdCl₂(dppf)·CH₂Cl₂, K₃PO₄, DMF, 80 °C, 5 h, 44% (**11i**); h) R¹-ONa/R¹-OH or *t*-BuOK/*t*-BuOH, CHCl₃, rt, 2-25 h, 25-69%.

The synthesis of nitrogen-containing ester analogs was performed in a different manner to avoid possible deactivation of the catalyst^[35] during Suzuki coupling reaction. Esterification was performed on the unprotected mannosides **1** and **4** and the crude products **3l-n** and **5l** were purified by means of preparative HPLC resulting in moderate yields (Scheme 2).



Scheme 2. a) R¹-OH, COMU, DIPEA, DMF, rt, 4-31 h, 14-53%.

Physicochemical and *in vitro* pharmacokinetic characterization

For estimating the oral absorption potential of the various ester prodrugs as well as their propensity to enzyme-mediated bioactivation, we conducted aqueous solubility, lipophilicity, permeability, and metabolic stability studies (for experimental data refer to Table 2). Aqueous solubility was of interest because the orally applied dose needs to be dissolved in the intestinal fluids prior to absorption.^[36] Lipophilicity was quantified by means of the octanol-water distribution coefficient at pH 7.4 ($\log D_{7.4}$).^[37] The parallel artificial membrane permeability assay (PAMPA) was performed to estimate the prodrugs' ability to diffuse through the intestinal membranes,^[38] while bi-directional permeation studies across a colorectal adenocarcinoma (Caco-2) cell monolayer were implemented to reveal active influx and efflux processes.^[39] Furthermore, the prodrugs were incubated with rat and human liver microsomes (RLM, HLM) for estimating their susceptibility to hydrolases localized in the endoplasmic reticulum of hepatocytes,^[40] while incubations with human plasma were performed to investigate the involvement of plasma-borne enzymes in ester hydrolysis.^[41]

Table 2. Pharmacokinetic parameters of different ester prodrugs of the FimH antagonists **1** and **4**. PAMPA, parallel artificial membrane permeability assay; P_e , effective permeability; P_{app} , apparent permeability; RLM, rat liver microsomes; HLM, human liver microsomes; n.d., not determined. The Caco-2 assay was performed at an initial compound concentration (c_0) of 62.5 μ M. Microsomal stability was determined with pooled male rat liver microsomes (0.125 mg/mL) and pooled human liver microsomes (0.125 mg/mL) at pH 7.4 and 37 °C. Plasma stability was determined with human plasma (50%) at pH 7.4 and 37 °C.

Cpd	PAMPA log P_e [cm/s]/pH	Caco-2 P_{app} [10^{-6} cm/s]		log $D_{7.4}$	Solubility [μ g/mL]/pH	RLM $t_{1/2}$ [min]	HLM $t_{1/2}$ [min]	Plasma $t_{1/2}$ [min]
		a→b	b→a					
1 ^[18]	no permeation	0.2±0.0	0.4±0.0	< -1.5	>3000 / 6.61	---	---	---
2 ^[18]	-4.6	5.3±0.6	18±1	2.32	11.9 / 6.53	3.1	36	>120
3a	-4.5±0.1 / 7.4	n.d.	n.d.	n.d.	3.9±0.1 / 7.4	n.d.	n.d.	n.d.
3b	-4.5±0.1 / 7.4	n.d.	n.d.	n.d.	2.2±0.5 / 7.4	n.d.	n.d.	n.d.
3c	-4.6 / 7.4	n.d.	n.d.	n.d.	0.8±0.2 / 7.4	n.d.	n.d.	n.d.
3d	-4.4±0.1 / 7.4	n.d.	n.d.	n.d.	14±1 / 7.4	n.d.	n.d.	n.d.
3e	-4.4±0.1 / 7.4	n.d.	n.d.	n.d.	3.8±0.6 / 7.4	n.d.	n.d.	n.d.
3k	-6.6±0.1 / 7.4	0.6±0.1	9.6±0.6	1.8±0.1	>160 / 7.4	>120	>120	>120
3f	-4.9±0.0 / 7.4	4.5±0.4	18±1	2.3±0.0	121±4 / 7.4	4.1	47	57
3g	-4.9±0.2 / 7.4	11±1	19±1	2.7±0.0	137±14 / 7.4	5.9	101	66
3h	-4.5±0.1 / 7.4	8.3±0.7	36±4	3.1±0.1	90±6 / 7.4	1.9	16	57
3i	-5.1±0.1 / 7.4	4.6±0.6	36±7	2.1±0.1	147±6 / 7.4	5.1	33	33
3l	-6.4±0.0 / 5.0 -6.2±0.1 / 7.4	0.9±0.1	27±0	1.6±0.0	>160 / 3.0 >160 / 7.4	>120	>120	6.2
3m	-5.5±0.0 / 5.0 -5.1±0.0 / 7.4	1.0±0.3	33±2	2.4±0.1	79±8 / 3.0 57±4 / 7.4	49	>120	3.7
3n	-6.3±0.2 / 5.0 -5.6±0.0 / 7.4	0.6±0.2	35±5	2.2±0.1	>120 / 3.0 >120 / 7.4	32	>120	86
4	-8.4±1.3 / 5.0 -8.6±1.6 / 7.4	n.d.	n.d.	-0.8±0.1	15±1 / 3.0 >200 / 7.4	---	---	---
5l	-6.7±0.2 / 5.0 -6.4±0.0 / 7.4	1.6	37	1.7±0.0	>160 / 3.0 >160 / 7.4	80	n.d.	17

Oral absorption. As previously reported, low aqueous solubility ($< 20 \mu\text{g/mL}$) is a primary drawback constraining oral absorption of the methyl ester **2**.^[18,42] Moreover, carrier-mediated efflux at the apical enterocyte membrane – revealed by the bi-directional Caco-2 permeation assay – probably interferes with the intestinal uptake of the prodrug, in spite of promising membrane permeability suggested by PAMPA ($\log P_e = -4.6$).^[43,44] Therefore, we expanded the alkyl promoiety with the aim to increase solubility and permeability.

In the first step, esters with simple alkyl promoieties (**3a-e**) were synthesized. They trend towards slightly higher effective permeability ($\log P_e$), as detected by PAMPA. However, replacing the methyl promoiety with an ethyl, propyl, butyl, isopropyl, or *tert*-butyl group further reduced the aqueous solubility of the prodrug and, as a consequence, its intestinal absorption potential.^[36]

In order to counteract decreasing aqueous solubility, we introduced ethyl promoieties functionalized with oxygenated or nitrogenated substituents.^[45] These esters (**3f-i**, **k-n**) were indeed more soluble than the initial methyl ester **2** and the prodrugs **3a-e**. Moreover, the 2-ethoxyethyl ester **3g** and the 2-isopropoxyethyl ester **3h** displayed a higher $\log D_{7.4}$ than the methyl ester, suggesting an increase in membrane permeability. On the other hand, the tertiary amines present in the compounds **3l** and **3n** induced a decrease in $\log D_{7.4}$ but a strong increase in aqueous solubility. The moderate lipophilicity of the 2-(dimethylamino)ethyl ester **3l** could in turn be slightly raised by replacing the *ortho*-chloro substituent with a trifluoromethyl moiety on the aromatic ring of the biphenyl aglycone adjacent to the anomeric position (\rightarrow **5l**). Effective permeability deduced from PAMPA ($\log P_e$) correlated with $\log D_{7.4}$, such that the most lipophilic ester **3h** showed optimal $\log P_e$ for membrane permeation (-4.5).^[43] In the case of the esters **3l-n** and **5l** bearing an amine functional group, we observed moreover a strong dependence of $\log P_e$ on the pH of the compound solution in the donor compartment of the PAMPA.

A bi-directional Caco-2 permeability screening at low initial compound concentrations in the donor chamber ($c_0 = 62.5 \mu\text{M}$) classified all heteroalkyl esters as apparent substrates of efflux transporters.^[44] Passive diffusion driven by the concentration gradient across the cell monolayer and active efflux given for intrinsic carrier substrates are considered as key determinants of the apparent net flux.^[46] Accordingly, moderately permeable aminoalkyl esters, such as compound **3l**, diffused slowly but were strongly recognized by the efflux carriers, resulting in a high efflux ratio ($b \rightarrow a/a \rightarrow b$). Since **3l** is well soluble in aqueous medium, the initial concentration (c_0) in the donor chambers could however be expanded to

825 μM , which increased the gradient and apparently saturated the transporter activity (Figure 2). As a result, apparent permeability ($P_{\text{app, a}\rightarrow\text{b}}$) in the range for successful oral absorption was achieved.

In contrast to the 2-aminoethyl esters, the highly permeable esters **3f-h** diffused more rapidly, which led to a lower efflux ratio and promising $P_{\text{app, a}\rightarrow\text{b}}$ under the screening conditions ($c_0 = 62.5 \mu\text{M}$). However, for the ester **3h** exhibiting the least favorable efflux ratio among those esters, the attempt to saturate the transporters was not successful due to insufficient aqueous solubility (90 $\mu\text{g/mL}$).

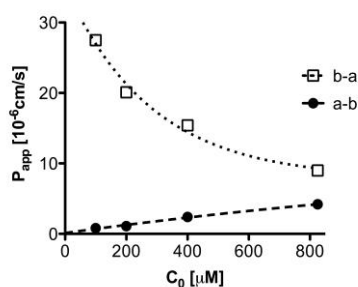


Figure 2. Apparent permeability (P_{app}) of ester **3l** through a Caco-2 cell monolayer. The assay was performed at different initial compound concentrations in the donor compartment (c_0), ranging from 100 μM to 825 μM . P_{app} (a \rightarrow b), permeability in the absorptive direction; P_{app} (b \rightarrow a), permeability in the secretory direction.

Enzyme-mediated bioactivation. Besides solubility and permeability, propensity to enzyme-mediated bioactivation was a key feature of our ester prodrug concept.^[31] Hydrolysis of the ester bond can be mediated by plasma-borne enzymes or by isozymes of the carboxylesterase (CES) superfamily associated to the endoplasmic reticulum of various tissues.^[41,47] The isozyme hCE1, highly expressed in hepatocytes but scarcely observed in enterocytes, and the isozyme hCE2, present in both hepatocytes and enterocytes, have been identified as major human CES.^[40] Since the prodrug approach might only be successful when hydrolysis takes place in the bloodstream or in the liver and not in the small intestines or in the enterocytes during absorption, high chemical stability of the ester bond and substrate specificity for plasma-borne hydrolases or hCE1 was aspired.

Incubations of the esters **3f-i**, **k-n**, and **5l** in buffer without active enzyme (pH 7.4, 37 $^{\circ}\text{C}$) showed a negligible degradation within one hour, suggesting high chemical stability of the prodrugs. With regard to the enzyme-mediated bioactivation, we identified different esterases to be involved in the conversion of the oxygen-containing esters **3f-i**, **k** and the amine-bearing esters **3l-n** and **5l** to the active parent compounds.

When we incubated the oxyethyl esters **3f-h**, **k** (initial concentration, $c_0 = 2 \mu\text{M}$ in TRIS-HCl 0.1 M, pH 7.4) with RLM (0.125 mg/mL, total incubation time = 60 min), we observed the previously described relationship between the lipophilicity of the ester and its propensity to hydrolysis by microsome-associated hydrolases.^[48,49] The 2-hydroxyethyl ester **3k**, i.e. the least lipophilic representative among the oxyethyl esters, showed stability during the entire incubation time ($t_{1/2} > 120 \text{ min}$). By contrast, the 2-methoxyethyl ester **3f**, 2-ethoxyethyl ester **3g**, and 2-isopropoxyethyl ester **3h** were all susceptible to degradation by microsome-associated enzymes, with the most lipophilic **3h** showing the shortest metabolic half-life. Nonetheless, the observed high rates of biotransformation by murine hydrolases did not correlate with the turnover by human enzymes. In fact, the incubations with HLM under similar assay conditions revealed important species differences in the observed half-lives (see Table 2), which need to be considered when predicting the rates of bioconversion in human from *in vivo* animal experiments.^[50]

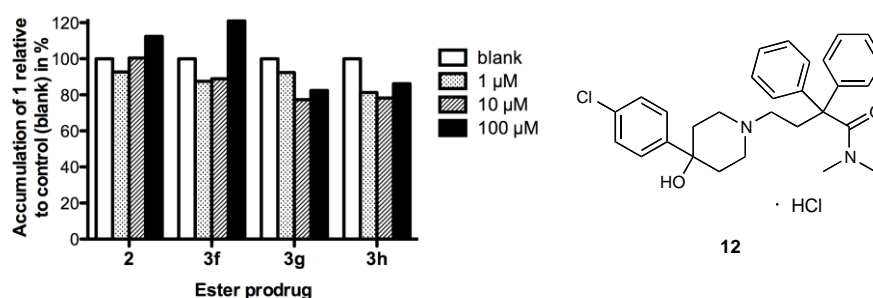


Figure 3. Human liver microsome (HLM) mediated hydrolysis of ester prodrug **2**, **3f**, **3g**, and **3h** in presence of loperamide hydrochloride (**12**), a specific inhibitor of the human carboxylesterase isotype 2 (hCE2). The bars represent the accumulation of the parent compound **1** in the incubation with inhibitor (1 μM , 10 μM , 100 μM) relative to the accumulation in the control experiment without loperamide (blank).

When bis(4-nitrophenyl) phosphate (BNPP, 1 mM) – an inhibitor of all CES isozymes – was added to the microsomal incubations of the esters **3f-h**, a strong decrease in the rates of hydrolysis was observed. These results suggest that enzymes of the CES superfamily are the main contributors to the bioactivation of these prodrugs.^[40] Otherwise, treating the HLM with loperamide (1 – 100 μM) – a specific inhibitor of the human CES isotype 2 (hCE2) – did not affect the rates of hydrolysis (Figure 3), which attributes the observed enzymatic turnover primarily to the hCE1 isozyme.^[51]

In contrast to the 2-oxyethyl esters, all 2-aminoethyl ester prodrugs **3l-n** and **5l** showed low susceptibility to hydrolysis by microsome-associated esterases. Indeed, the cationic tertiary amine present in these esters is supposed to establish strong interactions with negatively charged residues in the active site gorge of the CES and, as a consequence, to inhibit the hydrolytic activity.^[49] By contrast, the 2-(dimethylamino)ethyl esters **3l**, **5l**, and the 2-(piperidin-1-yl)ethyl ester **3m** were rapidly cleaved by plasma-borne enzymes. Since the 2-aminoethyl carboxylate present in these prodrugs is structurally related to choline esters, we postulated that they were recognized by the butyrylcholinesterase (BChE) present in human plasma.^[52,53] The metabolic turnover could indeed be inhibited by the specific cholinesterase inhibitor neostigmine bromide (**13**, Figure 4B), which confirms the strong contribution of BChE to the observed hydrolysis (Figure 4A).^[54] Against our expectations, the 2-morpholinoethyl promoiety in **3n**, known from marketed ester prodrugs, e.g. micophenolate mofetil (**14**, Figure 4B),^[55] was scarcely cleaved by microsomal or plasma-associated enzymes.

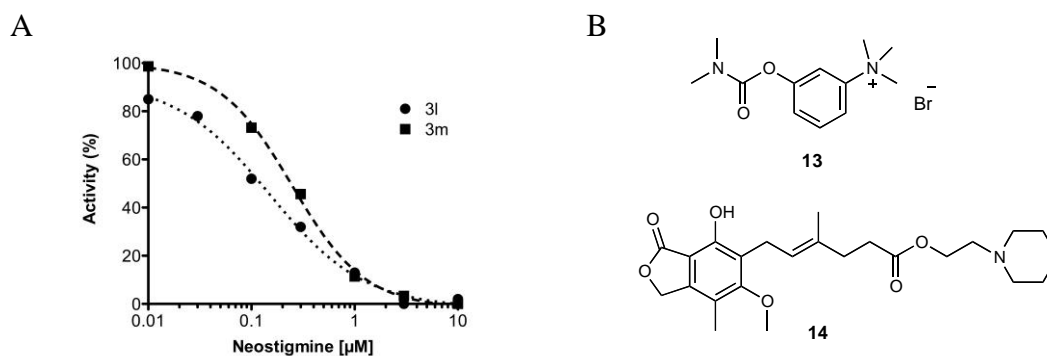


Figure 4. (A) Hydrolysis of the 2-(dimethylamino)ethyl ester **3l** and the 2-(piperidin-1-yl)ethyl ester **3m** by plasma-associated esterases in presence of the specific butyrylcholinesterase inhibitor neostigmine bromide (0.01 - 10 μM). The activity was calculated by dividing the metabolic $t_{1/2}$ observed in presence of the inhibitor neostigmine by the metabolic $t_{1/2}$ of the control experiment without inhibitor. (B) A chemical structure of neostigmine bromide (**13**) and micophenolate mofetil (**14**).

In summary, the prodrug approach proved successful to mask the polar character of the carboxylic acid and hence to increase permeability of the biphenyl α -D-mannopyranoside **1**. As opposed to merely aliphatic motifs present in **3a-e**, the oxyalkyl promoieties in **3f-h** enhanced both permeability and solubility. Nonetheless, aqueous solubility was still insufficient to reach concentrations necessary for efflux transporter saturation. Moreover, we suspect that, despite hydrolysis by hepatic CES, further metabolic modifications within the hepatocytes (e.g. glucuronidation of the free acid) or hepatobiliary excretion may take place

and constrain the systemic availability of the active principle.^[31] Otherwise, the 2-aminoethyl derivatives showed high aqueous solubility, compensating for moderate permeability and providing a promising overall absorption potential. Furthermore, the well soluble esters **3l** and **5l** displayed high propensity to hydrolysis by plasma-borne enzymes, which suggests rapid and quantitative conversion of the prodrug to the polar active principle within the bloodstream and thus low compound loss during the first pass through the liver.^[31]

With regard to the rate of enzyme-mediated bioactivation, rapid conversion, such as observed for the prodrugs **3h**, **3l** or **5l**, is not necessarily advantageous, since it favors rapid compound clearance from circulation, i.e. high initial concentrations in the bladder but only short-acting therapeutic effects. We therefore hypothesize that the slightly prolonged metabolic $t_{1/2}$ of the prodrug **3g** would allow maintaining the minimal therapeutic concentration in the urine for a longer period of time, thus reducing the dosing frequency.

Summary and Conclusion

Although described as potent and selective FimH antagonists, biaryl α -D-mannosides bearing carboxylic acid on the terminal aromatic ring have physicochemical profile unfavorable for an oral therapy. In a former publication, we introduced an ester prodrug approach rendering the biphenyl mannoside **1** orally available. The goal of the present study was to optimize the properties of the promoiety in order to enhance the intestinal uptake and the delivery of the pharmacologically active parent compound to the therapeutic target in the urinary bladder.

Introducing alkyl promoieties (i.e. ethyl, propyl, isopropyl, butyl, isopropyl, or *tert*-butyl) was unsuccessful due to markedly reduced aqueous solubility of the final molecules. By contrast, alkyl promoieties functionalized with oxygenated or nitrogenated substituents proved advantageous for masking the polar carboxylic acid substituent of the biphenyl aglycone and at the same time for raising the aqueous solubility of the prodrug. With regard to enzymatic bioactivation, we identified different esterases responsible for the hydrolysis of the alkoxyethyl esters and the aminoethyl derivatives. Whereas the class of the alkoxyethyl esters was recognized by the ER-associated CES expressed in hepatocytes, the aminoethyl derivatives were rapidly cleaved by the plasma-borne BChE, which implies immediate availability of the active principle in the bloodstream and lower non-renal clearance by phase II metabolic reactions or hepatobiliary excretion.

With respect to all ADME parameters determined *in vitro* (Table 2), the prodrugs **3g** and **5l** showed the most promising profiles. The 2-(dimethylamino)ethyl ester **5l** displayed high solubility, moderate permeability, and rapid hydrolysis mediated by the cholinesterase, which can lower the risk of non-renal clearance but also shorten the dosing interval of the treatment. On the other hand, the 2-ethoxyethyl ester **3g** exhibited moderate solubility, high permeability, and a slightly prolonged $t_{1/2}$, which may be beneficial in terms of dose regimen but also may increase the propensity to hepatic clearance. In order to evaluate the advantages and drawbacks of these two prodrugs, *in vivo* pharmacokinetic studies in mice should be conducted as a next step.

Experimental Section

Chemistry

General methods: NMR spectra were recorded on a Bruker Avance DMX-500 (500 MHz) spectrometer. Assignment of ^1H and ^{13}C NMR spectra was achieved using 2D methods (COSY, HSQC, HMBC). Chemical shifts are expressed in ppm using residual CHCl_3 , CHD_2OD or HDO as references. Optical rotations were measured using Perkin-Elmer Polarimeter 341. Electron spray ionization mass spectra (ESI-MS) were obtained on a Waters micromass ZQ Mass Spectrometer. The LC-HRMS analysis were carried out using a Agilent 1100 LC equipped with a photodiode array detector and a Micromass QTOF I equipped with a 4 GHz digital-time converter. Reactions were monitored by TLC using glass plates coated with silica gel 60 F₂₅₄ (Merck) and visualized by using UV light and/or by charring with a molybdate solution (a 0.02 M solution of ammonium cerium sulfate dihydrate and ammonium molybdate tetrahydrate in aqueous 10% H_2SO_4). MPLC separations were carried out on a CombiFlash Companion or R_f from Teledyne Isco equipped with RediSep normal-phase. LC-MS separations were carried out on a Waters system equipped with sample manager 2767, pump 2525, PDA 2996, column SunFireTM Prep C₁₈ OBDTM (5 μm , 19 x 150 mm), and Micromass ZQ. All compounds used for biological assays are at least of 95% purity based on HPLC analytical results. Commercially available reagents were purchased from Aldrich, Alfa Aesar, Acros Organics or Frontier Scientific. Solvents were purchased from Sigma-Aldrich or Acros and were dried prior to use where indicated. Methanol (MeOH), ethanol (EtOH), *n*-propanol (PrOH), isopropanol (*i*-PrOH), *n*-butanol (BuOH) and *tert*-butanol (*t*-BuOH) were dried by storing with activated molecular sieves 3Å or 4Å for at

least one day. Dichloromethane (DCM) was dried by filtration over Al₂O₃ (Fluka, type 5016 A basic) and stored over activated molecular sieves 4Å. Molecular sieves 3Å and 4Å were activated in vacuo at 200 °C for 30 min immediately before use.

General procedure A for Suzuki coupling reaction. A round-bottom flask was charged with **10**, boronate **6** or **7** and K₃PO₄, then evacuated and flushed with argon. Anhydrous DMF (0.5-4 mL) was added and the mixture was degassed in an ultrasonic bath for 10 min followed by the addition of PdCl₂(dppf)·CH₂Cl₂. The reaction was stirred at 80 °C under argon until completion (2-6 h). After cooling to rt, the mixture was diluted with EtOAc (30-50 mL) and washed with satd aq NaHCO₃ (2 x 20 mL) and H₂O (2 x 20 mL). The organic layer was dried over Na₂SO₄, concentrated in vacuo and purified by MPLC on silica gel to afford **11a-j**.

General procedure B for deacetylation. To a solution of protected mannoside **11** in a mixture of dry alcohol and chloroform, freshly prepared sodium alkoxide or potassium *tert*-butoxide was added. The mixture was stirred at rt under argon until completion (2-25 h). Then, the mixture was neutralized with Amberlyst-15 (H⁺) ion-exchange resin, filtered and concentrated in vacuo. The crude product was purified by MPLC on silica gel to afford **3a-i, k**.

General procedure C for esterification of compounds 1 and 4. To a solution of **1** or **4**, the corresponding alcohol and DIPEA in DMF was added COMU. The mixture was stirred at rt under argon until completion (4-31 h) and then concentrated in vacuo. The residue was dissolved in MeOH (1 mL) or MeCN (1 mL), passed through a nylon membrane syringe filter (pore size 0.45 µm) and purified by LC-MS (H₂O/MeCN + 0.2% HCO₂H) to afford **3l-n** and **5l** as solids after lyophilization from H₂O.

4-Ethoxycarbonylphenylboronic acid pinacol ester (7a). A round-bottom flask was charged with **6** (60 mg, 0.235 mmol), evacuated and flushed with argon. Then, dry EtOH (0.6 mL) and SOCl₂ (41 µL, 0.282 mmol, 2.4 eq) were added. The mixture was stirred at 60 °C for 2 h. The reaction mixture was concentrated in vacuo and purified by MPLC on silica gel (petroleum ether/EtOAc, 9:1) to afford **7a** (43 mg, 66%) as a colorless oil. Analytical data are in accordance with literature data.^[56]

4-Propoxycarbonylphenylboronic acid pinacol ester (7b). Prepared according to the procedure for **7a** from **6** (39 mg, 0.152 mmol) with SOCl₂ (12 μ L, 0.152 mmol, 1.0 eq) in dry PrOH (0.3 mL). After stirring for 6 h, the reaction mixture was diluted with EtOAc (40 mL) and washed with satd aq NaHCO₃ (20 mL). The organic layer was dried over Na₂SO₄, concentrated in vacuo and purified by MPLC on silica gel (petroleum ether/EtOAc, 9:1) to afford **7b** (23 mg, 52%) as a colorless oil. ¹H NMR (500 MHz, CDCl₃): δ = 7.95 (d, J = 8.2 Hz, 2H, Ar-H), 7.79 (d, J = 8.2 Hz, 2H, Ar-H), 4.21 (t, J = 6.7 Hz, 2H, OCH₂), 1.76-1.69 (m, 2H, CH₂), 1.28 (s, 12H, 2 C(CH₃)₂), 0.96 (t, J = 7.4 Hz, 3H, CH₃); ¹³C NMR (125 MHz, CDCl₃): δ = 166.92 (CO), 134.84, 132.91, 128.76 (6C, Ar-C), 84.36 (2C, 2 C(CH₃)₂), 66.82 (OCH₂), 25.08 (4C, 2 C(CH₃)₂), 22.31 (CH₂), 10.72 (CH₃); elemental analysis: Calcd (%) for C₁₆H₂₃BO₄: C 66.23, H 7.99, found: C 66.15, H 8.01.

4-Butoxycarbonylphenylboronic acid pinacol ester (7c). Prepared according to the procedure for **7a** from **6** (47 mg, 0.188 mmol) with SOCl₂ (17 μ L, 0.232 mmol, 1.2 eq) in dry BuOH (0.4 mL). After stirring for 6 h, the mixture was concentrated in vacuo and purified by MPLC on silica gel (petroleum ether/EtOAc, 9:1) to afford **7c** (37 mg, 65%) as a colorless oil. ¹H NMR (500 MHz, CDCl₃): δ = 7.94 (d, J = 8.2 Hz, 2H, Ar-H), 7.79 (d, J = 8.1 Hz, 2H, Ar-H), 4.25 (t, J = 6.7 Hz, 2H, OCH₂), 1.71-1.66 (m, 2H, CH₂), 1.44-1.37 (m, 2H, CH₂), 1.28 (s, 12H, 2 C(CH₃)₂), 0.91 (t, J = 7.4 Hz, 3H, CH₃); ¹³C NMR (125 MHz, CDCl₃): δ = 166.93 (CO), 134.84, 132.91, 128.75 (6C, Ar-C), 84.36 (2C, 2 C(CH₃)₂), 65.13 (OCH₂), 30.97 (CH₂), 25.08 (4C, 2 C(CH₃)₂), 19.47 (CH₂), 13.97 (CH₃); ESI-MS: m/z : Calcd for C₁₇H₂₅BNaO₄ [M+Na]⁺: 327.17, found: 326.98.

4-Isopropoxycarbonylphenylboronic acid pinacol ester (7d). To a solution of **6** (39 mg, 0.152 mmol) in CHCl₃ (1 mL) was added SOCl₂ (28 μ L, 0.380 mmol, 2.5 eq). The reaction mixture was stirred at 60 °C under argon. Dry *i*-PrOH (1 mL) and Et₃N (23 μ L, 0.167 mmol, 1.1 eq) were added after 2 h. When the reaction was complete (2.5 h), the mixture was concentrated in vacuo and the residue purified by MPLC on silica gel (petroleum ether/EtOAc, 9:1) to afford **7d** (14 mg, 32%) as a colorless oil. ¹H NMR (500 MHz, CDCl₃): δ = 7.94 (d, J = 8.2 Hz, 2H, Ar-H), 7.78 (d, J = 8.1 Hz, 2H, Ar-H), 5.18 (hept, J = 6.3 Hz, 1H, OCH), 1.71-1.66 (m, 2H, CH₂), 1.44-1.37 (m, 2H, CH₂), 1.31-1.29 (m, 18H, 2 C(CH₃)₂, CH(CH₃)₂); ¹³C NMR (125 MHz, CDCl₃): δ = 166.37 (CO), 134.79, 133.33, 128.74 (6C, Ar-

C), 84.36 (2C, 2 C(CH₃)₂), 68.67 (OCH), 25.10 (4C, 2 C(CH₃)₂), 22.16 (2C, CH(CH₃)₂); ESI-MS: *m/z*: Calcd for C₁₆H₂₃BNaO₄ [M+Na]⁺: 313.16, found: 312.99.

4-(2-Isopropoxyethoxycarbonyl)phenylboronic acid pinacol ester (7h). To a solution of **6** (100 mg, 0.391 mmol) in dry DCM (2 mL) under argon were added 2-isopropoxyethanol (91 μL, 0.782 mmol, 2.0 eq) and a catalytic amount of DMAP (4 mg, 0.033 mmol, 0.08 eq). Then, DIC (91 μL, 0.587 mmol, 1.5 eq) was added at 0 °C, the reaction was allowed to reach rt and stirred for 1 h. The reaction mixture was diluted with EtOAc (40 mL) and washed with 0.1 N HCl (10 mL), satd aq NaHCO₃ (20 mL) and H₂O (20 mL). The organic layer was dried over Na₂SO₄, concentrated in vacuo and purified by MPLC on silica gel (DCM/MeOH, 99:1) to afford **7h** (70 mg, 53%) as a colorless oil. ¹H NMR (500 MHz, CDCl₃): δ = 8.03 (d, *J* = 8.3 Hz, 2H, Ar-H), 7.86 (d, *J* = 8.1 Hz, 2H, Ar-H), 4.46-4.43 (m, 2H, COCH₃), 3.77-3.75 (m, 2H, CH₂O), 3.66 (hept, *J* = 6.1 Hz, 1H, OCH), 1.35 (s, 12H, 2 C(CH₃)₂), 1.18 (d, *J* = 6.1 Hz, 6H, CH(CH₃)₂); ¹³C NMR (125 MHz, CDCl₃): δ = 166.78 (CO), 134.76, 132.52, 128.82 (6C, Ar-C), 84.30 (2C, 2 C(CH₃)₂), 72.20 (OCH), 66.09 (CH₂O), 64.71 (COCH₂), 25.02 (4C, 2 C(CH₃)₂), 22.19 (2C, CH(CH₃)₂); elemental analysis: Calcd (%) for C₁₈H₂₇BO₅: C 64.69, H 8.14, found: C 65.05, H 8.21.

4-(2-Acetoxyethoxycarbonyl)phenylboronic acid pinacol ester (7j). Prepared according to the procedure for **7h** from **6** (100 mg, 0.403 mmol) and 2-hydroxyethyl acetate^[57] (0.150 mL) with DIC (94 μL, 0.605 mmol, 1.5 eq) and DMAP (4 mg, 0.033 mmol, 0.08 eq) in dry DCM (2 mL) to afford **7j** (71 mg, 53%) as a colorless oil. ¹H NMR (500 MHz, CD₃OD): δ = 8.00 (d, *J* = 8.2 Hz, 2H, Ar-H), 7.84 (d, *J* = 8.2 Hz, 2H, Ar-H), 4.53-4.51 (m, 2H, CH₂), 4.43-4.41 (m, 2H, CH₂), 2.06 (s, 3H, COCH₃), 1.36 (s, 12H, 2 C(CH₃)₂); ¹³C NMR (125 MHz, CD₃OD): δ = 172.63, 167.70 (2 CO), 135.69, 129.64 (6C, Ar-C), 85.53 (2C, 2 C(CH₃)₂), 64.17, 63.44 (2 OCH₂), 25.20 (4C, 2 C(CH₃)₂), 20.66 (COCH₃); ESI-MS: *m/z*: Calcd for C₁₇H₂₃BNaO₆ [M+Na]⁺: 357.15, found: 357.04.

2-Chloro-4-iodophenyl 2,3,4,6-tetra-O-acetyl-α-D-mannopyranoside (10). To a suspension of **8** (1.33 g, 3.42 mmol), phenol **9** (1.04 g, 4.10 mmol, 1.2 eq) and activated molecular sieves 4 Å (1.40 g) in dry DCM (10 mL), BF₃·Et₂O (1.67 mL, 13.7 mmol, 4.0 eq) was added dropwise at rt under argon. After 22 h of stirring at 40 °C, a second portion of BF₃·Et₂O (0.42 mL, 3.42 mmol, 1.0 eq) was added. The mixture was stirred at 40 °C for 28 h

and then filtered through Celite and the filtrate was diluted with EtOAc (100 mL), washed with satd aq NaHCO₃ (2 x 50 mL), H₂O (50 mL) and brine (20 mL). The organic layer was dried over Na₂SO₄ and concentrated in vacuo. The residue was purified by MPLC on silica gel (petroleum ether/EtOAc, 9:1) to afford **10** (1.25 g, 62%) as a white solid. Analytical data are with accordance with the literature data.^[20]

Ethyl 4'-(2,3,4,6-tetra-*O*-acetyl- α -D-mannopyranosyloxy)-3'-chlorobiphenyl-4-carboxylate (11a). Prepared according to general procedure A from **10** (83 mg, 0.142 mmol) and **7a** (43 mg, 0.156 mmol, 1.1 eq) with K₃PO₄ (93 mg, 0.411 mmol, 3.0 eq) and PdCl₂(dppf)·CH₂Cl₂ (3.4 mg, 4.2 μ mol, 0.03 eq) in anhydrous DMF (0.5 mL). Purified by MPLC on silica gel (petroleum ether/EtOAc, 7:3). Yield: 62 mg (62%) as colorless oil. $[\alpha]_D^{20} +66.4$ (*c* 1.00, CHCl₃); ¹H NMR (500 MHz, CDCl₃): δ = 8.02 (d, *J* = 8.4 Hz, 2H, Ar-H), 7.59 (d, *J* = 2.2 Hz, 1H, Ar-H), 7.51 (d, *J* = 8.4 Hz, 2H, Ar-H), 7.39 (dd, *J* = 2.2, 8.6 Hz, 1H, Ar-H), 7.18 (d, *J* = 8.6 Hz, 1H, Ar-H), 5.58-5.54 (m, 2H, H-1, H-3), 5.48 (dd, *J* = 1.8, 3.4 Hz, 1H, H-2), 5.33 (t, *J* = 10.1 Hz, 1H, H-4), 4.32 (q, *J* = 7.1 Hz, 2H, OCH₂), 4.22 (dd, *J* = 5.3, 12.3 Hz, 1H, H-6a), 4.12 (ddd, *J* = 2.1, 5.2, 10.1 Hz, 1H, H-5), 4.03 (dd, *J* = 2.2, 12.4 Hz, 1H, H-6b), 2.14, 2.00, 1.97, 1.96 (4 s, 12H, 4 COCH₃), 1.34 (t, *J* = 7.1 Hz, 3H, CH₃); ¹³C NMR (125 MHz, CDCl₃): δ = 170.61, 170.10, 169.92, 169.91, 166.45 (5 CO), 151.27, 143.48, 136.33, 130.36, 129.79, 129.44, 126.83, 126.64, 125.03, 117.39 (12C, Ar-C), 96.79 (C-1), 69.99 (C-5), 69.47 (C-2), 68.92 (C-3), 65.96 (C-4), 62.25 (C-6), 61.22 (OCH₂), 21.02, 20.86, 20.84, 20.82 (4 COCH₃), 14.51 (CH₃); elemental analysis: Calcd (%) for C₂₉H₃₁ClO₁₂: C 57.38, H 5.15, found: C 57.62, H 5.32.

Propyl 4'-(2,3,4,6-tetra-*O*-acetyl- α -D-mannopyranosyloxy)-3'-chlorobiphenyl-4-carboxylate (11b). Prepared according to general procedure A from **10** (35 mg, 0.060 mmol) and **7b** (19 mg, 0.065 mmol, 1.1 eq) with K₃PO₄ (39 mg, 0.179 mmol, 3.0 eq) and PdCl₂(dppf)·CH₂Cl₂ (2.3 mg, 2.8 μ mol, 0.05 eq) in DMF (0.5 mL). Purified by MPLC on silica gel (petroleum ether/EtOAc, 1:0-0:1). Yield: 26 mg (70%) as colorless oil. $[\alpha]_D^{20} +68.2$ (*c* 0.87, CHCl₃); ¹H NMR (500 MHz, CDCl₃): δ = 8.03 (d, *J* = 8.4 Hz, 2H, Ar-H), 7.60 (d, *J* = 2.2 Hz, 1H, Ar-H), 7.52 (d, *J* = 8.4 Hz, 2H, Ar-H), 7.39 (dd, *J* = 2.2, 8.6 Hz, 1H, Ar-H), 7.19 (d, *J* = 8.5 Hz, 1H, Ar-H), 5.57 (dd, *J* = 3.5, 10.1 Hz, 1H, H-3), 5.54 (d, *J* = 1.5 Hz, 1H, H-1), 5.49 (dd, *J* = 1.9, 3.4 Hz, 1H, H-2), 5.34 (t, *J* = 10.1 Hz, 1H, H-4), 4.25-4.21 (m, 3H, H-6a, OCH₂), 4.12 (ddd, *J* = 2.1, 5.2, 10.1 Hz, 1H, H-5), 4.03 (dd, *J* = 2.2, 12.3 Hz, 1H, H-

6b), 2.15, 2.01, 1.98, 1.97 (4 s, 12H, 4 COCH₃), 1.78-1.71 (m, 2H, CH₂), 0.98 (t, J = 7.4 Hz, 3H, CH₃); ¹³C NMR (125 MHz, CDCl₃): δ = 170.66, 170.16, 169.97, 169.96, 166.57 (5 CO), 151.32, 143.54, 136.40, 130.41, 129.86, 129.49, 126.90, 126.68, 125.09, 117.43 (12C, Ar-C), 96.84 (C-1), 70.03 (C-5), 69.52 (C-2), 68.96 (C-3), 66.85 (OCH₂), 66.01 (C-4), 62.29 (C-6), 22.33 (CH₂), 21.07, 20.90, 20.88, 20.86 (4 COCH₃), 10.72 (CH₃); ESI-MS: m/z : Calcd for C₃₀H₃₇ClNO₁₂ [M+NH₄]⁺: 638.20, found: 638.07.

Butyl 4'-(2,3,4,6-tetra-*O*-acetyl- α -D-mannopyranosyloxy)-3'-chlorobiphenyl-4-carboxylate (11c). Prepared according to general procedure A from **10** (52 mg, 0.090 mmol) and **7c** (30 mg, 0.099 mmol, 1.1 eq) with K₃PO₄ (59 mg, 0.270 mmol, 3.0 eq) and PdCl₂(dppf)·CH₂Cl₂ (3.9 mg, 4.5 μ mol, 0.05 eq) in DMF (0.5 mL). Purified by MPLC on silica gel (petroleum ether/EtOAc, 7:3). Yield: 33 mg (58%) as pink oil. $[\alpha]_D^{20}$ +105.1 (c 1.10, CHCl₃); ¹H NMR (500 MHz, CDCl₃): δ = 8.03 (d, J = 8.4 Hz, 2H, Ar-H), 7.61 (d, J = 2.2 Hz, 1H, Ar-H), 7.54 (d, J = 8.4 Hz, 2H, Ar-H), 7.41 (dd, J = 2.2, 8.6 Hz, 1H, Ar-H), 7.19 (d, J = 8.6 Hz, 1H, Ar-H), 5.57 (dd, J = 3.5, 10.1 Hz, 1H, H-3), 5.54 (d, J = 1.6 Hz, 1H, H-1), 5.49 (dd, J = 1.9, 3.4 Hz, 1H, H-2), 5.34 (t, J = 10.1 Hz, 1H, H-4), 4.28 (t, J = 6.6 Hz, 2H, OCH₂), 4.22 (dd, J = 5.3, 12.3 Hz, 1H, H-6a), 4.12 (ddd, J = 2.2, 5.2, 10.1 Hz, 1H, H-5), 4.04 (dd, J = 2.2, 12.3 Hz, 1H, H-6b), 2.15, 2.01, 1.98, 1.97 (4 s, 12H, 4 COCH₃), 1.73-1.67 (m, 2H, CH₂), 1.46-1.39 (m, 2H, CH₂), 0.92 (t, J = 7.4 Hz, 3H, CH₃); ¹³C NMR (125 MHz, CDCl₃): δ = 170.67, 170.17, 169.98, 169.97, 166.58 (5 CO), 151.33, 143.54, 136.41, 130.42, 129.87, 129.50, 126.90, 126.68, 125.09, 117.44 (12C, Ar-C), 96.85 (C-1), 70.04 (C-5), 69.53 (C-2), 68.96 (C-3), 66.02 (C-4), 65.16 (OCH₂), 62.30 (C-6), 31.00 (CH₂), 21.07, 20.91, 20.88, 20.87 (4 COCH₃), 19.49 (CH₂), 13.98 (CH₃); HRMS: m/z : Calcd for C₃₁H₃₅ClNaO₁₂ [M+Na]⁺: 657.1715, found: 657.1711.

Isopropyl 4'-(2,3,4,6-tetra-*O*-acetyl- α -D-mannopyranosyloxy)-3'-chlorobiphenyl-4-carboxylate (11d). Prepared according to general procedure A from **10** (26 mg, 0.044 mmol) and **7d** (14 mg, 0.048 mmol, 1.1 eq) with K₃PO₄ (29 mg, 0.132 mmol, 3.0 eq) and PdCl₂(dppf)·CH₂Cl₂ (1.5 mg, 1.8 μ mol, 0.04 eq) in DMF (0.5 mL). Purified by MPLC on silica gel (petroleum ether/EtOAc, 7:3). Yield: 22 mg (81%) as colorless oil. $[\alpha]_D^{20}$ +57.5 (c 1.05, CHCl₃); ¹H NMR (500 MHz, CDCl₃): δ = 8.02 (d, J = 8.5 Hz, 2H, Ar-H), 7.61 (d, J = 2.2 Hz, 1H, Ar-H), 7.53 (d, J = 8.5 Hz, 2H, Ar-H), 7.40 (dd, J = 2.2, 8.6 Hz, 1H, Ar-H), 7.19 (d, J = 8.3 Hz, 1H, Ar-H), 5.57 (dd, J = 3.5, 10.1 Hz, 1H, H-3), 5.54 (d, J = 1.6 Hz, 1H, H-1),

5.49 (dd, $J = 1.9, 3.4$ Hz, 1H, H-2), 5.34 (t, $J = 10.1$ Hz, 1H, H-4), 5.20 (hept, $J = 6.3$ Hz, 1H, OCH), 4.22 (dd, $J = 5.3, 12.3$ Hz, 1H, H-6a), 4.12 (ddd, $J = 2.2, 5.2, 10.1$ Hz, 1H, H-5), 4.03 (dd, $J = 2.3, 12.2$ Hz, 1H, H-6b), 2.15, 2.01, 1.98, 1.97 (4 s, 12H, 4 COCH₃), 1.38 (d, $J = 6.3$ Hz, 6H, CH(CH₃)₂); ¹³C NMR (125 MHz, CDCl₃): $\delta = 170.67, 170.17, 169.98, 169.97, 166.00$ (5 CO), 151.30, 143.44, 136.46, 130.39, 130.26, 129.49, 126.84, 126.68, 125.08, 117.43 (12C, Ar-C), 96.84 (C-1), 70.03 (C-5), 69.52 (C-2), 68.97 (C-3), 68.71 (OCH), 66.02 (C-4), 62.30 (C-6), 22.17 (2C, CH(CH₃)₂), 21.07, 20.91, 20.88, 20.87 (4 COCH₃); HRMS: m/z : Calcd for C₃₀H₃₃ClNaO₁₂ [M+Na]⁺: 643.1558, found: 643.1554.

tert-Butyl 4'-(2,3,4,6-tetra-*O*-acetyl- α -D-mannopyranosyloxy)-3'-chlorobiphenyl-4-carboxylate (11e). Prepared according to general procedure A from **10** (27 mg, 0.047 mmol) and 4-*tert*-butyloxycarbonylphenyl boronic pinacol ester (**7e**, 16 mg, 0.052 mmol, 1.1 eq) with K₃PO₄ (31 mg, 0.141 mmol, 3.0 eq) and PdCl₂(dppf)·CH₂Cl₂ (1.6 mg, 1.9 μ mol, 0.04 eq) in DMF (0.5 mL). Purified by MPLC on silica gel (petroleum ether/EtOAc, 7:3). Yield: 22 mg (74%) as colorless oil. $[\alpha]_D^{20} +64.9$ (c 1.09, CHCl₃); ¹H NMR (500 MHz, CDCl₃): $\delta = 7.97$ (d, $J = 8.4$ Hz, 2H, Ar-H), 7.59 (d, $J = 2.2$ Hz, 1H, Ar-H), 7.49 (d, $J = 8.4$ Hz, 2H, Ar-H), 7.38 (dd, $J = 2.2, 8.6$ Hz, 1H, Ar-H), 7.18 (d, $J = 8.8$ Hz, 1H, Ar-H), 5.57 (dd, $J = 3.5, 10.1$ Hz, 1H, H-3), 5.55 (d, $J = 1.5$ Hz, 1H, H-1), 5.49 (dd, $J = 1.9, 3.4$ Hz, 1H, H-2), 5.34 (t, $J = 10.1$ Hz, 1H, H-4), 4.22 (dd, $J = 5.3, 12.3$ Hz, 1H, H-6a), 4.12 (ddd, $J = 2.1, 5.3, 10.1$ Hz, 1H, H-5), 4.03 (dd, $J = 2.2, 12.3$ Hz, 1H, H-6b), 2.15, 2.01, 1.98, 1.97 (4 s, 12H, 4 COCH₃), 1.54 (s, 9H, C(CH₃)₃); ¹³C NMR (125 MHz, CDCl₃): $\delta = 170.68, 170.18, 169.99, 169.98, 165.68$ (5 CO), 151.26, 143.16, 136.55, 131.39, 130.30, 129.48, 126.77, 126.67, 125.08, 117.45 (12C, Ar-C), 96.86 (C-1), 81.40 (C(CH₃)₃), 70.04 (C-5), 69.54 (C-2), 68.98 (C-3), 66.04 (C-4), 62.31 (C-6), 28.43 (3C, C(CH₃)₃), 21.09, 20.92, 20.90, 20.88 (4 COCH₃); ESI-MS: m/z : Calcd for C₃₁H₃₅ClNaO₁₂ [M+Na]⁺: 657.17, found: 657.13.

2-Methoxyethyl 4'-(2,3,4,6-tetra-*O*-acetyl- α -D-mannopyranosyloxy)-3'-chloro-biphenyl-4-carboxylate (11f). 4-(2-Methoxyethoxycarbonyl)phenylboronic acid pinacol ester (**7f**) was prepared according to the procedure for **7a** from **6** (25 mg, 0.104 mmol) with SOCl₂ (11 μ L, 0.151 mmol, 1.5 eq) in 2-methoxyethanol (0.4 mL). The reaction mixture was concentrated in vacuo after 4 h. The crude product was used directly in the coupling reaction according to general procedure A with **10** (55 mg, 0.095 mmol), K₃PO₄ (61 mg, 0.285 mmol, 3.0 eq) and PdCl₂(dppf)·CH₂Cl₂ (3.1 mg, 3.8 μ mol, 0.04 eq) in DMF (1 mL). Purified by MPLC on silica

gel (petroleum ether/EtOAc, 3:2). Yield: 32 mg (52% over two steps) as colorless oil. $[\alpha]_D^{20} +60.9$ (*c* 1.26, CHCl₃); ¹H NMR (500 MHz, CDCl₃): δ = 8.05 (d, *J* = 8.4 Hz, 2H, Ar-H), 7.60 (d, *J* = 2.2 Hz, 1H, Ar-H), 7.52 (d, *J* = 8.4 Hz, 2H, Ar-H), 7.39 (dd, *J* = 2.2, 8.6 Hz, 1H, Ar-H), 7.19 (d, *J* = 8.9 Hz, 1H, Ar-H), 5.56 (dd, *J* = 3.5, 10.1 Hz, 1H, H-3), 5.54 (d, *J* = 1.5 Hz, 1H, H-1), 5.49 (dd, *J* = 1.9, 3.4 Hz, 1H, H-2), 5.34 (t, *J* = 10.1 Hz, 1H, H-4), 4.43-4.42 (m, 2H, CH₂), 4.22 (dd, *J* = 5.3, 12.3 Hz, 1H, H-6a), 4.12 (ddd, *J* = 2.2, 5.2, 10.1 Hz, 1H, H-5), 4.03 (dd, *J* = 2.2, 12.3 Hz, 1H, H-6b), 3.68-3.67 (m, 2H, CH₂), 3.37 (s, 3H, OCH₃), 2.14, 2.01, 1.98, 1.97 (4 s, 12H, 4 COCH₃); ¹³C NMR (125 MHz, CDCl₃): δ = 170.58, 170.07, 169.89, 169.88, 166.39 (5 CO), 151.26, 143.64, 136.25, 130.51, 129.41, 129.30, 126.81, 126.60, 125.00, 117.34 (12C, Ar-C), 96.74 (C-1), 70.69 (CH₂), 69.95 (C-5), 69.42 (C-2), 68.87 (C-3), 65.92 (C-4), 64.24 (CH₂), 62.20 (C-6), 59.19 (OCH₃), 20.98, 20.82, 20.79, 20.78 (4 COCH₃); ESI-MS: *m/z*: Calcd for C₃₀H₃₃ClNaO₁₃ [M+Na]⁺: 659.15, found: 659.12.

2-Ethoxyethyl 4'-(2,3,4,6-tetra-*O*-acetyl- α -D-mannopyranosyloxy)-3'-chloro-biphenyl-4-carboxylate (11g). 4-(2-Ethoxyethoxycarbonyl)phenylboronic acid pinacol ester (**7g**) was prepared according to the procedure for **7a** from **6** (40 mg, 0.161 mmol) with SOCl₂ (35 μ L, 0.484 mmol, 3.0 eq) in 2-ethoxyethanol (0.6 mL). After 6 h, the reaction mixture was diluted with DCM (40 mL) and washed with H₂O (4 x 30 mL). The organic layer was dried over Na₂SO₄ and concentrated in vacuo. The crude product was used directly in the coupling reaction according to general procedure A with **10** (47 mg, 0.081 mmol), K₃PO₄ (53 mg, 0.242 mmol, 3.0 eq) and PdCl₂(dppf)·CH₂Cl₂ (3.3 mg, 4.1 μ mol, 0.05 eq) in DMF (2 mL). Purified by MPLC on silica gel (petroleum ether/EtOAc, 1:0-0:1). Yield: 25 mg (47% over two steps) as colorless oil. $[\alpha]_D^{20} +54.5$ (*c* 1.15, CHCl₃); ¹H NMR (500 MHz, CDCl₃): δ = 8.12 (d, *J* = 8.4 Hz, 2H, Ar-H), 7.67 (d, *J* = 2.2 Hz, 1H, Ar-H), 7.59 (d, *J* = 8.4 Hz, 2H, Ar-H), 7.46 (dd, *J* = 2.2, 8.6 Hz, 1H, Ar-H), 7.27-7.25 (m, 1H, Ar-H), 5.64 (dd, *J* = 3.5, 10.1 Hz, 1H, H-3), 5.62 (d, *J* = 1.7 Hz, 1H, H-1), 5.56 (dd, *J* = 1.9, 3.4 Hz, 1H, H-2), 5.41 (t, *J* = 10.1 Hz, 1H, H-4), 4.50-4.48 (m, 2H, CH₂), 4.30 (dd, *J* = 5.3, 12.3 Hz, 1H, H-6a), 4.20 (ddd, *J* = 2.2, 5.2, 10.1 Hz, 1H, H-5), 4.11 (dd, *J* = 2.2, 12.2 Hz, 1H, H-6b), 3.80-3.78 (m, 2H, CH₂), 3.60 (q, *J* = 7.0 Hz, 2H, OCH₂CH₃), 2.22, 2.08, 2.05, 2.04 (4 s, 12H, 4 COCH₃), 1.24 (t, *J* = 7.0 Hz, 3H, CH₃); ¹³C NMR (125 MHz, CDCl₃): δ = 170.59, 170.09, 169.91, 169.89, 166.43 (5 CO), 151.28, 143.62, 136.29, 130.52, 129.43, 129.42, 126.83, 126.62, 125.02, 117.35 (12C, Ar-C), 96.77 (C-1), 69.96 (C-5), 69.45 (C-2), 68.89 (C-3), 68.56 (CH₂), 66.85

(OCH₂CH₃), 65.94 (C-4), 64.49 (CH₂), 62.22 (C-6), 21.00, 20.84, 20.81, 20.80 (4 COCH₃), 15.30 (CH₃); ESI-MS: *m/z*: Calcd for C₃₁H₃₅ClNaO₁₃ [M+Na]⁺: 673.17, found: 673.19.

2-Isopropoxyethyl 4'-(2,3,4,6-tetra-*O*-acetyl- α -D-mannopyranosyloxy)-3'-chlorobiphenyl-4-carboxylate (11h). Prepared according to general procedure A from **10** (105 mg, 0.180 mmol) and **7h** (60 mg, 0.180 mmol, 1.0 eq) with K₃PO₄ (118 mg, 0.540 mmol, 3.0 eq) and PdCl₂(dppf)·CH₂Cl₂ (7.3 mg, 9.0 μ mol, 0.05 eq) in DMF (2 mL). Purified by MPLC on silica gel (petroleum ether/EtOAc, 1:0-0:1). Yield: 67 mg (56%) as colorless oil. $[\alpha]_D^{20}$ +55.6 (*c* 1.10, CHCl₃); ¹H NMR (500 MHz, CDCl₃): δ = 8.11 (d, *J* = 8.4 Hz, 2H, Ar-H), 7.67 (d, *J* = 2.2 Hz, 1H, Ar-H), 7.59 (d, *J* = 8.4 Hz, 2H, Ar-H), 7.46 (dd, *J* = 2.2, 8.6 Hz, 1H, Ar-H), 7.26 (d, *J* = 8.4 Hz, 1H, Ar-H), 5.63 (dd, *J* = 3.5, 10.1 Hz, 1H, H-3), 5.61 (d, *J* = 1.3 Hz, 1H, H-1), 5.55 (dd, *J* = 1.8, 3.3 Hz, 1H, H-2), 5.40 (t, *J* = 10.1 Hz, 1H, H-4), 4.47-4.45 (m, 2H, CH₂), 4.29 (dd, *J* = 5.3, 12.3 Hz, 1H, H-6a), 4.20 (ddd, *J* = 2.1, 5.2, 10.0 Hz, 1H, H-5), 4.10 (dd, *J* = 2.1, 12.2 Hz, 1H, H-6b), 3.78-3.76 (m, 2H, CH₂), 3.67 (hept, *J* = 6.1 Hz, 1H, OCH), 2.21, 2.07, 2.05, 2.04 (4 s, 12H, 4 COCH₃), 1.22 (d, *J* = 6.1 Hz, 6H, CH(CH₃)₂); ¹³C NMR (125 MHz, CDCl₃): δ = 170.59, 170.09, 169.91, 169.89, 166.43 (5 CO), 151.28, 143.59, 136.30, 130.49, 129.49, 129.44, 126.83, 126.61, 125.03, 117.36 (12C, Ar-C), 96.78 (C-1), 72.20 (OCH), 69.97 (C-5), 69.45 (C-2), 68.89 (C-3), 66.12 (CH₂), 65.95 (C-4), 64.76 (CH₂), 62.22 (C-6), 22.21 (2C, CH(CH₃)₂), 21.00, 20.84, 20.81, 20.80 (4 COCH₃); ESI-MS: *m/z*: Calcd for C₃₂H₃₇ClNaO₁₃ [M+Na]⁺: 687.18, found: 687.23.

2-(2-Ethoxyethoxy)ethyl 4'-(2,3,4,6-tetra-*O*-acetyl- α -D-mannopyranosyloxy)-3'-chlorobiphenyl-4-carboxylate (11i). 4-(2-(2-ethoxyethoxy)ethoxycarbonyl)phenyl-boronic acid pinacol ester (**7i**) was prepared according to the procedure for **7h** from **6** (75 mg, 0.196 mmol) and 2-(2-ethoxyethoxy)ethanol (40 μ L, 0.196 mmol, 1.0 eq) with DIC (54 μ L, 0.235 mmol, 1.2 eq) and DMAP (2 mg, 0.016 mmol, 0.08 eq) in DCM (2 mL). The major impurities were removed by MPLC on silica gel (DCM/MeOH, 99:1) and the product was used directly in the coupling reaction according to general procedure A with **10** (79 mg, 0.135 mmol), K₃PO₄ (89 mg, 0.405 mmol, 3.0 eq) and PdCl₂(dppf)·CH₂Cl₂ (5.5 mg, 6.8 μ mol, 0.05 eq) in DMF (2 mL). Purified by MPLC on silica gel (petroleum ether/EtOAc, 3:2). Yield: 60 mg (44% over two steps) as colorless oil. $[\alpha]_D^{20}$ +58.6 (*c* 1.15, CHCl₃); ¹H NMR (500 MHz, CDCl₃): δ = 8.06-8.04 (m, 2H, Ar-H), 7.60 (d, *J* = 2.2 Hz, 1H, Ar-H), 7.53-7.51 (m, 2H, Ar-H), 7.39 (dd, *J* = 2.3, 8.6 Hz, 1H, Ar-H), 7.19 (m, 1H, Ar-H), 5.57 (dd, *J* =

3.5, 10.1 Hz, 1H, H-3), 5.54 (d, $J = 1.7$ Hz, 1H, H-1), 5.49 (dd, $J = 1.9, 3.4$ Hz, 1H, H-2), 5.34 (t, $J = 10.1$ Hz, 1H, H-4), 4.45-4.43 (m, 2H, CH₂), 4.22 (dd, $J = 5.3, 12.3$ Hz, 1H, H-6a), 4.12 (ddd, $J = 2.2, 5.2, 10.1$ Hz, 1H, H-5), 4.03 (dd, $J = 2.2, 12.3$ Hz, 1H, H-6b), 3.80-3.78 (m, 2H, CH₂), 3.65-3.63 (m, 2H, CH₂), 3.56-3.54 (m, 2H, CH₂), 3.47 (q, $J = 7.0$ Hz, 2H, OCH₂CH₃), 2.15, 2.01, 1.98, 1.97 (4 s, 12H, 4 COCH₃), 1.14 (t, $J = 7.0$ Hz, 3H, CH₃); ¹³C NMR (125 MHz, CDCl₃): $\delta = 170.60, 170.10, 169.91, 169.90, 166.40$ (5 CO), 151.28, 143.63, 136.28, 130.52, 129.44, 129.40, 126.83, 126.62, 125.02, 117.35 (12C, Ar-C), 96.77 (C-1), 70.92, 70.00 (2C, 2 CH₂), 69.96 (C-5), 69.45 (C-2), 69.39 (CH₂), 68.89 (C-3), 66.86 (OCH₂CH₃), 65.94 (C-4), 64.37 (CH₂), 62.22 (C-6), 21.00, 20.84, 20.82, 20.80 (4 COCH₃), 15.29 (CH₃); ESI-MS: m/z : Calcd for C₃₃H₃₉ClNaO₁₄ [M+Na]⁺: 717.19, found: 717.27.

2-Acetoxyethyl 4'-(2,3,4,6-tetra-*O*-acetyl- α -D-mannopyranosyloxy)-3'-chloro-biphenyl-4-carboxylate (11j). Prepared according to general procedure A from **10** (120 mg, 0.205 mmol) and **7j** (69 mg, 0.205 mmol, 1.0 eq) with K₃PO₄ (135 mg, 0.618 mmol, 3.0 eq) and PdCl₂(dppf)·CH₂Cl₂ (8.4 mg, 10.3 μ mol, 0.05 eq) in DMF (2 mL). Purified by MPLC on silica gel (petroleum ether/EtOAc, 3:2). Yield: 79 mg (58%) as colorless oil. $[\alpha]_D^{20} +43.9$ (c 0.75, CHCl₃); ¹H NMR (500 MHz, CDCl₃): $\delta = 8.11$ (d, $J = 8.4$ Hz, 2H, Ar-H), 7.67 (d, $J = 2.2$ Hz, 1H, Ar-H), 7.60 (d, $J = 8.4$ Hz, 2H, Ar-H), 7.46 (dd, $J = 2.3, 8.6$ Hz, 1H, Ar-H), 7.27 (m, 1H, Ar-H), 5.64 (dd, $J = 3.5, 10.1$ Hz, 1H, H-3), 5.62 (d, $J = 1.7$ Hz, 1H, H-1), 5.56 (dd, $J = 1.9, 3.4$ Hz, 1H, H-2), 5.41 (t, $J = 10.1$ Hz, 1H, H-4), 4.54-4.53 (m, 2H, CH₂), 4.45-4.43 (m, 2H, CH₂), 4.30 (dd, $J = 5.3, 12.3$ Hz, 1H, H-6a), 4.19 (ddd, $J = 2.2, 5.2, 10.1$ Hz, 1H, H-5), 4.11 (dd, $J = 2.2, 12.3$ Hz, 1H, H-6b), 2.22, 2.11, 2.08, 2.05, 2.04 (5 s, 15H, 5 COCH₃); ¹³C NMR (125 MHz, CDCl₃): $\delta = 171.01, 170.61, 170.12, 169.93, 169.90, 166.19$ (6 CO), 151.35, 143.86, 136.21, 130.53, 129.46, 129.05, 126.93, 126.64, 125.07, 117.37 (12C, Ar-C), 96.79 (C-1), 69.99 (C-5), 69.46 (C-2), 68.90 (C-3), 65.95 (C-4), 62.97, 62.33 (2C, 2 CH₂), 62.23 (C-6), 21.02, 21.00, 20.85, 20.83, 20.82 (5 COCH₃); HRMS: m/z : Calcd for C₃₁H₃₃ClNaO₁₄ [M+Na]⁺: 687.1457, found: 687.1450.

Ethyl 3'-chloro-4'-(α -D-mannopyranosyloxy)biphenyl-4-carboxylate (3a). Prepared according to general procedure B from **11a** (18 mg, 0.030 mmol) with 1 M EtONa/EtOH (160 μ L) in EtOH/CHCl₃ (4 mL, 1:1). Purified by MPLC on silica gel (DCM/MeOH, 17:3). Yield: 9 mg (69%) as a white solid. $[\alpha]_D^{20} +105.0$ (c 0.60, MeOH); ¹H NMR (500 MHz, CD₃OD): $\delta = 8.07$ (d, $J = 8.5$ Hz, 2H, Ar-H), 7.73 (d, $J = 2.3$ Hz, 1H, Ar-H), 7.70 (d, $J = 8.5$

Hz, 2H, Ar-H), 7.59 (dd, $J = 2.3, 8.6$ Hz, 1H, Ar-H), 7.49 (d, $J = 8.7$ Hz, 1H, Ar-H), 5.61 (d, $J = 1.6$ Hz, 1H, H-1), 4.38 (q, $J = 7.1$ Hz, 2H, OCH₂), 4.12 (dd, $J = 1.8, 3.3$ Hz, 1H, H-2), 4.00 (dd, $J = 3.4, 9.5$ Hz, 1H, H-3), 3.80-3.71 (m, 3H, H-4, H-6a, H-6b), 3.65 (ddd, $J = 2.4, 5.4, 9.8$ Hz, 1H, H-5), 1.40 (t, $J = 7.1$ Hz, 3H, CH₃); ¹³C NMR (125 MHz, CD₃OD): $\delta = 167.86$ (CO), 153.35, 145.15, 136.26, 131.15, 130.50, 129.76, 127.79, 127.74, 125.38, 118.61 (12C, Ar-C), 100.73 (C-1), 76.02 (C-5), 72.40 (C-3), 71.84 (C-2), 68.22 (C-4), 62.66 (C-6), 62.19 (OCH₂), 14.61 (CH₃); HRMS: m/z : Calcd for C₂₁H₂₃ClNaO₈ [M+Na]⁺: 461.0979, found: 461.0972.

Propyl 3'-chloro-4'-(α -D-mannopyranosyloxy)biphenyl-4-carboxylate (3b). Prepared according to general procedure B from **11b** (22 mg, 0.035 mmol) with 1 M PrONa/PrOH (150 μ L) in PrOH/CHCl₃ (2 mL, 1:1). Purified by MPLC on silica gel (DCM/MeOH, 17:3). Yield: 9 mg (56%) as a white solid. $[\alpha]_D^{20} +90.0$ (c 0.90, MeOH); ¹H NMR (500 MHz, CD₃OD): $\delta = 8.08$ (d, $J = 8.5$ Hz, 2H, Ar-H), 7.74 (d, $J = 2.3$ Hz, 1H, Ar-H), 7.72 (d, $J = 8.5$ Hz, 2H, Ar-H), 7.59 (dd, $J = 2.3, 8.6$ Hz, 1H, Ar-H), 7.47 (d, $J = 8.7$ Hz, 1H, Ar-H), 5.61 (d, $J = 1.5$ Hz, 1H, H-1), 4.29 (t, $J = 6.6$ Hz, 2H, OCH₂), 4.12 (dd, $J = 1.8, 3.3$ Hz, 1H, H-2), 4.02 (dd, $J = 3.4, 9.5$ Hz, 1H, H-3), 3.81-3.71 (m, 3H, H-4, H-6a, H-6b), 3.65 (ddd, $J = 2.4, 5.5, 9.9$ Hz, 1H, H-5), 1.85-1.78 (m, 2H, CH₂), 1.06 (t, $J = 7.4$ Hz, 3H, CH₃); ¹³C NMR (125 MHz, CD₃OD): $\delta = 167.91$ (CO), 153.35, 145.16, 136.28, 131.14, 130.47, 129.76, 127.80, 127.76, 125.37, 118.61 (12C, Ar-C), 100.73 (C-1), 76.02 (C-5), 72.40 (C-3), 71.84 (C-2), 68.22 (C-4), 67.74 (OCH₂), 62.66 (C-6), 23.18 (CH₂), 10.80 (CH₃); HRMS: m/z : Calcd for C₂₂H₂₅ClNaO₈ [M+Na]⁺: 475.1136, found: 475.1131.

Butyl 3'-chloro-4'-(α -D-mannopyranosyloxy)biphenyl-4-carboxylate (3c). Prepared according to general procedure B from **11c** (33 mg, 0.052 mmol) with 1 M BuONa/BuOH (200 μ L) in BuOH/CHCl₃ (3 mL, 2:1). An additional portion of 1 M BuONa/BuOH (200 μ L) was added after 2 h. Purified by MPLC on silica gel (DCM/MeOH, 9:1). Yield: 9 mg (37%) as a white solid. $[\alpha]_D^{20} +78.5$ (c 0.95, MeOH); ¹H NMR (500 MHz, CD₃OD): $\delta = 8.07$ (d, $J = 8.5$ Hz, 2H, Ar-H), 7.74 (d, $J = 2.2$ Hz, 1H, Ar-H), 7.71 (d, $J = 8.5$ Hz, 2H, Ar-H), 7.60 (dd, $J = 2.3, 8.6$ Hz, 1H, Ar-H), 7.47 (d, $J = 8.7$ Hz, 1H, Ar-H), 5.61 (d, $J = 1.3$ Hz, 1H, H-1), 4.34 (t, $J = 6.5$ Hz, 2H, OCH₂), 4.12 (dd, $J = 1.8, 3.3$ Hz, 1H, H-2), 4.00 (dd, $J = 3.5, 9.5$ Hz, 1H, H-3), 3.80-3.71 (m, 3H, H-4, H-6a, H-6b), 3.65 (ddd, $J = 2.4, 5.5, 9.8$ Hz, 1H, H-5), 1.81-1.75 (m, 2H, CH₂), 1.55-1.48 (m, 2H, CH₂), 1.01 (t, $J = 7.4$ Hz, 3H, CH₃); ¹³C NMR (125

MHz, CD₃OD): δ = 167.91 (CO), 153.36, 145.17, 136.29, 131.15, 130.48, 129.77, 127.80, 127.76, 125.38, 118.61 (12C, Ar-C), 100.73 (C-1), 76.02 (C-5), 72.40 (C-3), 71.84 (C-2), 68.22 (C-4), 65.99 (OCH₂), 62.66 (C-6), 31.94, 20.33 (2 CH₂), 14.08 (CH₃); HRMS: m/z : Calcd for C₂₃H₂₇ClNaO₈ [M+Na]⁺: 489.1292, found: 489.1291.

Isopropyl 3'-chloro-4'-(α -D-mannopyranosyloxy)biphenyl-4-carboxylate (3d). Prepared according to general procedure B from **11d** (21 mg, 0.034 mmol) with 1 M *i*-PrONa/*i*-PrOH (200 μ L) in *i*-PrOH/CHCl₃ (1.5 mL, 2:1). An additional portion of 0.5 M *i*-PrONa/*i*-PrOH (500 μ L) was added after 6.5 h. Purified by MPLC on silica gel (DCM/MeOH, 9:1). Yield: 9.5 mg (62%) as a white solid. $[\alpha]_D^{20}$ +89.4 (*c* 0.90, MeOH); ¹H NMR (500 MHz, CD₃OD): δ = 8.06 (d, *J* = 8.5 Hz, 2H, Ar-H), 7.73 (d, *J* = 2.3 Hz, 1H, Ar-H), 7.70-7.69 (m, 2H, Ar-H), 7.61 (dd, *J* = 2.3, 8.7 Hz, 1H, Ar-H), 7.47 (d, *J* = 8.7 Hz, 1H, Ar-H), 5.61 (d, *J* = 1.6 Hz, 1H, H-1), 5.23 (hept, *J* = 6.3 Hz, 1H, OCH), 4.12 (dd, *J* = 1.8, 3.3 Hz, 1H, H-2), 4.00 (dd, *J* = 3.4, 9.5 Hz, 1H, H-3), 3.81-3.71 (m, 3H, H-4, H-6a, H-6b), 3.64 (ddd, *J* = 2.4, 5.4, 9.8 Hz, 1H, H-5), 1.38 (d, *J* = 6.3 Hz, 6H, CH(CH₃)₂); ¹³C NMR (125 MHz, CD₃OD): δ = 167.38 (CO), 153.34, 145.07, 136.31, 131.10, 130.85, 129.76, 127.78, 127.70, 125.37, 118.61 (12C, Ar-C), 100.73 (C-1), 76.02 (C-5), 72.40 (C-3), 71.84 (C-2), 69.87 (OCH), 68.22 (C-4), 62.66 (C-6), 22.14 (2C, CH(CH₃)₂); HRMS: m/z : Calcd for C₂₂H₂₅ClNaO₈ [M+Na]⁺: 475.1136, found: 475.1132.

***tert*-Butyl 3'-chloro-4'-(α -D-mannopyranosyloxy)biphenyl-4-carboxylate (3e).** Prepared according to general procedure B from **11e** (17 mg, 0.027 mmol) with *t*-BuOK (49 mg, 0.441 mmol, 16 eq) in *t*-BuOH/CHCl₃ (2 mL, 3:1). Purified by MPLC on silica gel (DCM/MeOH, 9:1). Yield: 8 mg (63%) as a colorless solid. $[\alpha]_D^{20}$ +82.4 (*c* 0.40, MeOH); ¹H NMR (500 MHz, CD₃OD): δ = 8.01 (d, *J* = 8.5 Hz, 2H, Ar-H), 7.73 (d, *J* = 2.2 Hz, 1H, Ar-H), 7.67 (d, *J* = 8.5 Hz, 2H, Ar-H), 7.59 (dd, *J* = 2.3, 8.6 Hz, 1H, Ar-H), 7.47 (d, *J* = 8.7 Hz, 1H, Ar-H), 5.61 (d, *J* = 1.3 Hz, 1H, H-1), 4.12 (dd, *J* = 1.8, 3.2 Hz, 1H, H-2), 4.00 (dd, *J* = 3.4, 9.5 Hz, 1H, H-3), 3.81-3.71 (m, 3H, H-4, H-6a, H-6b), 3.64 (ddd, *J* = 2.4, 5.4, 9.6 Hz, 1H, H-5), 1.61 (s, 9H, C(CH₃)₃); ¹³C NMR (125 MHz, CD₃OD): δ = 167.13 (CO), 153.29, 144.78, 136.39, 131.99, 131.02, 129.74, 127.76, 127.60, 125.36, 118.61 (12C, Ar-C), 100.74 (C-1), 82.35 (C(CH₃)₃), 76.01 (C-5), 72.40 (C-3), 71.84 (C-2), 68.22 (C-4), 62.66 (C-6), 28.43 (3C, C(CH₃)₃); HRMS: m/z : Calcd for C₂₃H₂₇ClNaO₈ [M+Na]⁺: 489.1292, found: 489.1286.

2-Methoxyethyl 3'-chloro-4'-(α -D-mannopyranosyloxy)biphenyl-4-carboxylate (3f).

Prepared according to general procedure B from **11f** (16 mg, 0.025 mmol) with *t*-BuOK (56 mg, 0.502 mmol, 20 eq) in *t*-BuOH/CHCl₃ (6 mL, 5:1). An additional portion of *t*-BuOH (3 mL) was added after 17 h and additional portions of *t*-BuOK were added after 17 h (40 eq) and 22 h (8 eq). Purified by MPLC on silica gel (DCM/MeOH, 9:1). Yield: 3 mg (25%) as a white wax. $[\alpha]_D^{20}$ +92.3 (*c* 0.30, MeOH); ¹H NMR (500 MHz, CD₃OD): δ = 8.10 (d, *J* = 8.5 Hz, 2H, Ar-H), 7.75 (d, *J* = 2.3 Hz, 1H, Ar-H), 7.72 (d, *J* = 8.5 Hz, 2H, Ar-H), 7.61 (dd, *J* = 2.3, 8.6 Hz, 1H, Ar-H), 7.48 (d, *J* = 8.7 Hz, 1H, Ar-H), 5.61 (d, *J* = 1.6 Hz, 1H, H-1), 4.48-4.46 (m, 2H, CH₂), 4.12 (dd, *J* = 1.8, 3.3 Hz, 1H, H-2), 4.00 (dd, *J* = 3.4, 9.5 Hz, 1H, H-3), 3.80-3.71 (m, 5H, CH₂, H-4, H-6a, H-6b), 3.64 (ddd, *J* = 2.3, 5.4, 9.7 Hz, 1H, H-5), 3.43 (s, 3H, OCH₃); ¹³C NMR (125 MHz, CD₃OD): δ = 167.75 (CO), 153.38, 145.30, 136.27, 131.29, 130.19, 129.78, 127.82, 127.77, 125.39, 118.62 (12C, Ar-C), 100.73 (C-1), 76.03 (C-5), 72.40 (C-3), 71.84 (C-2), 71.65 (CH₂), 68.22 (C-4), 65.17 (CH₂), 62.66 (C-6), 59.18 (OCH₃); HRMS: *m/z*: Calcd for C₂₂H₂₅ClNaO₉ [M+Na]⁺: 491.1085, found: 491.1080.

2-Ethoxyethyl 3'-chloro-4'-(α -D-mannopyranosyloxy)biphenyl-4-carboxylate (3g).

Prepared according to general procedure B from **11g** (12.5 mg, 0.019 mmol) with *t*-BuOK (51 mg, 0.432 mmol, 23 eq) in *t*-BuOH/CHCl₃ (6 mL, 5:1). An additional portion of *t*-BuOK (23 eq) was added after 19 h. Purified by MPLC on silica gel (DCM/MeOH, 9:1). Yield: 6 mg (67%) as a colorless solid. $[\alpha]_D^{20}$ +70.1 (*c* 0.55, MeOH); ¹H NMR (500 MHz, CD₃OD): δ = 8.11-8.09 (m, 2H, Ar-H), 7.74 (d, *J* = 2.3 Hz, 1H, Ar-H), 7.72-7.71 (m, 2H, Ar-H), 7.60 (dd, *J* = 2.3, 8.6 Hz, 1H, Ar-H), 7.47 (d, *J* = 8.7 Hz, 1H, Ar-H), 5.61 (d, *J* = 1.6 Hz, 1H, H-1), 4.47-4.45 (m, 2H, CH₂), 4.12 (dd, *J* = 1.8, 3.4 Hz, 1H, H-2), 4.00 (dd, *J* = 3.4, 9.5 Hz, 1H, H-3), 3.81-3.71 (m, 5H, H-4, H-6a, H-6b, CH₂), 3.65 (m, 1H, H-5), 3.61 (q, *J* = 7.0 Hz, 2H, OCH₂CH₃), 1.22 (t, *J* = 7.0 Hz, 3H, CH₃); ¹³C NMR (125 MHz, CD₃OD): δ = 167.77 (CO), 153.37, 145.27, 136.27, 131.28, 130.22, 129.78, 127.82, 127.76, 125.38, 118.61 (12C, Ar-C), 100.73 (C-1), 76.02 (C-5), 72.40 (C-3), 71.84 (C-2), 69.56 (CH₂), 68.22 (C-4), 67.67 (OCH₂CH₃), 65.40 (CH₂), 62.22 (C-6), 15.44 (CH₃); ESI-MS: *m/z*: Calcd for C₂₃H₂₇ClNaO₉ [M+Na]⁺: 505.1241, found: 505.1234.

2-Isopropoxyethyl 3'-chloro-4'-(α -D-mannopyranosyloxy)biphenyl-4-carboxylate (3h).

Prepared according to general procedure B from **11h** (48 mg, 0.072 mmol) with *t*-BuOK (42 mg, 0.361 mmol, 5.0 eq) in *t*-BuOH/CHCl₃ (5.5 mL, 10:1). Additional portions of *t*-BuOK

were added every 30 min (5.0 eq, 5.0 eq and 1.0 eq). Purified by MPLC on silica gel (DCM/MeOH, 9:1). Yield: 24 mg (67%) as a white solid. $[\alpha]_D^{20} +74.6$ (*c* 0.30, MeOH); ^1H NMR (500 MHz, CD_3OD): δ = 8.09 (d, *J* = 8.5 Hz, 2H, Ar-H), 7.74 (d, *J* = 2.2 Hz, 1H, Ar-H), 7.71 (d, *J* = 8.5 Hz, 2H, Ar-H), 7.60 (dd, *J* = 2.3, 8.6 Hz, 1H, Ar-H), 7.47 (d, *J* = 8.7 Hz, 1H, Ar-H), 5.61 (d, *J* = 1.4 Hz, 1H, H-1), 4.45-4.43 (m, 2H, CH_2), 4.12 (dd, *J* = 1.8, 3.2 Hz, 1H, H-2), 4.00 (dd, *J* = 3.4, 9.5 Hz, 1H, H-3), 3.81-3.69 (m, 6H, CH_2 , H-4, H-6a, H-6b, OCH), 3.65 (ddd, *J* = 2.3, 5.4, 9.7 Hz, 1H, H-5), 1.08 (d, *J* = 6.1 Hz, 6H, $\text{CH}(\text{CH}_3)_2$); ^{13}C NMR (125 MHz, CD_3OD): δ = 167.79 (CO), 153.37, 145.26, 136.26, 131.26, 130.62, 129.77, 127.81, 127.76, 125.38, 118.61 (12C, Ar-C), 100.73 (C-1), 76.02 (C-5), 73.45 (OCH), 72.40 (C-3), 71.83 (C-2), 68.21 (C-4), 67.22 (CH_2), 65.70 (CH_2), 62.66 (C-6), 22.38 (2C, $\text{CH}(\text{CH}_3)_2$); HRMS: *m/z*: Calcd for $\text{C}_{24}\text{H}_{29}\text{ClNaO}_9$ $[\text{M}+\text{Na}]^+$: 519.1398, found: 519.1395.

2-(2-Ethoxyethoxy)ethyl 3'-chloro-4'-(α -D-mannopyranosyloxy)biphenyl-4-carboxylate (3i). Prepared according to general procedure B from **11i** (14 mg, 0.020 mmol) with *t*-BuOK (4 mg, 0.034 mmol, 1.7 eq) in *t*-BuOH (2 mL). An additional portion of *t*-BuOK (1.7 eq) was added after 2.5 h. Purified by MPLC on silica gel (DCM/MeOH, 9:1). Yield: 4.2 mg (40%) as a white wax. $[\alpha]_D^{20} +76.4$ (*c* 0.40, MeOH); ^1H NMR (500 MHz, CD_3OD): δ = 8.11-8.09 (m, 2H, Ar-H), 7.74 (d, *J* = 2.3 Hz, 1H, Ar-H), 7.72-7.70 (m, 2H, Ar-H), 7.60 (dd, *J* = 2.3, 8.6 Hz, 1H, Ar-H), 7.48 (d, *J* = 8.7 Hz, 1H, Ar-H), 5.61 (d, *J* = 1.7, 1H, H-1), 4.49-4.46 (m, 2H, CH_2), 4.12 (dd, *J* = 1.8, 3.4 Hz, 1H, H-2), 4.00 (dd, *J* = 3.4, 9.5 Hz, 1H, H-3), 3.86-3.84 (m, 2H, CH_2), 3.80-3.69 (m, 5H, H-6a, H-6b, H-4, OCH₂), 3.65 (ddd, *J* = 2.4, 5.4, 9.8 Hz, 1H, H-5), 3.62-3.60 (m, 2H, CH_2), 3.53 (q, *J* = 7.0 Hz, 2H, OCH₂CH₃), 1.17 (t, *J* = 7.0 Hz, 3H, CH₃); ^{13}C NMR (125 MHz, CD_3OD): δ = 167.76 (CO), 153.37, 145.27, 136.26, 131.30, 130.24, 129.77, 127.81, 127.75, 125.38, 118.61 (12C, Ar-C), 100.73 (C-1), 76.02 (C-5), 72.40 (C-3), 71.84 (C-2), 71.68, 70.92, 70.22 (3C, CH_2), 68.22 (C-4), 67.62 (CH_2), 65.35 (OCH₂CH₃), 62.66 (C-6), 15.41 (CH₃); HRMS: *m/z*: Calcd for $\text{C}_{25}\text{H}_{31}\text{ClNaO}_{10}$ $[\text{M}+\text{Na}]^+$: 549.1503, found: 549.1498.

2-Hydroxyethyl 3'-chloro-4'-(α -D-mannopyranosyloxy)biphenyl-4-carboxylate (3k). Prepared according to general procedure B from **11j** (36 mg, 0.054 mmol) with *t*-BuOK (32 mg, 0.271 mmol, 5.0 eq) in *t*-BuOH/ CHCl_3 (5.5 mL, 10:1). Additional portions of *t*-BuOK (10 eq) were added after 2 h and 24 h. Purified by MPLC on silica gel (DCM/MeOH, 9:1). Yield: 8 mg (32%) as a white wax. $[\alpha]_D^{20} +79.5$ (*c* 0.65, MeOH); ^1H NMR (500 MHz,

CD₃OD): δ = 8.13 (d, J = 8.5 Hz, 2H, Ar-H), 7.74 (d, J = 2.3 Hz, 1H, Ar-H), 7.71 (d, J = 8.5 Hz, 2H, Ar-H), 7.60 (dd, J = 2.3, 8.6 Hz, 1H, Ar-H), 7.47 (d, J = 8.7 Hz, 1H, Ar-H), 5.61 (d, J = 1.6 Hz, 1H, H-1), 4.41-4.39 (m, 2H, CH₂), 4.12 (dd, J = 1.8, 3.3 Hz, 1H, H-2), 4.00 (dd, J = 3.4, 9.5 Hz, 1H, H-3), 3.89-3.87 (m, 2H, CH₂), 3.80-3.71 (m, 3H, H-4, H-6a, H-6b), 3.65 (ddd, J = 2.4, 5.4, 9.7 Hz, 1H, H-5); ¹³C NMR (125 MHz, CD₃OD): δ = 167.93 (CO), 153.36, 145.23, 136.29, 131.35, 130.29, 129.77, 127.80, 127.72, 125.38, 118.62 (12C, Ar-C), 100.73 (C-1), 76.02 (C-5), 72.40 (C-3), 71.83 (C-2), 68.22 (C-4), 67.63 (CH₂), 62.66 (C-6), 61.16 (CH₂); HRMS: m/z : Calcd for C₂₁H₂₃ClNaO₉ [M+Na]⁺: 477.0928, found: 477.0921.

2-(Dimethylamino)ethyl 3'-chloro-4'-(α -D-mannopyranosyloxy)biphenyl-4-carboxylate (3l). Prepared according to general procedure C from **1** (19 mg, 0.044 mmol) and 2-(dimethylamino)ethanol (13 μ L, 0.132 mmol, 3.0 eq) with DIPEA (23 μ L, 0.132 mmol, 3.0 eq) and COMU (39 mg, 0.088 mmol, 2.0 eq) in DMF (2 mL). Purified by preparative LC-MS (RP-18, H₂O/MeCN, 19:1-3:7, + 0.2% HCOOH). Yield: 8.2 mg (39%) as a white solid. $[\alpha]_D^{20}$ +62.7 (c 0.75, MeOH); ¹H NMR (500 MHz, CD₃OD): δ = 8.15 (d, J = 8.4 Hz, 2H, Ar-H), 7.75-7.73 (m, 3H, Ar-H), 7.60 (dd, J = 2.2, 8.6 Hz, 1H, Ar-H), 7.48 (d, J = 8.7 Hz, 1H, Ar-H), 5.61 (d, J = 1.5 Hz, 1H, H-1), 4.69-4.67 (m, 2H, CH₂), 4.11 (dd, J = 1.8, 3.3 Hz, 1H, H-2), 4.00 (dd, J = 3.4, 9.5 Hz, 1H, H-3), 3.80-3.71 (m, 3H, H-4, H-6a, H-6b), 3.64 (ddd, J = 2.4, 5.5, 9.7 Hz, 1H, H-5), 3.57-3.55 (m, 2H, CH₂), 2.97 (s, 6H, N(CH₃)₂); ¹³C NMR (125 MHz, CD₃OD): δ = 167.18 (CO), 153.46, 145.69, 136.03, 131.54, 129.77, 129.38, 127.83, 125.41, 118.61 (12C, Ar-C), 100.69 (C-1), 76.03 (C-5), 72.39 (C-3), 71.82 (C-2), 68.21 (C-4), 62.66 (C-6), 60.42, 57.65 (2 CH₂), 44.16 (2C, N(CH₃)₂); HRMS: m/z : Calcd for C₂₃H₂₉ClNO₈ [M+H]⁺: 482.1582, found: 482.1578.

2-Piperidinoethyl 3'-chloro-4'-(α -D-mannopyranosyloxy)biphenyl-4-carboxylate (3m). Prepared according to general procedure C from **1** (46 mg, 0.112 mmol) and 1-(2-hydroxyethyl)piperidine (59 μ L, 0.448 mmol, 4.0 eq) with DIPEA (58 μ L, 0.336 mmol, 3.0 eq) and COMU (99 mg, 0.224 mmol, 2.0 eq) in DMF (4 mL). Purified by preparative LC-MS (RP-18, H₂O/MeCN, 19:1-1:19, + 0.2% HCOOH). Yield: 7.8 mg (13%) as a yellowish solid. $[\alpha]_D^{20}$ +64.3 (c 0.25, MeOH); ¹H NMR (500 MHz, CD₃OD): δ = 8.12 (d, J = 8.4 Hz, 2H, Ar-H), 7.75-7.73 (m, 3H, Ar-H), 7.61 (dd, J = 2.2, 8.6 Hz, 1H, Ar-H), 7.48 (d, J = 8.7 Hz, 1H, Ar-H), 5.62 (d, J = 1.4 Hz, 1H, H-1), 4.62-4.60 (m, 2H, CH₂), 4.12 (dd, J = 1.8, 3.2 Hz, 1H, H-2), 4.00 (dd, J = 3.4, 9.5 Hz, 1H, H-3), 3.81-3.71 (m, 3H, H-4, H-6a, H-6b), 3.64 (ddd, J =

2.4, 5.5, 9.6 Hz, 1H, H-5), 3.23 (m, 2H, CH₂N), 3.02 (br s, 4H, 2 NCH₂), 1.81-1.76 (m, 4H, 2 CH₂), 1.62-1.60 (m, 2H, (CH₂)₂CH₂); ¹³C NMR (125 MHz, CD₃OD): δ = 167.23 (CO), 153.47, 145.69, 136.03, 131.49, 129.78, 129.44, 127.86, 127.83, 125.42, 118.62 (12C, Ar-C), 100.70 (C-1), 76.04 (C-5), 72.40 (C-3), 71.82 (C-2), 68.22 (C-4), 62.67 (C-6), 60.19 (CH₂), 57.01 (CH₂N), 54.93 (2 NCH₂), 24.31 (2C, 2 CH₂), 22.65 ((CH₂)₂CH₂); HRMS: m/z : Calcd for C₂₆H₃₃ClNO₈ [M+H]⁺: 522.1895, found: 522.1889.

2-Morpholinoethyl 3'-chloro-4'-(α -D-mannopyranosyloxy)biphenyl-4-carboxylate (3n).

Prepared according to general procedure C from **1** (20 mg, 0.049 mmol) and 4-(2-hydroxyethyl)morpholine (18 μ L, 0.147 mmol, 3.0 eq) with DIPEA (25 μ L, 0.146 mmol, 3.0 eq) and COMU (42 mg, 0.095 mmol, 2.0 eq) in DMF (2 mL). The major impurities were removed by MPLC on silica gel (DCM/MeOH, 8:2) followed by purification by preparative LC-MS (RP-18, H₂O/MeCN, 19:1-1:19, + 0.2% HCOOH). Yield: 3.2 mg (13%) as a yellowish solid. $[\alpha]_D^{20}$ +72.5 (c 0.35, MeOH); ¹H NMR (500 MHz, CD₃OD): δ = 8.12 (d, J = 8.4 Hz, 2H, Ar-H), 7.75-7.72 (m, 3H, Ar-H), 7.61 (dd, J = 2.2, 8.6 Hz, 1H, Ar-H), 7.48 (d, J = 8.7 Hz, 1H, Ar-H), 5.61 (d, J = 1.4 Hz, 1H, H-1), 4.59-4.57 (m, 2H, OCH₂), 4.12 (dd, J = 1.8, 3.3 Hz, 1H, H-2), 4.00 (dd, J = 3.4, 9.5 Hz, 1H, H-3), 3.81-3.71 (m, 7H, 2 CH₂O, H-4, H-6a, H-6b), 3.64 (ddd, J = 2.3, 5.4, 9.6 Hz, 1H, H-5), 3.13-3.11 (m, 2H, CH₂N), 2.92 (m, 4H, 2 NCH₂); ¹³C NMR (125 MHz, CD₃OD): δ = 167.53 (CO), 153.43, 145.47, 136.17, 131.37, 129.93, 129.78, 127.81, 125.41, 118.62 (12C, Ar-C), 100.72 (C-1), 76.04 (C-5), 72.40 (C-3), 71.83 (C-2), 68.22 (C-4), 66.78 (2C, 2 CH₂O), 62.67 (C-6), 61.95 (OCH₂), 57.94 (CH₂N), 54.55 (2C, 2 NCH₂); HRMS: m/z : Calcd for C₂₅H₃₁ClNO₉ [M+H]⁺: 524.1687, found: 524.1684.

2-(Dimethylamino)ethyl 3'-trifluoromethyl-4'-(α -D-mannopyranosyloxy)-biphenyl-4-carboxylate (5l).

Prepared according to general procedure C from **4**^[21] (60 mg, 0.135 mmol) and 2-(dimethylamino)ethanol (82 μ L, 0.810 mmol, 6.0 eq) with DIPEA (69 μ L, 0.405 mmol, 3.0 eq) and COMU (119 mg, 0.270 mmol, 2.0 eq) in DMF (4 mL). Purified by preparative LC-MS (RP-18, H₂O/MeCN, 19:1-1:19, + 0.2% HCOOH). Yield: 37 mg (53%) as a white solid. $[\alpha]_D^{20}$ +80.9 (c 1.00, MeOH); ¹H NMR (500 MHz, CD₃OD): δ = 8.17 (d, J = 8.4 Hz, 2H, Ar-H), 7.91-7.89 (m, 2H, Ar-H), 7.76 (d, J = 8.4 Hz, 2H, Ar-H), 7.61 (d, J = 8.4 Hz, 1H, Ar-H), 5.66 (d, J = 1.2 Hz, 1H, H-1), 4.66-4.64 (m, 2H, OCH₂), 4.06 (dd, J = 1.8, 3.3 Hz, 1H, H-2), 3.94 (dd, J = 3.4, 9.5 Hz, 1H, H-3), 3.81-3.71 (m, 3H, H-4, H-6a, H-6b), 3.58

(ddd, $J = 2.3, 5.6, 9.6$ Hz, 1H, H-5), 3.45-3.43 (m, 2H, CH₂N), 2.87 (s, 6H, N(CH₃)₂); ¹³C NMR (125 MHz, CD₃OD): $\delta = 167.23$ (CO), 155.61, 145.55, 134.59, 133.46, 131.58, 129.67, 127.89, 126.46, 126.41, 126.07, 123.90, 121.00, 120.76, 120.51, 117.83 (13C, Ar-C, CF₃), 100.27 (C-1), 76.13 (C-5), 72.24 (C-3), 71.73 (C-2), 68.11 (C-4), 62.68 (C-6), 60.95 (OCH₂), 57.79 (CH₂N), 44.41 (2C, N(CH₃)₂); HRMS: m/z : Calcd for C₂₄H₂₉F₃NO₈ [M+H]⁺: 516.1845, found: 516.1840.

Physicochemical and in vitro pharmacokinetic studies

Materials: Dimethyl sulfoxide (DMSO), 1-propanol, 1-octanol, Dulbecco's Modified Eagle's Medium (DMEM) high glucose, Penicillin-Streptomycin (solution stabilized, with 10'000 units Penicillin and 10 mg Streptomycin/mL), L-glutamine solution (200 mM), magnesium chloride, bis(4-nitrophenyl) phosphate (BNPP), Loperamide hydrochloride, and Neostigmine bromide were purchased from Sigma-Aldrich (St. Louis, MI, USA). PRISMA HT universal buffer, GIT-0 Lipid Solution, and Acceptor Sink Buffer were ordered from pIon (Woburn, MA, USA). MEM non-essential amino acids solution 10 mM (100X), fetal bovine serum (FBS), and DMEM without sodium pyruvate and phenol red were bought from Invitrogen (Carlsbad, CA, USA). Acetonitrile (MeCN) and methanol (MeOH) were ordered from Acros Organics (Geel, Belgium). Human plasma was purchased from Biopredic (Rennes, France). Pooled male rat liver microsomes (Sprague Dawley), and pooled human liver microsomes were ordered from BD Bioscience (Woburn, MA, USA). The Caco-2 cells were kindly provided by Prof G. Imanidis, FHNW, Muttentz, Switzerland and originated from the American Type Culture Collection (Rockville, MD, USA).

Aqueous solubility. Solubility was determined in a 96-well format using the μ SOL Explorer solubility analyzer (pIon, version 3.4.0.5). For each compound, measurements were performed at two pH values (3.0, 7.4) in triplicate. Six wells of a deep well plate, i.e. three wells per pH value, were filled with 300 μ L of PRISMA HT universal buffer adjusted to pH 3.0 or 7.4 by adding the requested amount of NaOH (0.5 M). Aliquots (3 μ L) of a compound stock solution (40-100 mM in DMSO) were added and thoroughly mixed. The final sample concentration was 0.4-1.0 mM, the residual DMSO concentration was 1.0% (v/v) in the buffer solutions. After 15 h, the solutions were filtrated (0.2 μ m 96-well filter plates) using a vacuum to collect manifold (Whatman Ltd., Maidstone, UK) to remove any

precipitates. Equal amounts of filtrate and 1-propanol were mixed and transferred to a 96-well plate for UV/Vis detection (190 to 500 nm, SpectraMax 190, Molecular Devices, Silicon Valley, CA, USA). The amount of material dissolved was calculated by comparison with UV/Vis spectra obtained from reference samples, which were prepared by dissolving compound stock solution in a 1:1 mixture of buffer and 1-propanol (final concentrations 0.067-0.167 mM).

log $D_{7.4}$ determination. The in silico prediction tool ALOGPS^[58] was used to estimate the log P values of the compounds. Depending on these values, the compounds were classified into three categories: hydrophilic compounds (log P below zero), moderately lipophilic compounds (log P between zero and one) and lipophilic compounds (log P above one). For each category, two different ratios (volume of 1-octanol to volume of buffer) were defined as experimental parameters (Table 3).

Table 3. Compound classification based on estimated log P values.

compound type	log P	ratios (1-octanol: buffer)
hydrophilic	< 0	30:140, 40:130
moderately lipophilic	0 - 1	70:110, 110:70
lipophilic	> 1	3:180, 4:180

Equal amounts of phosphate buffer (0.1 M, pH 7.4) and 1-octanol were mixed and shaken vigorously for 5 min to saturate the phases. The mixture was left until separation of the two phases occurred, and the buffer was retrieved. Stock solutions of the test compounds were diluted with buffer to a concentration of 1 μ M. For each compound, six determinations, *i.e.* three determinations per 1-octanol:buffer ratio, were performed in different wells of a 96-well plate. The respective volumes of buffer containing analyte (1 μ M) were pipetted to the wells and covered by saturated 1-octanol according to the chosen volume ratio. The plate was sealed with aluminium foil, shaken (1350 rpm, 25 °C, 2 h) on a Heidolph Titramax 1000 plate-shaker (Heidolph Instruments GmbH & Co. KG, Schwabach, Germany) and centrifuged (2000 rpm, 25 °C, 5 min, 5804 R Eppendorf centrifuge, Hamburg, Germany). The aqueous phase was transferred to a 96-well plate for analysis by liquid chromatography-mass spectrometry (LC-MS, see below).

The $\log D_{7.4}$ coefficients were calculated from the 1-octanol:buffer ratio (o:b), the initial concentration of the analyte in buffer (1 μ M), and the concentration of the analyte in buffer (c_B) with Equation 1:

$$\log D_{7.4} = \log \left(\frac{1\mu M - c_B}{c_B} \times \frac{1}{o:b} \right) \quad (\text{eq. 1})$$

The average of the three $\log D_{7.4}$ values per 1-octanol:buffer ratio was calculated. If the two means obtained for a compound did not differ by more than 0.1 units, the results were accepted.

Parallel artificial membrane permeability assay (PAMPA). Effective permeability ($\log P_e$) was determined in a 96-well format with the PAMPA.^[38] For each compound, measurements were performed at two pH values (5.0, 7.4) in quadruplicate. Eight wells of a deep well plate, i.e. four wells per pH-value, were filled with 650 μ L of PRISMA HT universal buffer adjusted to pH 5.0 or 7.4 by adding the requested amount of NaOH (0.5 M). Samples (150 μ L) were withdrawn from each well to determine the blank spectra by UV-spectroscopy (190 to 500 nm, SpectraMax 190). Then, analyte dissolved in DMSO (10 mM) was added to the remaining buffer to yield 50 μ M solutions. To exclude precipitation, the optical density was measured at 650 nm, with 0.01 being the threshold value. Solutions exceeding this threshold were filtrated. Afterwards, samples (150 μ L) were withdrawn to determine the reference spectra. Further 200 μ L was transferred to each well of the donor plate of the PAMPA sandwich (pIon, P/N 110 163). The filter membranes at the bottom of the acceptor plate were infused with 5 μ L of GIT-0 Lipid Solution and 200 μ L of Acceptor Sink Buffer was filled into each acceptor well. The sandwich was assembled, placed in the GutBoxTM, and left undisturbed for 16 h. Then, it was disassembled and samples (150 μ L) were transferred from each donor and acceptor well to UV-plates. Quantification was done by UV/Vis-spectroscopy. Effective permeability ($\log P_e$) was calculated from the compound flux deduced from the UV/Vis spectra, the filter area, and the initial sample concentration in the donor well with the aid of the PAMPA Explorer Software (pIon, version 3.5).

Colorectal adenocarcinoma (Caco-2) cell permeation assay. Caco-2 cells were cultivated in tissue culture flasks (BD Biosciences, Franklin Lakes, NJ, USA) with DMEM high glucose medium, containing L-glutamine (2 mM), nonessential amino acids (0.1 mM),

Penicillin (100 U/mL), Streptomycin (100 µg/mL), and fetal bovine serum (10%). The cells were kept at 37 °C in humidified air containing 5% CO₂, and the medium was changed every second day. When approximately 90% confluence was reached, the cells were split in a 1:10 ratio and distributed to new tissue culture flasks. At passage numbers between 60 and 65, they were seeded at a density of 5.3 x 10⁵ cells per well to Transwell 6-well plates (Corning Inc., Corning, NY, USA) with 2.5 mL of culture medium in the basolateral and 2 mL in the apical compartment. The medium was renewed on alternate days. Permeation experiments were performed between days 19 and 21 post seeding. Previously to the experiment, the integrity of the Caco-2 monolayers was evaluated by measuring the transepithelial electrical resistance (TEER) with an Endohm tissue resistance instrument (World Precision Instruments Inc., Sarasota, FL, USA). Only wells with TEER values higher than 250 Ω cm² were used. To inhibit carboxylesterase activity, the Caco-2 cell monolayers were pre-incubated with bis(4-nitrophenyl) phosphate (BNPP, 200 µM) dissolved in transport medium (DMEM without sodium pyruvate and phenol red) for 40 min.^[59] Experiments were performed in the apical-to-basolateral (absorptive) and basolateral-to-apical (secretory) directions in triplicate. Transport medium was withdrawn from the donor compartments of three wells and replaced by the same volume of compound stock solutions (in DMSO) to reach an initial sample concentration of 62.5 µM, 100 µM, 200 µM, 400 µM, or 825 µM. The Transwell plate was shaken (600 rpm, 37 °C) on a Heidolph Titramax 1000 plate-shaker. Samples (40 µL) were withdrawn from the donor and acceptor compartments 30 min after initiation of the experiment and the concentrations were determined by LC-MS (see below). Apparent permeability (P_{app}) was calculated according to Equation 2:

$$P_{app} = \frac{dQ}{dt} \times \frac{1}{A \times c_0} \quad (\text{eq. 2})$$

where dQ/dt is the compound flux (mol s⁻¹), A the surface area of the monolayer (cm²), and c_0 the initial concentration in the donor compartment (mol cm⁻³).^[44] After the experiment, TEER values were assessed again for each well and results from wells with values below 250 Ω cm² were discarded.

In vitro metabolism: microsomal stability

Metabolic stability study. Incubations were performed in triplicate in a 96-well format on an Eppendorf Thermomixer Comfort. The reaction mixture (270 µL) consisting of liver

microsomes (0.139 $\mu\text{g/mL}$), TRIS-HCl buffer (0.1 M, pH 7.4) and MgCl_2 (2 mM) was preheated (37 $^{\circ}\text{C}$, 500 rpm, 10 min), and the incubation was initiated by adding 30 μL of compound solution (20 μM) in TRIS-HCl buffer. The final concentration of the compound was 2 μM , and the microsomal concentration was 0.125 mg/mL. At the beginning of the experiment ($t = 0$ min) and after an incubation time of 5, 10, 20, 40, and 60 min, samples (40 μL) were transferred to 120 μL of ice-cooled MeCN or MeOH and centrifuged (3600 rpm, 4 $^{\circ}\text{C}$, 10 min). Then, 80 μL of supernatant was transferred to a 96-well plate for LC-MS analysis (see below). The metabolic half-life ($t_{1/2}$) was calculated from the slope of the linear regression from the log percentage remaining compound versus incubation time relationship. Control experiments were performed in parallel by preincubating the microsomes with the specific carboxylesterase inhibitor BNPP (1 mM) for 5 min before addition of the compound solution.^[40]

Inhibition study. Test compounds were dissolved in DMSO to 1 mM and then diluted with TRIS-HCl buffer (0.1 M, pH 7.4) containing MgCl_2 (2 mM) to a concentration of 6 μM . Loperamide hydrochloride was dissolved in DMSO to 20 mM, 2 mM, and 0.2 mM and then diluted with TRIS-HCl buffer containing MgCl_2 to a concentration of 750 μM , 75 μM , and 7.5 μM . Human liver microsomes were suspended in TRIS-HCl buffer containing MgCl_2 to a concentration of 30 $\mu\text{g/mL}$. Compound solution (100 μL) and microsome suspension (200 μL) mixed with Loperamide solution or blank buffer (50 μL) were preheated (37 $^{\circ}\text{C}$, 500 rpm, 15 min) in separate wells of a 96-well plate. The incubation was initiated by transferring 200 μL of microsome suspension containing Loperamide to the compound solution. The final compound concentration was 2 μM , the microsomal concentration was 20 $\mu\text{g/mL}$, and the Loperamide concentration was 100 μM , 10 μM , 1 μM , and 0 μM (blank). At the beginning of the experiment ($t = 0$ min) and after an incubation time of 10, 20, 30, 45, and 60 min, samples (20 μL) were transferred to 60 μL of ice-cooled MeOH and analysed by LC-MS (see below). The metabolic turnover was assessed as accumulation of product **1** versus incubation time.

In vitro metabolism: plasma stability

Metabolic stability study. Incubations were performed in triplicates in a 96-well format according to the procedure described by Di et al.^[60] Human plasma was centrifuged (4 $^{\circ}\text{C}$, 3000 rpm, 10 min) to remove particulates before use. Compounds were dissolved in DMSO

to 80 μM and then diluted with phosphate buffer (0.1 M, pH 7.4) to a concentration of 8 μM . Plasma (156 μL) was mixed with phosphate buffer (84 μL) and preheated (37 $^{\circ}\text{C}$, 500 rpm, 10 min). The incubation was initiated by adding 80 μL of compound solution. The final compound concentration was 2 μM and the plasma concentration was 50% in buffer pH 7.4. At the beginning of the experiment ($t = 0$ min) and after an incubation time of 15, 30, 60, and 120 min, samples (50 μL) were transferred to 150 μL of ice-cooled MeOH, frozen (-20 $^{\circ}\text{C}$, 10 min) and centrifuged (3600 rpm, 4 $^{\circ}\text{C}$, 10 min). The supernatant (80 μL) was transferred to a 96-well plate for LC-MS analysis (see below). The metabolic half-life ($t_{1/2}$) was calculated from the slope of the linear regression from the log percentage remaining compound versus incubation time relationship. To monitor non-enzymatic compound degradation, incubations in absence of human plasma were run in parallel.

Inhibition study. Human plasma and test compound were processed as described above. Neostigmine bromide was dissolved in DMSO to 10 mM, 3 mM, 1 mM, 0.3 mM, 0.1 mM, 0.03 mM, and 0.01 mM and then diluted with phosphate buffer (0.1 M, pH 7.4) to a concentration of 80 μM , 24 μM , 8 μM , 2.4 μM , 0.8 μM , 0.24 μM , and 0.08 μM . Human plasma (156 μL) mixed with phosphate buffer (44 μL) was preheated (37 $^{\circ}\text{C}$, 500 rpm, 10 min). Then, Neostigmine bromide solution or blank buffer (40 μL) was added for preincubation (37 $^{\circ}\text{C}$, 500 rpm, 5 min). The incubation was initiated by adding 80 μL of compound solution. The final compound concentration was 2 μM , the plasma concentration was 50% in buffer pH 7.4, and the Neostigmine bromide concentration was 10 μM , 3 μM , 1 μM , 0.3 μM , 0.1 μM , 0.03 μM , 0.01 μM , and 0 μM (blank). At the beginning of the experiment ($t = 0$ min) and after an incubation time of 5, 10, 30, and 60 min, samples (50 μL) were transferred to 150 μL of ice-cooled MeOH, frozen (-20 $^{\circ}\text{C}$, 10 min), and centrifuged (3600 rpm, 4 $^{\circ}\text{C}$, 10 min). The supernatant (80 μL) was transferred to a 96-well plate for LC-MS analysis (see below). Metabolic activity was calculated from the slope of the linear regression from the log percentage remaining compound versus incubation time relationship.

LC-MS measurements. Analyses were performed using a 1100/1200 Series HPLC System coupled to a 6410 Triple Quadrupole mass detector (Agilent Technologies, Inc., Santa Clara, CA, USA) equipped with electrospray ionization. The system was controlled with the Agilent MassHunter Workstation Data Acquisition software (version B.01.04). The column used was an Atlantis[®] T3 C18 column (2.1 x 50 m) with a 3- μm particle size (Waters Corp., Milford, MA, USA). The mobile phase consisted of eluent A: H₂O containing 0.1% formic acid (for **1**,

3f-i, **3l-n**, **4**, and **5l**), or 10 mM ammonium acetate, pH 5.0 in 95:5 H₂O:MeCN (for **2**, **3a-e**, **3k**); and eluent B: MeCN containing 0.1% formic acid. The flow rate was maintained at 0.6 mL/min. The gradient was ramped from 95% A/5% B to 5% A/95% B over 1 min, and then hold at 5% A/95% B for 0.1 min. The system was then brought back to 95% A/5% B, resulting in a total duration of 4 min. MS parameters such as fragmentor voltage, collision energy, polarity were optimized individually for each drug, and the molecular ion was followed for each compound in the multiple reaction monitoring mode. The concentrations of the analytes were quantified by the Agilent Mass Hunter Quantitative Analysis software (version B.01.04).

Supporting Information

NMR spectra and HPLC traces to document purity of the test compounds.

Acknowledgement

The authors gratefully acknowledge the financial support by the Swiss National Science Foundation (grant no. xy).

References

- [1] Hooton, T. M.; Besser, R.; Foxman, B.; Fritsche, T. R.; Nicolle, L. E. Acute uncomplicated cystitis in an era of increasing antibiotic resistance: a proposed approach to empirical therapy. *Clin. Infect. Dis.* **2004**, *39*, 75-80.
- [2] Fihn, S. D. Acute Uncomplicated Urinary Tract Infection in Women. *N. Engl. J. Med.* **2003**, *349*, 259-266.
- [3] Sanchez, G. V.; Master, R. N.; Karlowsky, J. A.; Bordon, J. M. In vitro antimicrobial resistance of urinary Escherichia coli isolates among U.S. outpatients from 2000 to 2010. *Antimicrob. Agents Chemother.* **2012**, *56*, 2181-2183.
- [4] Sharon, N. Carbohydrates as future anti-adhesion drugs for infectious diseases. *Biochim. Biophys. Acta.* **2006**, *1760*, 527-537.
- [5] Westerlund-Wikström, B.; Korhonen, T.K. Molecular structure of adhesin domains in Escherichia coli fimbriae. *Int. J. Med. Microbiol.* **2005**, *295*, 479–486.

-
- [6] Wiles, T. J.; Kulesus, R. R.; Mulvey, M. A. Origins and virulence mechanisms of uropathogenic *Escherichia coli*. *Exp. Mol. Pathol.* **2008**, *85*, 11-19.
- [7] Schilling, J. D.; Mulvey, M. A.; Hultgren, S. J. Structure and function of *Escherichia coli* type 1 pili: new insight into the pathogenesis of urinary tract infections. *J. Infect. Dis.* **2001**, *183* (Suppl 1), S36-S40.
- [8] Capitani, G.; Eidam, O.; Glockshuber, R.; Grütter, M. G. Structural and functional insights into the assembly of type 1 pili from *Escherichia coli*. *Microbes Infect.* **2006**, *8*, 2284-2290.
- [9] Firon, N.; Ofek, I.; Sharon, N. Interaction of mannose-containing oligosaccharides with the fimbrial lectin of *Escherichia coli*. *Biochem. Biophys. Res. Commun.* **1982**, *105*, 1426-1432.
- [10] Firon, N.; Ofek, I.; Sharon, N. Carbohydrate specificity of the surface lectins of *Escherichia coli*, *Klebsiella pneumoniae*, and *Salmonella typhimurium*. *Carbohydr. Res.* **1983**, *120*, 235-249.
- [11] Firon, N.; Ashkenazi, S.; Mirelman, D.; Ofek, I.; Sharon, N. Aromatic alpha-glycosides of mannose are powerful inhibitors of the adherence of type 1 fimbriated *Escherichia coli* to yeast and intestinal epithelial cells. *Infect. Immun.* **1987**, *55*, 472-476.
- [12] Pieters, R. J. Maximising multivalency effects in protein-carbohydrate interactions. *Org. Biomol. Chem.* **2009**, *7*, 2013-2025.
- [13] Imberty, A.; Chabre, Y. M.; Roy, R. Glycomimetics and glycodendrimers as high affinity microbial anti-adhesins. *Chem. Eur. J.* **2008**, *14*, 7490-7499.
- [14] Hartmann, M.; Lindhorst, T. K. The bacterial lectin FimH, a target for drug discovery – carbohydrate inhibitors of type 1 fimbriae-mediated bacterial adhesion. *Eur. J. Org. Chem.* **2011**, 3583-3609.
- [15] Bouckaert, J.; Berglund, J.; Schembri, M.; Genst, E. D.; Cools, L.; Wuhler, M.; Hung, C. S.; Pinkner, J.; Slättergard, R.; Zavialov, A.; Choudhury, D.; Langermann, S.; Hultgren, S. J.; Wyns, L.; Klemm, P.; Oscarson, S.; Knight, S. D.; Greve, H. D. Receptor binding studies disclose a novel class of high-affinity inhibitors of the *Escherichia coli* FimH adhesin. *Mol. Microbiol.* **2005**, *55*, 441– 455.
- [16] Sperling, O.; Fuchs, A.; Lindhorst, T. K. Evaluation of the carbohydrate recognition domain of the bacterial adhesin FimH: Design, synthesis and binding properties of mannoside ligands. *Org. Biomol. Chem.* **2006**, *4*, 3913– 3922.

- [17] Han, Z.; Pinkner, J. S.; Ford, B.; Obermann, R.; Nolan, W.; Wildman, S. A.; Hobbs, D.; Ellenberger, T.; Cusumano, C. K.; Hultgren, S. J.; Janetka, J. W. Structure-based drug design and optimization of mannoside bacterial FimH antagonists. *J. Med. Chem.* **2010**, *53*, 4779–4792.
- [18] Klein, T.; Abgottspon, D.; Wittwer, M.; Rabbani, S.; Herold, J.; Jiang, X.; Kleeb, S.; Lüthi, C.; Scharenberg, M.; Bezençon, J.; Gubler, E.; Pang, L.; Smieško, M.; Cutting, B.; Schwardt, O.; Ernst, B. FimH antagonists for the oral treatment of urinary tract infections: from design and synthesis to in vitro and in vivo evaluation. *J. Med. Chem.* **2010**, *53*, 8627–8641.
- [19] Schwardt, O.; Rabbani, S.; Hartmann, M.; Abgottspon, D.; Wittwer, M.; Kleeb, S.; Zalewski, A.; Smieško, M.; Cutting, B.; Ernst, B. Design, synthesis and biological evaluation of mannosyl triazoles as FimH antagonists. *Bioorg. Med. Chem.* **2011**, *19*, 6454-6473.
- [20] Jiang, X.; Abgottspon, D.; Kleeb, S.; Rabbani, S.; Scharenberg, M.; Wittwer, M.; Haug, M.; Schwardt, O.; Ernst, B. Antiadhesion therapy for urinary tract infections – A balanced PK/PD profile proved to be key for success. *J. Med. Chem.* **2012**, *55*, 4700–4713.
- [21] Pang, L.; Kleeb, S.; Lemme, K.; Rabbani, S.; Scharenberg, M.; Zalewski, A.; Schädler, F.; Schwardt, O.; Ernst, B. FimH antagonists: structure-activity and structure-property relationships for biphenyl α -D-mannopyranosides. *ChemMedChem* **2012**, *7*, 1404–1422.
- [22] Choudhury, D.; Thompson, A.; Stojanoff, V.; Langermann, S.; Pinkner, J.; Hultgren, S. J.; Knight, S. D. X-ray structure of the FimC-FimH chaperone-adhesin complex from uropathogenic *Escherichia coli*. *Science* **1999**, *285*, 1061-1066.
- [23] Hung, C. S.; Bouckaert, J.; Hung, D.; Pinkner, J.; Widberg, C.; DeFusco, A.; Auguste, C. G.; Strouse, R.; Langermann, S.; Waksman, G.; Hultgren, S. J. Structural basis of tropism of *Escherichia coli* to the bladder during urinary tract infection. *Mol. Microbiol.* **2002**, *44*, 903-915.
- [24] Wellens, A.; Garofalo, C.; Nguyen, H.; Van Gerven, N.; Slättegård, R.; Hernalsteens, J. P.; Wyns, L.; Oscarson, S.; De Greve, H.; Hultgren, S.; Bouckaert, J. Intervening with urinary tract infections using anti-adhesives based on the crystal structure of the FimH-oligomannose-3 complex. *PLoS One* **2008**, *3*, e2040.
- [25] Wellens, A.; Lahmann, M.; Touaibia, M.; Vaucher, J.; Oscarson, S.; Roy, R.; Remaut, H.; Bouckaert, J. The tyrosine gate as a potential entropic lever in the

- receptor-binding site of the bacterial adhesin FimH. *Biochemistry* **2012**, *51*, 4790–4799.
- [26] Han, Z.; Pinkner, J. S.; Ford, B.; Chorell, E.; Crowley, J. M.; Cusumano, C. K.; Campbell, S.; Henderson, J. P.; Hultgren, S. J.; Janetka, J. W. Lead optimization studies on FimH antagonists: discovery of potent and orally bioavailable ortho-substituted biphenyl mannosides. *J. Med. Chem.* **2012**, *55*, 3945–3959.
- [27] Winiwarter, S.; Bonham, N. M.; Ax, F.; Hallberg, A.; Lennernäs, H.; Karlén, A. Correlation of human jejunal permeability (in vivo) of drugs with experimentally and theoretically derived parameters. A multivariate data analysis approach. *J. Med. Chem.* **1998**, *41*, 4939-4949.
- [28] Waring, M. J. Lipophilicity in drug discovery. *Expert Opin. Drug Discov.* **2010**, *5*, 235-248.
- [29] van De Waterbeemd, H.; Smith, D. A.; Beaumont, K.; Walker, D. K. Property-based design: optimization of drug absorption and pharmacokinetics. *J. Med. Chem.* **2001**, *44*, 1313-1333.
- [30] Varma, M. V. S.; Feng, B.; Obach, R. S.; Troutman, M. D.; Chupka, J.; Miller, H. R.; El-Kattan, A. Physicochemical determinants of human renal clearance. *J. Med. Chem.* **2009**, *52*, 4844-4852.
- [31] Beaumont, K.; Webster, R.; Gardner, I.; Dack, K. Design of ester prodrugs to enhance oral absorption of poorly permeable compounds: challenges to the discovery scientist. *Curr. Drug Metab.* **2003**, *4*, 461-485.
- [32] Ettmayer, P.; Amidon, G. L.; Clement, B.; Testa, B. Lessons learned from marketed and investigational prodrugs. *J. Med. Chem.* **2004**, *47*, 2393-2404.
- [33] Neises, B.; Steglich, W. Simple method for the esterification of carboxylic acids. *Angew. Chem. Int. Ed.* **1978**, *17*, 522-524.
- [34] Miyaura, N.; Suzuki, A. Palladium-catalyzed cross-coupling reactions of organoboron compounds. *Chem. Rev.* **1995**, *95*, 2457-2483.
- [35] Caron, S.; Massett, S. S.; Bogle, D. E.; Castaldi, M. J.; Braish, T. F. An efficient and cost-effective synthesis of 2-phenyl-3-aminopyridine. *Org. Process Res. Dev.* **2001**, *5*, 254–256.
- [36] Lipinski, C. A. Drug-like properties and the causes of poor solubility and poor permeability. *J. Pharmacol. Toxicol. Methods* **2000**, *44*, 235-249.
- [37] Dearden, J. C.; Bresnen, G. M. The measurement of partition coefficients. *QSAR Comb. Sci.* **1988**, *7*, 133-144.

- [38] Kansy, M.; Senner, F.; Gubernator, K. Physicochemical high throughput screening: parallel artificial membrane permeation assay in the description of passive absorption processes. *J. Med. Chem.* **1998**, *41*, 1007-1010.
- [39] Artursson, P.; Karlsson, J. Correlation between oral drug absorption in humans and apparent drug permeability coefficients in human intestinal epithelial (Caco-2) cells. *Biochem. Biophys. Res. Commun.* **1991**, *175*, 880-885.
- [40] Taketani, M.; Shii, M.; Ohura, K.; Ninomiya, S.; Imai, T. Carboxylesterase in the liver and small intestine of experimental animals and human. *Life Sci.* **2007**, *81*, 924-932.
- [41] Li, B.; Sedlacek, M.; Manoharan, I.; Boopathy, R.; Duysen, E. G.; Masson, P.; Lockridge, O. Butyrylcholinesterase, paraoxonase, and albumin esterase, but not carboxylesterase, are present in human plasma. *Biochem. Pharmacol.* **2005**, *70*, 1673-1684.
- [42] Ishikawa, M.; Hashimoto, Y. Improvement in aqueous solubility in small molecule drug discovery programs by disruption of molecular planarity and symmetry. *J. Med. Chem.* **2011**, *54*, 1539-1554.
- [43] Avdeef, A.; Bendels, S.; Di, L.; Faller, B.; Kansy, M.; Sugano, K.; Yamauchi, Y. PAMPA – critical factors for better predictions of absorption. *J. Pharm. Sci.* **2007**, *96*, 2893-2909.
- [44] Hubatsch, I.; Ragnarsson, E. G. E.; Artursson, P. Determination of drug permeability and prediction of drug absorption in Caco-2 monolayers. *Nat. Protoc.* **2007**, *2*, 2111-2119.
- [45] Testa, B.; Mayer, J. M. *Hydrolysis in Drug and Prodrug Metabolism, Chemistry, Biochemistry, and Enzymology*, Helvetica Chimica Acta, Zurich, **2003**, pp. 425-434.
- [46] Seelig, A.; Gerebtzoff, G. Enhancement of drug absorption by noncharged detergents through membrane and P-glycoprotein binding. *Expert Opin. Drug. Metab. Toxicol.* **2006**, *2*, 733-752.
- [47] Liederer, B. M.; Borchardt, R. T. Enzymes involved in the bioconversion of ester-based prodrugs. *J. Pharm. Sci.* **2006**, *95*, 1177-1195.
- [48] Hatfield, J. M.; Wierdl, M.; Wadkins, R. M.; Potter, P. M. Modifications of human carboxylesterase for improved prodrug activation. *Expert Opin. Drug Metab. Toxicol.* **2008**, *4*, 1153-1165.

- [49] Vistoli, G.; Pedretti, A.; Mazzolari, A.; Testa, B. In silico prediction of human carboxylesterase-1 (hCES1) metabolism combining docking analyses and MD simulations. *Bioorg. Med. Chem.* **2010**, *18*, 320-329.
- [50] Naritomi, Y.; Terashita, S.; Kimura, S.; Suzuki, A.; Kagayama, A.; Sugiyama, Y. Prediction of human hepatic clearance from in vivo animal experiments and in vitro metabolic studies with liver microsomes from animals and humans. *Drug Metab. Dispos.* **2001**, *29*, 1316-1324.
- [51] Jewell, C.; Ackermann, C.; Payne, N. A.; Fate, G.; Voorman, R.; Williams, F. M. Specificity of procaine and ester hydrolysis by human, minipig, and rat skin and liver. *Drug Metab. Dispos.* **2007**, *35*, 2015-2022.
- [52] Nicolet, Y.; Lockridge, O.; Masson, P.; Fontecilla-Camps, J. C.; Nachon, F. Crystal structure of human butyrylcholinesterase and of its complexes with substrate and products. *J. Biol. Chem.* **2003**, *278*, 41141-41147.
- [53] Darvesh, S.; Hopkins, D. A.; Geula, C. Neurobiology of butyrylcholinesterase. *Nat. Rev. Neurosci.* **2003**, *4*, 131-138.
- [54] Sunew, K. Y.; Hicks, R. G. Effects of neostigmine and pyridostigmine on duration of succinylcholine action and pseudocholinesterase activity. *Anesthesiology* **1978**, *49*, 188-191.
- [55] Fujiyama, N.; Miura, M.; Kato, S.; Sone, T.; Isobe, M.; Satoh, S. Involvement of carboxylesterase 1 and 2 in the hydrolysis of mycophenolate mofetil. *Drug Metab. Dispos.* **2010**, *38*, 2210-2217.
- [56] Murata, M.; Watanabe, S.; Masuda, Y. Novel palladium(0)-catalyzed coupling reaction of dialkoxyborane with aryl halides: convenient synthetic route to arylboronates. *J. Org. Chem.* **1997**, *62*, 6458-6459.
- [57] Das, B.; Thirupathi, P. A highly selective and efficient acetylation of alcohols and amines with acetic anhydride using NaHSO₄·SiO₂ as a heterogeneous catalyst. *J. Mol. Catal. A. Chem.* **2007**, *269*, 12-16.
- [58] a) VCCLAB, Virtual Computational Chemistry Laboratory, 2005, <http://www.vcclab.org> (accessed April 8, 2013); b) Tetko, I. V.; Gasteiger, J.; Todeschini, R.; Mauri, A.; Livingstone, D.; Ertl, P.; Palyulin, V. A.; Radchenko, E. V.; Zefirov, N. S.; Makarenko, A. S.; Tanchuk, V. Y.; Prokopenko, V. V. Virtual computational chemistry laboratory-design and description. *J. Comput. Aided Mol. Des.* **2005**, *19*, 453-463.

- [59] Ohura, K.; Nozawa, T.; Murakami, K.; Imai, T. Evaluation of transport mechanism of prodrugs and parent drugs formed by intracellular metabolism in Caco-2 cells with modified carboxylesterase activity: temocapril as a model case. *J. Pharm. Sci.* **2011**, *100*, 3985-3994.
- [60] Di, L.; Kerns, E. H.; Hong, Y.; Chen, H. Development and application of high throughput plasma stability assay for drug discovery. *Int. J. Pharm.* **2005**, *297*, 110-119.

2.2 Paper 2: Prodruggability of Carbohydrates – Oral FimH Antagonists

This manuscript focuses on improving membrane permeability of 4'-(methylsulfonyl)-biphenyl-4-yl α -D-mannopyranoside by means of an ester prodrug approach. Various lipophilic acyl groups are incorporated into the sugar moiety masking the polar hydroxyl group 6-OH. Moreover, the propensity of the prodrugs to the enzyme-mediated hydrolysis was studied in detail.

Contribution to the project:

Wojciech Schönemann was involved in the design of the prodrugs and their chemical synthesis together with the master student Philipp Dätwyler who he supervised. Furthermore, he was responsible for reviewing of the manuscript and writing the synthetic part.

This paper was published in the *Canadian Journal of Chemistry*.

Schönemann, W.*; Kleeb, S.*; Dätwyler, P.; Schwardt, O.; Ernst, B. Prodruggability of carbohydrates — oral FimH antagonists. *Can. J. Chem.* **2016**, *94*, 909-919.

* These authors contributed equally to the project.

© 2016 Canadian Journal of Chemistry



Prodruggability of carbohydrates — oral FimH antagonists

Wojciech Schönemann, Simon Kleeb, Philipp Dätwyler, Oliver Schwardt, and Beat Ernst

Abstract: The bacterial lectin FimH is a promising therapeutic target for the nonantibiotic prevention and treatment of urinary tract infections. In this communication, an ester prodrug approach is described to achieve oral bioavailability for FimH antagonists. By introducing short-chain acyl promoieties at the C-6 position of a biphenyl α -D-mannopyranoside, prodrugs with an excellent absorption potential were obtained. The human carboxylesterase 2 was identified as a main enzyme mediating rapid bioconversion to the active principle. Despite their propensity to hydrolysis within the enterocytes during absorption, these ester prodrugs present a considerable progress in the development of orally available FimH antagonists.

Key words: FimH antagonists, oral bioavailability, ester prodrugs, enzyme-mediated bioconversion, renal excretion.

Résumé: La lectine bactérienne FimH est une cible thérapeutique prometteuse pour la prévention et le traitement sans antibiotiques des infections des voies urinaires. Dans la présente communication, nous décrivons une approche faisant appel à un promédicament à base d'ester pour permettre l'obtention d'une biodisponibilité orale à l'administration d'antagonistes de la protéine FimH. En ajoutant des groupements labiles acylés à courtes chaînes en position C-6 d'un biphényle- α -D-mannopyranoside, nous avons obtenu des promédicaments dotés d'un excellent potentiel d'absorption. Nous avons établi que la carboxylestérase 2 humaine était la principale enzyme assurant une bioconversion rapide de ces promédicaments en leur principe actif. Malgré leur propension à l'hydrolyse à l'intérieur des entérocytes au cours de l'absorption, ces promédicaments à base d'ester représentent un progrès considérable sur le plan du développement d'antagonistes de la protéine FimH biodisponibles après administration par voie orale. [Traduit par la Rédaction]

Mots-clés : antagonistes de la protéine FimH, biodisponibilité orale, promédicaments à base d'ester, bioconversion enzymatique, excrétion rénale.

Introduction

Urinary tract infections (UTIs) primarily caused by uropathogenic *Escherichia coli* (UPEC) are among the most prevalent infectious diseases worldwide and are treated with antibiotics as first line therapy.¹ However, frequent and repeated use of antibiotics can lead to antimicrobial resistance and treatment failure, corroborating the need for alternative therapeutic strategies.² Bacterial adhesion to urothelial cells is a crucial first step of the infection cycle, preventing UPEC from being washed out by urine flow and enabling the bacteria to infect urothelial cells.³ This initial adhesion is mediated by the mannose-specific lectin FimH localized at the tip of bacterial type 1 pili.⁴ FimH consists of a lectin domain hosting the carbohydrate recognition domain (CRD) and a pilin domain regulating the switch between the low- and high-affinity states of the CRD.⁵ The CRD interacts with the mannoseylated glycoprotein uropod 1a on the surface of urothelial cells and thereby initiates the bacterial infection.

More than three decades ago, Firon et al. introduced FimH antagonists as a novel class of therapeutics for prevention and treatment of UTI.⁶ Since then, several alkyl and aryl α -D-mannopyranosides with nanomolar affinities towards the FimH-CRD were reported.⁷ In vivo pharmacokinetic studies with orally bioavailable biphenyl α -D-mannopyranosides in a mouse model were first performed in 2010,^{7d} and since then, additional reports describing orally active FimH antagonists have been published.^{7e,7g} In either case, high oral dosages

(≥50 mg/kg) were necessary to achieve the minimal effective concentrations required for anti-adhesive effects in the bladder. The antagonists were furthermore rapidly eliminated from circulation, such that the therapeutic effect — upon a single dose — could be maintained only for a few hours.

When despite high oral dosages only low antagonist concentration can be detected in the urine, the reasons are either low intestinal absorption (i.e., due to low aqueous solubility or low membrane permeability) or extensive nonrenal elimination.⁸ Moreover, undesirably fast renal excretion of the systemically available fraction is due to high glomerular filtration, i.e., low plasma protein binding (PPB), or poor reabsorption in the renal tubules.⁹ We recently reported ester prodrugs of antagonist **1** (Fig. 1) where the carboxylic acid moiety on the terminal ring of the biphenyl aglycone is masked as ester, leading to increased intestinal absorption.^{7d} In a second approach, we replaced the carboxylic acid moiety by bioisosteres to raise lipophilicity and PPB and, consequently, to slow down excretion of the systemically available antagonist into the bladder.¹⁰ In the case of the cyanide **3**, the physicochemical profile allowed for excellent oral absorption and sustained renal excretion, whereas other bioisosteres, e.g., the *p*-methylsulfonyl-biphenyl mannoside **4a**, were too polar for absorption.

A common feature of carbohydrate derivatives is their high polarity, resulting from their many hydroxyl groups. By peracylation the hydrophilic character can be markedly reduced, leading

Received 30 November 2015. Accepted 10 February 2016.

W. Schönemann,* S. Kleeb,* P. Dätwyler, O. Schwardt, and B. Ernst. Institute of Molecular Pharmacy, Pharmcenter, University of Basel, Klingelbergstrasse 50, CH-4056 Basel, Switzerland.

Corresponding author: Beat Ernst (email: beat.ernst@unibas.ch).

*These authors contributed equally to the project.

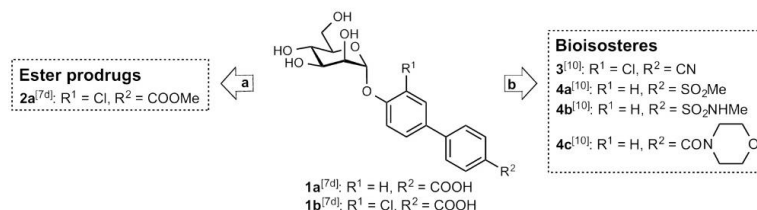
Copyright remains with the author(s) or their institution(s). Permission for reuse (free in most cases) can be obtained from RightsLink.

This article is part of a Special Issue dedicated to Professor David Bundle in recognition of his seminal contributions and lifetime achievements in the fields of carbohydrate chemistry and glycobiology.

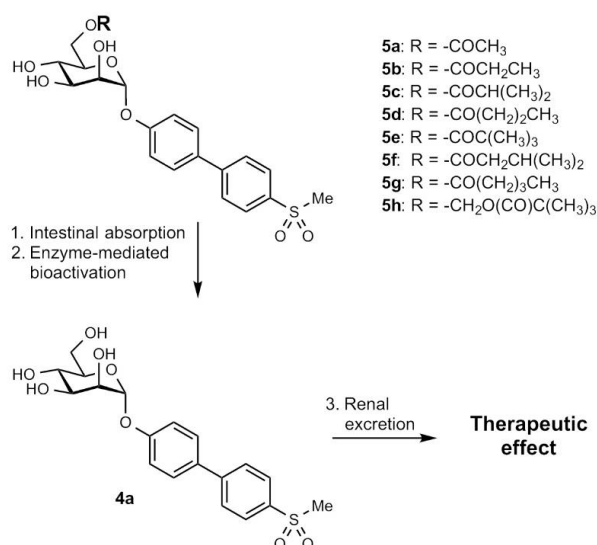
Can. J. Chem. 94: 909–919 (2016) dx.doi.org/10.1139/cjc-2015-0582

Published at www.nrcresearchpress.com/cjc on 21 March 2016.

Fig. 1. Pharmacokinetics of biphenyl α -D-mannopyranosides improved by (a) an ester prodrug approach^{7d} and (b) bioisosteric modifications.¹⁰ Compared to the parent carboxylates **1a** and **1b**, the ester prodrugs **2a–2c** exhibit oral availability; with bioisosteres of the carboxylates **1a** and **1b**, a prolonged renal excretion (\rightarrow **4a–4c**) and improved oral bioavailability (\rightarrow **3**) could be achieved.



Scheme 1. Proposed mode of action. Ester prodrugs of the biphenyl α -D-mannopyranoside **4a** are hydrolyzed upon absorption by esterases. The active principle **4a** is excreted renally and binds to FimH lectins located at the tip of type 1 pili of UPECs in the bladder, resulting in a therapeutic effect.^{7d}



to an increased cellular uptake.^{11a,11b} However, polyacylated carbohydrate derivatives may also exhibit disadvantages, like low solubility and complex in vivo pharmacokinetic profiles due to different rates for deacylation leading to numerous metabolic intermediates, whereof each metabolite could be renally excreted individually.

In the present communication, we describe an ester prodrug strategy applied for the optimization of the pharmacokinetic parameters relevant for oral absorption of methylsulfonyl bioisostere **4a**. As opposed to peracylation, only one of the hydroxyl groups was acylated. For the adjustment of lipophilicity and metabolic hydrolysis, the aliphatic esters were elongated or branched, thereby paving the way for orally available prodrugs with sustained excretion of the pharmacologically active principle **4a** into the bladder (Scheme 1).

Results and discussion

Synthesis of prodrugs **5a–5h**

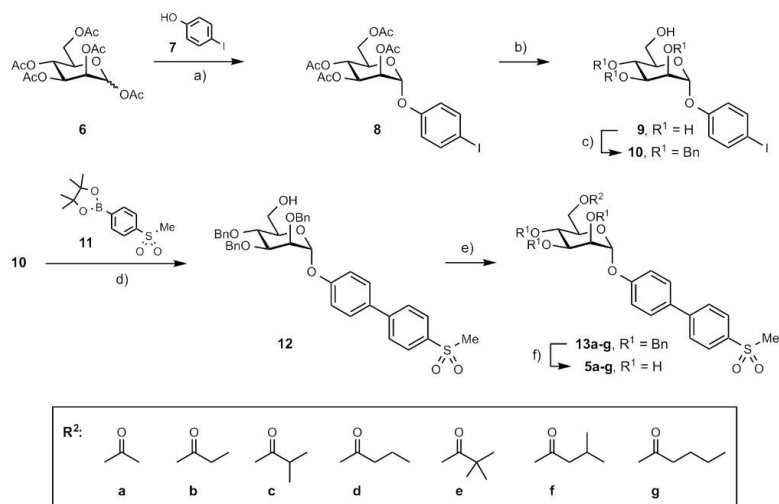
For the acylation, we selected the C-6 hydroxyl group of the mannose moiety of antagonist **4a** because the steric accessibility of the 6-position guarantees successful enzymatic hydrolysis. In the prodrugs **5a–5g**, the C-6 hydroxyl group is directly acylated, whereas in prodrug **5h**, an additional acetal linker was introduced

to further improve the accessibility of the metabolic cleavage site. Upon hydrolysis of the ester, the resulting hemiacetal intermediate is expected to collapse spontaneously, releasing the active principal as well as formaldehyde.

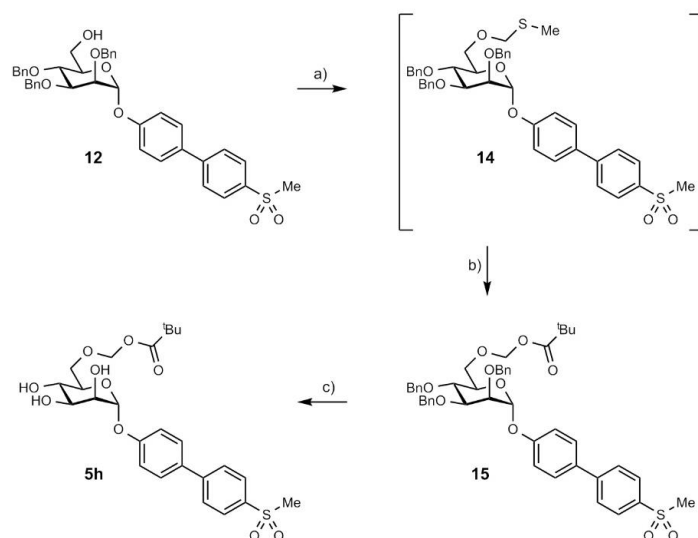
The synthetic route applied for the synthesis of the prodrugs **5a–5g** is depicted in Scheme 2. BF₃·Et₂O-promoted mannosylation of *p*-iodophenol **7** (\rightarrow **8**) followed by deacetylation under standard Zemplén conditions yielded mannoside **9**. Selective protection of the primary alcohol in **9** with *tert*-butyldimethylsilyl chloride followed by benzylation of the remaining three hydroxyl groups and, finally, removal of the TBDMS group under acidic conditions was performed according to one of the representative procedures to give intermediate **10**.¹² Suzuki cross-coupling with 4-(methanesulfonyl)phenylboronic acid pinacol ester (**11**) afforded mannoside **12**.¹³ Then the promoity in the 6-position was introduced with acetic anhydride (\rightarrow **13a**) or corresponding acid chlorides (\rightarrow **13b–13g**). The prodrugs **5a–5g** were finally obtained after hydrogenolysis in the presence of palladium hydroxide on carbon.

For the synthesis of **5h** (Scheme 3), a modified final acylation strategy was necessary, since a methylene linker had to be introduced between the 6-OH of the mannose moiety and the acyl group. A convenient approach involves methylthiomethyl ether

Scheme 2. (a) $\text{BF}_3 \cdot \text{Et}_2\text{O}$, CH_2Cl_2 , 4 Å MS, 40 °C, 30 h, 67%; (b) $\text{MeONa} \cdot \text{MeOH}$, rt, 27 h, 61%; (c) (i) TBDMSCl, imidazole, DMF, 0 °C → rt, 18 h; (ii) BnBr , NaH, TBAI, DMF, 0 °C → rt, 5 h, (iii) H_2SO_4 (1 M), MeOH, 0 °C, 18 h, 58% (for three steps); (d) $\text{PdCl}_2(\text{dppf}) \cdot \text{CH}_2\text{Cl}_2$, K_3PO_4 , DMF, 80 °C, 19 h, 86%; (e) Ac_2O or $\text{R}^2\text{-Cl}$, DMAP, pyridine, 0 °C → 60 °C, 3–24 h, 58%–91%; (f) $\text{Pd}(\text{OH})_2/\text{C}$, H_2 (1 bar), EtOH, rt.



Scheme 3. (a) Ac_2O , AcOH, DMSO, 4 Å MS, rt, 23 h; (b) PivOH, NIS, 0 °C → rt, 15 h, 33%; (c) $\text{Pd}(\text{OH})_2/\text{C}$, H_2 (1 bar), EtOH, rt.



for a subsequent introduction of diverse acyl groups. Starting from **12**, the methylthiomethyl ether **14** was obtained according to a previously described procedure.¹⁴ After removal of the main impurities by flash chromatography, this intermediate was coupled with pivalic acid in presence of *N*-iodosuccinimide yielding the pivaloyloxymethyl ester **15**.¹⁵ Finally, debenzoylation by hydrogenolysis gave prodrug **5h**.

Physicochemical and pharmacokinetic properties

Table 1 summarizes the physicochemical and pharmacokinetic properties of the ester prodrugs **5a–5h**, i.e., their aqueous solubility,¹⁶ lipophilicity as quantified by the octanol–water partition

coefficient ($\log P$),¹⁷ and permeability determined with the parallel artificial membrane permeability assay (PAMPA)¹⁸ as well as with colorectal adenocarcinoma cells (Caco-2).¹⁹ Table 1 also includes metabolic stability data, describing the susceptibility of the ester prodrugs to hydrolysis by rat and human liver associated esterases.²⁰

Lipophilicity and permeability

Our primary goal, namely to increase lipophilicity and permeability of the biphenyl mannoside **4a**, could clearly be achieved. The $\log P$ coefficients increased in parallel with the number of carbons of the acyl moiety. Whereas acetate **5a** was only

Table 1. Physicochemical and pharmacokinetic parameters of different ester prodrugs **5a–5h**.

Compound	log P^a	Solubility ($\mu\text{g/mL}$) ^b	PAMPA log P_e (cm/s) ^c	Caco-2 P_{app} (10^{-6} cm/s) ^d			RLM $t_{1/2}$ (min) ^e	HLM $t_{1/2}$ (min)
				a \rightarrow b (absorptive)	b \rightarrow a (secretory)	b \rightarrow a/a \rightarrow b		
4a ¹⁰	0.4 \pm 0.0	246 \pm 17	−7.2 \pm 0.0	0.4 \pm 0.0	1.8 \pm 0.1	5.0		
5a	0.9 \pm 0.1	146 \pm 6	−5.4 \pm 0.1	1.8 \pm 0.7	17.7 \pm 1.1	10	33	nd
5b	1.5 \pm 0.1	253 \pm 10	−5.0 \pm 0.0	4.0 \pm 0.6	15.2 \pm 0.7	3.8	6.5	3.0
5c	1.8 \pm 0.1	61 \pm 1	−4.6 \pm 0.0	10.5 \pm 0.9	19.5 \pm 0.1	1.9	3.7	nd
5d	1.8 \pm 0.0	145 \pm 9	−4.7 \pm 0.1	17.3 \pm 1.9	23.5 \pm 1.2	1.4	1.8	1.1
5e	2.3 \pm 0.1	58 \pm 7	−4.6 \pm 0.1	14.1 \pm 1.2	19.8 \pm 3.3	1.4	15	nd
5f	2.1 \pm 0.1	65 \pm 4	−4.4 \pm 0.0	17.8 \pm 2.4	24.3 \pm 3.0	1.4	2.0	nd
5g	2.2 \pm 0.1	149 \pm 5	−4.5 \pm 0.1	18.1 \pm 0.2	29.4 \pm 4.0	1.6	<1	<1
5h	2.1 \pm 0.1	154 \pm 12	−4.5 \pm 0.1	9.4 \pm 1.3	30.3 \pm 3.2	3.2	44	nd

Note: The indicated values represent the mean \pm SD of replicate determinations.

^aOctanol–water partition coefficients (log P) were determined by a miniaturized shake-flask procedure in sextuplicate.¹⁷

^bKinetic aqueous solubility was measured in triplicate.¹⁶

^c P_e = effective permeability: diffusion through an artificial membrane was determined by the parallel artificial membrane permeability assay (PAMPA) in quadruplicate.¹⁸

^d P_{app} = apparent permeability: permeation through a Caco-2 cell monolayer was assessed in the absorptive (a \rightarrow b) and secretory (b \rightarrow a) direction in triplicate. The initial compound concentration (C_0) in the donor chamber was 62.5 μM .¹⁹

^eMicrosomal stability was determined with pooled male rat liver microsomes (RLM) (0.125 mg/mL) and pooled human liver microsomes (HLM) (0.125 mg/mL) at pH 7.4 and 37 °C. The initial compound concentration was 2 μM . The concentration of the prodrug in the incubation was monitored by LC-MS and $t_{1/2}$ was calculated from the slope of the linear regression from the log percentage compound remaining versus incubation time relationship.²⁰

slightly more lipophilic than the parent compound **4a**, propionate **5b**, isobutyrate **5c**, and butyrate **5d** exhibited markedly elevated lipophilicity. The aspired log P values above 2 could be reached in the case of pivaloate **5e**, pivaloyloxymethyl **5h**, isovalerate **5f**, and valerate **5g**. Furthermore, the effective permeability (log P_e) deduced from PAMPA rose proportionally to log P . Log P_e values above −5.7 are a strong indication for intestinal absorption, whereas those above −6.3 propose only a moderate potential. The PAMPA values for prodrugs **5a** and **5b** (log P_e −5.4 and −5.0) indicate a relevant improvement in membrane permeability compared to parent compound **4a** (log P_e −7.2) and optimal permeability for the more lipophilic esters **5c–5h** (log P_e −4.7 to −4.4).²¹

In addition to PAMPA, bi-directional permeation studies through a monolayer of Caco-2 cells were performed to reveal passive permeation as well as carrier-mediated transport through the cell membranes lining the small intestines.¹⁹ By treatment with bis(4-nitrophenyl) phosphate (BNPP), the esterases expressed by Caco-2 cells were inhibited,²⁰ enabling the study of membrane permeation independent of enzyme-mediated hydrolysis.²² Apparent permeability (P_{app}) derived from the experiments in the absorptive direction (apical \rightarrow basal) paralleled the trends observed in lipophilicity (log P) and PAMPA (log P_e). Whereas **5a** and **5b** exhibited low permeability ($P_{app} < 5 \times 10^{-6}$ cm/s), high permeability ($P_{app} > 9 \times 10^{-6}$ cm/s) was detected for the remaining prodrugs. For the most polar prodrugs **5a** and **5b**, high P_{app} in the secretory direction (basal \rightarrow apical) is leading to unfavorable efflux ratios (b \rightarrow a/a \rightarrow b). In these cases, efflux carrier activity probably outbalanced the slow diffusion in the absorptive direction.²³ Otherwise, the more lipophilic prodrugs **5c–5g** diffused more rapidly and therefore appeared only as weak efflux transporter substrates. Finally, the performance of **5h** remains in the high-permeability range. However, its overall evaluation is worsened when the efflux ratio of 3.2 is taken into account.

Solubility

For achieving oral bioavailability, quantitative dissolution of the orally administered prodrug in the intestine is an additional requirement.²⁴ Regarding aqueous solubility, the prodrugs listed in Table 1 can be divided into two categories: esters with branched acyl promoieties (isobutyrate **5c**, pivaloate **5e**, and isovalerate **5f**) were sparsely soluble in aqueous medium (around 60 $\mu\text{g/mL}$), whereas the linear esters (acetate **5a**, propionate **5b**, butyrate **5d**,

and valerate **5g**) and the extended pivaloyloxymethyl ester in **5h** showed solubility values of at least 145 $\mu\text{g/mL}$. Provided that the prodrugs are applied at a therapeutic dose of at most 1 mg/kg body weight, aqueous solubility of 52 $\mu\text{g/mL}$ should be aspired,²⁴ which could barely be achieved with the branched-chain derivatives. By contrast, the prodrugs **5a**, **5b**, **5d**, **5g**, and **5h** markedly exceeded this minimum solubility criterion for quantitative intestinal absorption.

Considering the two pivotal criteria for oral absorption — aqueous solubility and membrane permeability — the prodrug **5b** (high solubility, moderate permeability) as well as the derivatives **5d** and **5g** (moderate solubility, high permeability) showed the most promising profiles for a successful absorption.

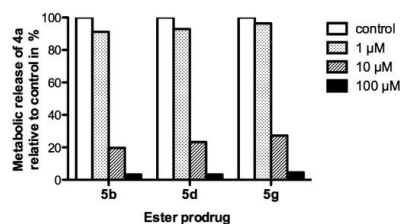
Gastrointestinal stability

Other prerequisites for developing orally bioavailable prodrugs are chemical stability under the conditions encountered in the gastrointestinal tract as well as resistance to hydrolysis during the absorption phase.²⁵ To assess the stability of the esters against hydrolysis under acidic and physiological conditions, the butyrate **5d** was dissolved in phosphate buffer (20 mM, pH 2.5 and 7.4) and acetate buffer (20 mM, pH 5.0) at 37 °C and stirred for 3 h.²⁶ At physiological or acidic pH, **5d** proved to be stable. We therefore expect only marginal prodrug loss in the strongly acidic environment of the stomach and the slightly acidic environment of the proximal small bowel.²⁷

Enzymatic hydrolysis

Whereas the prodrug has to fulfill stability requirements prior to absorption, it should be rapidly cleaved once in circulation.²⁵ Enzymatic ester hydrolysis is undesirable during absorption but necessary once the prodrug has reached circulation. It is mediated by plasma-borne esterases or, as in case of many ester prodrugs, by the carboxylesterase (CES) localized in the endoplasmic reticulum of different tissues.²⁸ The CES superfamily encloses various isozymes classified into five subfamilies. The isozymes human carboxylesterase isotype 1 (hCE1), highly expressed in the liver but scarcely observed in the gastrointestinal tract, and human carboxylesterase isotype 2 (hCE2), present in both liver and small intestine, have been identified as major human CES.^{20,29} To estimate the prodrugs' propensity to CES-mediated hydrolysis irrespective of the type of isozyme involved, we incubated the prodrugs **5a–5h** (initial concentration = 2 μM) with rat liver microsomes (RLM)

Fig. 2. Human liver microsome mediated hydrolysis of ester prodrugs **5b**, **5d**, and **5g** in presence of loperamide (1, 10, and 100 μ M), a specific inhibitor of the human carboxylesterase isotype 2. The bars represent the metabolic release of the parent compound **4a** in the presence of different concentrations of inhibitor (1, 10, and 100 μ M) relative to the accumulation in the control experiment without loperamide.



(0.125 mg/mL in TRIS-HCl 0.1 M, pH 7.4 at 37 °C). In a further step, we assessed the most promising esters **5b**, **5d**, and **5g** using human liver microsomes (HLM) (0.125 mg/mL). The metabolic half-lives ($t_{1/2}$) derived from the microsomal incubations revealed two major trends: first, an increasing susceptibility to hydrolysis along with increased lipophilicity of the linear esters and, second, sterically hindered branched acyl moieties, such as present in pivaloate **5e** and pivaloyloxymethyl **5h**, hampering the enzymatic turnover. Moreover, exposing the pivaloate ester by an acetal linker (\rightarrow **5h**) actually did not increase the rate of enzyme-mediated hydrolysis.

Rapid hydrolysis as detected for the propionate, butyrate, and valerate esters (**5b**, **5d**, and **5g**) is essential for the release of the pharmacologically active principle. However, the prodrug approach might only be successful when the cleavage takes place in liver and plasma and not in the small intestines during absorption or, more precisely, when the hydrolysis is mediated by the isozyme hCE1 rather than by hCE2.²⁵ Since liver microsomes prepared by differential centrifugation from a crude liver homogenate contain both CES, selective inhibition of only one reveals which isozyme is mainly involved. Therefore, loperamide (a specific inhibitor of hCE2) was added during the incubation of **5b**, **5d**, and **5g** with HLM.³⁰ Figure 2 summarizes the hydrolytic activity in presence of the hCE2 specific inhibitor at ascending concentrations (1, 10, and 100 μ M). The metabolic turnover of the esters **5b**, **5d**, and **5g** was in fact inhibited by loperamide, which attributes the hydrolysis to the hCE2 isozyme.³⁰ Recognition of the employed promoieties by isotype 2 correlates with the reported substrate specificity of the two isozymes. Accordingly, hCE2 prefers esters with a relatively small acyl moiety and a large alcohol group, whereas hCE1 primarily catalyzes the hydrolysis of esters with a large acyl but small alcohol moiety.²⁰ Bioconversion mediated by isotype 2 might interfere with the intestinal absorption, even in the case of the well-soluble and permeable prodrugs **5b**, **5d**, and **5g**. By hydrolysis within the enterocytes, the polar active principle **4a** is formed and likely effluxed back into the gut lumen instead into the portal blood.²⁵

Conclusions

Several short-chain fatty acids (propionic acid, butyric acid, and valeric acid) were identified as useful acyl promoieties for optimizing the intestinal absorption potential of the biphenyl mannoside **4a**. We showed that acylation of only one hydroxyl group on the sugar moiety was sufficient to improve lipophilicity into the range required for membrane permeability, whilst sufficient solubility could be sustained. Moreover, the introduced ester promoieties are stable in acidic conditions of the gastrointestinal

tract; however, they are fast hydrolyzed by esterases upon absorption.

The downside of acylation of a hydroxyl group of the sugar moiety could be premature cleavage of the promoieties by hCE2 located in the enterocytes. Therefore, choosing the appropriate prodrug moiety should be guided by enzymatic stability studies. Furthermore, the half-life of the prodrug should allow that the majority of the prodrug is absorbed unchanged.

For proving the benefits of the prodrug approach on oral bioavailability and for assessing whether the intestinal uptake is affected by concomitant hydrolysis, in vivo pharmacokinetic studies in a mouse model are currently performed.

Experimental section

Synthesis

General methods

NMR spectra were recorded on a Bruker Avance DMX-500 (500 MHz) spectrometer. Assignment of ^1H and ^{13}C NMR spectra was achieved using 2D methods (COSY, HSQC, and HMBC). Chemical shifts are expressed in ppm using residual CHCl_3 , CHD_2OD , or HDO as references. Optical rotations were measured using a Perkin-Elmer Polarimeter 341. Electron spray ionization mass spectra (ESI-MS) were obtained on a Waters micromass ZQ mass spectrometer. The LC-HRMS analyses were carried out using an Agilent 1100 LC equipped with a photodiode array detector and a Micromass QTOF I equipped with a 4 GHz digital-time converter. Reactions were monitored by TLC using glass plates coated with silica gel 60 F₂₅₄ (Merck) and visualized by using UV light and (or) by charring with a molybdate solution (a 0.02 M solution of ammonium cerium sulfate dihydrate and ammonium molybdate tetrahydrate in aqueous 10% H_2SO_4). MPLC separations were carried out on a CombiFlash Companion or Rf from Teledyne Isco equipped with RediSep normal-phase columns. All compounds used for biological assays are at least of 97% purity based on HPLC analytical results. Commercially available reagents were purchased from Aldrich, Alfa Aesar, ABCR, or Acros Organics. Solvents were purchased from Sigma-Aldrich or ACS and were dried prior to use where indicated. Methanol (MeOH), pyridine, and dimethyl sulfoxide (DMSO) were dried by storing with activated molecular sieves of 3 or 4 Å for at least 1 day. Dichloromethane (DCM) was dried by filtration over Al_2O_3 (Fluka, type 5016 A basic). Molecular sieves of 3 and 4 Å were activated in vacuo at 500 °C for 1 h immediately before use.

General procedure A for esterification

To a solution of **12** in dry pyridine (2 mL) were added Ac_2O or the corresponding acyl chloride and a catalytic amount of dimethylaminopyridine (DMAP). The mixture was stirred at rt under argon until the reaction was complete (monitored by TLC) and then diluted with ethyl acetate (EtOAc) and washed with H_2O and brine. The organic layer was dried over Na_2SO_4 , concentrated in vacuo, and co-evaporated with xylene. The residue was purified by MPLC on silica gel (petroleum ether – EtOAc, 7:3) to afford **13a–13g**.

General procedure B for hydrogenolysis

A solution of **13a–13g** or **15** in EtOH was stirred under hydrogen (1 bar) in the presence of $\text{Pd}(\text{OH})_2/\text{C}$ (E101 NE/W, 20% Pd) at rt until the reaction was complete (monitored by TLC) and then filtered through Celite, washed with methanol (MeOH), and concentrated in vacuo. The residue was purified by MPLC on silica gel (DCM–MeOH) to give **5a–5h**.

4-Iodophenyl 2,3,4,6-tetra-O-acetyl- α -D-mannopyranoside (**8**)

Penta-O-acetyl-D-mannopyranose (15.0 g, 45.4 mmol), 4-iodophenol (11.2 g, 50.0 mmol, 1.1 equiv.), and activated molecular sieves of 4 Å (2.00 g) were stirred in dry DCM (60 mL) under argon. After 1 h, a first

portion of $\text{BF}_3 \cdot \text{Et}_2\text{O}$ (10 mL, 81 mmol, 1.8 equiv.) was added dropwise followed by the addition of a second portion (6.8 mL, 55.2 mmol, 1.2 equiv.) 4 h later. The reaction was stirred at 40 °C for 30 h. The reaction mixture was filtered through Celite and the filtrate was diluted with EtOAc (250 mL), washed with satd aq NaHCO_3 (3 × 100 mL) and brine (100 mL). The organic layer was dried over Na_2SO_4 and concentrated in vacuo. The residue was crystallized from Et_2O –hexane (1:1) to give **8**. The mother liquor was concentrated and **8** was crystallized again from Et_2O –hexane (2:1). The filtrate was concentrated and purified by MPLC on silica gel (petroleum ether – EtOAc, 9:1). Compound **8** was obtained in an overall yield of 67% (16.8 g). Analytical data were in accordance with literature data.³¹

4-Iodophenyl α -D-mannopyranoside (9)

To a solution of **8** (16.8 g, 30.5 mmol) in dry MeOH (100 mL) was added freshly prepared 1 M MeONa–MeOH (2 mL) under argon. The reaction mixture was stirred overnight at rt and then neutralized with Amberlyst-15 (H^+) ion-exchange resin, filtered, and concentrated in vacuo. Recrystallization from ethanol (250 mL) afforded white crystals of **9**. The mother liquor was concentrated and purified by MPLC on silica gel (DCM–MeOH, 9:1). Compound **9** was obtained in an overall yield of 61% (7.10 g). $[\alpha]_D^{20} + 106.5$ (c 1.00, MeOH). ^1H NMR (500 MHz, CD_3OD): δ = 7.61 (d, J = 8.9 Hz, 2H, Ar-H), 6.96 (d, J = 8.9 Hz, 2H, Ar-H), 5.48 (d, J = 1.4 Hz, 1H, H-1), 4.01 (dd, J = 1.8, 3.2 Hz, 1H, H-2), 3.89 (dd, J = 3.4, 9.4 Hz, 1H, H-3), 3.80–3.69 (m, 3H, H-4, H-6a, H-6b), 3.57 ppm (ddd, J = 2.4, 5.4, 9.7 Hz, 1H, H-5). ^{13}C NMR (125 MHz, CD_3OD): δ = 157.84, 139.52, 120.15 (5C, Ar-C), 100.13 (C-1), 85.31 (Ar-C), 75.52 (C-5), 72.32 (C-3), 71.84 (C-2), 68.28 (C-4), 62.65 ppm (C-6). HRMS: m/z : calcd. for $\text{C}_{12}\text{H}_{15}\text{INO}_6$ [$\text{M}+\text{Na}$] $^+$: 404.9811; found: 404.9808.

4-Iodophenyl 2,3,4-tri-O-benzyl- α -D-mannopyranoside (10)

To a stirred solution of **9** (6.61 g, 17.3 mmol) in dry DMF (17 mL) were added TBDMSCl (2.61 g, 17.3 mmol, 1.0 equiv.) and imidazole (2.35 g, 34.6 mmol, 2.0 equiv.) under argon at 0 °C. After 1 h, the reaction mixture was removed from the ice bath and allowed to reach rt. Another portion of TBDMSCl (0.26 g, 1.73 mmol, 0.1 equiv.) was added after 15 h. The reaction was stirred for 3 h until **9** was completely consumed. The reaction mixture was diluted with DCM (200 mL) and washed with satd aq NaHCO_3 (2 × 150 mL) and brine (150 mL). The organic layer was dried over Na_2SO_4 , concentrated in vacuo, and co-evaporated with toluene (2 × 100 mL) to afford 9.60 g of crude product. The obtained compound (6.01 g) was dissolved in dry DMF (28 mL) under argon. Sodium hydride (1.75 g, 43.6 mmol, 60% in mineral oil) was added to the stirred solution together with an additional portion of DMF (16 mL) at 0 °C followed by the addition of BnBr (6.47 mL, 54.5 mmol). The reaction mixture was removed from the ice bath and allowed to reach rt. Bu_4NI (0.88 g, 2.42 mmol) was added after 2 h. When the reaction was complete after another 2 h, the mixture was diluted with EtOAc (250 mL) and washed with satd aq NaHCO_3 (150 mL), H_2O (150 mL), and brine (100 mL). The organic layer was dried over Na_2SO_4 , concentrated in vacuo, and co-evaporated with toluene (75 mL) to afford 10.8 g of a yellowish product. The crude compound (10.8 g) was then dissolved in MeOH (70 mL) under argon and a solution of H_2SO_4 in MeOH (1 M, 560 mL) was added dropwise. The reaction was stirred at 0 °C until completion (18 h, monitored by TLC) and then the mixture was diluted with EtOAc (100 mL) and washed with satd aq NaHCO_3 (100 mL), H_2O (100 mL), and brine (100 mL). The aqueous layer was extracted with EtOAc (100 mL). The combined organic layers were dried over Na_2SO_4 , concentrated in vacuo, and the major impurities were removed by MPLC on silica gel (petroleum ether – EtOAc, 85:15). The crude **10** was crystallized from petroleum ether – EtOAc (3:1). The mother liquor was concentrated and the residue was recrystallized from MeOH (20 mL). Compound **10** was obtained in an overall yield of 58% (4.32 g) over three steps. $[\alpha]_D^{20} + 55.9$ (c 1.00, EtOAc). ^1H NMR (500 MHz, CDCl_3): δ = 7.48 (d, J = 8.7 Hz, 2H, Ar-H),

7.35–7.24 (m, 15H, Ar-H), 6.67 (d, J = 8.7 Hz, 2H, Ar-H), 5.49 (d, J = 1.7 Hz, 1H, H-1), 4.90 (d, J = 10.9 Hz, 1H, PhCH_2O), 4.78 (d, J = 12.2 Hz, 1H, PhCH_2O), 4.70–4.62 (m, 4H, PhCH_2O), 4.07–4.02 (m, 2H, H-4, H-3), 3.89 (br s, 1H, H-2), 3.70–3.69 (m, 2H, H-6a, H-6b), 3.62 (m, 1H, H-5), 1.81 ppm (s, 1H, OH). ^{13}C NMR (125 MHz, CDCl_3): δ = 155.93, 138.53, 138.42, 138.35, 138.09, 128.61, 128.58, 128.19, 128.03, 127.95, 127.86, 127.80, 118.73 (23C, Ar-C), 96.66 (C-1), 85.12 (Ar-C), 79.88 (C-3 or C-4), 75.40 (PhCH_2O), 74.74 (C-2), 74.43 (C-3 or C-4), 73.38 (PhCH_2O), 73.28 (C-5), 72.69 (PhCH_2O), 62.06 ppm (C-6). ESI-MS: m/z : calcd. for $\text{C}_{33}\text{H}_{33}\text{INO}_6$ [$\text{M}+\text{Na}$] $^+$: 675.12, found: 675.18.

4'-(Methylsulfonyl)-biphenyl-4-yl 2,3,4-tri-O-benzyl- α -D-mannopyranoside (12)

Compounds **10** (2.50 g, 3.83 mmol) and **11** (843 mg, 4.21 mmol) were dissolved in dry DMF (20 mL) under argon. The mixture was degassed in an ultrasonic bath and flushed with argon for 5 min followed by the addition of K_3PO_4 (2.44 g, 11.5 mmol, 3.0 equiv.) and $\text{Pd}(\text{dppf})\text{Cl}_2 \cdot \text{CH}_2\text{Cl}_2$ (156 mg, 0.19 mmol, 0.05 equiv.). The mixture was stirred at 80 °C for 19 h. The reaction mixture was diluted with EtOAc (200 mL), washed with H_2O (2 × 120 mL) and brine (120 mL), dried over Na_2SO_4 , and concentrated in vacuo. The residue was purified by MPLC on silica gel (petroleum ether – EtOAc, 1:1) to give **12** (2.24 g, 86%) as a white solid. $[\alpha]_D^{20} + 70.8$ (c 1.01, EtOAc). ^1H NMR (500 MHz, CDCl_3): δ = 7.99–7.97 (m, 2H, Ar-H), 7.72–7.70 (m, 2H, Ar-H), 7.53–7.52 (m, 2H, Ar-H), 7.42–7.29 (m, 15H, Ar-H), 7.08–7.06 (m, 2H, Ar-H), 5.58 (d, J = 1.9 Hz, 1H, H-1), 4.97 (d, J = 10.9 Hz, 1H, PhCH_2O), 4.87 (d, J = 12.3 Hz, 1H, PhCH_2O), 4.78–4.69 (m, 4H, PhCH_2O), 4.16–4.09 (m, 2H, H-3, H-4), 4.00 (d, J = 2.2 Hz, 1H, H-2), 3.79–3.73 (m, 3H, H-5, H-6a, H-6b), 3.09 ppm (s, 3H, SO_2CH_3). ^{13}C NMR (125 MHz, CDCl_3): δ = 156.68, 146.14, 138.87, 138.46, 138.35, 138.15, 133.34, 128.78, 128.65, 128.63, 128.24, 128.09, 128.06, 128.02, 127.91, 127.84, 127.67, 116.99 (30C, Ar-C), 96.67 (C-1), 80.00 (C-3 or C-4), 75.46 (PhCH_2O), 74.79 (C-2), 74.59 (C-3 or C-4), 73.41 (PhCH_2O), 73.31 (C-5), 72.74 (PhCH_2O), 62.25 (C-6), 44.79 ppm (SO_2CH_3). ESI-MS: m/z : calcd. for $\text{C}_{40}\text{H}_{40}\text{NaO}_8\text{S}$ [$\text{M}+\text{Na}$] $^+$: 703.23, found: 703.26.

4'-(Methylsulfonyl)-biphenyl-4-yl 6-O-acetyl-2,3,4-tri-O-benzyl- α -D-mannopyranoside (13a)

Prepared according to the general procedure A from **12** (100 mg, 0.147 mmol), Ac_2O (27 μL , 0.294 mmol, 2.0 equiv.), and DMAP (1 mg, 0.008 mmol, 0.05 eq). The reaction was started at 0 °C and allowed to warm up to rt. Yield: 104 mg (96%) as a colorless oil. $[\alpha]_D^{20} + 70.0$ (c 1.00, CHCl_3). ^1H NMR (500 MHz, CDCl_3): δ = 7.90 (d, J = 8.5 Hz, 2H, Ar-H), 7.63 (d, J = 8.4 Hz, 2H, Ar-H), 7.46 (d, J = 8.8 Hz, 2H, Ar-H), 7.33–7.17 (m, 15H, Ar-H), 7.03 (d, J = 8.7 Hz, 2H, Ar-H), 5.52 (d, J = 1.7 Hz, 1H, H-1), 4.88 (d, J = 10.8 Hz, 1H, PhCH_2O), 4.77–4.63 (m, 4H, PhCH_2O), 4.54 (d, J = 10.8 Hz, 1H, PhCH_2O), 4.26–4.18 (m, 2H, H-6a, H-6b), 4.07 (dd, J = 3.0, 9.2 Hz, 1H, H-3), 3.98–3.92 (m, 2H, H-2, H-4), 3.81 (m, 1H, H-5), 2.99 (s, 3H, SO_2CH_3), 1.92 ppm (s, 3H, COCH_3). ^{13}C NMR (125 MHz, CDCl_3): δ = 170.83 (CO), 156.71, 146.07, 138.84, 138.29, 138.10, 138.09, 133.31, 128.64, 128.59, 128.57, 128.55, 128.24, 128.05, 127.99, 127.95, 127.93, 127.90, 127.84, 127.61, 117.12 (30C, Ar-C), 96.43 (C-1), 79.97 (C-3), 75.34 (PhCH_2O), 74.48 (C-2), 74.32 (C-4), 73.05, 72.56 (2 PhCH_2O), 71.01 (C-5), 63.21 (C-6), 44.74 (SO_2CH_3), 20.95 ppm (COCH_3). ESI-MS: m/z : calcd. for $\text{C}_{42}\text{H}_{42}\text{NaO}_9\text{S}$ [$\text{M}+\text{Na}$] $^+$: 745.24, found: 745.31.

4'-(Methylsulfonyl)-biphenyl-4-yl 2,3,4-tri-O-benzyl-6-O-propionyl- α -D-mannopyranoside (13b)

Prepared according to the general procedure A from **12** (70 mg, 0.103 mmol), propionyl chloride (33 μL , 0.309 mmol, 3.0 equiv.), and DMAP (1 mg, 0.008 mmol, 0.08 equiv.). The reaction was started at rt and then warmed up to 60 °C. Yield: 38 mg (58%) as a colorless oil. $[\alpha]_D^{20} + 63.0$ (c 1.84, CHCl_3). ^1H NMR (500 MHz, CDCl_3): δ = 7.97 (d, J = 8.4 Hz, 2H, Ar-H), 7.70 (d, J = 8.4 Hz, 2H, Ar-H), 7.51 (d, J = 8.7 Hz, 2H, Ar-H), 7.41–7.27 (m, 15H, Ar-H), 7.10 (d, J = 8.7 Hz, 2H, Ar-H), 5.58 (d, J = 1.5 Hz, 1H, H-1), 4.95 (d, J = 10.7 Hz, 1H, PhCH_2O), 4.83 (d, J = 12.3 Hz, 1H, PhCH_2O), 4.77–4.72 (m, 3H, PhCH_2O), 4.60 (d,

$J = 10.7$ Hz, 1H, PhCH₂O), 4.34–4.28 (m, 2H, H-6a, H-6b), 4.14 (dd, $J = 3.0$, 9.2 Hz, 1H, H-3), 4.03 (t, $J = 9.5$ Hz, 1H, H-4), 3.99 (m, 1H, H-2), 3.88 (ddd, $J = 2.4$, 4.4, 9.8 Hz, 1H, H-5), 3.08 (s, 3H, SO₂CH₃), 2.27 (q, $J = 7.5$ Hz, 2H, CH₂COO), 1.07 ppm (t, $J = 7.6$ Hz, 3H, CH₃). ¹³C NMR (125 MHz, CDCl₃): $\delta = 174.29$ (CO), 156.77, 146.18, 138.89, 138.36, 138.17, 138.15, 137.46, 137.16, 133.37, 128.70, 128.65, 128.63, 128.61, 128.29, 128.12, 128.01, 127.99, 127.97, 127.92, 127.68, 118.42, 117.18 (30C, Ar-C), 96.44 (C-1), 80.02 (C-3), 75.44 (PhCH₂O), 74.61 (C-2), 74.50 (C-4), 73.15, 72.65 (2 PhCH₂O), 71.19 (C-5), 63.14 (C-6), 44.80 (SO₂CH₃), 27.66 (CH₂COO), 9.21 ppm (CH₃). ESI-MS: m/z : calcd. for C₄₃H₄₄NaO₅S [M+Na]⁺: 759.26, found: 759.13.

4'-(Methylsulfonyl)-biphenyl-4-yl 2,3,4-tri-O-benzyl-6-O-isobutyryl- α -D-mannopyranoside (13c)

Prepared according to the general procedure A from **12** (70 mg, 0.103 mmol), isobutyryl chloride (33 μ L, 0.309 mmol, 3.0 equiv.), and DMAP (2 mg, 0.016 mmol, 0.16 equiv.). The reaction was started at rt and then warmed up to 60 °C. Yield: 63 mg (82%) as a colorless oil. [α]_D²⁰ + 60.0 (c 3.17, CHCl₃). ¹H NMR (500 MHz, CDCl₃): $\delta = 7.96$ (d, $J = 8.4$ Hz, 2H, Ar-H), 7.68 (d, $J = 8.4$ Hz, 2H, Ar-H), 7.49 (d, $J = 8.7$ Hz, 2H, Ar-H), 7.39–7.26 (m, 15H, Ar-H), 7.09 (d, $J = 8.7$ Hz, 2H, Ar-H), 5.57 (d, $J = 1.6$ Hz, 1H, H-1), 4.94 (d, $J = 10.6$ Hz, 1H, PhCH₂O), 4.81 (d, $J = 12.2$ Hz, 1H, PhCH₂O), 4.74–4.71 (m, 3H, PhCH₂O), 4.58 (d, $J = 10.6$ Hz, 1H, PhCH₂O), 4.35 (dd, $J = 1.7$, 11.9 Hz, 1H, H-6a), 4.25 (dd, $J = 5.2$, 11.9 Hz, 1H, H-6b), 4.12 (dd, $J = 3.0$, 9.2 Hz, 1H, H-3), 4.00 (t, $J = 9.5$ Hz, 1H, H-4), 3.97 (m, 1H, H-2), 3.86 (ddd, $J = 1.6$, 5.0, 9.8 Hz, 1H, H-5), 3.06 (s, 3H, SO₂CH₃), 2.49 (hept, $J = 7.0$ Hz, 1H, CH(CH₃)₂), 1.09 (d, $J = 7.0$ Hz, 3H, CH₃), 1.06 ppm (d, $J = 7.0$ Hz, 3H, CH₃). ¹³C NMR (125 MHz, CDCl₃): $\delta = 176.85$ (CO), 156.73, 146.17, 138.85, 138.33, 138.14, 133.31, 128.67, 128.62, 128.56, 128.22, 128.06, 128.01, 127.95, 127.90, 127.64, 117.14 (30C, Ar-C), 96.34 (C-1), 79.96 (C-3), 75.48 (PhCH₂O), 74.67 (C-2), 74.61 (C-4), 73.16, 72.63 (2 PhCH₂O), 71.32 (C-5), 62.98 (C-6), 44.77 (SO₂CH₃), 34.10 (CH), 19.12, 18.92 ppm (2 CH₃). ESI-MS: m/z : calcd. for C₄₄H₄₆NaO₅S [M+Na]⁺: 773.28, found: 773.28.

4'-(Methylsulfonyl)-biphenyl-4-yl 2,3,4-tri-O-benzyl-6-O-butyryl- α -D-mannopyranoside (13d)

Prepared according to the general procedure A from **12** (54 mg, 0.080 mmol), butyryl chloride (10 μ L, 0.094 mmol, 1.2 equiv.), and DMAP (1 mg, 0.008 mmol, 0.1 equiv.). The reaction mixture was stirred at rt. Yield: 45 mg (75%) as a colorless oil. [α]_D²⁰ + 68.6 (c 1.13, CHCl₃). ¹H NMR (500 MHz, CDCl₃): $\delta = 8.02$ (d, $J = 8.4$ Hz, 2H, Ar-H), 7.75 (d, $J = 8.5$ Hz, 2H, Ar-H), 7.56 (d, $J = 8.8$ Hz, 2H, Ar-H), 7.45–7.32 (m, 15H, Ar-H), 7.15 (d, $J = 8.8$ Hz, 2H, Ar-H), 5.64 (d, $J = 1.7$ Hz, 1H, H-1), 5.00 (d, $J = 10.7$ Hz, 1H, PhCH₂O), 4.87 (d, $J = 12.3$ Hz, 1H, PhCH₂O), 4.81–4.77 (m, 3H, PhCH₂O), 4.65 (d, $J = 10.7$ Hz, 1H, PhCH₂O), 4.40–4.33 (m, 2H, H-6a, H-6b), 4.19 (dd, $J = 3.0$, 9.2 Hz, 1H, H-3), 4.07 (t, $J = 9.5$ Hz, 1H, H-4), 4.04 (m, 1H, H-2), 3.92 (ddd, $J = 2.2$, 4.6, 9.8 Hz, 1H, H-5), 3.12 (s, 3H, SO₂CH₃), 2.29 (t, $J = 7.5$ Hz, 2H, CH₂COO), 1.67–1.59 (m, 2H, CH₂), 0.91 ppm (t, $J = 7.4$ Hz, 3H, CH₃). ¹³C NMR (125 MHz, CDCl₃): $\delta = 173.42$ (CO), 156.72, 146.10, 138.83, 138.31, 138.12, 138.10, 133.27, 128.64, 128.59, 128.57, 128.55, 128.21, 128.05, 127.98, 127.95, 127.93, 127.91, 127.86, 127.60, 117.10 (30C, Ar-C), 96.37 (C-1), 79.95 (C-3), 75.40 (PhCH₂O), 74.58, 74.49 (C-2, C-4), 73.10, 72.59 (2 PhCH₂O), 71.17 (C-5), 62.94 (C-6), 44.73 (SO₂CH₃), 36.23 (CH₂COO), 18.47 (CH₂), 13.80 ppm (CH₃). ESI-MS: m/z : calcd. for C₄₄H₄₆NaO₅S [M+Na]⁺: 773.28, found: 773.44.

4'-(Methylsulfonyl)-biphenyl-4-yl 2,3,4-tri-O-benzyl-6-O-pivaloyl- α -D-mannopyranoside (13e)

Prepared according to the general procedure A from **12** (100 mg, 0.147 mmol), pivaloyl chloride (36 μ L, 0.294 mmol, 2.0 equiv.), and DMAP (1 mg, 0.008 mmol, 0.05 equiv.). The reaction was started at rt and then warmed up to 60 °C. Yield: 101 mg (90%) as a colorless oil. [α]_D²⁰ + 88.7 (c 1.02, CHCl₃). ¹H NMR (500 MHz, CDCl₃): $\delta = 7.90$ (d, $J = 8.4$ Hz, 2H, Ar-H), 7.62 (d, $J = 8.4$ Hz, 2H, Ar-H), 7.44 (d, $J = 8.7$ Hz, 2H, Ar-H), 7.35–7.20 (m, 15H, Ar-H), 7.05 (d, $J = 8.7$ Hz, 2H,

Ar-H), 5.53 (d, $J = 1.6$ Hz, 1H, H-1), 4.90 (d, $J = 10.6$ Hz, 1H, PhCH₂O), 4.77 (d, $J = 12.2$ Hz, 1H, PhCH₂O), 4.68–4.65 (m, 3H, PhCH₂O), 4.55 (d, $J = 10.7$ Hz, 1H, PhCH₂O), 4.36 (dd, $J = 1.5$, 11.8 Hz, 1H, H-6a), 4.15–4.08 (m, 2H, H-3, H-6b), 3.98–3.93 (m, 2H, H-2, H-4), 3.82 (ddd, $J = 1.3$, 5.3, 9.8 Hz, 1H, H-5), 2.99 (s, 3H, SO₂CH₃), 1.05 ppm (s, 9H, C(CH₃)₃). ¹³C NMR (125 MHz, CDCl₃): $\delta = 178.19$ (CO), 156.61, 146.05, 138.75, 138.25, 138.07, 133.16, 128.59, 128.52, 128.46, 128.11, 127.97, 127.91, 127.84, 127.83, 127.52, 127.59, 117.08 (30C, Ar-C), 96.13 (C-1), 79.84 (C-3), 75.40 (PhCH₂O), 74.71, 74.64 (C-2, C-4), 73.11, 72.50 (2 PhCH₂O), 71.33 (C-5), 63.07 (C-6), 44.62 (SO₂CH₃), 38.82 (C(CH₃)₃), 27.17 ppm (C(CH₃)₃). ESI-MS: m/z : calcd. for C₄₅H₄₈NaO₅S [M+Na]⁺: 787.29, found: 787.36.

4'-(Methylsulfonyl)-biphenyl-4-yl 2,3,4-tri-O-benzyl-6-O-isovaleryl- α -D-mannopyranoside (13f)

Prepared according to the general procedure A from **12** (38 mg, 0.056 mmol), isovaleryl chloride (27 μ L, 0.223 mmol, 4.0 equiv.), and DMAP (1 mg, 0.008 mmol, 0.14 equiv.). The reaction mixture was stirred at rt. Yield: 35 mg (81%) as a colorless oil. [α]_D²⁰ + 59.0 (c 0.93, CHCl₃). ¹H NMR (500 MHz, CDCl₃): $\delta = 7.99$ (d, $J = 8.4$ Hz, 2H, Ar-H), 7.72 (d, $J = 8.4$ Hz, 2H, Ar-H), 7.53 (d, $J = 8.7$ Hz, 2H, Ar-H), 7.42–7.29 (m, 15H, Ar-H), 7.11 (d, $J = 8.7$ Hz, 2H, Ar-H), 5.59 (d, $J = 1.6$ Hz, 1H, H-1), 4.97 (d, $J = 10.7$ Hz, 1H, PhCH₂O), 4.84 (d, $J = 12.3$ Hz, 1H, PhCH₂O), 4.77–4.74 (m, 3H, PhCH₂O), 4.62 (d, $J = 10.7$ Hz, 1H, PhCH₂O), 4.38 (dd, $J = 1.9$, 11.9 Hz, 1H, H-6a), 4.29 (dd, $J = 4.9$, 12.0 Hz, 1H, H-6b), 4.15 (dd, $J = 3.0$, 9.2 Hz, 1H, H-3), 4.04 (t, $J = 9.5$ Hz, 1H, H-4), 4.00 (m, 1H, H-2), 3.88 (ddd, $J = 1.8$, 4.8, 9.8 Hz, 1H, H-5), 3.09 (s, 3H, SO₂CH₃), 2.16 (d, $J = 7.1$ Hz, 2H, CH₂COO), 2.04 (m, 1H, CH(CH₃)₂), 0.89 (d, $J = 3.0$ Hz, 3H, CH₃), 0.88 ppm (d, $J = 3.0$ Hz, 3H, CH₃). ¹³C NMR (125 MHz, CDCl₃): $\delta = 172.93$ (CO), 156.76, 146.14, 138.85, 138.33, 138.15, 138.13, 133.29, 128.66, 128.62, 128.60, 128.58, 128.22, 128.09, 127.98, 127.96, 127.94, 127.89, 127.62, 117.11 (30C, Ar-C), 96.39 (C-1), 79.97 (C-3), 75.45 (PhCH₂O), 74.61, 74.57 (C-2, C-4), 73.13, 72.62 (2 PhCH₂O), 71.22 (C-5), 62.89 (C-6), 44.77 (SO₂CH₃), 43.48 (CH₂COO), 25.70 (CH(CH₃)₂), 22.56 ppm (2 CH₃). ESI-MS: m/z : calcd. for C₄₅H₄₈NaO₅S [M+Na]⁺: 787.29, found: 787.46.

4'-(Methylsulfonyl)-biphenyl-4-yl 2,3,4-tri-O-benzyl-6-O-valeryl- α -D-mannopyranoside (13g)

Prepared according to the general procedure A from **12** (69 mg, 0.101 mmol), valeryl chloride (49 μ L, 0.404 mmol, 4.0 equiv.), and DMAP (1 mg, 0.008 mmol, 0.08 equiv.). The reaction was started at rt and then warmed up to 60 °C. Yield: 70 mg (91%) as a yellowish oil. [α]_D²⁰ + 63.9 (c 1.00, CHCl₃). ¹H NMR (500 MHz, CDCl₃): $\delta = 7.90$ (d, $J = 8.4$ Hz, 2H, Ar-H), 7.64 (d, $J = 8.4$ Hz, 2H, Ar-H), 7.45 (d, $J = 8.7$ Hz, 2H, Ar-H), 7.33–7.20 (m, 15H, Ar-H), 7.03 (d, $J = 8.7$ Hz, 2H, Ar-H), 5.52 (d, $J = 1.5$ Hz, 1H, H-1), 4.88 (d, $J = 10.7$ Hz, 1H, PhCH₂O), 4.76 (d, $J = 12.3$ Hz, 1H, PhCH₂O), 4.70–4.63 (m, 3H, PhCH₂O), 4.53 (d, $J = 10.7$ Hz, 1H, PhCH₂O), 4.28–4.21 (m, 2H, H-6a, H-6b), 4.07 (dd, $J = 3.0$, 9.2 Hz, 1H, H-3), 3.95 (t, $J = 9.5$ Hz, 1H, H-4), 3.92 (m, 1H, H-2), 3.81 (ddd, $J = 2.3$, 4.4, 9.8 Hz, 1H, H-5), 3.01 (s, 3H, SO₂CH₃), 2.19 (t, $J = 9.5$ Hz, 2H, CH₂COO), 1.50–1.44 (m, 2H, CH₂), 1.24–1.17 (m, 2H, CH₂), 0.77 ppm (t, $J = 7.4$ Hz, 3H, CH₃). ¹³C NMR (125 MHz, CDCl₃): $\delta = 173.63$ (CO), 156.76, 146.12, 138.84, 138.32, 138.14, 138.12, 133.29, 128.65, 128.60, 128.59, 128.57, 128.22, 128.06, 127.99, 127.97, 127.94, 127.92, 127.88, 127.61, 117.12 (30C, Ar-C), 96.43 (C-1), 79.97 (C-3), 75.21 (PhCH₂O), 74.59, 74.52 (C-2, C-4), 73.11, 72.60 (2 PhCH₂O), 71.17 (C-5), 63.01 (C-6), 44.75 (SO₂CH₃), 34.04 (CH₂COO), 27.00, 22.35 (2 CH₂), 13.78 ppm (CH₃). ESI-MS: m/z : calcd. for C₄₅H₄₈NaO₅S [M+Na]⁺: 787.29, found: 787.66.

4'-(Methylsulfonyl)-biphenyl-4-yl 2,3,4-tri-O-benzyl-6-O-pivaloyloxymethyl- α -D-mannopyranoside (15)

Compound **12** (250 mg, 0.367 mmol) was dissolved in dry DMSO under argon followed by the addition of Ac₂O (2 mL) and AcOH (0.2 mL). The reaction was stirred at rt for 19 h. The mixture was diluted with EtOAc (50 mL) and washed with satd aq NaHCO₃ (2 \times 50 mL) and brine (50 mL). The organic layer was dried over Na₂SO₄,

concentrated in vacuo, and purified by MPLC on silica gel (petroleum ether – EtOAc, 7:3) to afford 153 mg of **14**. The intermediate **14** (113 mg) was dissolved in dry DMF (2 mL) under argon and PivOH (47 mg, 0.460 mmol) and NIS (52 mg, 0.230 mmol) were added. The reaction was quenched after 17 h with Et₃N (0.100 mL). Then, the mixture was diluted with EtOAc (50 mL) and washed with satd aq NaHCO₃ (50 mL), H₂O (50 mL) and brine (50 mL). The organic layer was dried over Na₂SO₄, concentrated in vacuo and purified by MPLC on silica gel (petroleum ether – EtOAc, 7:3). Compound **15** was obtained in an overall yield of 33% (72 mg) over two steps. [α]_D²⁰ + 64.3 (c 0.58, CHCl₃). ¹H NMR (500 MHz, CDCl₃): δ = 7.84 (d, *J* = 8.4 Hz, 2H, Ar-H), 7.63 (d, *J* = 8.4 Hz, 2H, Ar-H), 7.45 (d, *J* = 8.7 Hz, 2H, Ar-H), 7.32–7.21 (m, 15H, Ar-H), 7.02 (d, *J* = 8.7 Hz, 2H, Ar-H), 5.50 (d, *J* = 1.6 Hz, 1H, H-1), 5.22 (s, 2H, OCH₂O), 4.88 (d, *J* = 10.9 Hz, 1H, PhCH₂O), 4.75 (d, *J* = 12.4 Hz, 1H, PhCH₂O), 4.70 (d, *J* = 12.4 Hz, 1H, PhCH₂O), 4.65–4.62 (m, 2H, PhCH₂O), 4.59 (d, *J* = 11.0 Hz, 1H, PhCH₂O), 4.05–3.97 (m, 2H, H-3, H-4), 3.90 (m, 1H, H-2), 3.83 (dd, *J* = 4.4, 10.7 Hz, 1H, H-6a), 3.78–3.72 (m, 2H, H-5, H-6b), 2.99 (s, 3H, SO₂CH₃), 1.08 ppm (s, 9H, C(CH₃)₃). ¹³C NMR (125 MHz, CDCl₃): δ = 178.10 (CO), 156.90, 146.19, 138.83, 138.47, 138.19, 133.28, 128.74, 128.60, 128.59, 128.55, 128.08, 128.00, 127.98, 127.86, 127.83, 127.67, 117.16 (30C, Ar-C), 96.74 (C-1), 89.94 (OCH₂O), 80.00 (C-2), 75.25 (PhCH₂O), 74.55, 74.50 (C-2, C-4), 73.16, 72.62 (2 PhCH₂O), 72.38 (C-5), 69.04 (C-6), 44.78 (SO₂CH₃), 39.04 (C(CH₃)₃), 27.17 ppm (C(CH₃)₃). ESI-MS: *m/z*: calcd. for C₄₆H₅₀NaO₉S [M+Na]⁺: 817.30, found: 817.39.

4'-(Methylsulfonyl)-biphenyl-4-yl 6-O-acetyl- α -D-mannopyranoside (**5a**)

Prepared according to the general procedure B from **13a** (50 mg, 0.069 mmol) with 15 mg of Pd(OH)₂/C (E101 NE/W, 20% Pd) in EtOH (5 mL). Purified by MPLC on silica gel (DCM–MeOH, 9:1). Yield: 24 mg (75%) as a white solid. [α]_D²⁰ + 101.2 (c 0.19, MeOH). ¹H NMR (500 MHz, CD₃OD): δ = 8.02 (d, *J* = 8.5 Hz, 2H, Ar-H), 7.88 (d, *J* = 8.5 Hz, 2H, Ar-H), 7.71 (d, *J* = 8.8 Hz, 2H, Ar-H), 7.26 (d, *J* = 8.6 Hz, 2H, Ar-H), 5.57 (d, *J* = 1.5 Hz, 1H, H-1), 4.39 (dd, *J* = 1.9, 11.8 Hz, 1H, H-6a), 4.24 (dd, *J* = 6.4, 11.8 Hz, 1H, H-6b), 4.08 (dd, *J* = 1.8, 3.4 Hz, 1H, H-2), 3.94 (dd, *J* = 3.4, 9.0 Hz, 1H, H-3), 3.82–3.73 (m, 2H, H-4, H-5), 3.18 (s, 3H, SO₂CH₃), 1.93 ppm (s, 3H, CH₃). ¹³C NMR (125 MHz, CD₃OD): δ = 172.68 (CO), 158.24, 147.29, 140.20, 134.42, 129.59, 129.03, 128.47, 118.37 (12C, Ar-C), 99.90 (C-1), 73.02 (C-5), 72.39 (C-3), 71.77 (C-2), 68.52 (C-4), 64.81 (C-6), 44.48 (SO₂CH₃), 20.69 ppm (CH₃). HRMS: *m/z*: calcd. for C₂₁H₂₄NaO₉S [M+Na]⁺: 475.1039, found: 475.1037.

4'-(Methylsulfonyl)-biphenyl-4-yl 6-O-propionyl- α -D-mannopyranoside (**5b**)

Prepared according to the general procedure B from **13b** (28 mg, 0.038 mmol) with 20 mg of Pd(OH)₂/C (E101 NE/W, 20% Pd) in EtOH (5 mL). Purified by MPLC on silica gel (DCM–MeOH, 1:0 to 9:1). Yield: 11 mg (59%) as a white oil. [α]_D²⁰ + 93.8 (c 0.50, MeOH). ¹H NMR (500 MHz, CD₃OD): δ = 8.02 (d, *J* = 8.4 Hz, 2H, Ar-H), 7.87 (d, *J* = 8.4 Hz, 2H, Ar-H), 7.70 (d, *J* = 8.7 Hz, 2H, Ar-H), 7.25 (d, *J* = 8.7 Hz, 2H, Ar-H), 5.58 (d, *J* = 1.0 Hz, 1H, H-1), 4.42 (dd, *J* = 1.6, 11.7 Hz, 1H, H-6a), 4.23 (dd, *J* = 6.7, 11.7 Hz, 1H, H-6b), 4.09 (d, *J* = 1.6 Hz, 1H, H-2), 3.95 (dd, *J* = 3.4, 9.1 Hz, 1H, H-3), 3.82–3.73 (m, 2H, H-4, H-5), 3.18 (s, 3H, SO₂CH₃), 2.25 (dq, *J* = 2.8, 7.6 Hz, 2H, CH₂COO), 1.02 ppm (t, *J* = 7.6 Hz, 3H, CH₃). ¹³C NMR (125 MHz, CD₃OD): δ = 175.92 (CO), 158.18, 147.26, 140.19, 134.37, 129.57, 129.03, 128.45, 118.34 (12C, Ar-C), 99.75 (C-1), 73.11 (C-5), 72.39 (C-3), 71.74 (C-2), 68.57 (C-4), 64.75 (C-6), 44.48 (SO₂CH₃), 28.20 (CH₂COO), 9.31 ppm (CH₃). HRMS: *m/z*: calcd. for C₂₂H₂₆NaO₉S [M+Na]⁺: 489.1195, found: 489.1192.

4'-(Methylsulfonyl)-biphenyl-4-yl 6-O-isobutyryl- α -D-mannopyranoside (**5c**)

Prepared according to the general procedure B from **13c** (40 mg, 0.053 mmol) with 25 mg of Pd(OH)₂/C (E101 NE/W, 20% Pd) in EtOH (4 mL). Purified by MPLC on silica gel (DCM–MeOH, 1:0 to 9:1). Yield: 18 mg (70%) as a white oil. [α]_D²⁰ + 109.8 (c 0.85, MeOH).

¹H NMR (500 MHz, CD₃OD): δ = 8.02 (d, *J* = 8.4 Hz, 2H, Ar-H), 7.86 (d, *J* = 8.5 Hz, 2H, Ar-H), 7.68 (d, *J* = 8.7 Hz, 2H, Ar-H), 7.25 (d, *J* = 8.7 Hz, 2H, Ar-H), 5.60 (d, *J* = 1.1 Hz, 1H, H-1), 4.45 (dd, *J* = 1.6, 11.7 Hz, 1H, H-6a), 4.20 (dd, *J* = 7.0, 11.7 Hz, 1H, H-6b), 4.09 (dd, *J* = 1.7, 3.2 Hz, 1H, H-2), 3.95 (dd, *J* = 3.4, 9.1 Hz, 1H, H-3), 3.82–3.72 (m, 2H, H-4, H-5), 3.18 (s, 3H, SO₂CH₃), 2.45 (hept, *J* = 7.0 Hz, 1H, CH(CH₃)₂), 1.06 (d, *J* = 7.0 Hz, 3H, CH₃), 1.02 ppm (d, *J* = 7.0 Hz, 3H, CH₃). ¹³C NMR (125 MHz, CD₃OD): δ = 178.50 (CO), 158.14, 147.26, 140.17, 134.34, 129.60, 129.02, 128.43, 118.29 (12C, Ar-C), 99.61 (C-1), 73.27 (C-5), 72.37 (C-3), 71.71 (C-2), 68.57 (C-4), 64.84 (C-6), 44.48 (SO₂CH₃), 35.12 (CH), 19.23, 19.14 ppm (2 CH₃). HRMS: *m/z*: calcd. for C₂₃H₂₈NaO₉S [M+Na]⁺: 503.1352, found: 503.1353.

4'-(Methylsulfonyl)-biphenyl-4-yl 6-O-butyryl- α -D-mannopyranoside (**5d**)

Prepared according to the general procedure B from **13d** (45 mg, 0.060 mmol) with 40 mg of Pd(OH)₂/C (E101 NE/W, 20% Pd) in EtOH (5 mL). Purified by MPLC on silica gel (DCM–MeOH, 9:1). Yield: 21 mg (72%) as a colorless oil. [α]_D²⁰ + 97.3 (c 1.05, MeOH). ¹H NMR (500 MHz, CD₃OD): δ = 8.01 (d, *J* = 8.5 Hz, 2H, Ar-H), 7.87 (d, *J* = 8.5 Hz, 2H, Ar-H), 7.69 (d, *J* = 8.8 Hz, 2H, Ar-H), 7.24 (d, *J* = 8.8 Hz, 2H, Ar-H), 5.58 (d, *J* = 1.4 Hz, 1H, H-1), 4.43 (dd, *J* = 1.8, 11.7 Hz, 1H, H-6a), 4.20 (dd, *J* = 6.9, 11.7 Hz, 1H, H-6b), 4.08 (dd, *J* = 1.7, 3.3 Hz, 1H, H-2), 3.93 (dd, *J* = 3.4, 9.1 Hz, 1H, H-3), 3.79 (m, 1H, H-5), 3.73 (m, 1H, H-4), 3.17 (s, 3H, SO₂CH₃), 2.21–2.17 (m, 2H, CH₂COO), 1.55–1.47 (m, 2H, CH₂), 0.83 ppm (t, *J* = 7.4 Hz, 3H, CH₃). ¹³C NMR (125 MHz, CD₃OD): δ = 175.09 (CO), 158.18, 147.24, 140.19, 134.31, 129.56, 129.03, 128.43, 118.31 (12C, Ar-C), 99.70 (C-1), 73.17 (C-5), 72.39 (C-3), 71.74 (C-2), 68.59 (C-4), 64.72 (C-6), 44.47 (SO₂CH₃), 36.88 (CH₂COO), 19.29 (CH₃), 13.92 ppm (CH₃). HRMS: *m/z*: calcd. for C₂₃H₂₈NaO₉S [M+Na]⁺: 503.1352, found: 503.1350.

4'-(Methylsulfonyl)-biphenyl-4-yl 6-O-pivaloyl- α -D-mannopyranoside (**5e**)

Prepared according to the general procedure B from **13e** (50 mg, 0.065 mmol) with 15 mg of Pd(OH)₂/C (E101 NE/W, 20% Pd) in EtOH (5 mL). Purified by MPLC on silica gel (DCM–MeOH, 9:1). Yield: 24 mg (73%) as a white oil. [α]_D²⁰ + 96.0 (c 1.18, MeOH). ¹H NMR (500 MHz, CD₃OD): δ = 8.02 (d, *J* = 8.5 Hz, 2H, Ar-H), 7.85 (d, *J* = 8.6 Hz, 2H, Ar-H), 7.68 (d, *J* = 8.7 Hz, 2H, Ar-H), 7.26 (d, *J* = 8.9 Hz, 2H, Ar-H), 5.62 (d, *J* = 1.5 Hz, 1H, H-1), 4.45 (dd, *J* = 1.7, 11.7 Hz, 1H, H-6a), 4.15 (dd, *J* = 7.4, 11.7 Hz, 1H, H-6b), 4.09 (dd, *J* = 1.8, 3.4 Hz, 1H, H-2), 3.96 (dd, *J* = 3.4, 9.2 Hz, 1H, H-3), 3.81 (ddd, *J* = 1.6, 7.4, 9.2 Hz, 1H, H-5), 3.73 (t, *J* = 9.6 Hz, 1H, H-4), 3.18 (s, 3H, SO₂CH₃), 1.07 ppm (s, 9H, C(CH₃)₃). ¹³C NMR (125 MHz, CD₃OD): δ = 179.92 (CO), 158.09, 147.28, 140.16, 134.31, 129.65, 129.03, 128.43, 118.26 (12C, Ar-C), 99.43 (C-1), 73.38 (C-5), 72.35 (C-3), 71.68 (C-2), 68.59 (C-4), 65.14 (C-6), 44.48 (SO₂CH₃), 39.72 (C(CH₃)₃), 27.43 ppm (C(CH₃)₃). HRMS: *m/z*: calcd. for C₂₄H₃₀NaO₉S [M+Na]⁺: 517.1508, found: 517.1507.

4'-(Methylsulfonyl)-biphenyl-4-yl 6-O-isovaleryl- α -D-mannopyranoside (**5f**)

Prepared according to the general procedure B from **13f** (34 mg, 0.044 mmol) with 40 mg of Pd(OH)₂/C (E101 NE/W, 20% Pd) in EtOH (7 mL). Purified by MPLC on silica gel (DCM–MeOH, 9:1). Yield: 12 mg (55%) as a colorless oil. [α]_D²⁰ + 120.3 (c 0.60, MeOH). ¹H NMR (500 MHz, CD₃OD): δ = 8.02 (d, *J* = 8.5 Hz, 2H, Ar-H), 7.88 (d, *J* = 8.5 Hz, 2H, Ar-H), 7.70 (d, *J* = 8.8 Hz, 2H, Ar-H), 7.25 (d, *J* = 8.8 Hz, 2H, Ar-H), 5.58 (d, *J* = 1.3 Hz, 1H, H-1), 4.45 (dd, *J* = 1.6, 11.7 Hz, 1H, H-6a), 4.18 (dd, *J* = 7.0, 11.7 Hz, 1H, H-6b), 4.07 (dd, *J* = 1.7, 3.3 Hz, 1H, H-2), 3.94 (dd, *J* = 3.4, 9.2 Hz, 1H, H-3), 3.79 (m, 1H, H-5), 3.72 (m, 1H, H-4), 3.17 (s, 3H, SO₂CH₃), 2.09 (dd, *J* = 3.0, 7.2 Hz, 2H, CH₂COO), 1.95 (m, 1H, CH(CH₃)₂), 0.83 ppm (app-t, *J* = 6.3 Hz, 6H, 2 CH₃). ¹³C NMR (125 MHz, CD₃OD): δ = 174.55 (CO), 158.20, 147.24, 140.19, 134.28, 129.57, 129.03, 128.42, 118.30 (12C, Ar-C), 99.69 (C-1), 73.25 (C-5), 72.39 (C-3), 71.74 (C-2), 68.60 (C-4), 64.72 (C-6), 44.47 (SO₂CH₃), 44.16 (CH₂COO), 26.67 (CH(CH₃)₂), 22.68, 22.66 ppm (2 CH₃). HRMS: *m/z*: calcd. for C₂₄H₃₀NaO₉S [M+Na]⁺: 517.1508, found: 517.1499.

4'-(Methylsulfonyl)-biphenyl-4-yl 6-O-valeryl- α -D-mannopyranoside (5g)

Prepared according to the general procedure B from **13g** (51 mg, 0.067 mmol) with 40 mg of Pd(OH)₂/C (E101 NE/W, 20% Pd) in EtOH (15 mL). Purified by MPLC on silica gel (DCM–MeOH, 95:5). Yield: 25 mg (76%) as a white solid. $[\alpha]_D^{20} + 111.4$ (c 1.00, MeOH). ¹H NMR (500 MHz, CD₃OD): δ = 7.99 (d, *J* = 8.5 Hz, 2H, Ar-H), 7.85 (d, *J* = 8.5 Hz, 2H, Ar-H), 7.68 (d, *J* = 8.8 Hz, 2H, Ar-H), 7.23 (d, *J* = 8.8 Hz, 2H, Ar-H), 5.56 (d, *J* = 1.4 Hz, 1H, H-1), 4.41 (dd, *J* = 1.8, 11.7 Hz, 1H, H-6a), 4.18 (dd, *J* = 7.0, 11.7 Hz, 1H, H-6b), 4.05 (dd, *J* = 1.7, 3.3 Hz, 1H, H-2), 3.91 (dd, *J* = 3.4, 9.1 Hz, 1H, H-3), 3.77 (m, 1H, H-5), 3.70 (t, *J* = 9.6 Hz, 1H, H-4), 3.15 (s, 3H, SO₂CH₃), 2.21–2.17 (m, 2H, CH₂COO), 1.48–1.42 (m, 2H, CH₂), 1.24–1.17 (m, 2H, CH₂), 0.79 ppm (t, *J* = 7.4 Hz, 3H, CH₃). ¹³C NMR (125 MHz, CD₃OD): δ = 175.26 (CO), 163.63, 158.20, 147.22, 140.20, 134.28, 129.56, 129.02, 128.41, 118.31 (12C, Ar-C), 99.73 (C-1), 73.18 (C-5), 72.40 (C-3), 71.74 (C-2), 68.60 (C-4), 64.75 (C-6), 44.48 (SO₂CH₃), 34.71 (CH₂COO), 27.96, 23.20 (2 CH₂), 13.99 ppm (CH₃). HRMS: *m/z*: calcd. for C₂₄H₃₀NaO₉S [M+Na]⁺: 517.1508, found: 517.1499.

4'-(Methylsulfonyl)-biphenyl-4-yl 6-O-pivaloyloxymethyl- α -D-mannopyranoside (5h)

Prepared according to the general procedure B from **15** (36 mg, 0.045 mmol) with 30 mg of Pd(OH)₂/C (E101 NE/W, 20% Pd) in EtOH (5 mL). Purified by MPLC on silica gel (DCM–MeOH, 95:5). Yield: 10 mg (24%) as a white solid. $[\alpha]_D^{20} + 111.4$ (c 1.00, MeOH). ¹H NMR (500 MHz, CD₃OD): δ = 7.99 (d, *J* = 8.5 Hz, 2H, Ar-H), 7.86 (d, *J* = 8.5 Hz, 2H, Ar-H), 7.67 (d, *J* = 8.8 Hz, 2H, Ar-H), 7.23 (d, *J* = 8.8 Hz, 2H, Ar-H), 5.52 (d, *J* = 1.6 Hz, 1H, H-1), 5.26 (s, 2H, OCH₂O), 4.03 (dd, *J* = 1.8, 3.3 Hz, 1H, H-2), 3.91–3.90 (m, 2H, H-3, H-6a), 3.85 (m, 1H, H-6b), 3.75–3.71 (m, 2H, H-4, H-5), 3.15 (s, 3H, SO₂CH₃), 1.19 ppm (s, 9H, C(CH₃)₃). ¹³C NMR (125 MHz, CD₃OD): δ = 179.44 (CO), 158.49, 147.36, 140.16, 134.45, 129.65, 129.01, 128.50, 118.44 (12C, Ar-C), 100.20 (C-1), 90.45 (OCH₂O), 74.36 (C-5), 72.42 (C-2), 71.83 (C-3), 70.53 (C-6), 68.32 (C-4), 44.48 (SO₂CH₃), 39.92 (C(CH₃)₃), 27.39 ppm (C(CH₃)₃). HRMS: *m/z*: calcd. for C₂₅H₃₂NaO₁₀S [M + Na]⁺: 547.1614, found: 547.1607.

Pharmacokinetic assays

Materials

DMSO, 1-propanol, 1-octanol, Dulbecco's modified Eagle's medium (DMEM) high glucose, penicillin–streptomycin (solution stabilized, with 10 000 units of penicillin/mL and 10 mg of streptomycin/mL), L-glutamine solution (200 mM), magnesium chloride, ammonium acetate, BNPP, and loperamide hydrochloride were purchased from Sigma-Aldrich (St. Louis, Missouri). PRISMA HT universal buffer, GIT-0 Lipid Solution, and Acceptor Sink Buffer were ordered from plon (Woburn, Massachusetts). MEM nonessential amino acids solution 10 mM (100x), fetal bovine serum (FBS), and DMEM without sodium pyruvate and phenol red were bought from Invitrogen (Carlsbad, California). Acetonitrile (MeCN) and MeOH were ordered from Acros Organics (Geel, Belgium). Pooled male RLM (Sprague–Dawley) and pooled HLM were ordered from BD Bioscience (Franklin Lakes, New Jersey). The Caco-2 cells were kindly provided by Prof G. Imanidis, FHNW, Muttentz, Switzerland, and originated from the American Type Culture Collection (Rockville, Maryland).

Log *P* determination

The *in silico* prediction tool ALOGPS³² was used to estimate the octanol–water partition coefficients (log *P*) of the compounds. Depending on these values, the compounds were classified into three categories: hydrophilic compounds (log *P* below zero), moderately lipophilic compounds (log *P* between zero and one) and lipophilic compounds (log *P* above 1). For each category, two different ratios (volume of 1-octanol to volume of buffer) were defined as experimental parameters (Table 2).

Equal amounts of phosphate buffer (0.1 M, pH 7.4) and 1-octanol were mixed and shaken vigorously for 5 min to saturate the

Table 2. Compound classification based on estimated log *P* values.

Compound type	log <i>P</i>	Ratios (1-octanol:buffer)
Hydrophilic	<0	30:140, 40:130
Moderately lipophilic	0–1	70:110, 110:70
Lipophilic	>1	3:180, 4:180

phases. The mixture was left until separation of the two phases occurred, and the buffer was retrieved. Stock solutions of the test compounds were diluted with buffer to a concentration of 1 μ M. For each compound, three determinations per 1-octanol:buffer ratio were performed in different wells of a 96-well plate. The respective volumes of buffer containing analyte (1 μ M) were pipetted to the wells and covered by saturated 1-octanol according to the chosen volume ratio. The plate was sealed with aluminum foil, shaken (1350 rpm, 25 °C, 2 h) on a Heidolph Titramax 1000 plate-shaker (Heidolph Instruments GmbH & Co. KG, Schwabach, Germany), and centrifuged (2000 rpm, 25 °C, 5 min) (5804 R Eppendorf centrifuge, Hamburg, Germany). The aqueous phase was transferred to a 96-well plate for analysis by liquid chromatography – mass spectrometry (LC-MS) (see below).

The log *P* coefficients were calculated from the 1-octanol:buffer ratio (o:b), the initial concentration of the analyte in buffer (1 μ M), and the concentration of the analyte in buffer (*c_B*) with eq. 1:

$$(1) \quad \log P = \log \left(\frac{1 \mu\text{M} - c_B}{c_B} \times \frac{1}{o:b} \right)$$

The average of the three log *P* values per 1-octanol:buffer ratio was calculated. If the two means obtained for a compound did not differ by more than 0.1 unit, the results were accepted.

PAMPA

Effective permeability (log *P_e*) was determined in a 96-well format with PAMPA.¹⁸ For each compound, measurements were performed at pH 7.4 in quadruplicate. Four wells of a deep well plate were filled with 650 μ L of PRISMA HT universal buffer, adjusted to pH 7.4 by adding the requested amount of NaOH (0.5 M). Samples (150 μ L) were withdrawn from each well to determine the blank spectra by UV/Vis-spectroscopy (190–500 nm) (SpectraMax 190, Molecular Devices, Silicon Valley, California). Then, analyte dissolved in DMSO (10 mM) was added to the remaining buffer to yield 50 μ M solutions. To exclude precipitation, the optical density (OD) was measured at 650 nm, and solutions exceeding OD 0.01 were filtrated. Afterwards, samples (150 μ L) were withdrawn to determine the reference spectra. A further 200 μ L was transferred to each well of the donor plate of the PAMPA sandwich (plon, P/N 110 163). The filter membranes at the bottom of the acceptor plate were infused with 5 μ L of GIT-0 Lipid Solution and 200 μ L of Acceptor Sink Buffer was filled into each acceptor well. The sandwich was assembled, placed in the GutBoxTM, and left undisturbed for 16 h. Then, it was disassembled and samples (150 μ L) were transferred from each donor and acceptor well to UV plates for determination of the UV/Vis spectra. Effective permeability (log *P_e*) was calculated from the compound flux deduced from the spectra, the filter area, and the initial sample concentration in the donor well with the aid of the PAMPA Explorer Software (plon, version 3.5).

Caco-2 cell permeation assay

Caco-2 cells were cultivated in tissue culture flasks (BD Biosciences, Franklin Lakes, New Jersey) with DMEM high glucose medium containing L-glutamine (2 mM), nonessential amino acids (0.1 mM), penicillin (100 U/mL), streptomycin (100 μ g/mL), and FBS (10%). The cells were kept at 37 °C in humidified air containing 5% CO₂, and the medium was changed every second day. When ap-

proximately 90% confluence was reached, the cells were split in a 1:10 ratio and distributed to new tissue culture flasks. At passage numbers between 60 and 65, they were seeded at a density of 5.3×10^5 cells/well to Transwell 6-well plates (Corning Inc., Corning, New York) with 2.5 mL of culture medium in the basolateral and 2 mL in the apical compartment. The medium was renewed on alternate days. Permeation experiments were performed between days 19 and 21 postseeding. Previously to the experiment, the integrity of the Caco-2 monolayers was evaluated by measuring the transepithelial electrical resistance (TEER) with an Endohm tissue resistance instrument (World Precision Instruments Inc., Sarasota, Florida). Only wells with TEER values higher than $250 \Omega \cdot \text{cm}^2$ were used. To inhibit CES activity, the Caco-2 cell monolayers were pre-incubated with BNPP (200 μM) dissolved in transport medium (DMEM without sodium pyruvate and phenol red) for 40 min.^{22b} Experiments were performed in the apical-to-basolateral (absorptive) and basolateral-to-apical (secretory) directions in triplicate. Transport medium was withdrawn from the donor compartments and replaced by the same volume of compound stock solution (10 mM in DMSO) to reach an initial sample concentration of 62.5 μM . The Transwell plate was shaken (600 rpm, 37 °C) on a Heidolph Titramax 1000 plate-shaker. Samples (40 μL) were withdrawn from the donor and acceptor compartments 30 min after initiation of the experiment and the concentrations were determined by LC-MS (see below). Apparent permeability (P_{app}) was calculated according to eq. 2:

$$(2) \quad P_{\text{app}} = \frac{dQ}{dt} \times \frac{1}{A \times c_0}$$

where dQ/dt is the compound flux (mol s^{-1}), A is the surface area of the monolayer (cm^2), and c_0 is the initial concentration in the donor compartment (mol cm^{-3}).³³ After the experiment, TEER values were measured again and results from wells with values below $250 \Omega \cdot \text{cm}^2$ were discarded.

Aqueous solubility

Solubility was determined in a 96-well format using the μSOL Explorer solubility analyzer (pion, version 3.4.0.5). For each compound, measurements were performed in triplicate. Three wells of a deep well plate were filled with 300 μL of PRISMA HT universal buffer, adjusted to pH 7.4 by adding the requested amount of NaOH (0.5 M). Aliquots (3 μL) of a compound stock solution (40–100 mM in DMSO) were added and thoroughly mixed. The final sample concentration was 0.4–1.0 mM and the residual DMSO concentration was 1.0% (v/v). Fifteen hours after initiation of the experiment, the solutions were filtrated (0.2 μm 96-well filter plates) using a vacuum to collect manifold (Whatman Ltd., Maidstone, UK) to remove any precipitates. Equal amounts of filtrate and 1-propanol were mixed and transferred to a 96-well plate for UV detection (190–500 nm). The amount of material dissolved was calculated by comparison with UV spectra obtained from reference samples, which were prepared by dissolving compound stock solution in a 1:1 mixture of buffer and 1-propanol (final concentrations 0.067–0.167 mM).

Enzymatic hydrolysis by liver microsome associated CES

Incubations were performed in triplicate in a 96-well format on an Eppendorf Thermomixer Comfort. The reaction mixture (270 μL) consisting of liver microsomes (0.139 $\mu\text{g/mL}$), TRIS-HCl buffer (0.1 M, pH 7.4), and MgCl_2 (2 mM) was preheated (37 °C, 500 rpm, 10 min), and the incubation was initiated by adding 30 μL of compound solution (20 μM) in TRIS-HCl buffer. The final concentration of the compound was 2 μM , and the microsomal concentration was 0.125 mg/mL . At the beginning of the experiment ($t = 0$ min) and after an incubation time of 2, 5, 10, 20, and 30 min, samples (40 μL) were transferred to 120 μL of ice-cooled

MeOH and centrifuged (3700 rpm, 4 °C, 10 min). Then, 80 μL of supernatant was transferred to a 96-well plate for analysis by LC-MS (see below). The metabolic half-life ($t_{1/2}$) was calculated from the slope of the linear regression from the log percentage remaining compound versus incubation time relationship. Control experiments were performed in parallel by preincubating the microsomes with the specific CES inhibitor BNPP (1 mM) for 5 min before addition of the compound solution.²⁰

Isozyme specific inhibition of CES-mediated hydrolysis

Test compounds were dissolved in DMSO to 1 mM and then diluted with TRIS-HCl buffer (0.1 M, pH 7.4) containing MgCl_2 (2 mM) to a concentration of 6 μM . Loperamide hydrochloride was dissolved in DMSO to 20, 2, and 0.2 mM and then diluted with TRIS-HCl buffer containing MgCl_2 to a concentration of 750, 75, and 7.5 μM . HLM were suspended in TRIS-HCl buffer containing MgCl_2 to a concentration of 30 $\mu\text{g/mL}$. Compound solution (100 μL) and microsomal suspension (200 μL) mixed with loperamide solution or blank buffer (50 μL) were preheated (37 °C, 500 rpm, 15 min) in separate wells of a 96-well plate. The incubation was initiated by transferring 200 μL of microsome suspension containing loperamide to the compound solution. The final compound concentration was 2 μM , the microsomal concentration was 0.02 mg/mL , and the loperamide concentration was 100, 10, 1, and 0 μM (blank). At the beginning of the experiment ($t = 0$ min) and after an incubation time of 10, 20, 30, 45, and 60 min, samples (20 μL) were transferred to 60 μL of ice-cooled MeOH and analyzed by LC-MS (see below). The metabolic turnover was assessed as accumulation of product **4a** versus incubation time.³⁰

LC-MS measurements

Analyses were performed using a 1100/1200 Series HPLC system coupled to a 6410 Triple Quadrupole mass detector (Agilent Technologies, Inc., Santa Clara, California) equipped with electrospray ionization. The system was controlled with the Agilent MassHunter Workstation Data Acquisition software (version B.01.04). The column used was an Atlantis® T3 C18 column (2.1 \times 50 mm) with a 3 μm particle size (Waters Corp., Milford, Massachusetts). The mobile phase consisted of eluent A (10 mM ammonium acetate, pH 5.0 in 95:5 H_2O -MeCN) and eluent B (MeCN containing 0.1% formic acid). The flow rate was maintained at 0.6 mL/min. The gradient was ramped from 95% A – 5% B to 5% A – 95% B over 1 min and then held at 5% A – 95% B for 0.1 min. The system was then brought back to 95% A – 5% B, resulting in a total duration of 4 min. MS parameters such as fragmentor voltage, collision energy, and polarity were optimized individually for each drug, and the molecular ion was followed for each compound in the multiple reaction monitoring mode. The concentrations of the analytes were quantified by the Agilent Mass Hunter Quantitative Analysis software (version B.01.04).

Supplementary material

Supplementary material is available with the article through the journal Web site at <http://nrcresearchpress.com/doi/suppl/10.1139/cjc-2015-0582>. NMR spectra and HPLC traces to document purity of the test compounds.

Acknowledgement

Financial support from the Swiss National Science Foundation (SNF 200020-129935) is gratefully acknowledged.

References

- (1) (a) Fihn, S. D. *N. Engl. J. Med.* **2003**, 349, 259. doi:10.1056/NEJMc030027; (b) Hooton, T. M.; Besser, R.; Foxman, B.; Fritzsche, T. R.; Nicolle, L. E. *Clin. Infect. Dis.* **2004**, 39, 75. doi:10.1086/422145.
- (2) Sanchez, G. V.; Master, R. N.; Karlowsky, J. A.; Bordon, J. M. *Antimicrob. Agents Chemother.* **2012**, 56, 2181. doi:10.1128/AAC.06060-11.
- (3) Schilling, J. D.; Mulvey, M. A.; Hultgren, S. J. *J. Infect. Dis.* **2001**, 183 (Suppl. 1), S36. doi:10.1086/318855.

- (4) Capitani, G.; Eidam, O.; Glockshuber, R.; Grütter, M. G. *Microbes Infect.* **2006**, *8*, 2284. doi:10.1016/j.micinf.2006.03.013.
- (5) (a) Sharon, N. *Biochim. Biophys. Acta* **2006**, *1760*, 527. doi:10.1016/j.bbagen.2005.12.008; (b) Le Trong, L.; Aprikian, P.; Kidd, B. A.; Forero-Shelton, M.; Tchesnokova, V.; Rajagopal, P.; Rodriguez, V.; Interlandi, G.; Klevit, R.; Vogel, V.; Stenkamp, R. E.; Sokurenko, E. V.; Thomas, W. E. *Cell* **2010**, *141*, 645. doi:10.1016/j.cell.2010.03.038.
- (6) (a) Firon, N.; Ofek, I.; Sharon, N. *Biochem. Biophys. Res. Commun.* **1982**, *105*, 1426. doi:10.1016/0006-291X(82)90947-0; (b) Firon, N.; Ofek, I.; Sharon, N. *Carbohydr. Res.* **1983**, *120*, 235. doi:10.1016/0008-6215(83)88019-7; (c) Firon, N.; Ashkenazi, S.; Mirelman, D.; Ofek, I.; Sharon, N. *Infect. Immun.* **1987**, *55*, 472.
- (7) (a) Bouckaert, J.; Berglund, J.; Schembri, M.; Genst, E. D.; Cools, L.; Wührer, M.; Hung, C. S.; Pinkner, J.; Slättergard, R.; Zavialov, A.; Choudhury, D.; Langermann, S.; Hultgren, S. J.; Wyns, L.; Klemm, P.; Oscarson, S.; Knight, S. D.; Greve, H. D. *Mol. Microbiol.* **2005**, *55*, 441. doi:10.1111/j.1365-2958.2004.04415.x; (b) Sperling, O.; Fuchs, A.; Lindhorst, T. K. *Org. Biomol. Chem.* **2006**, *4*, 3913. doi:10.1039/b610745a; (c) Han, Z.; Pinkner, J. S.; Ford, B.; Obermann, R.; Nolan, W.; Wildman, S. A.; Hobbs, D.; Ellenberger, T.; Cusumano, C. K.; Hultgren, S. J.; Janetka, J. W. *J. Med. Chem.* **2010**, *53*, 4779. doi:10.1021/jm100438s; (d) Klein, T.; Abgottspon, D.; Wittwer, M.; Rabbani, S.; Herold, J.; Jiang, X.; Kleeb, S.; Lüthi, C.; Scharenberg, M.; Bezençon, J.; Gubler, E.; Pang, L.; Smiesko, M.; Cutting, B.; Schwardt, O.; Ernst, B. *J. Med. Chem.* **2010**, *53*, 8627. doi:10.1021/jm101011y; (e) Schwardt, O.; Rabbani, S.; Hartmann, M.; Abgottspon, D.; Wittwer, M.; Kleeb, S.; Zalewski, A.; Smiesko, M.; Cutting, B.; Ernst, B. *Bioorg. Med. Chem.* **2011**, *19*, 6454. doi:10.1016/j.bmc.2011.08.057; (f) Cusumano, C. K.; Pinkner, J. S.; Han, Z.; Greene, S. E.; Ford, B. A.; Crowley, J. R.; Henderson, J. P.; Janetka, J. W.; Hultgren, S. J. *Sci. Transl. Med.* **2011**, *3*, 109ra115. doi:10.1126/scitranslmed.3003021; (g) Han, Z.; Pinkner, J. S.; Ford, B.; Chorem, E.; Crowley, J. M.; Cusumano, C. K.; Campbell, S.; Henderson, J. P.; Hultgren, S. J.; Janetka, J. W. *J. Med. Chem.* **2012**, *55*, 3945. doi:10.1021/jm300165m; (h) Jiang, X.; Abgottspon, D.; Kleeb, S.; Rabbani, S.; Scharenberg, M.; Wittwer, M.; Haug, M.; Schwardt, O.; Ernst, B. *J. Med. Chem.* **2012**, *55*, 4700. doi:10.1021/jm300192x; (i) Pang, L.; Kleeb, S.; Lemme, K.; Rabbani, S.; Scharenberg, M.; Zalewski, A.; Schädler, F.; Schwardt, O.; Ernst, B. *ChemMedChem* **2012**, *7*, 1404. doi:10.1002/cmdc.201200125.
- (8) (a) Smith, D. A.; Jones, B. C.; Walker, D. K. *Med. Res. Rev.* **1996**, *16*, 243. doi:10.1002/(SICI)1098-1128(199605)16:3<243::AID-MED2>3.3.CO;2-R; (b) van de Waterbeemd, H.; Smith, D. A.; Beaumont, K.; Walker, D. K. *J. Med. Chem.* **2001**, *44*, 1313. doi:10.1021/jm000407e.
- (9) Feng, B.; LaPerle, J. L.; Chang, G.; Varma, M. V. *Expert Opin. Drug Metab. Toxicol.* **2010**, *6*, 939. doi:10.1517/17425255.2010.482930.
- (10) Kleeb, S.; Pang, L.; Mayer, K.; Eris, D.; Sigl, A.; Preston, R. C.; Zihlmann, P.; Sharpe, T.; Jakob, R. P.; Abgottspon, D.; Hutter, A. S.; Scharenberg, M.; Jiang, X.; Navarra, G.; Rabbani, S.; Smiesko, M.; Lüdin, N.; Bezençon, J.; Schwardt, O.; Maier, T.; Ernst, B. *J. Med. Chem.* **2015**, *58*, 2221. doi:10.1021/jm501524q.
- (11) (a) Saxon, E.; Bertozzi, C. R. *Science* **2000**, *287*, 2007. doi:10.1126/science.287.5460.2007; (b) Sarkar, A. K.; Fritz, T. A.; Taylor, W. H.; Esko, J. D. *Proc. Natl. Acad. Sci. U.S.A.* **1995**, *92*, 3323. doi:10.1073/pnas.92.8.3323.
- (12) Fokt, I.; Skora, S.; Conrad, C.; Madden, T.; Emmett, M.; Priebe, W. *Carbohydr. Res.* **2013**, *368*, 111. doi:10.1016/j.carres.2012.11.021.
- (13) Prieto, M.; Zurita, E.; Rosa, E.; Muñoz, L.; Lloyd-Williams, P.; Giral, E. *J. Org. Chem.* **2004**, *69*, 6812. doi:10.1021/jo0491612.
- (14) Pojer, P. M.; Angyal, S. J. *Aust. J. Chem.* **1978**, *31*, 1031. doi:10.1071/CH9781031.
- (15) Ali, A.; van den Berg, R. J. B. H. N.; Overkleeft, H. S.; van der Marel, G. A.; Codee, J. D. C. *Tetrahedron* **2010**, *32*, 6121. doi:10.1016/j.tet.2010.06.007.
- (16) Avdeef, A. In *Pharmacokinetic Optimization in Drug Research: Biological, Physicochemical and Computational Strategies*; Testa, B., van de Waterbeemd, H., Folkers, G., Guy, R., Eds.; Helvetica Chimica Acta: Zurich, 2001; pp. 305–326.
- (17) Dearden, J. C.; Bresnen, G. M. *QSAR Comb. Sci.* **1988**, *7*, 133.
- (18) Kansy, M.; Sennner, F.; Gubernator, K. *J. Med. Chem.* **1998**, *41*, 1007. doi:10.1021/jm970530e.
- (19) Artursson, P.; Karlsson, J. *Biochem. Biophys. Res. Commun.* **1991**, *175*, 880. doi:10.1016/0006-291X(91)91647-U.
- (20) (a) Imai, T.; Taketani, M.; Shii, M.; Hosokawa, M.; Chiba, K. *Drug Metab. Dispos.* **2006**, *34*, 1734. doi:10.1124/dmd.106.009381; (b) Taketani, M.; Shii, M.; Ohura, K.; Ninomiya, S.; Imai, T. *Life Sci.* **2007**, *81*, 924. doi:10.1016/j.lfs.2007.07.026.
- (21) Avdeef, A.; Bendels, S.; Di, L.; Faller, B.; Kansy, M.; Sugano, K.; Yamauchi, Y. *J. Pharm. Sci.* **2007**, *96*, 2893. doi:10.1002/jps.21068.
- (22) (a) Imai, T.; Imoto, M.; Sakamoto, H.; Hashimoto, M. *Drug Metab. Dispos.* **2005**, *33*, 1185. doi:10.1124/dmd.105.004226; (b) Ohura, K.; Sakamoto, H.; Ninomiya, S.; Imai, T. *Drug Metab. Dispos.* **2010**, *38*, 323. doi:10.1124/dmd.109.029413.
- (23) Seelig, A.; Gerebtzoff, G. *Expert Opin. Drug. Metab. Toxicol.* **2006**, *2*, 733. doi:10.1517/17425255.2.5.733.
- (24) Lipinski, C. A. *J. Pharmacol. Toxicol. Methods* **2000**, *44*, 235. doi:10.1016/S1056-8719(00)00107-6.
- (25) (a) Beaumont, K.; Webster, R.; Gardner, I.; Dack, K. *Curr. Drug Metab.* **2003**, *4*, 461. doi:10.2174/1389200033489253; (b) Ettmayer, P.; Amidon, G. L.; Clement, B.; Testa, B. *J. Med. Chem.* **2004**, *47*, 2393. doi:10.1021/jm0303812.
- (26) Nielsen, A. B.; Buur, A.; Larsen, C. *Eur. J. Pharm. Sci.* **2005**, *24*, 433. doi:10.1016/j.ejps.2004.12.007.
- (27) Evans, D. F.; Pye, G.; Bramley, R.; Clark, A. G.; Dyson, T. J.; Hardcastle, J. D. *Gut* **1988**, *29*, 1035. doi:10.1136/gut.29.8.1035.
- (28) (a) Li, B.; Sedlacek, M.; Manoharan, I.; Boopathy, R.; Duysen, E. G.; Masson, P.; Lockridge, O. *Biochem. Pharmacol.* **2005**, *70*, 1673. doi:10.1016/j.bcp.2005.09.002; (b) Liederer, B. M.; Borchardt, R. T. *J. Pharm. Sci.* **2006**, *95*, 1177. doi:10.1002/jps.20542.
- (29) Satoh, T.; Hosokawa, M. *Chem. Biol. Interact.* **2006**, *162*, 195. doi:10.1016/j.cbi.2006.07.001.
- (30) (a) Quinney, S. K.; Sanghani, S. P.; Davis, W. I.; Hurley, T. D.; Sun, Z.; Murry, D. J.; Bosron, W. F. *J. Pharmacol. Exp. Ther.* **2005**, *313*, 1011. doi:10.1124/jpet.104.081265; (b) Wang, J.; Williams, E. T.; Bourgea, J.; Wong, Y. N.; Patten, C. J. *Drug Metab. Dispos.* **2011**, *39*, 1329. doi:10.1124/dmd.111.039628.
- (31) Roy, R.; Das, S. K.; Santoyo-González, F.; Hernández-Mateo, F.; Dam, T. K.; Brewer, C. F. *Chem. Eur. J.* **2000**, *6*, 1757. doi:10.1002/(SICI)1521-3765(20000515)6:10<1757::AID-CHEM1757>3.0.CO;2-5.
- (32) (a) VCCLAB, Virtual Computational Chemistry Laboratory, 2005; available from <http://www.vcclab.org> (accessed November 19, 2012); (b) Tetko, I. V.; Gasteiger, J.; Todeschini, R.; Mauri, A.; Livingstone, D.; Ertl, P.; Palyulin, V. A.; Radchenko, E. V.; Zefirov, N. S.; Makarenko, A. S.; Tanchuk, V. Y.; Prokopenko, V. V. *J. Comput. Aided Mol. Des.* **2005**, *19*, 453. doi:10.1007/s10822-005-8694-y.
- (33) Hubatsch, I.; Ragnarsson, E. G. E.; Artursson, P. *Nat. Protoc.* **2007**, *2*, 2111. doi:10.1038/nprot.2007.303.

2.3 Chapter 3: Antagonists Targeting the Arg98 Residue of FimH Adhesin

The following chapter describes our approach to establish a stable interaction with Arg98 of the FimH protein using elongated fragments attached via amide bond to the terminal ring of biaryl mannosides. The involvement of Arg98 to binding was evaluated by comparing activities of obtained antagonists towards the wild type and R98A mutant of FimH. Furthermore, the physicochemical properties of the new antagonists were determined.

Contribution to the project:

Wojciech Schönemann designed and synthesized all, previously not reported, FimH antagonists described in this chapter. Furthermore, he is responsible for the writing of the entire chapter.

Dr. Simon Kleeb and Dr. Jacqueline Bezençon determined physicochemical properties of new FimH antagonists. Dr. Said Rabbani measured affinity of new FimH antagonists in competitive binding assay.

Abbreviations: UPEC, uropathogenic *Escherichia coli*; UTI, urinary tract infection; CRD, carbohydrate-recognition domain; P , octanol-water partition coefficient; P_{app} , apparent permeability; P_e , effective permeability; PAMPA, parallel artificial membrane permeability assay.

Introduction

Urinary tract infections (UTIs) are among the most common bacterial infections worldwide. Millions of people suffer from UTI, in particular women.^[1] More than 25% suffering from UTI will experience a recurrent infection within six months.^[2] This makes UTIs a serious medical and economical issue.^[3] Uropathogenic *Escherichia coli* (UPEC) are the most prevalent causative factor of UTI accounting for 70-95% of the reported cases.^[4] The frequent use of antimicrobials led to increased antibiotic-resistance making alternative treatment strategies a pressing need.^[5]

UPEC employ adhesin FimH located on the tip of their type 1 pili to attach to urothelia cells of the host and to induce the infection.^[6,7] In addition, adherent bacteria cannot be removed from the bladder by the bulk flow of urine. The high-mannosylated glycoprotein uroplakin 1a (UP1a) expressed on urothelial cells is a natural ligand for the carbohydrate recognition domain (CRD) of FimH.^[8] Therefore, carbohydrate mimetics capable of blocking the adherence of UPEC can be employed as anti-adhesive drugs substituting antibiotics in the treatment of UTI.

Almost three decades ago, Sharon and co-workers reported several aryl mannosides capable of inhibiting yeast agglutination in the presence of *E. coli*.^[9-11] In the following decades, numerous high-affinity monovalent^[12-23] and multivalent^[24-30] FimH antagonists were synthesized. All FimH antagonists consist of a mannose moiety interacting with a negatively charged pocket of FimH-CRD and a lipophilic aglycone interacting with so called tyrosine gate composed of Tyr48, Ile52 and Tyr137. It was postulated that Arg98 could also contribute to the binding in the case of biphenyl α -D-mannosides bearing an appropriate substituent in *meta*-position of the outer phenyl ring by forming hydrogen bonds or a salt bridge with the guanidine of Arg98 (Figure 1A).^[16] However, in a first published example with a methyl carboxylate directly linked to the *meta*-position of the outer aromatic ring of the biphenyl aglycone (\rightarrow **1**) the geometry of the hydrogen bond deduced from the crystal structure (PDB ID: 3MCY) is unfavorable to form a strong interaction. Moreover, a carboxylic acid located in the same position being capable of establishing strong electrostatic interactions reduced the affinity.

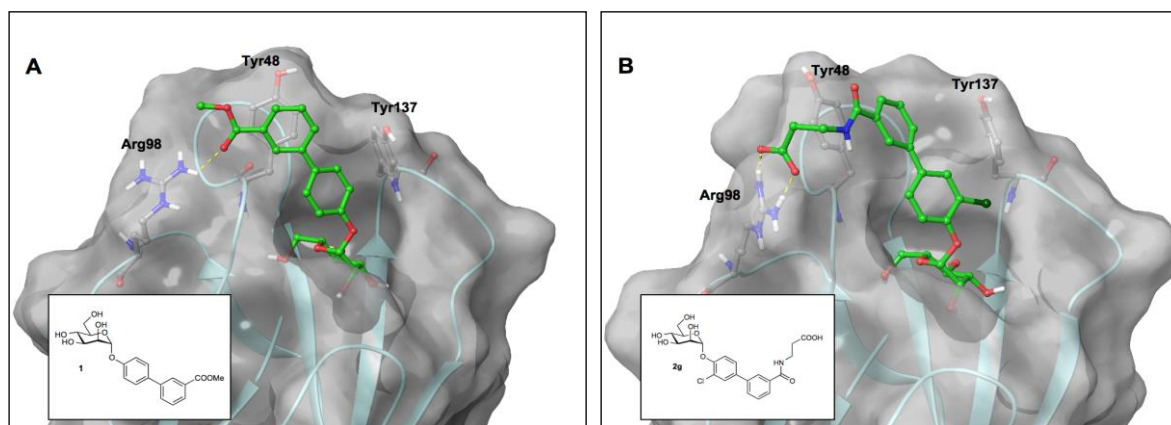


Figure 1. A) Crystal structure of **1** co-crystallized with the FimH lectin domain (PDB ID: 3MCY);^[12] B) Binding mode of amino acid derivative **2g** stabilized by a salt bridge with Arg98 as observed in MD simulation.^[31]

This obviously contradictory result encouraged us to investigate the role of Arg98 in binding FimH antagonists in more detail. Pang *et al.* previously reported on biphenyl mannosides containing an elongated carboxylate side chain in *para*-position designed to reach Arg98.^[20] However, this modification led to a reduction of the affinity. To establish stable interactions with Arg98, we expanded this approach by introducing linear amino acids of different lengths in *meta*- and *para*-position (e.g. **2g**, Figure 1B) as well as substituting a terminal phenyl by pyrrole ring. Moreover, we replaced carboxylate by other groups capable of accepting hydrogen bond, i.e. pyridine derivatives and hydroxyl-bearing fragments (Figure 2). The antagonists most successful in the binding assay with wild type FimH were also tested with the R98A mutant. Since all antagonists bind to wild type FimH with nanomolar affinity, we evaluated physicochemical properties of these compounds or their ester prodrugs in order to estimate their potential use as orally bioavailable drugs.

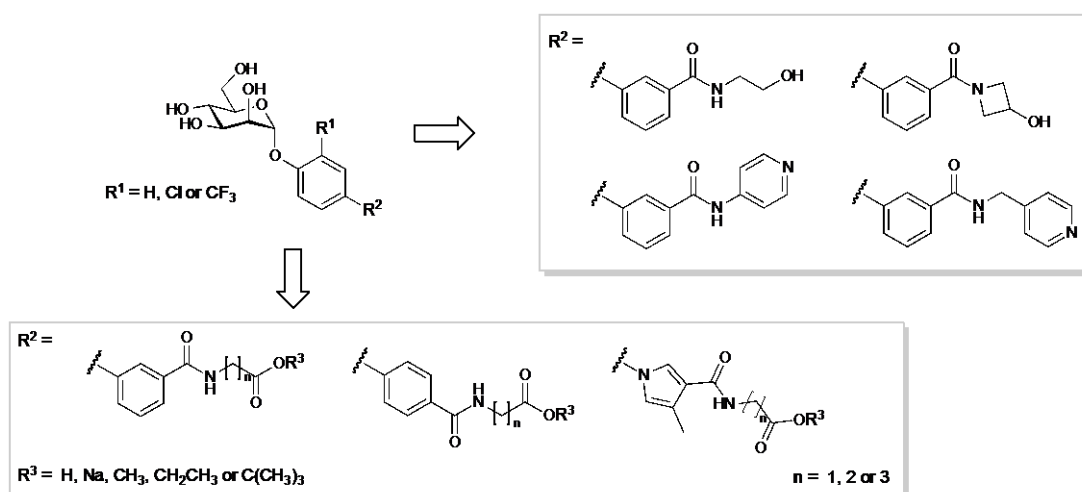
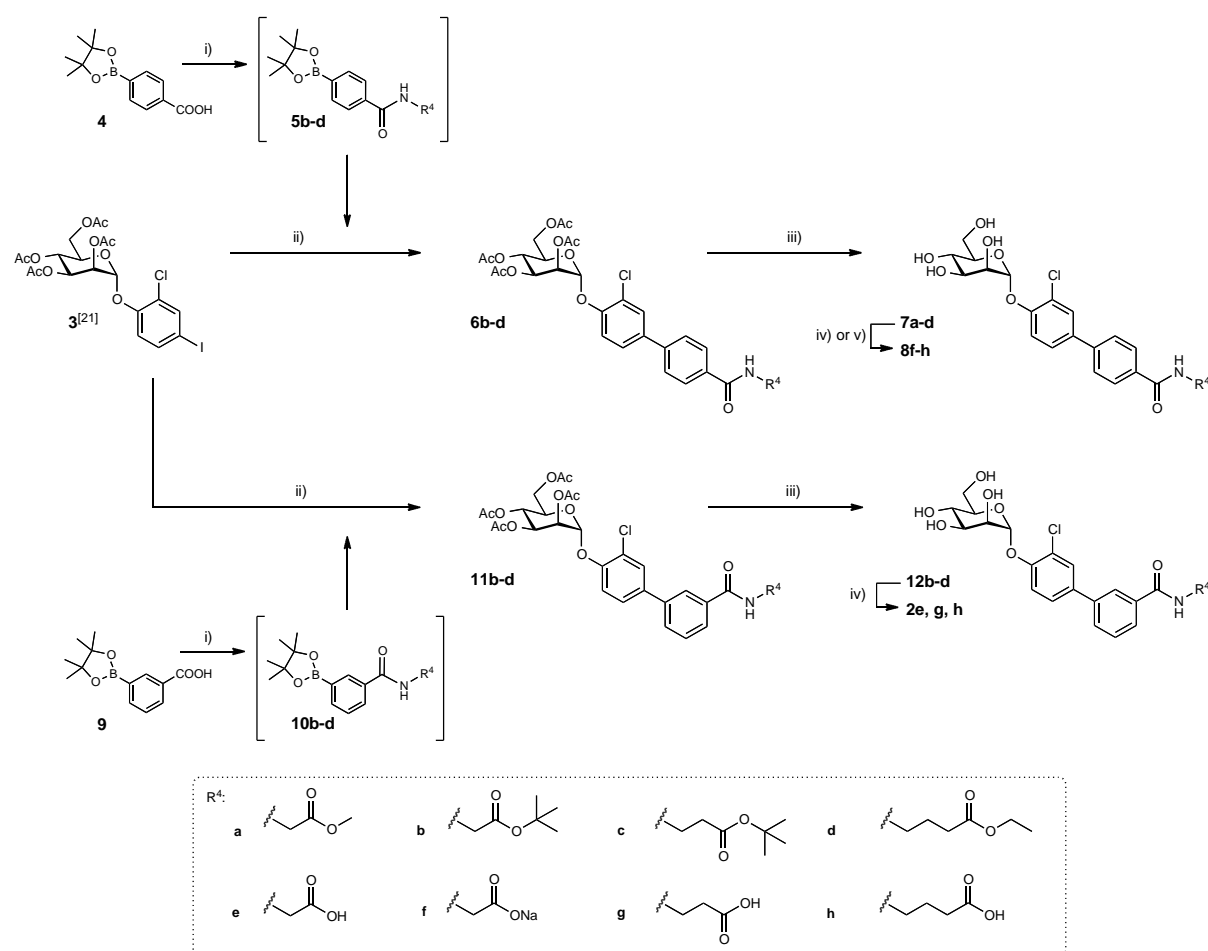


Figure 2. Modifications of the aglycone of a FimH antagonist introduced in order to establish new interactions with Arg98.

Results and Discussion

Synthesis

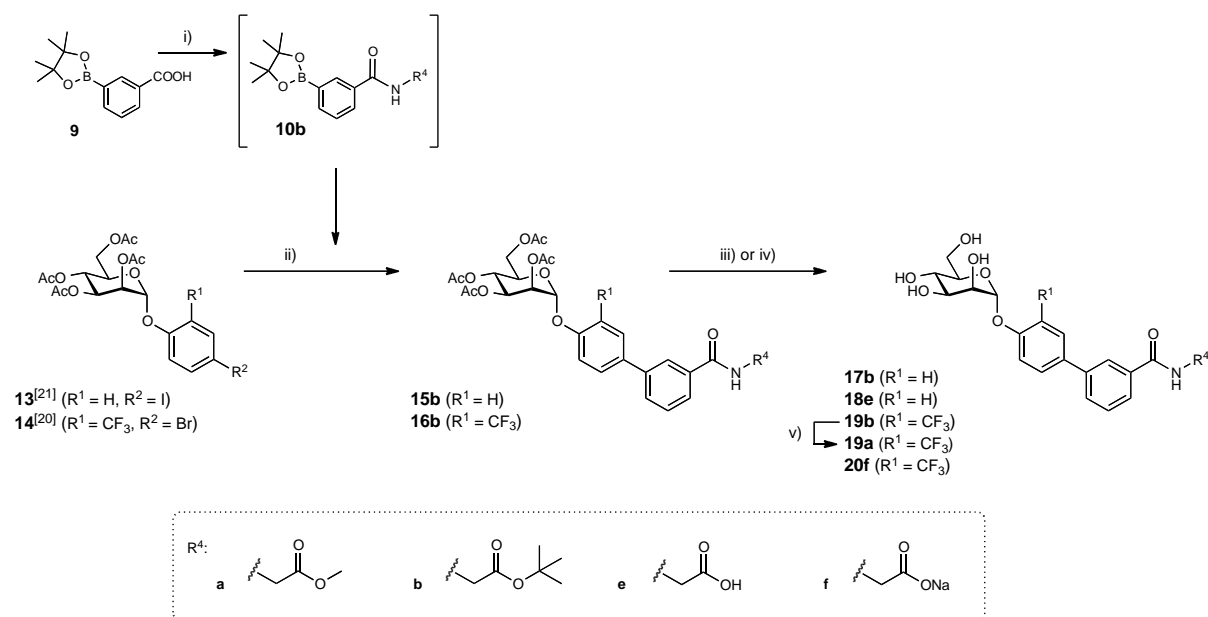
Commercially available boronates **4** and **9** were coupled with corresponding protected amino acids using COMU reagent to yield the boronate amide intermediates **5b-d** and **10b-d**, respectively. The boronate derivatives underwent directly Suzuki cross-coupling reaction^[32] with peracetylated mannoside **3**^[21] affording the protected biphenyl mannosides **6b-d** and **11b-d** in moderate yields (Scheme 1). In order to avoid transesterification on the aglycone, a mixture of the corresponding alcohol and alkoxide in chloroform were used for deprotection (\rightarrow **7b-d**, **12b-d**). Additionally, compound **6b** underwent transesterification with MeONa/MeOH to obtain methyl ester **7a**. Saponification of the resulting prodrugs **7a**, **7c**, **7d** and **12b-d** gave the test compounds **8f-h** and **2e, g, h**, respectively.



Scheme 1. i) $R^4-NH_2 \cdot HCl$, COMU, DIPEA, DMF or MeCN, rt, 3-20 h; ii) $PdCl_2(dppf) \cdot CH_2Cl_2$, K_3PO_4 , DMF, 80 °C, 3-21 h, 34-66%; iii) MeONa/MeOH, EtONa/EtOH or *t*-BuOK/*t*-BuOH, $CHCl_3$, rt, 1.5-35 h, 42-65%; iv)

1. aq. NaOH, MeOH, rt, 2-6 h; 2. Amberlyst-15 (H⁺), 43-61% for **2e**, **2g**, **2h**, **8g**, **8h**; v) aq. NaOH, MeOH, rt, 0.5 h, 86% for **8f**.

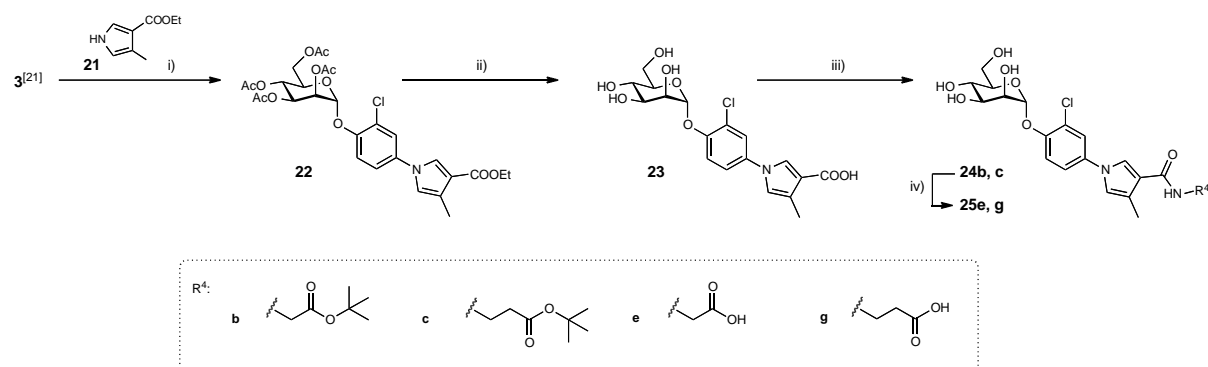
A similar strategy was applied to the synthesis of **18e** and **20f** (Scheme 2). First, **9** was coupled with glycine *tert*-butyl ester followed by a Suzuki coupling reaction with **13**^[21] and **14**^[20] to yield **15b** and **16b**, respectively. Deacetylation was achieved with potassium *tert*-butoxide in *tert*-butanol. These reaction conditions resulted in the formation of *tert*-butyl ester prodrugs **17b** and **19b** as well as active principles **18e** and **20f**. The ester cleavage might have occurred via E2 elimination of isobutylene by potassium *tert*-butoxide. Transesterification of **19b** with MeONa/MeOH gave methyl ester **19a** in moderate yield.



Scheme 2. i) R⁴-NH₂·HCl, COMU, DIPEA, DMF, rt, 3-7 h; ii) PdCl₂(dppf)·CH₂Cl₂, K₃PO₄, DMF, 80 °C, 19-20 h, 49-72%; iii) 1. *t*-BuOK/*t*-BuOH, rt, 1.5-3 h; 2. Amberlyst-15 (H⁺), 36-44% for **17b**, **18e**, **19b**; iv) 1. *t*-BuOK/*t*-BuOH, rt, 1.5-3 h; 2. Amberlyst-15 (H⁺); 3. 0.5 M NaOH, 31% for **20f**; v) MeONa/MeOH, rt, 1.5 h, 65%.

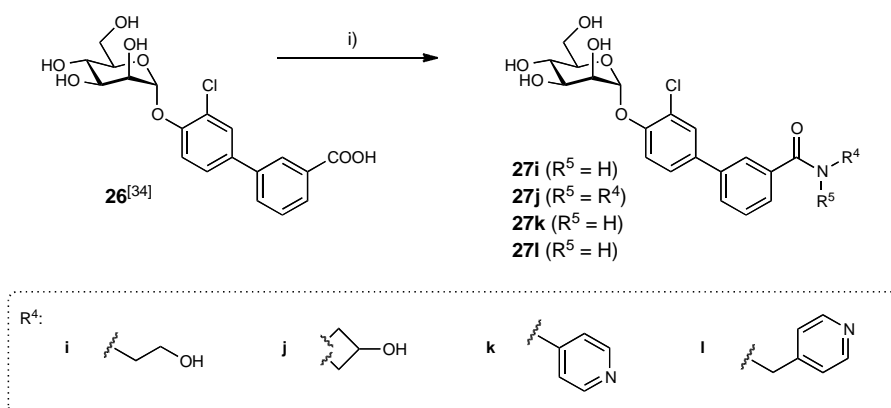
The synthesis of pyrrole-containing analogue of **2e** and **2g** is depicted in Scheme 3. Commercially available pyrrole **21** was coupled with mannoside **3**^[21] in copper-diamine-catalyzed *N*-arylation^[33] followed by reprotection of the sugar moiety by acetylation to give **22** in a good yield. After treatment with MeONa/MeOH followed by an aqueous solution of sodium hydroxide, fully deprotected **23** was obtained. The compound **23** was then coupled with glycine *tert*-butyl ester and β-alanine *tert*-butyl ester by means of COMU reagent to

afford **24b** and **24c**. Subsequently, the ester prodrugs were saponified to yield test compounds **25e** and **25g**.



Scheme 3. i) 1. CuI, *trans*-1,2-diaminocyclohexane, K_3PO_4 , 1,4-dioxane, 100 °C, 19 h; 2. Ac_2O , pyridine, 60 °C, 2 h, 88%; ii) 1. MeONa/MeOH, rt, 1.5 h; 2. aq. NaOH, MeOH, rt, 15.5 h; 3. AcOH, 26%; iii) $R^4\text{-NH}_2\cdot\text{HCl}$, COMU, DIPEA or TEA, DMF, rt, 16 h, 45-52%; iv) 1. aq. NaOH, MeOH, rt, 16 h; 2. AcOH, 63%.

In order to study different hydrogen bond acceptors in *meta*-position, additional amide derivatives were synthesized (Scheme 4). Previously described **26**^[34] was treated with corresponding amines and COMU reagent. The crude products were purified by preparative HPLC. The desired test compounds **27i-l** were obtained in moderate to good yields.



Scheme 4. i) $R^4\text{-NH}_2$ or $R^4\text{-NH}\cdot\text{HCl}$, COMU, DIPEA or TEA, DMF, rt, 5-15 h, 55-83%.

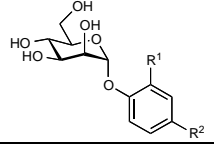
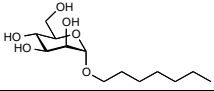
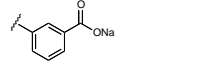
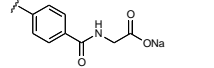
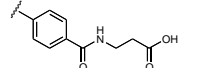
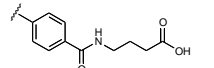
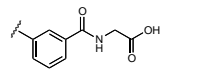
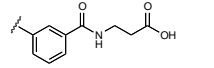
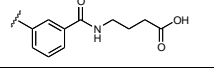
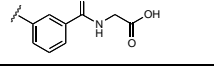
Binding affinity

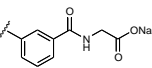
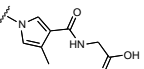
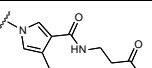
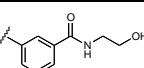
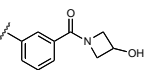
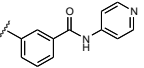
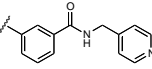
The binding properties of the amino acid-substituted biaryl α -D-mannopyranosides **2e**, **2g**, **2h**, **8f-h**, **18e**, **20f**, **25e**, **25g** and the amide derivatives **27i-l** were determined in a cell-free

competitive binding assay with the wild type FimH-CRD (Table 1).^[35] Subsequently, the affinities of the most active antagonists (**2e** & **2g**) were measured in the binding assay with the R98A mutant of FimH-CRD (Table 2).

Cell-free competitive binding assay. The activities of all antagonists were measured twice in duplicate for each concentration. *n*-Heptyl α -D-mannopyranoside (**28**) was used as the reference compound each time in parallel with a new batch of antagonists to ensure comparability. The affinities are referred to the activity of **28** as rIC_{50} . Affinity data for the wild type FimH-CRD are summarized in Table 1, those for R98A mutant of FimH-CRD in Table 2.

Table 1. Binding affinities of FimH antagonists for the FimH-CRD. The IC_{50} values were determined by the cell-free competitive binding assay.^[35] The rIC_{50} values are quotient of the IC_{50} of the compound of interest and the IC_{50} of the reference compound **28**. The rIC_{50} values below 1.0 indicate antagonists, which are more active than the reference **28** and rIC_{50} above 1.0 that they are less active than the reference **28**.

Entry	Compd			IC_{50} [nM]	rIC_{50}
		R ¹	R ²		
1	28			44.0-104.0	1
2	29 ^[34]	Cl		12.3	0.19
3	8f	Cl		14.2	0.32
4	8g	Cl		22.2	0.40
5	8h	Cl		29.5	0.54
6	2e	Cl		13.6	0.21
7	2g	Cl		12.6	0.20
8	2h	Cl		26.4	0.48
9	18e	H		80.1	0.98

10	20f	CF ₃		31.9	0.31
11	25e	Cl		71.0	1.20
12	25g	Cl		48.4	0.81
13	27i	Cl		53.1	0.89
14	27j	Cl		48.1	0.81
15	27k	Cl		32.5	0.55
16	27l	Cl		41.0	0.69

All antagonists substituted with amino acid fragments in *meta*- (\rightarrow **2e**, **2g**, **2h**) and *para*- (\rightarrow **8f-h**) position of the terminal phenyl ring showed affinities in a low nanomolar range. The glycine derivatives **2e** and **8f** were the most active in *meta*- and *para*-series, respectively. However, no improvement in affinity compared to a derivative without an amino acid fragment (\rightarrow **29**) could be detected. In the case of *para*-substitution, we observed a constant drop in affinity in parallel to the elongation of the amino acid moiety. By contrast, *meta*-substituted antagonists did not follow exactly the same trend. Thus, exchanging glycine (\rightarrow **8f**) by β -alanine (\rightarrow **8g**) in *para*-position resulted in a slight reduction of the affinity, whereas the same exchange in *meta*-position (**2e** \rightarrow **2g**) was not detrimental. Although the difference is rather small, this result may suggest additional interactions between **2g** and the protein.

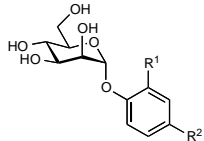
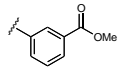
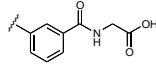
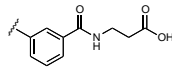
To improve activity of **2e**, we modified the *ortho*-substitution of the phenyl ring adjacent to the anomeric position by either removing the chloro substituent (\rightarrow **18e**) or replacing it by a trifluoromethyl group (\rightarrow **20f**). In previous studies, this strategy proved to be beneficial when CF₃ was applied.^[19,20] However, in our case, both modifications were deleterious for binding to FimH.

The replacement of the terminal phenyl ring by pyrrole (\rightarrow **25e** & **25g**) was not advantageous either, decreasing the affinity several times compared to their counterparts **2e** and **2g**. Reducing the carboxylic acid in **2e** to the alcohol (\rightarrow **27i**) and rigidifying the aliphatic chain

(→ **27j**) as well as substituting the amino acid fragment with the pyridine ring (→ **27k** & **27l**) resulted in worse binding.

Han *et al.* reported an enhanced activity of the antagonist bearing a methyl ester in *meta*-position (→ **1**).^[16] The beneficial effect was partly attributed to the formation of the hydrogen bond with Arg98. In order to establish if Arg98 is involved in the binding of **1** and our strongest antagonists **2e** and **2g**, we determined the affinities of these compounds for the R98A mutant of FimH compared to the wild type (Table 2). For all compounds, no significant difference in the affinity for the wild type and the R98A mutant was observed. Therefore, the contribution of Arg98 to the binding of tested FimH antagonists can be excluded. Noteworthy is the fact that these amino acid fragments did not change the affinity compared to the reference **29** until the longest amino acid was introduced (→ **2h**).

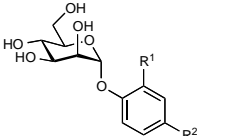
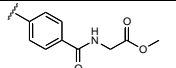
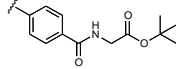
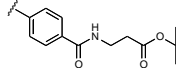
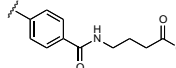
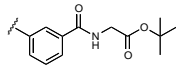
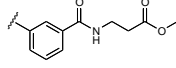
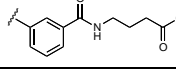
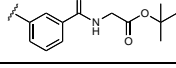
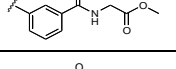
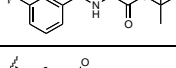
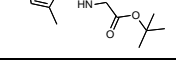
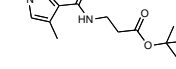
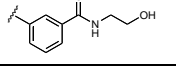
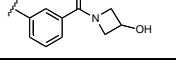
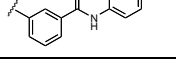
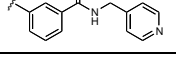
Table 2. Binding affinities of FimH antagonists to the wild type and R98A mutant of FimH-CRD.

Entry	Compd			WT	R98A
		R ¹	R ²	IC ₅₀ [nM]	IC ₅₀ [nM]
1	1	H		30.6	30.4
2	2e	Cl		13.6	13.4
3	2g	Cl		12.6	12.5

Physicochemical and in vitro pharmacokinetic characterization.

Despite the lack of improvement in affinity, the synthesized antagonists still bind to FimH-CRD in the low nanomolar range and the introduced modifications may beneficially influence parameters relevant for oral bioavailability. In order to estimate their absorption potential, we measured aqueous solubility^[36], lipophilicity^[37] and permeability by an artificial membrane permeability assay (PAMPA).^[38] The obtained results are summarized in Table 3.

Table 3. Structural and physicochemical properties of ester prodrugs and amide derivatives.

Entry	Compd			$\log D_{7.4}^a$	Solubility ^b [$\mu\text{g/ml}$]/pH	PAMPA ^c $\log P_e$ [log cm/s]/pH
		R ¹	R ²			
1	7a	Cl		1.7 ± 0.1	> 120 / 7.4	-10 / 7.4
2	7b	Cl		2.6 ± 0.0	128 ± 3 / 7.4	-6.5 ± 0.1 / 7.4
3	7c	Cl		2.7 ± 0.1	151 ± 5 / 7.4	-6.5 ± 0.1 / 7.4
4	7d	Cl		2.2 ± 0.1	119 ± 3 / 7.4	-9.5 ± 1.0 / 7.4
5	12b	Cl		2.4 ± 0.1	300 ± 8 / 7.4	-6.4 ± 0.1 / 7.4
6	12c	Cl		2.6 ± 0.1	256 ± 11 / 7.4	-6.3 ± 0.1 / 7.4
7	12d	Cl		2.1 ± 0.2	> 400 / 7.4	-7.7 ± 1.6 / 7.4
8	17b	H		2.0 ± 0.1	321 ± 10 / 7.4	-9.3 ± 1.3 / 7.4
9	19a	CF ₃		1.7 ± 0.1	> 360 / 7.4	-10 / 7.4
10	19b	CF ₃		2.8 ± 0.0	224 ± 6 / 7.4	-8.2 ± 2.1 / 7.4
11	24b	Cl		2.1 ± 0.0	249 ± 22 / 7.4	-10 / 7.4
12	24c	Cl		2.2 ± 0.0	181 ± 17 / 7.4	-10 / 7.4
13	27i	Cl		0.9 ± 0.1	336 ± 33 / 7.4	-9.4 ± 1.2 / 7.4
14	27j	Cl		0.8 ± 0.0	261 ± 20 / 7.4	-10 / 7.4
15	27k	Cl		2.4 ± 0.1	118 ± 8 / 3.0 53 ± 11 / 7.4	-10 / 5.0 -9.5 ± 1.0 / 7.4
16	27l	Cl		1.8 ± 0.1	306 ± 17 / 3.0 192 ± 20 / 7.4	-10 / 5.0 -10 / 7.4

The indicated values represent the mean \pm standard deviation (SD) of replicate determinations.

^a Octanol-water distribution coefficients ($\log D_{7.4}$) were determined by a miniaturized shake-flask procedure at pH 7.4 in sextuplicate.^[37]

^b Kinetic aqueous solubility was measured in 96-well format at pH 3.0 and 7.4 in triplicate using the μ SOL Explorer solubility analyzer.^[36]

^c P_e = effective permeability: diffusion through an artificial membrane was determined at pH 5.0 and 7.4 by the parallel artificial membrane permeability assay (PAMPA) in quadruplicate.^[38]

All *para*-substituted derivatives (**7a-d**, Table 3, entries 1-4) showed moderate solubility (> 119 μ g/ml). Concerning lipophilicity, the *tert*-butyl ester prodrugs (**7b** & **7c**) reached one of the highest values in the series. The elevated lipophilicity correlates with improved permeability as determined with PAMPA. Although *tert*-butyl ester markedly increased diffusion rate through the membrane ($\log P_e$ -6.5), these prodrugs are still poorly permeable.^[39]

After shifting the amide group to *meta*-position (\rightarrow **12b-d**, entries 5-7), aqueous solubility was noticeably increased compared to their *para*-substituted analogues. By contrast, no big changes in lipophilicity and permeability could be observed. Nevertheless, prodrug **12c** had effective permeability in a range predicted for moderate permeation ($\log P_e > -6.3$ ^[39]).

For a further modification of the aglycone, the terminal phenyl ring was replaced by pyrroles (\rightarrow **24b** & **24c**, entries 11 & 12). In addition, the esterified amino acid fragments were substituted by various metabolically stable groups (\rightarrow **27i-l**, entries 13-16). Unfortunately, all of these FimH antagonists exhibited very poor absorption potential.

Conclusions

In summary, we synthesized a series of biphenyl mannoside derivatives substituted with different amino acid fragments in *meta*- and *para*-position of the terminal phenyl ring, either in the acid or ester form. In addition, we obtained pyrrole-substituted analogues of the amino acid derivatives. Finally, we replaced the carboxylic acid fragments by metabolically stable groups linked to the biphenyl aglycone via amide bond in *meta*-position. All of the antagonists showed affinities in a nanomolar range. However, only glycine and β -alanine derivatives (**2e**, **2g**, **8f**, **8g**) were particularly active. We tested **2e**, **2g** and previously reported **1** in the competitive binding assay against R98A FimH mutant in order to elucidate the influence of Arg98 on binding. We did not observe any difference in the affinities of these antagonists between the wild type and the R98A mutant. This indicates no beneficial interaction of Arg98 with these antagonists and calls into question the importance of this

amino acid for binding. The antagonists **2e** and **2g** will be co-crystallized with the FimH lectin domain to verify if the high affinity results from the interaction with other side chains of the protein.

We also determined the physicochemical properties of the ester prodrugs and the metabolically stable amide derivatives. We observed that *meta*-position is more favorable for solubility than *para*-position. Unfortunately, almost all measured compounds showed poor permeability in the PAMPA. Only prodrug **12c** reached the moderate permeability. This, together with high solubility and the high affinity of the active principle, makes **12c** the best candidate for the orally available drug.

Experimental section

General methods: NMR spectra were recorded on a Bruker Avance DMX-500 (500 MHz) spectrometer. Assignment of ^1H and ^{13}C NMR spectra was achieved using 2D methods (COSY, HSQC, HMBC). Chemical shifts are expressed in ppm using residual CHCl_3 , CHD_2OD or HDO as references. Optical rotations were measured using Perkin-Elmer Polarimeter 341. Electron spray ionization mass spectra (ESI-MS) were obtained on a Waters micromass ZQ Mass Spectrometer. The LC-HRMS analysis were carried out using a Agilent 1100 LC equipped with a photodiode array detector and a Micromass QTOF I equipped with a 4 GHz digital-time converter. Reactions were monitored by TLC using glass plates coated with silica gel 60 F₂₅₄ (Merck) and visualized by using UV light and/or by charring with a molybdate solution (a 0.02 M solution of ammonium cerium sulfate dihydrate and ammonium molybdate tetrahydrate in aqueous 10% H_2SO_4). MPLC separations were carried out on a CombiFlash Companion or R_f from Teledyne Isco equipped with RediSep normal-phase or RP-18 flash columns. LC-MS separations were carried out on a Waters system equipped with sample manager 2767, pump 2525, PDA 2996, column SunFire™ Prep C18 OBD™ (5 μm , 19 x 150 mm), and Micromass ZQ. Size-exclusion chromatography was performed on Bio-Gel P-2 Gel (45–90 mm) from Bio-Rad (Reinach, Switzerland). All compounds used for biological assays are at least of 96% purity based on HPLC analytical results. Commercially available reagents were purchased from Sigma-Aldrich, Alfa Aesar, Acros Organics or Combi-Blocks. Solvents were purchased from Sigma-Aldrich or Acros Organics and were dried prior to use where indicated. Methanol (MeOH), ethanol (EtOH) and *tert*-butanol (*t*-BuOH) were dried by storing with activated molecular sieves 3Å or 4Å

for at least one day. Dichloromethane (DCM) was dried by filtration over Al_2O_3 (Fluka, type 5016 A basic). Molecular sieves 4\AA were activated in vacuo at $200\text{ }^\circ\text{C}$ for 30 min immediately before use.

General procedure A. To a solution of **4** or **9** and C-protected amino acid in anhydrous DMF or MeCN under argon, DIPEA and COMU were added. After stirring for 3-20 h, the mixture was diluted with EtOAc (20 mL) and washed with 1 N HCl (2 x 5 mL), satd aq NaHCO_3 (2 x 10 mL) and brine (10 mL). The organic layer was dried over Na_2SO_4 , concentrated in vacuo and co-evaporated with toluene (2 x 10 mL). The crude product was mixed with **3**^[21], **13**^[21] or **14**^[20] and dissolved in anhydrous DMF under argon. Then, K_3PO_4 and $\text{PdCl}_2(\text{dppf})\cdot\text{CH}_2\text{Cl}_2$ were added and the reaction was stirred at $80\text{ }^\circ\text{C}$ until completion (3-21 h). The mixture was diluted with EtOAc (20 mL) and washed with H_2O (2 x 20 mL). The organic layer was dried over Na_2SO_4 , concentrated in vacuo and co-evaporated with toluene (2 x 10 mL). The residue was purified by MPLC on silica gel to yield **6b-d**, **11b-d**, **15b** and **16b**.

General procedure B. The protected mannoside was dissolved in a mixture of dry alcohol under argon and a freshly prepared solution of sodium alkoxide or potassium *tert*-butoxide was added. The reaction was stirred at rt until completion (1.5-35 h). Then, the mixture was neutralized with Amberlyst-15 (H^+) ion-exchange resin, filtered and concentrated in vacuo. The residue was purified by MPLC on silica gel to give **7a-d**, **12b-d**, **17b**, **18e**, **19a**, **19b** and **20f**.

General procedure C. To a solution of **7b-d**, **12b-d**, **24b** or **24c** in MeOH, 0.2-1.0 M aq NaOH was added. The reaction was stirred at rt until completion (0.5-16 h). The mixture was acidified to pH 3-4 with Amberlyst-15 (H^+) ion-exchange resin, filtered and concentrated in vacuo. The residue was purified by MPLC (RP-18) to yield **2e**, **2g**, **2h**, **8g**, **8h** and **25e**, **25g**.

General procedure D. To a mixture of **23** or **26**^[34] and H-Gly-O*t*Bu·HCl, H- β -Ala-O*t*Bu·HCl or the corresponding amine in anhydrous DMF were added DIPEA or TEA and COMU. The reaction was stirred for 5-16 h under argon. Then, the mixture was concentrated in vacuo and co-evaporated with xylene (10 mL). The residue was dissolved in MeOH (1

mL) or MeCN (1 mL) and passed through a nylon membrane syringe filter (pore size 0.45 μm) and purified by LC-MS ($\text{H}_2\text{O}/\text{MeCN}$, + 0.2% HCO_2H) to yield **24b**, **24c** and **27i-l**.

tert-Butyl [4'-(2,3,4,6-tetra-*O*-acetyl- α -D-mannopyranosyloxy)-3'-chlorobiphenyl-4-carbonyl]-glycinate (6b). Prepared according to general procedure A from **4** (50 mg, 0.199 mmol) and H-Gly-*O**t*Bu·HCl, (34 mg, 0.199 mmol, 1.0 eq) with DIPEA (104 μL , 0.605 mmol, 3.0 eq) and COMU (86 mg, 0.199 mmol, 1.0 eq) in MeCN (2 mL), followed by reaction with **3**^[21] (108 mg, 0.184 mmol), K_3PO_4 (117 mg, 0.540 mmol, 3.0 eq) and $\text{PdCl}_2(\text{dppf})\cdot\text{CH}_2\text{Cl}_2$ (6.0 mg, 7.4 μmol , 0.04 eq) in DMF (2 mL). Purified by MPLC on silica gel (petroleum ether/EtOAc, 7:3-0:1). Yield: 56 mg (44% over two steps) as colorless oil. $[\alpha]_D^{20} +50.5$ (*c* 1.00, CHCl_3); ^1H NMR (500 MHz, CDCl_3): δ = 7.88 (d, *J* = 8.3 Hz, 2H, Ar-H), 7.66 (d, *J* = 2.2 Hz, 1H, Ar-H), 7.59 (d, *J* = 8.4 Hz, 2H, Ar-H), 7.45 (dd, *J* = 2.2, 8.6 Hz, 1H, Ar-H), 7.24 (m, 1H, Ar-H), 6.67 (t, *J* = 4.7 Hz, 1H, NH), 5.64 (dd, *J* = 3.5, 10.0 Hz, 1H, H-3), 5.61 (d, *J* = 1.6 Hz, 1H, H-1), 5.56 (dd, *J* = 1.9, 3.4 Hz, 1H, H-2), 5.41 (t, *J* = 10.1 Hz, 1H, H-4), 4.30 (dd, *J* = 5.3, 12.3 Hz, 1H, H-6a), 4.19 (ddd, *J* = 2.2, 5.3, 10.3 Hz, 1H, H-5), 4.16 (d, *J* = 4.7 Hz, 2H, NHCH_2) 4.10 (dd, *J* = 2.2, 12.3 Hz, 1H, H-6b), 2.22, 2.08, 2.05, 2.04 (4 s, 12H, 4 COCH_3), 1.45 ppm (s, 9H, $\text{C}(\text{CH}_3)_3$); ^{13}C NMR (125 MHz, CDCl_3): δ = 170.62, 170.11, 169.92, 169.41, 166.88 (6 CO), 151.21, 142.50, 136.29, 133.09, 129.38, 127.89, 127.10, 126.56, 125.04, 117.39 (12C, Ar-C), 96.80 (C-1), 82.83 ($\text{C}(\text{CH}_3)_3$), 69.97 (C-5), 69.47 (C-2), 68.91 (C-3), 65.97 (C-4), 62.24 (C-6), 42.72 (NHCH_2), 28.24 (3C, $\text{C}(\text{CH}_3)_3$), 21.02, 20.85, 20.82 ppm (4C, 4 COCH_3); ESI-MS: *m/z*: Calcd for $\text{C}_{33}\text{H}_{38}\text{ClNNaO}_{13}$ $[\text{M}+\text{Na}]^+$: 714.19, found: 714.24.

tert-Butyl 3-[4'-(2,3,4,6-tetra-*O*-acetyl- α -D-mannopyranosyloxy)-3'-chlorobiphenyl-4-carboxamido]-propanoate (6c). Prepared according to general procedure A from **4** (51 mg, 0.199 mmol) and H- β -Ala-*O**t*Bu·HCl (42 mg, 0.218 mmol, 1.1 eq) with DIPEA (102 μL , 0.594 mmol, 3.0 eq) and COMU (131 mg, 0.297 mmol, 1.5 eq) in DMF (2 mL), followed by reaction with **3**^[21] (105 mg, 0.180 mmol), K_3PO_4 (118 mg, 0.540 mmol, 3.0 eq) and $\text{PdCl}_2(\text{dppf})\cdot\text{CH}_2\text{Cl}_2$ (8.8 mg, 10.8 μmol , 0.06 eq) in DMF (3 mL). Purified by MPLC on silica gel (petroleum ether/EtOAc, 6:4). Yield: 58 mg (46% over two steps) as colorless oil. $[\alpha]_D^{20} +60.0$ (*c* 1.06, CHCl_3); ^1H NMR (500 MHz, CDCl_3): δ = 7.82 (d, *J* = 8.2 Hz, 2H, Ar-H), 7.64 (d, *J* = 2.1 Hz, 1H, Ar-H), 7.57 (d, *J* = 8.2 Hz, 2H, Ar-H), 7.43 (dd, *J* = 2.1, 8.6 Hz, 1H, Ar-H), 7.24 (d, *J* = 8.6 Hz, 1H, Ar-H), 6.96 (t, *J* = 5.7 Hz, 1H, NH), 5.62 (dd, *J* = 3.5,

10.1 Hz, 1H, H-3), 5.60 (d, $J = 1.2$ Hz, 1H, H-1), 5.54 (dd, $J = 1.8, 3.2$ Hz, 1H, H-2), 5.39 (t, $J = 10.1$ Hz, 1H, H-4), 4.28 (dd, $J = 5.3, 12.3$ Hz, 1H, H-6a), 4.18 (ddd, $J = 2.0, 5.2, 10.0$ Hz, 1H, H-5), 4.09 (dd, $J = 2.0, 12.2$ Hz, 1H, H-6b), 3.70 (app dd, $J = 5.8, 11.5$ Hz, 2H, NHCH_2), 2.56 (t, $J = 5.8$ Hz, 2H, CH_2CO), 2.20, 2.06, 2.04, 2.02 (4 s, 12H, 4 COCH_3), 1.46 ppm (s, 9H, $\text{C}(\text{CH}_3)_3$); ^{13}C NMR (125 MHz, CDCl_3): $\delta = 172.42$ (CH_2CO), 170.56, 170.06, 169.88, 169.86 (4 CO), 166.86 (CONH), 151.12, 142.20, 136.29, 133.61, 129.30, 127.73, 127.02, 126.49, 124.97, 117.37 (12C, Ar-C), 96.75 (C-1), 81.41 ($\text{C}(\text{CH}_3)_3$), 69.93 (C-5), 69.42 (C-2), 68.87 (C-3), 65.92 (C-4), 62.20 (C-6), 35.66 (NHCH_2), 35.13 (CH_2CO), 28.24 (3C, $\text{C}(\text{CH}_3)_3$), 20.97, 20.81, 20.78, 20.77 ppm (4 COCH_3); HRMS: m/z : Calcd for $\text{C}_{34}\text{H}_{40}\text{ClNNaO}_{13}$ $[\text{M}+\text{Na}]^+$: 728.2086, found: 728.2085; elemental analysis: Calcd (%) for $\text{C}_{34}\text{H}_{40}\text{ClNO}_{13}$: C 57.83, H 5.71, N 1.98 found: C 57.68, H 5.89, N 2.06.

Ethyl 4-[4'-(2,3,4,6-tetra-*O*-acetyl- α -D-mannopyranosyloxy)-3'-chlorobiphenyl-4-carboxamido]-butanoate (6d). Prepared according to general procedure A from **4** (51 mg, 0.199 mmol) and ethyl 4-aminobutyrate hydrochloride (37 mg, 0.218 mmol, 1.1 eq) with DIPEA (102 μL , 0.594 mmol, 3.0 eq) and COMU (131 mg, 0.297 mmol, 1.5 eq) in DMF (2 mL), followed by reaction with **3**^[21] (105 mg, 0.180 mmol), K_3PO_4 (118 mg, 0.540 mmol, 3.0 eq) and $\text{PdCl}_2(\text{dppf})\cdot\text{CH}_2\text{Cl}_2$ (8.8 mg, 10.8 μmol , 0.06 eq) in DMF (3 mL). Purified by MPLC on silica gel (petroleum ether/EtOAc, 1:1). Yield: 43 mg (34% over two steps) as colorless oil. $[\alpha]_D^{20} +60.5$ (c 0.86, CHCl_3); ^1H NMR (500 MHz, CDCl_3): $\delta = 7.85$ (d, $J = 8.2$ Hz, 2H, Ar-H), 7.64 (d, $J = 2.1$ Hz, 1H, Ar-H), 7.57 (d, $J = 8.3$ Hz, 2H, Ar-H), 7.44 (dd, $J = 2.1, 8.6$ Hz, 1H, Ar-H), 7.24 (d, $J = 8.6$ Hz, 1H, Ar-H), 6.75 (t, $J = 5.0$ Hz, 1H, NH), 5.62 (dd, $J = 3.5, 10.1$ Hz, 1H, H-3), 5.60 (d, $J = 1.1$ Hz, 1H, H-1), 5.54 (dd, $J = 1.8, 3.3$ Hz, 1H, H-2), 5.39 (t, $J = 10.1$ Hz, 1H, H-4), 4.28 (dd, $J = 5.3, 12.3$ Hz, 1H, H-6a), 4.18 (ddd, $J = 2.1, 5.2, 10.0$ Hz, 1H, H-5), 4.15-4.08 (m, 3H, OCH_2 , H-6b), 3.52 (app dd, $J = 6.3, 12.0$ Hz, 2H, NHCH_2), 2.45 (t, $J = 6.9$ Hz, 2H, CH_2CO), 2.20, 2.06, 2.04, 2.03 (4 s, 12H, 4 COCH_3), 1.97 (p, $J = 6.8$ Hz, 2H, CH_2), 1.23 ppm (t, $J = 7.1$ Hz, 3H, CH_3); ^{13}C NMR (125 MHz, CDCl_3): $\delta = 174.08$ (CH_2CO), 170.57, 170.07, 169.89, 169.87 (4 CO), 167.08 (CONH), 151.12, 142.13, 136.30, 133.57, 129.30, 127.72, 126.99, 126.48, 124.97, 117.37 (12C, Ar-C), 96.76 (C-1), 69.93 (C-5), 69.42 (C-2), 68.88 (C-3), 65.92 (C-4), 62.20 (C-6), 60.84 (OCH_2), 40.01 (NHCH_2), 32.25 (CH_2CO), 24.41 (CH_2), 20.97, 20.81, 20.79, 20.78 (4 COCH_3), 14.30 ppm (CH_3); ESI-MS: m/z : Calcd for $\text{C}_{33}\text{H}_{39}\text{ClNO}_{13}$ $[\text{M}+\text{H}]^+$: 692.21, found: 692.21.

Methyl [3'-chloro-4'-(α -D-mannopyranosyloxy)biphenyl-4-carbonyl]-glycinate (7a).

Prepared according to general procedure B from **6b** (55 mg, 0.079 mmol) using 1 M MeONa/MeOH (500 μ L) in dry MeOH (2 mL). Purified by MPLC on silica gel (DCM/MeOH, 19:3). Yield: 16 mg (42%) as colorless oil. $[\alpha]_D^{20} +81.2$ (*c* 0.98, MeOH); ^1H NMR (500 MHz, CD_3OD): δ = 7.93 (d, *J* = 8.5 Hz, 2H, Ar-H), 7.72 (d, *J* = 2.3 Hz, 1H, Ar-H), 7.70 (d, *J* = 8.5 Hz, 2H, Ar-H), 7.58 (dd, *J* = 2.3, 8.6 Hz, 1H, Ar-H), 7.46 (d, *J* = 8.7 Hz, 1H, Ar-H), 5.61 (d, *J* = 1.6 Hz, 1H, H-1), 4.14 (s, 2H, NHCH_2), 4.12 (dd, *J* = 1.8, 3.3 Hz, 1H, H-2), 4.00 (dd, *J* = 3.4, 9.5 Hz, 1H, H-3), 3.81-3.74 (m, 6H, H-4, H-6a, H-6b, OCH_3), 3.65 ppm (ddd, *J* = 2.4, 5.4, 9.7 Hz, 1H, H-5); ^{13}C NMR (125 MHz, CD_3OD): δ = 171.97, 170.10 (2 CO), 153.23, 144.03, 136.38, 133.76, 129.68, 129.14, 127.77, 127.71, 125.36, 118.64 (12C, Ar-C), 100.74 (C-1), 76.01 (C-5), 72.40 (C-3), 71.84 (C-2), 68.22 (C-4), 62.66 (C-6), 52.67 (OCH_3), 42.41 ppm (NHCH_2); HRMS: *m/z*: Calcd for $\text{C}_{22}\text{H}_{24}\text{ClNNaO}_9$ $[\text{M}+\text{Na}]^+$: 504.1037, found: 504.1037.

***tert*-Butyl [3'-chloro-4'-(α -D-mannopyranosyloxy)biphenyl-4-carbonyl]-glycinate (7b).**

Prepared according to general procedure B from **6b** (145 mg, 0.210 mmol) using *t*-BuOK (75 mg, 0.630 mmol, 3.0 eq) in dry *t*-BuOH/ CHCl_3 (4 mL, 3:1). An additional portion of *t*-BuOH (4 mL) was added after 18 h and additional portions of *t*-BuOK (12 eq) were added after 18, 22 and 23 h. Purified by MPLC on silica gel (DCM/MeOH, 19:3). Yield: 63 mg (57%) as a white solid. $[\alpha]_D^{20} +80.0$ (*c* 0.44, MeOH); ^1H NMR (500 MHz, CD_3OD): δ = 7.93 (d, *J* = 8.4 Hz, 2H, Ar-H), 7.73 (d, *J* = 2.2 Hz, 1H, Ar-H), 7.70 (d, *J* = 8.4 Hz, 2H, Ar-H), 7.59 (dd, *J* = 2.2, 8.6 Hz, 1H, Ar-H), 7.47 (d, *J* = 8.7 Hz, 1H, Ar-H), 5.61 (d, *J* = 1.4 Hz, 1H, H-1), 4.12 (dd, *J* = 1.8, 3.2 Hz, 1H, H-2), 4.03 (br s, 2H, NHCH_2), 4.00 (dd, *J* = 3.4, 9.5 Hz, 1H, H-3), 3.81-3.71 (m, 3H, H-4, H-6a, H-6b), 3.65 (ddd, *J* = 2.3, 5.3, 9.5 Hz, 1H, H-5), 1.50 ppm (s, 9H, $\text{C}(\text{CH}_3)_3$); ^{13}C NMR (125 MHz, CD_3OD): δ = 170.67, 170.10 (2 CO), 153.23, 143.98, 136.43, 133.98, 129.69, 129.11, 127.78, 127.72, 125.37, 118.65 (12C, Ar-C), 100.75 (C-1), 82.89 ($\text{C}(\text{CH}_3)_3$), 76.01 (C-5), 72.40 (C-3), 71.84 (C-2), 68.22 (C-4), 62.66 (C-6), 43.35 (NHCH_2), 28.31 ppm (3C, $\text{C}(\text{CH}_3)_3$); HRMS: *m/z*: Calcd for $\text{C}_{25}\text{H}_{30}\text{ClNNaO}_9$ $[\text{M}+\text{Na}]^+$: 546.1507, found: 546.1505.

***tert*-Butyl 3-[3'-chloro-4'-(α -D-mannopyranosyloxy)biphenyl-4-carboxamido]-propanoate (7c).** Prepared according to general procedure B from **6c** (45 mg, 0.064 mmol) with *t*-BuOK (23 mg, 0.191 mmol, 3.0 eq) in dry *t*-BuOH (5 mL). An additional portion of *t*-

BuOK (3.0 eq) was added after 1 h. Purified by MPLC on silica gel (DCM/MeOH, 9:1). Yield: 22 mg (65%) as colorless oil. $[\alpha]_D^{20} +79.8$ (*c* 1.05, MeOH); ^1H NMR (500 MHz, CD_3OD): δ = 7.87 (d, *J* = 8.5 Hz, 2H, Ar-H), 7.71 (d, *J* = 2.3 Hz, 1H, Ar-H), 7.67 (d, *J* = 8.5 Hz, 2H, Ar-H), 7.57 (dd, *J* = 2.3, 8.6 Hz, 1H, Ar-H), 7.45 (d, *J* = 8.7 Hz, 1H, Ar-H), 5.60 (d, *J* = 1.6 Hz, 1H, H-1), 4.12 (dd, *J* = 1.8, 3.3 Hz, 1H, H-2), 4.00 (dd, *J* = 3.4, 9.5 Hz, 1H, H-3), 3.81-3.71 (m, 3H, H-4, H-6a, H-6b), 3.67-3.61 (m, 3H, H-5, NHCH_2), 2.59 (t, *J* = 6.9 Hz, 2H, CH_2CO), 1.45 ppm (s, 9H, $\text{C}(\text{CH}_3)_3$); ^{13}C NMR (125 MHz, CD_3OD): δ = 172.87 (CO), 169.74 (CONH), 153.18, 143.74, 136.41, 134.38, 129.65, 128.96, 127.72, 127.68, 125.34, 118.63 (12C, Ar-C), 100.73 (C-1), 81.96 ($\text{C}(\text{CH}_3)_3$), 75.99 (C-5), 72.39 (C-3), 71.83 (C-2), 68.21 (C-4), 62.65 (C-6), 37.15 (NHCH_2), 36.17 (CH_2CO), 28.33 ppm (3C, $\text{C}(\text{CH}_3)_3$); HRMS: *m/z*: Calcd for $\text{C}_{26}\text{H}_{32}\text{ClNNaO}_9$ $[\text{M}+\text{Na}]^+$: 560.1663, found: 560.1653.

Ethyl 4-[3'-chloro-4'-(α -D-mannopyranosyloxy)biphenyl-4-carboxamido]-butanoate (7d). Prepared according to general procedure B from **6d** (43 mg, 0.062 mmol) using 1 M EtONa/EtOH (400 μL) in dry EtOH (6 mL). Purified by MPLC on silica gel (DCM/MeOH, 9:1). Yield: 21 mg (64%) as colorless oil. $[\alpha]_D^{20} +79.6$ (*c* 1.05, MeOH); ^1H NMR (500 MHz, CD_3OD): δ = 7.78 (d, *J* = 8.4 Hz, 2H, Ar-H), 7.71 (d, *J* = 2.2 Hz, 1H, Ar-H), 7.67 (d, *J* = 8.4 Hz, 2H, Ar-H), 7.57 (dd, *J* = 2.2, 8.6 Hz, 1H, Ar-H), 7.45 (d, *J* = 8.7 Hz, 1H, Ar-H), 5.60 (d, *J* = 1.4 Hz, 1H, H-1), 4.13-4.09 (m, 3H, H-2, OCH_2), 4.00 (dd, *J* = 3.4, 9.5 Hz, 1H, H-3), 3.81-3.71 (m, 3H, H-4, H-6a, H-6b), 3.65 (ddd, *J* = 2.3, 5.4, 9.7 Hz, 1H, H-5), 3.44 (t, *J* = 6.9 Hz, 2H, NHCH_2), 2.42 (t, *J* = 7.3 Hz, 2H, CH_2CO), 1.94 (p, *J* = 7.2 Hz, 2H, CH_2), 1.24 ppm (t, *J* = 7.1 Hz, 3H, CH_3); ^{13}C NMR (125 MHz, CD_3OD): δ = 175.04 (CO), 169.85 (CONH), 153.17, 143.67, 136.44, 134.48, 129.64, 128.97, 127.70, 127.67, 125.34, 118.63 (12C, Ar-C), 100.73 (C-1), 75.99 (C-5), 72.40 (C-3), 71.83 (C-2), 68.22 (C-4), 62.66 (C-6), 61.57 (OCH_2), 40.35 (NHCH_2), 32.55 (CH_2CO), 25.82 (CH_2), 14.49 ppm (CH_3); HRMS: *m/z*: Calcd for $\text{C}_{25}\text{H}_{30}\text{ClNNaO}_9$ $[\text{M}+\text{Na}]^+$: 546.1507, found: 546.1507.

Sodium [3'-chloro-4'-(α -D-mannopyranosyloxy)biphenyl-4-carbonyl]-glycinate (8f). To a solution of **7a** (8 mg, 0.017 mmol) in MeOH, 0.2 M aq. NaOH (10 mL) was added. The reaction was stirred at rt until completion (0.5 h). The mixture was neutralized to pH 8 with Amberlyst-15 (H^+) ion-exchange resin, filtered and concentrated in vacuo. The crude product was purified by MPLC on RP-18 ($\text{H}_2\text{O}/\text{MeOH}$, 19:1-1:19) followed by size-exclusion chromatography (P-2 gel, H_2O). Yield: 7 mg (86%) as a white solid. $[\alpha]_D^{20} +54.6$ (*c* 0.70,

H₂O); ¹H NMR (500 MHz, D₂O): δ = 7.79 (d, J = 8.5 Hz, 2H, Ar-H), 7.59 (d, J = 2.2 Hz, 1H, Ar-H), 7.54 (d, J = 8.5 Hz, 2H, Ar-H), 7.45 (dd, J = 2.2, 8.6 Hz, 1H, Ar-H), 7.26 (d, J = 8.7 Hz, 1H, Ar-H), 5.65 (d, J = 1.5 Hz, 1H, H-1), 4.22 (dd, J = 1.8, 3.3 Hz, 1H, H-2), 4.11 (dd, J = 3.5, 9.5 Hz, 1H, H-3), 3.97 (s, 2H, NHCH₂), 3.79-3.71 ppm (m, 4H, H-4, H-5, H-6a, H-6b); ¹³C NMR (125 MHz, D₂O): δ = 176.71, 169.55 (2 CO), 160.97, 150.49, 141.87, 134.82, 131.96, 128.51, 127.70, 126.55, 126.45, 123.91, 117.59 (12C, Ar-C), 98.48 (C-1), 73.86 (C-5), 70.42 (C-3), 69.74 (C-2), 66.44 (C-4), 60.58 (C-6), 43.81 ppm (NHCH₂); HRMS: m/z : Calcd for C₂₁H₂₁ClNNa₂O₉ [M+Na]⁺: 512.0700, found: 512.0696.

3-[3'-Chloro-4'-(α -D-mannopyranosyloxy)biphenyl-4-carboxamido]-propanoic acid (8g). Prepared according to general procedure C from **7c** (13 mg, 0.024 mmol) with 0.4 M aq. NaOH (10 mL). Purified by MPLC on RP-18 (H₂O/MeOH, 19:1-1:19). Yield: 6 mg (52%) as a white solid. $[\alpha]_D^{20}$ +85.4 (c 0.60, MeOH); ¹H NMR (500 MHz, CD₃OD): δ = 7.88 (d, J = 8.4 Hz, 2H, Ar-H), 7.72 (d, J = 2.2 Hz, 1H, Ar-H), 7.68 (d, J = 8.4 Hz, 2H, Ar-H), 7.58 (dd, J = 2.3, 8.6 Hz, 1H, Ar-H), 7.46 (d, J = 8.7 Hz, 1H, Ar-H), 5.60 (d, J = 1.5 Hz, 1H, H-1), 4.12 (dd, J = 1.8, 3.3 Hz, 1H, H-2), 4.00 (dd, J = 3.4, 9.5 Hz, 1H, H-3), 3.81-3.70 (m, 3H, H-4, H-6a, H-6b), 3.66-3.64 (m, 3H, H-5, NHCH₂), 2.64 ppm (t, J = 6.9 Hz, 2H, CH₂CO); ¹³C NMR (125 MHz, CD₃OD): δ = 175.66 (CO), 169.80 (CONH), 153.19, 143.74, 136.46, 134.41, 129.66, 128.98, 127.72, 127.69, 125.35, 118.64 (12C, Ar-C), 100.75 (C-1), 76.00 (C-5), 72.40 (C-3), 71.84 (C-2), 68.22 (C-4), 62.66 (C-6), 37.24 (NHCH₂), 35.25 ppm (CH₂CO); HRMS: m/z : Calcd for C₂₂H₂₄ClNNaO₉ [M+Na]⁺: 504.1037, found: 504.1029.

4-[3'-Chloro-4'-(α -D-mannopyranosyloxy)biphenyl-4-carboxamido]-butanoic acid (8h). Prepared according to general procedure C from **7d** (7 mg, 0.013 mmol) with 0.2 M aq. NaOH (10 mL). Purified by MPLC on RP-18 (H₂O/MeOH, 19:1-1:19). Yield: 4 mg (61%) as colorless oil. $[\alpha]_D^{20}$ +91.1 (c 0.60, MeOH); ¹H NMR (500 MHz, CD₃OD): δ = 7.89 (d, J = 8.4 Hz, 2H, Ar-H), 7.72 (d, J = 2.2 Hz, 1H, Ar-H), 7.68 (d, J = 8.4 Hz, 2H, Ar-H), 7.58 (dd, J = 2.2, 8.6 Hz, 1H, Ar-H), 7.47 (d, J = 8.7 Hz, 1H, Ar-H), 5.60 (d, J = 1.4 Hz, 1H, H-1), 4.12 (dd, J = 1.8, 3.3 Hz, 1H, H-2), 4.00 (dd, J = 3.4, 9.5 Hz, 1H, H-3), 3.81-3.71 (m, 3H, H-4, H-6a, H-6b), 3.65 (ddd, J = 2.3, 5.3, 9.7 Hz, 1H, H-5), 3.45 (t, J = 6.9 Hz, 2H, NHCH₂), 2.40 (t, J = 7.3 Hz, 2H, CH₂CO), 1.94 ppm (p, J = 7.1 Hz, 2H, CH₂); ¹³C NMR (125 MHz, CD₃OD): δ = 177.63 (CO), 169.89 (CONH), 153.19, 143.68, 136.50, 134.55, 129.66, 128.99, 127.72, 127.68, 125.35, 118.65 (12C, Ar-C), 100.76 (C-1), 76.01 (C-5), 72.40 (C-3), 71.85 (C-2),

68.23 (C-4), 62.66 (C-6), 40.54 (NHCH₂), 32.77 (CH₂CO), 25.99 ppm (CH₂); HRMS: *m/z*: Calcd for C₂₃H₂₆ClNNaO₉ [M+Na]⁺: 518.1194, found: 518.1188.

***tert*-Butyl [4'-(2,3,4,6-tetra-*O*-acetyl- α -D-mannopyranosyloxy)-3'-chlorobiphenyl-3-carbonyl]-glycinate (11b).** Prepared according to general procedure A from **9** (50 mg, 0.198 mmol) and H-Gly-*Ot*Bu-HCl (37 mg, 0.218 mmol, 1.1 eq) with DIPEA (102 μ L, 0.594 mmol, 3.0 eq) and COMU (131 mg, 0.297 mmol, 1.5 eq) in DMF (2 mL), followed by reaction with **3**^[21] (105 mg, 0.180 mmol), K₃PO₄ (118 mg, 0.540 mmol, 3.0 eq) and PdCl₂(dppf)·CH₂Cl₂ (8.8 mg, 10 μ mol, 0.06 eq) in DMF (2 mL). Purified by MPLC on silica gel (petroleum ether/EtOAc, 13:7). Yield: 50 mg (44% over two steps) as colorless oil. [α]_D²⁰ +63.1 (*c* 0.84, CHCl₃); ¹H NMR (500 MHz, CDCl₃): δ = 7.97 (br s, 1H, Ar-H), 7.75 (br d, *J* = 7.7 Hz, 1H, Ar-H), 7.65-7.63 (m, 2H, Ar-H), 7.48 (t, *J* = 7.7 Hz, 1H, Ar-H), 7.43 (dd, *J* = 2.2, 8.5 Hz, 1H, Ar-H), 7.23 (d, *J* = 8.6 Hz, 1H, Ar-H), 6.76 (t, *J* = 4.4 Hz, 1H, NH), 5.62 (dd, *J* = 3.5, 10.0 Hz, 1H, H-3), 5.59 (d, *J* = 1.5 Hz, 1H, H-1), 5.55 (dd, *J* = 1.8, 3.4 Hz, 1H, H-2), 5.39 (t, *J* = 10.1 Hz, 1H, H-4), 4.29 (dd, *J* = 5.4, 12.2 Hz, 1H, H-6a), 4.19 (ddd, *J* = 2.1, 5.3, 10.1 Hz, 1H, H-5), 4.15 (d, *J* = 4.8 Hz, 2H, NHCH₂), 4.09 (dd, *J* = 2.1, 12.2 Hz, 1H, H-6b), 2.20, 2.06, 2.03, 2.03 (4 s, 12H, 4 COCH₃), 1.50 ppm (s, 9H, C(CH₃)₃); ¹³C NMR (125 MHz, CDCl₃): δ = 170.59, 170.04, 169.87 (4C, 4 CO), 169.34 (CH₂CO), 167.11 (CONH), 150.98, 139.76, 136.45, 134.78, 130.09, 129.30, 126.49, 126.04, 125.85, 124.93, 117.39 (12C, Ar-C), 96.77 (C-1), 82.75 (C(CH₃)₃), 69.90 (C-5), 69.43 (C-2), 68.89 (C-3), 65.94 (C-4), 62.22 (C-6), 42.68 (NHCH₂), 28.19 (3C, C(CH₃)₃), 20.97, 20.81, 20.79 ppm (4C, 4 COCH₃); ESI-MS: *m/z*: Calcd for C₃₃H₃₈ClNNaO₁₃ [M+Na]⁺: 714.19, found: 714.24.

***tert*-Butyl 3-[4'-(2,3,4,6-tetra-*O*-acetyl- α -D-mannopyranosyloxy)-3'-chlorobiphenyl-3-carboxamido]-propanoate (11c).** Prepared according to general procedure A from **9** (50 mg, 0.202 mmol) and H- β -Ala-*Ot*Bu-HCl (58 mg, 0.302 mmol, 1.5 eq) with DIPEA (103 μ L, 0.604 mmol, 3.0 eq) and COMU (129 mg, 0.302 mmol, 1.5 eq) in DMF (3 mL), followed by reaction with **3**^[21] (131 mg, 0.224 mmol), K₃PO₄ (147 mg, 0.672 mmol, 3.0 eq) and PdCl₂(dppf)·CH₂Cl₂ (9.1 mg, 11.2 μ mol, 0.05 eq) in DMF (3 mL). Purified by MPLC on silica gel (petroleum ether/EtOAc, 8:2-3:7). Yield: 104 mg (66% over two steps) as colorless oil. [α]_D²⁰ +54.2 (*c* 0.81, CHCl₃); ¹H NMR (500 MHz, CDCl₃): δ = 7.93 (s, 1H, Ar-H), 7.67 (d, *J* = 7.7 Hz, 1H, Ar-H), 7.63-7.61 (m, 2H, Ar-H), 7.47-7.41 (m, 2H, Ar-H), 7.22 (d, *J* = 8.6 Hz, 1H, Ar-H), 7.01 (t, *J* = 2.1 Hz, 1H, NH), 5.61 (dd, *J* = 3.5, 10.0 Hz, 1H, H-3), 5.58 (d, *J* =

1.4 Hz, 1H, H-1), 5.53 (dd, $J = 1.8, 3.3$ Hz, 1H, H-2), 5.38 (t, $J = 10.1$ Hz, 1H, H-4), 4.27 (dd, $J = 5.4, 12.2$ Hz, 1H, H-6a), 4.18 (ddd, $J = 2.1, 5.3, 10.0$ Hz, 1H, H-5), 4.08 (dd, $J = 2.1, 12.2$ Hz, 1H, H-6b), 3.68 (app q, $J = 5.8$ Hz, 2H, NHCH_2), 2.55 (t, $J = 5.9$ Hz, 2H, CH_2CO), 2.19, 2.05, 2.02, 2.01 (4 s, 12H, 4 COCH_3), 1.44 ppm (s, 9H, $\text{C}(\text{CH}_3)_3$); ^{13}C NMR (125 MHz, CDCl_3): $\delta = 172.27$ (CH_2CO), 170.53, 170.00, 169.82 (4C, 4 CO), 167.10 (CONH), 150.92, 139.63, 136.45, 135.38, 129.76, 129.22, 129.21, 126.40, 125.83, 125.76, 124.88, 117.35 (12C, Ar-C), 96.73 (C-1), 81.34 ($\text{C}(\text{CH}_3)_3$), 69.86 (C-5), 69.38 (C-2), 68.84 (C-3), 65.89 (C-4), 62.17 (C-6), 35.68 (NHCH_2), 35.09 (CH_2CO), 28.19 (3C, $\text{C}(\text{CH}_3)_3$), 20.92, 20.76, 20.74 ppm (4C, 4 COCH_3); HRMS: m/z : Calcd for $\text{C}_{34}\text{H}_{40}\text{ClNNaO}_{13}$ $[\text{M}+\text{Na}]^+$: 728.2086, found: 728.2081; elemental analysis: Calcd (%) for $\text{C}_{34}\text{H}_{40}\text{ClNO}_{13}$: C 57.83, H 5.71, N 1.98 found: C 57.90, H 5.86, N 2.33.

Ethyl 4-[4'-(2,3,4,6-tetra-*O*-acetyl- α -D-mannopyranosyloxy)-3'-chlorobiphenyl-3-carboxamido]-butanoate (11d). Prepared according to general procedure A from **9** (50 mg, 0.198 mmol) and ethyl 4-aminobutyrate hydrochloride (37 mg, 0.218 mmol, 1.1 eq) with DIPEA (102 μL , 0.594 mmol, 3.0 eq) and COMU (131 mg, 0.297 mmol, 1.5 eq) in DMF (2 mL), followed by reaction with **3**^[21] (105 mg, 0.180 mmol), K_3PO_4 (118 mg, 0.540 mmol, 3.0 eq) and $\text{PdCl}_2(\text{dppf})\cdot\text{CH}_2\text{Cl}_2$ (8.8 mg, 10.8 μmol , 0.06 eq) in DMF (3 mL). Purified by MPLC on silica gel (petroleum ether/EtOAc, 1:0-0:1). Yield: 42 mg (34% over two steps) as colorless oil. $[\alpha]_D^{20} +52.8$ (c 1.00, CHCl_3); ^1H NMR (500 MHz, CDCl_3): $\delta = 7.97$ (m, 1H, Ar-H), 7.73 (br d, $J = 7.7$ Hz, 1H, Ar-H), 7.67 (d, $J = 2.2$ Hz, 1H, Ar-H), 7.63 (br d, $J = 7.9$ Hz, 1H, Ar-H), 7.49-7.44 (m, 2H, Ar-H), 7.23 (d, $J = 8.6$ Hz, 1H, Ar-H), 6.86 (t, $J = 4.9$ Hz, 1H, NH), 5.62 (dd, $J = 3.5, 10.0$ Hz, 1H, H-3), 5.59 (d, $J = 1.5$ Hz, 1H, H-1), 5.54 (dd, $J = 1.8, 3.4$ Hz, 1H, H-2), 5.39 (t, $J = 10.1$ Hz, 1H, H-4), 4.29 (dd, $J = 5.3, 12.2$ Hz, 1H, H-6a), 4.19 (ddd, $J = 2.1, 5.3, 10.1$ Hz, 1H, H-5), 4.15-4.08 (m, 3H, H-6b, OCH_2), 3.53 (app dd, $J = 6.4, 12.2$ Hz, 2H, NHCH_2), 2.46 (t, $J = 6.8$ Hz, 2H, CH_2CO), 2.20, 2.06, 2.04, 2.03 (4 s, 12H, 4 COCH_3), 1.98 (p, $J = 6.7$ Hz, 2H, CH_2), 1.23 ppm (t, $J = 7.1$ Hz, 3H, CH_3); ^{13}C NMR (125 MHz, CDCl_3): $\delta = 174.23$ (CH_2CO), 170.60, 170.07, 169.90, 169.88 (4 CO), 167.28 (CONH), 150.97, 139.61, 136.55, 135.34, 129.74, 129.28, 129.27, 126.46, 126.01, 125.66, 124.94, 117.39 (12C, Ar-C), 96.80 (C-1), 69.92 (C-5), 69.44 (C-2), 68.90 (C-3), 65.95 (C-4), 62.22 (C-6), 60.91 (OCH_2), 40.51 (NHCH_2), 32.34 (CH_2CO), 24.29 (CH_2), 20.98, 20.82, 20.80 (4C, 4 COCH_3), 14.30 ppm (CH_3); HRMS: m/z : Calcd for $\text{C}_{33}\text{H}_{38}\text{ClNNaO}_{13}$ $[\text{M}+\text{Na}]^+$: 714.1929, found: 714.1926.

***tert*-Butyl [3'-chloro-4'-(α -D-mannopyranosyloxy)biphenyl-3-carbonyl]-glycinate (**12b**).**

Prepared according to general procedure B from **11b** (45 mg, 0.065 mmol) using *t*-BuOK (23 mg, 0.195 mmol, 3.0 eq) in dry *t*-BuOH (5 mL). An additional portion of *t*-BuOK (3.0 eq) was added after 2.5 h. Purified by MPLC on silica gel (DCM/MeOH, 9:1). Yield: 18 mg (53%) as colorless oil. $[\alpha]_D^{20} +68.3$ (*c* 0.83, MeOH); ^1H NMR (500 MHz, CD_3OD): δ = 8.08 (m, 1H, Ar-H), 7.82 (br d, *J* = 7.8 Hz, 1H, Ar-H), 7.78 (br d, *J* = 8.2 Hz, 1H, Ar-H), 7.74 (d, *J* = 2.2 Hz, 1H, Ar-H), 7.59 (dd, *J* = 2.2, 8.6 Hz, 1H, Ar-H), 7.55 (t, *J* = 7.8 Hz, 1H, Ar-H), 7.47 (d, *J* = 8.6 Hz, 1H, Ar-H), 5.60 (d, *J* = 1.4 Hz, 1H, H-1), 4.12 (dd, *J* = 1.8, 3.2 Hz, 1H, H-2), 4.03 (s, 2H, NHCH_2), 4.01 (dd, *J* = 3.4, 9.5 Hz, 1H, H-3), 3.81-3.71 (m, 3H, H-4, H-6a, H-6b), 3.66 (ddd, *J* = 2.3, 5.4, 9.7 Hz, 1H, H-5), 1.50 ppm (s, 9H, $\text{C}(\text{CH}_3)_3$); ^{13}C NMR (125 MHz, CD_3OD): δ = 170.69 (CH_2CO), 170.32 (CONH), 153.03, 141.02, 136.72, 135.86, 131.01, 130.33, 129.65, 127.61, 127.39, 126.65, 125.36, 118.69 (12C, Ar-C), 100.78 (C-1), 82.94 ($\text{C}(\text{CH}_3)_3$), 75.99 (C-5), 72.40 (C-3), 71.85 (C-2), 68.23 (C-4), 62.66 (C-6), 43.36 (NHCH_2), 28.31 ppm (3C, $\text{C}(\text{CH}_3)_3$); HRMS: *m/z*: Calcd for $\text{C}_{25}\text{H}_{30}\text{ClNNaO}_9$ $[\text{M}+\text{Na}]^+$: 546.1507, found: 546.1499.

***tert*-Butyl 3-[3'-chloro-4'-(α -D-mannopyranosyloxy)biphenyl-3-carboxamido]-propanoate (**12c**).**

Prepared according to general procedure B from **11c** (87 mg, 0.123 mmol) using *t*-BuOK (46 mg, 0.370 mmol, 3.0 eq) in dry *t*-BuOH (10 mL). An additional portion of *t*-BuOK (3.0 eq) was added after 1.5 h. Purified by MPLC on silica gel (DCM/MeOH, 9:1). Yield: 28 mg (42%) as colorless oil. $[\alpha]_D^{20} +70.8$ (*c* 1.30, MeOH); ^1H NMR (500 MHz, CD_3OD): δ = 8.01 (t, *J* = 1.5 Hz, 1H, Ar-H), 7.78-7.75 (m, 2H, Ar-H), 7.73 (d, *J* = 2.2 Hz, 1H, Ar-H), 7.58 (dd, *J* = 2.3, 8.6 Hz, 1H, Ar-H), 7.53 (t, *J* = 7.8 Hz, 1H, Ar-H), 7.46 (d, *J* = 8.6 Hz, 1H, Ar-H), 5.60 (d, *J* = 1.5 Hz, 1H, H-1), 4.12 (dd, *J* = 1.8, 3.3 Hz, 1H, H-2), 4.01 (dd, *J* = 3.4, 9.5 Hz, 1H, H-3), 3.81-3.71 (m, 3H, H-4, H-6a, H-6b), 3.68-3.62 (m, 3H, H-5, NHCH_2), 2.59 (t, *J* = 6.9 Hz, 2H, CH_2CO), 1.45 ppm (s, 9H, $\text{C}(\text{CH}_3)_3$); ^{13}C NMR (125 MHz, CD_3OD): δ = 172.87 (CH_2CO), 169.98 (CONH), 153.01, 140.96, 136.72, 136.29, 130.81, 130.28, 129.62, 127.59, 127.27, 126.53, 125.35, 118.68 (12C, Ar-C), 100.77 (C-1), 81.98 ($\text{C}(\text{CH}_3)_3$), 75.98 (C-5), 72.40 (C-3), 71.85 (C-2), 68.22 (C-4), 62.65 (C-6), 37.20 (NHCH_2), 36.16 (CH_2CO), 28.34 ppm (3C, $\text{C}(\text{CH}_3)_3$); HRMS: *m/z*: Calcd for $\text{C}_{26}\text{H}_{32}\text{ClNNaO}_9$ $[\text{M}+\text{Na}]^+$: 560.1663, found: 560.1660.

Ethyl 4-[3'-chloro-4'-(α -D-mannopyranosyloxy)biphenyl-3-carboxamido]-butanoate (12d). Prepared according to general procedure B from **11d** (42 mg, 0.061 mmol) using 1 M EtONa/EtOH (400 μ L) in dry EtOH (7 mL). Purified by MPLC on silica gel (DCM/MeOH, 9:1). Yield: 17 mg (53%) as colorless oil. $[\alpha]_D^{20} +71.3$ (*c* 1.07, MeOH); ^1H NMR (500 MHz, CD_3OD): δ = 8.03 (s, 1H, Ar-H), 7.80-7.74 (m, 3H, Ar-H), 7.58 (dd, *J* = 2.2, 8.6 Hz, 1H, Ar-H), 7.53 (t, *J* = 7.8 Hz, 1H, Ar-H), 7.46 (d, *J* = 8.6 Hz, 1H, Ar-H), 5.60 (d, *J* = 1.2 Hz, 1H, H-1), 4.13-4.09 (m, 3H, H-2, OCH_2), 4.01 (dd, *J* = 3.4, 9.5 Hz, 1H, H-3), 3.81-3.71 (m, 3H, H-4, H-6a, H-6b), 3.66 (ddd, *J* = 2.3, 5.3, 9.6 Hz, 1H, H-5), 3.45 (t, *J* = 6.9 Hz, 2H, NHCH_2), 2.43 (t, *J* = 7.3 Hz, 2H, CH_2CO), 1.95 (p, *J* = 7.1 Hz, 2H, CH_2), 1.23 ppm (t, *J* = 7.1 Hz, 3H, CH_3); ^{13}C NMR (125 MHz, CD_3OD): δ = 175.09 (CH_2CO), 170.02 (CONH), 153.01, 140.96, 136.79, 136.35, 130.75, 130.26, 129.65, 127.61, 127.30, 126.51, 125.35, 118.69 (12C, Ar-C), 100.79 (C-1), 75.99 (C-5), 72.41 (C-3), 71.86 (C-2), 68.23 (C-4), 62.66 (C-6), 61.58 (OCH_2), 40.42 (NHCH_2), 32.59 (CH_2CO), 25.76 (CH_2), 14.49 ppm (CH_3); HRMS: *m/z*: Calcd for $\text{C}_{25}\text{H}_{30}\text{ClNNaO}_9$ $[\text{M}+\text{Na}]^+$: 546.1507, found: 546.1501.

[3'-Chloro-4'-(α -D-mannopyranosyloxy)biphenyl-4-carbonyl]-glycine (2e). Prepared according to general procedure C from **12b** (15 mg, 0.029 mmol) with 0.2 M aq. NaOH (10 mL). The mixture was acidified with an excess of AcOH. Purified by MPLC on RP-18 ($\text{H}_2\text{O}/\text{MeOH}$, 19:1-1:19) followed by LC-MS ($\text{H}_2\text{O}/\text{MeCN}$, 19:1-1:19, + 0.2% HCO_2H). Yield: 8 mg (60%) as a white solid. $[\alpha]_D^{20} +91.0$ (*c* 0.80, MeOH); ^1H NMR (500 MHz, CD_3OD): δ = 8.09 (m, 1H, Ar-H), 7.84 (br d, *J* = 7.8 Hz, 1H, Ar-H), 7.78 (br d, *J* = 8.0 Hz, 1H, Ar-H), 7.75 (d, *J* = 2.2 Hz, 1H, Ar-H), 7.59 (dd, *J* = 2.2, 8.6 Hz, 1H, Ar-H), 7.55 (t, *J* = 7.8 Hz, 1H, Ar-H), 7.47 (d, *J* = 8.6 Hz, 1H, Ar-H), 5.60 (d, *J* = 1.4 Hz, 1H, H-1), 4.13-4.11 (m, 3H, H-2, NHCH_2), 4.01 (dd, *J* = 3.4, 9.5 Hz, 1H, H-3), 3.81-3.71 (m, 3H, H-4, H-6a, H-6b), 3.66 ppm (ddd, *J* = 2.3, 5.4, 9.7 Hz, 1H, H-5); ^{13}C NMR (125 MHz, CD_3OD): δ = 173.55 (CO), 170.20 (CONH), 153.03, 141.00, 136.76, 135.88, 130.98, 130.29, 129.65, 127.62, 127.42, 126.69, 125.36, 118.69 (12C, Ar-C), 100.79 (C-1), 75.99 (C-5), 72.41 (C-3), 71.86 (C-2), 68.23 (C-4), 62.66 (C-6), 42.59 ppm (NHCH_2); HRMS: *m/z*: Calcd for $\text{C}_{21}\text{H}_{22}\text{ClNNaO}_9$ $[\text{M}+\text{Na}]^+$: 490.0881, found: 490.0874.

3-[3'-Chloro-4'-(α -D-mannopyranosyloxy)biphenyl-3-carboxamido]-propanoic acid (2g). Prepared according to general procedure C from **12c** (16 mg, 0.030 mmol) with 1 M aq. NaOH (10 mL) in MeOH (3 mL). The mixture was acidified with an excess of AcOH.

Purified by MPLC on RP-18 (H₂O/MeOH, 19:1-1:19, + 0.1% TFA) solvent system. Yield: 11 mg (79%) as a white solid. $[\alpha]_D^{20} +92.4$ (*c* 0.40, MeOH); ¹H NMR (500 MHz, CD₃OD): δ = 8.03 (m, 1H, Ar-H), 7.79-7.74 (m, 3H, Ar-H), 7.59 (dd, *J* = 2.2, 8.6 Hz, 1H, Ar-H), 7.53 (t, *J* = 7.8 Hz, 1H, Ar-H), 7.46 (d, *J* = 8.6 Hz, 1H, Ar-H), 5.60 (d, *J* = 1.4 Hz, 1H, H-1), 4.12 (dd, *J* = 1.8, 3.3 Hz, 1H, H-2), 4.01 (dd, *J* = 3.4, 9.5 Hz, 1H, H-3), 3.81-3.71 (m, 3H, H-4, H-6a, H-6b), 3.68-3.64 (m, 3H, H-5, NHCH₂), 2.63 ppm (t, *J* = 6.9 Hz, 2H, CH₂CO); ¹³C NMR (125 MHz, CD₃OD): δ = 176.44 (CO), 169.95 (CONH), 153.02, 140.99, 136.83, 136.34, 130.79, 130.26, 129.66, 127.64, 127.29, 126.54, 125.35, 118.69 (12C, Ar-C), 100.81 (C-1), 75.99 (C-5), 72.41 (C-3), 71.87 (C-2), 68.24 (C-4), 62.66 (C-6), 37.48 (NHCH₂), 35.53 ppm (CH₂CO); HRMS: *m/z*: Calcd for C₂₂H₂₄ClNNaO₉ [M+Na]⁺: 504.1037, found: 504.1034.

3-[3'-Chloro-4'-(α -D-mannopyranosyloxy)biphenyl-3-carboxamido]-butanoic acid (2h).

Prepared according to general procedure C from **12d** (15 mg, 0.029 mmol) with 0.2 M aq. NaOH (10 mL). Purified by MPLC on RP-18 (H₂O/MeOH, 19:1-1:19). Yield: 6 mg (43%) as colorless oil. $[\alpha]_D^{20} +78.1$ (*c* 0.60, MeOH); ¹H NMR (500 MHz, CD₃OD): δ = 8.04 (m, 1H, Ar-H), 7.80 (br d, *J* = 7.8 Hz, 1H, Ar-H), 7.76-7.74 (m, 2H, Ar-H), 7.59 (dd, *J* = 2.2, 8.6 Hz, 1H, Ar-H), 7.53 (t, *J* = 7.8 Hz, 1H, Ar-H), 7.47 (d, *J* = 8.6 Hz, 1H, Ar-H), 5.60 (d, *J* = 1.3 Hz, 1H, H-1), 4.12 (dd, *J* = 1.8, 3.2 Hz, 1H, H-2), 4.01 (dd, *J* = 3.4, 9.5 Hz, 1H, H-3), 3.81-3.71 (m, 3H, H-4, H-6a, H-6b), 3.66 (ddd, *J* = 2.3, 5.3, 9.7 Hz, 1H, H-5), 3.46 (t, *J* = 6.9 Hz, 2H, NHCH₂), 2.39 (t, *J* = 7.2 Hz, 2H, CH₂CO), 1.94 ppm (p, *J* = 7.1 Hz, 2H, CH₂); ¹³C NMR (125 MHz, CD₃OD): δ = 177.81 (CO), 170.05 (CONH), 153.01, 140.97, 136.84, 136.41, 130.73, 130.25, 129.66, 127.64, 127.30, 126.54, 125.35, 118.69 (12C, Ar-C), 100.80 (C-1), 75.99 (C-5), 72.41 (C-3), 71.86 (C-2), 68.23 (C-4), 62.66 (C-6), 40.64 (NHCH₂), 33.04 (CH₂CO), 26.03 ppm (CH₂); HRMS: *m/z*: Calcd for C₂₃H₂₆ClNNaO₉ [M+Na]⁺: 518.1194, found: 518.1189.

tert-Butyl [4'-(2,3,4,6-tetra-*O*-acetyl- α -D-mannopyranosyloxy)-biphenyl-3-carbonyl]-glycinate (15b). Prepared according to general procedure A from **9** (100 mg, 0.403 mmol) and H-Gly-*O**t*Bu-HCl (100 mg, 0.597 mmol, 1.5 eq) with DIPEA (400 μ L, 2.336 mmol, 5.8 eq) and COMU (262 mg, 0.612 mmol, 1.5 eq) in DMF (2 mL), followed by reaction with **13**^[21] (171 mg, 0.310 mmol), K₃PO₄ (204 mg, 0.930 mmol, 3.0 eq) and PdCl₂(dppf)·CH₂Cl₂ (15.0 mg, 18.6 μ mol, 0.06 eq) in DMF (3 mL). Purified by MPLC on silica gel (petroleum ether/EtOAc, 3:2). Yield: 147 mg (72% over two steps) as colorless oil. $[\alpha]_D^{20} +64.1$ (*c* 1.16,

CHCl₃); ¹H NMR (500 MHz, CDCl₃): δ = 7.98 (s, 1H, Ar-H), 7.71 (d, *J* = 7.6 Hz, 1H, Ar-H), 7.64 (d, *J* = 7.7 Hz, 1H, Ar-H), 7.52 (dd, *J* = 8.6 Hz, 2H, Ar-H), 7.45 (t, *J* = 7.7 Hz, 1H, Ar-H), 7.14 (d, *J* = 8.6 Hz, 2H, Ar-H), 6.81 (br s, 1H, NH), 5.57-5.55 (m, 2H, H-1, H-3), 5.45 (dd, *J* = 1.7, 3.3 Hz, 1H, H-2), 5.36 (t, *J* = 10.0 Hz, 1H, H-4), 4.27 (dd, *J* = 5.1, 12.0 Hz, 1H, H-6a), 4.13-4.05 (m, 4H, H-5, H-6b, NHCH₂), 2.19, 2.04, 2.02, 2.01 (4 s, 12H, 4 COCH₃), 1.48 ppm (s, 9H, C(CH₃)₃); ¹³C NMR (125 MHz, CDCl₃): δ = 170.58, 170.03, 170.00, 169.79 (5C, 5 CO), 167.31 (CONH), 155.45, 140.90, 135.12, 134.58, 130.05, 129.10, 128.44, 125.73, 125.53, 116.95 (12C, Ar-C), 95.88 (C-1), 82.60 (C(CH₃)₃), 69.43 (C-2), 69.31 (C-5), 68.49 (C-3), 66.00 (C-4), 62.18 (C-6), 42.62 (NHCH₂), 28.13 (3C, C(CH₃)₃), 20.92, 20.74 ppm (4C, 4 COCH₃); ESI-MS: *m/z*: Calcd for C₃₃H₃₉NNaO₁₃ [M+Na]⁺: 680.23, found: 680.38.

***tert*-Butyl [4'-(2,3,4,6-tetra-*O*-acetyl-α-D-mannopyranosyloxy)-3'-trifluoromethyl-biphenyl-3-carbonyl]-glycinate (16b).** Prepared according the general procedure A from **9** (150 mg, 0.604 mmol) and H-Gly-*O**t*Bu·HCl (151 mg, 0.889 mmol, 1.5 eq) with DIPEA (609 μL, 3.557 mmol, 6.0 eq) and COMU (405 mg, 0.891 mmol, 1.5 eq) in DMF (4 mL), followed by reaction with **14**^[20] (230 mg, 0.403 mmol), K₃PO₄ (264 mg, 1.209 mmol, 3.0 eq) and PdCl₂(dppf)·CH₂Cl₂ (15.0 mg, 24.0 μmol, 0.06 eq) in DMF (5 mL). Purified by MPLC on silica gel (petroleum ether/EtOAc, 1:0-0:1). Yield: 144 mg (49% over two steps) as colorless oil. [α]_D²⁰ +56.6 (*c* 1.10, CHCl₃); ¹H NMR (500 MHz, CDCl₃): δ = 7.99 (s, 1H, Ar-H), 7.82 (d, *J* = 1.9 Hz, 1H, Ar-H), 7.75 (br d, *J* = 7.8 Hz, 1H, Ar-H), 7.70 (dd, *J* = 2.1, 8.7 Hz, 1H, Ar-H), 7.65 (br d, *J* = 8.0 Hz, 1H, Ar-H), 7.48 (t, *J* = 7.7 Hz, 1H, Ar-H), 7.32 (d, *J* = 8.7 Hz, 1H, Ar-H), 6.84 (t, *J* = 4.7 Hz, 1H, NH), 5.67 (d, *J* = 1.5 Hz, 1H, H-1), 5.55 (dd, *J* = 3.4, 10.1 Hz, 1H, H-3), 5.48 (dd, *J* = 1.9, 3.3 Hz, 1H, H-2), 5.44 (t, *J* = 9.9 Hz, 1H, H-4), 4.28 (dd, *J* = 5.7, 12.9 Hz, 1H, H-6a), 4.14 (d, *J* = 4.9 Hz, 2H, NHCH₂), 4.09-4.06 (m, 2H, H-5, H-6b), 2.20, 2.05, 2.03, 2.02 (4 s, 12H, 4 COCH₃), 1.49 ppm (s, 9H, C(CH₃)₃); ¹³C NMR (125 MHz, CDCl₃): δ = 170.53, 169.99, 169.85, 169.70 (4 CO), 169.33 (CH₂CO), 167.07 (CONH), 152.76, 139.69, 134.89, 134.82, 131.88, 130.50, 129.34, 126.09, 126.05, 125.94, 123.26 (q, *J* = 273.0 Hz), 120.52 (q, *J* = 31.3 Hz), 115.93 (13C, 12 Ar-C, CF₃), 95.79 (C-1), 82.72 (C(CH₃)₃), 69.97 (C-5), 69.24 (C-2), 68.69 (C-3), 65.67 (C-4), 62.11 (C-6), 42.64 (NHCH₂), 28.14 (3C, C(CH₃)₃), 20.91, 20.76, 20.75, 20.70 ppm (4 COCH₃); ESI-MS: *m/z*: Calcd for C₃₄H₃₈F₃NNaO₁₃ [M+Na]⁺: 748.22, found: 748.38.

tert-Butyl [4'-(α -D-mannopyranosyloxy)-biphenyl-3-carbonyl]-glycinate (17b). [4'-(α -D-Mannopyranosyloxy)-biphenyl-3-carbonyl]-glycine (**18e**). Prepared according to general procedure B from **15b** (109 mg, 0.166 mmol) with *t*-BuOK (58 mg, 0.498 mmol, 3.0 eq) in *t*-BuOH (10 mL). An additional portion of *t*-BuOK (3.0 eq) was added after 1.5 h. The crude products were purified by MPLC on silica gel (DCM/MeOH, 9:1) to afford **17b** (36 mg, 44%) as colorless oil or by MPLC on silica gel (DCM/MeOH, 9:1-0:1) followed by MPLC on RP-18 (H₂O/MeOH, 19:1-1:19, + 0.1% TFA) to afford **18e** (26 mg, 36%) as colorless oil.

17b: $[\alpha]_D^{20} +97.3$ (*c* 1.17, MeOH); ¹H NMR (500 MHz, CD₃OD): δ = 8.07 (m, 1H, Ar-H), 7.79-7.75 (m, 2H, Ar-H), 7.61 (d, *J* = 8.7 Hz, 2H, Ar-H), 7.52 (t, *J* = 7.8 Hz, 1H, Ar-H), 7.22 (d, *J* = 8.7 Hz, 2H, Ar-H), 5.54 (d, *J* = 1.3 Hz, 1H, H-1), 4.04-4.03 (m, 3H, H-2, NHCH₂), 3.94 (dd, *J* = 3.4, 9.5 Hz, 1H, H-3), 3.80-3.72 (m, 3H, H-4, H-6a, H-6b), 3.63 (ddd, *J* = 2.5, 5.1, 9.7 Hz, 1H, H-5), 1.49 ppm (s, 9H, C(CH₃)₃); ¹³C NMR (125 MHz, CD₃OD): δ = 170.69, 170.53 (2 CO), 157.82, 142.34, 135.69, 135.53, 130.99, 130.13, 129.21, 126.75, 126.59, 118.20 (12C, Ar-C), 100.15 (C-1), 82.90 (C(CH₃)₃), 75.43 (C-5), 72.42 (C-3), 71.97 (C-2), 68.34 (C-4), 62.66 (C-6), 43.36 (NHCH₂), 28.31 ppm (3C, C(CH₃)₃); HRMS: *m/z*: Calcd for C₂₅H₃₁ClNNaO₉ [M+Na]⁺: 512.1897, found: 512.1887.

18e: $[\alpha]_D^{20} +93.1$ (*c* 0.87, MeOH); ¹H NMR (500 MHz, CD₃OD): δ = 8.08 (m, 1H, Ar-H), 7.80-7.76 (m, 2H, Ar-H), 7.62 (d, *J* = 8.7 Hz, 2H, Ar-H), 7.52 (t, *J* = 7.8 Hz, 1H, Ar-H), 7.22 (d, *J* = 8.7 Hz, 2H, Ar-H), 5.54 (d, *J* = 1.4 Hz, 1H, H-1), 4.12 (s, 2H, NHCH₂), 4.04 (dd, *J* = 1.8, 3.3 Hz, 1H, H-2), 3.93 (dd, *J* = 3.4, 9.5 Hz, 1H, H-3), 3.80-3.72 (m, 3H, H-4, H-6a, H-6b), 3.63 ppm (ddd, *J* = 2.5, 5.1, 9.7 Hz, 1H, H-5); ¹³C NMR (125 MHz, CD₃OD): δ = 173.27 (CO), 170.59 (CONH), 157.93, 142.44, 135.76, 135.65, 131.09, 130.21, 129.31, 126.88, 126.73, 118.29 (12C, Ar-C), 100.26 (C-1), 75.53 (C-5), 72.52 (C-3), 72.08 (C-2), 68.44 (C-4), 62.77 (C-6), 42.40 ppm (NHCH₂); HRMS: *m/z*: Calcd for C₂₁H₂₃NNaO₉ [M+Na]⁺: 456.1271, found: 456.1261.

Methyl [4'-(α -D-mannopyranosyloxy)-3'-trifluoromethyl-biphenyl-3-carbonyl]-glycinate (19a). Prepared according to general procedure B from **19b** (20 mg, 0.036 mmol) with 1 M MeONa/MeOH (600 μ L) in MeOH (2 mL). Purified by MPLC on silica gel (DCM/MeOH, 3:1). Yield: 12 mg (65%) as colorless oil. $[\alpha]_D^{20} +87.3$ (*c* 0.60, MeOH); ¹H NMR (500 MHz, CD₃OD): δ = 8.11 (m, 1H, Ar-H), 7.91-7.89 (m, 2H, Ar-H), 7.86 (m, 1H, Ar-H), 7.82 (m, 1H, Ar-H), 7.62-7.56 (m, 2H, Ar-H), 5.66 (d, *J* = 1.3 Hz, 1H, H-1), 4.15 (s, 2H, NHCH₂), 4.07

(dd, $J = 1.8, 3.2$ Hz, 1H, H-2), 3.95 (dd, $J = 3.4, 9.5$ Hz, 1H, H-3), 3.82-3.71 (m, 6H, H-4, H-6a, H-6b, CH₃), 3.60 ppm (ddd, $J = 2.2, 5.6, 9.6$ Hz, 1H, H-5); ¹³C NMR (125 MHz, CD₃OD): $\delta = 171.98$ (CH₂CO), 170.27 (CONH), 155.26, 141.04, 135.74, 135.21, 133.29, 131.18, 130.44, 127.55, 126.74, 126.32 (q, $J = 5.6$ Hz), 120.98, 120.74, 117.82 (13C, 12 Ar-C, CF₃), 100.33 (C-1), 76.09 (C-5), 72.26 (C-3), 71.76 (C-2), 68.14 (C-4), 62.70 (C-6), 52.69 (OCH₃), 42.43 ppm (NHCH₂); HRMS: m/z : Calcd for C₂₃H₂₄F₃NNaO₉ [M+Na]⁺: 538.1301, found: 538.1288.

tert-Butyl [4'-(α -D-mannopyranosyloxy)-3'-trifluoromethyl-biphenyl-3-carbonyl]-glycinate (19b). Sodium [4'-(α -D-mannopyranosyloxy)-3'-trifluoromethyl-biphenyl-3-carbonyl]-glycinate (**20f**). Prepared according to general procedure B from **16b** (132 mg, 0.182 mmol) with *t*-BuOK (64 mg, 0.546 mmol, 3.0 eq) in *t*-BuOH (20 mL). An additional portion of *t*-BuOK (3.0 eq) was added after 1 h. The crude products were purified by MPLC on silica gel (DCM/MeOH, 9:1) to afford **19b** (44 mg, 44%) as colorless oil or by MPLC on silica gel (DCM/MeOH, 9:1-0:1), after which the intermediate was converted into the sodium salt with 0.5 M NaOH (3 mL) and purified by size-exclusion chromatography (P-2 gel, H₂O) to afford **20f** (29 mg, 31%) as a white solid.

19b: $[\alpha]_D^{20} +83.4$ (*c* 1.10, MeOH); ¹H NMR (500 MHz, CD₃OD): $\delta = 8.12$ (m, 1H, Ar-H), 7.92-7.89 (m, 2H, Ar-H), 7.86 (br d, $J = 7.8$ Hz, 1H, Ar-H), 7.82 (br d, $J = 8.1$ Hz, 1H, Ar-H), 7.63-7.57 (m, 2H, Ar-H), 5.68 (d, $J = 1.1$ Hz, 1H, H-1), 4.09 (dd, $J = 1.7, 3.2$ Hz, 1H, H-2), 4.06 (s, 2H, NHCH₂), 3.97 (dd, $J = 3.4, 9.5$ Hz, 1H, H-3), 3.85-3.74 (m, 3H, H-4, H-6a, H-6b), 3.62 (ddd, $J = 2.2, 5.6, 9.6$ Hz, 1H, H-5), 1.52 ppm (s, 9H, C(CH₃)₃); ¹³C NMR (125 MHz, CD₃OD): $\delta = 170.68, 170.26$ (2 CO), 155.22, 140.97, 135.92, 135.18, 133.26, 131.07, 130.41, 127.51, 126.70, 126.29 (q, $J = 5.2$ Hz), 125.54 (q, $J = 272.7$ Hz), 120.83 (q, $J = 30.7$ Hz), 117.79 (13C, 12 Ar-C, CF₃), 100.29 (C-1), 82.94 (C(CH₃)₃), 76.07 (C-5), 72.25 (C-3), 71.75 (C-2), 68.13 (C-4), 62.68 (C-6), 43.37 (NHCH₂), 28.30 ppm (3C, C(CH₃)₃); HRMS: m/z : Calcd for C₂₆H₃₀F₃NNaO₉ [M+Na]⁺: 580.1770, found: 580.1763.

20f: $[\alpha]_D^{20} +45.7$ (*c* 0.97, H₂O); ¹H NMR (500 MHz, D₂O): $\delta = 7.71$ (m, 2H, Ar-H), 7.55 (m, 2H, Ar-H), 7.47 (br d, $J = 7.9$ Hz, 1H, Ar-H), 7.41 (t, $J = 7.7$ Hz, 1H, Ar-H), 7.24 (d, $J = 8.4$ Hz, 1H, Ar-H), 5.61 (d, $J = 1.1$ Hz, 1H, H-1), 4.14 (dd, $J = 1.8, 3.2$ Hz, 1H, H-2), 4.02 (dd, $J = 3.4, 9.7$ Hz, 1H, H-3), 3.96 (s, 2H, NHCH₂), 3.81-3.76 (m, 3H, H-4, H-6a, H-6b), 3.66 ppm (ddd, $J = 3.2, 4.6, 9.8$ Hz, 1H, H-5); ¹³C NMR (125 MHz, D₂O): $\delta = 176.64$ (CH₂CO), 169.46 (CONH), 152.37, 138.61, 133.65, 132.91, 131.62, 129.76, 129.23, 126.03, 125.12, 124.94,

115.77 (13C, Ar-C, CF₃), 97.34 (C-1), 73.78 (C-5), 70.31 (C-3), 69.70 (C-2), 66.34 (C-4), 60.60 (C-6), 43.83 ppm (NHCH₂); HRMS: *m/z*: Calcd for C₂₂H₂₂F₃NNaO₉ [M+H]⁺: 524.1144, found: 524.1141.

Ethyl 1-[4-(2,3,4,6-tetra-*O*-acetyl- α -D-mannopyranosyloxy)-3-chlorophenyl]-4-methyl-1*H*-pyrrole-3-carboxylate (22). To a solution of **3**^[21] (400 mg, 0.684 mmol) and **21** (130 mg, 0.821 mmol, 1.2 eq) in 1,4-dioxane (1.6 mL) were added K₃PO₄ (314 mg, 1.44 mmol, 2.1 eq), CuI (6.6 mg, 34.2 μ mol, 0.05 eq) and *trans*-1,2-diaminocyclohexane (8.2 μ L, 0.068 mmol, 0.1 eq) under argon. The reaction was stirred at 100 °C for 19 h, then the mixture was filtered through Celite, concentrated in vacuo and co-evaporated with xylene (10 mL). The crude product was dissolved in dry pyridine (5 mL) and Ac₂O (260 μ L, 2.76 mmol, 4.0 eq) was added. The mixture was stirred at 60 °C for 2 h, then diluted with EtOAc (50 mL) and washed with H₂O (3 x 20 mL) and brine (20 mL). The organic layer was dried over Na₂SO₄, concentrated in vacuo and co-evaporated with xylene (2 x 10 mL). The crude compound was purified by MPLC on silica gel (petroleum ether/EtOAc, 1:0-0:1) solvent system to give **22** (366 mg, 88%) as colorless oil. Analytical data are in accordance with literature data.^[34]

1-[3-Chloro-4-(α -D-mannopyranosyloxy)phenyl]-4-methyl-1*H*-pyrrole-3-carboxylic acid (23). A solution of **22** (366 mg, 0.600 mmol) in MeOH (10 mL) was treated with freshly prepared 1 M MeONa/MeOH (600 μ L) at rt for 1.5 h under argon. Then, 2 M aq. NaOH (20 mL) was added and stirring was continued for 8.5 h. The reaction mixture was acidified with an excess of AcOH and concentrated. The crude product was purified by MPLC on RP-18 (H₂O/MeOH, 19:1-1:19) to afford **23** (65 mg, 26%) as a white solid. Analytical data are in accordance with literature data.^[34]

***tert*-Butyl (1-[3-chloro-4-(α -D-mannopyranosyloxy)phenyl]-4-methyl-1*H*-pyrrole-3-carbonyl)-glycinate (24b).** Prepared according to general procedure D from **23** (18 mg, 0.043 mmol) and H-Gly-*Ot*Bu·HCl (15 mg, 0.087 mmol, 2.0 eq) with TEA (34 μ L, 0.258 mmol, 6.0 eq) and COMU (37 mg, 0.087 mmol, 2.0 eq) in DMF (2 mL). Purified by preparative LC-MS (H₂O/MeCN, 19:1-1:19, +0.2% HCOOH). Yield: 10 mg (45%) as colorless oil. [α]_D²⁰ +58.9 (*c* 0.90, MeOH); ¹H NMR (500 MHz, CD₃OD): δ = 7.63 (d, *J* = 2.4 Hz, 1H, Ar-H), 7.57 (d, *J* = 2.7 Hz, 1H, Ar-H), 7.46 (d, *J* = 8.9 Hz, 1H, Ar-H), 7.39 (dd, *J* = 2.7, 8.9 Hz, 1H, Ar-H), 6.97 (m, 1H, Ar-H), 5.55 (d, *J* = 1.5 Hz, 1H, H-1), 4.11 (dd, *J* = 1.8,

3.3 Hz, 1H, H-2), 3.99-3.96 (m, 3H, H-3, NHCH₂), 3.81-3.70 (m, 3H, H-4, H-6a, H-6b), 3.65 (ddd, $J = 2.2, 5.6, 9.7$ Hz, 1H, H-5), 2.29 (s, 3H, CH₃), 1.49 ppm (s, 9H, C(CH₃)₃); ¹³C NMR (125 MHz, CD₃OD): $\delta = 171.17, 168.32$ (2 CO), 151.62, 136.57, 125.81, 123.05, 122.78, 120.83, 120.73, 120.41, 119.39 (10C, Ar-C), 101.09 (C-1), 82.78 (C(CH₃)₃), 76.07 (C-5), 72.38 (C-3), 71.81 (C-2), 68.23 (C-4), 62.69 (C-6), 42.81 (NHCH₂), 28.32 (3C, C(CH₃)₃), 11.73 ppm (CH₃); HRMS: m/z : Calcd for C₂₄H₃₁ClN₂NaO₉ [M+Na]⁺: 549.1616, found: 549.1617.

tert-Butyl (1-[3-chloro-4-(α -D-mannopyranosyloxy)phenyl]-4-methyl-1H-pyrrole-3-carboxamido)-propanoate (24c). Prepared according to general procedure D from **23** (25 mg, 0.060 mmol) and H- β -Ala-O t Bu-HCl (23 mg, 0.121 mmol, 2.0 eq) with DIPEA (62 μ L, 0.360 mmol, 6.0 eq) and COMU (53 mg, 0.121 mmol, 2.0 eq) in DMF (2 mL). Purified by MPLC on silica gel (DCM/MeOH, 9:1) followed by preparative LC-MS (H₂O/MeCN, 19:1-1:19, + 0.2% HCOOH). Yield: 17 mg (52%) as colorless oil. $[\alpha]_D^{20} +69.2$ (c 0.85, MeOH); ¹H NMR (500 MHz, CD₃OD): $\delta = 7.56$ (d, $J = 2.4$ Hz, 1H, Ar-H), 7.55 (d, $J = 2.7$ Hz, 1H, Ar-H), 7.45 (d, $J = 8.9$ Hz, 1H, Ar-H), 7.36 (dd, $J = 2.7, 8.9$ Hz, 1H, Ar-H), 6.94 (m, 1H, Ar-H), 5.54 (d, $J = 1.5$ Hz, 1H, H-1), 4.11 (dd, $J = 1.8, 3.2$ Hz, 1H, H-2), 3.97 (dd, $J = 3.4, 9.5$ Hz, 1H, H-3), 3.81-3.70 (m, 3H, H-4, H-6a, H-6b), 3.64 (ddd, $J = 2.2, 5.6, 9.7$ Hz, 1H, H-5), 3.55 (t, $J = 6.8$ Hz, 2H, NHCH₂), 2.54 (t, $J = 6.8$ Hz, 2H, CH₂CO), 2.27 (s, 3H, CH₃), 1.46 ppm (s, 9H, C(CH₃)₃); ¹³C NMR (125 MHz, CD₃OD): $\delta = 173.11$ (CH₂CO), 168.10 (CONH), 151.57, 136.56, 125.80, 122.97, 122.79, 122.47, 121.23, 120.64, 120.34, 119.39 (10C, Ar-C), 101.08 (C-1), 81.93 (C(CH₃)₃), 76.06 (C-5), 72.37 (C-3), 71.80 (C-2), 68.23 (C-4), 62.68 (C-6), 36.44 (CH₂CO, NHCH₂), 28.34 (3C, C(CH₃)₃), 11.76 ppm (CH₃); HRMS: m/z : Calcd for C₂₅H₃₃ClN₂NaO₉ [M+Na]⁺: 563.1772, found: 563.1772.

(1-[3-Chloro-4-(α -D-mannopyranosyloxy)phenyl]-4-methyl-1H-pyrrole-3-carbonyl)-glycine (25e). Prepared according to general procedure C from **24b** (9 mg, 0.017 mmol) with 1 M aq NaOH (1 mL) in MeOH (1 mL). The mixture was acidified with an excess of AcOH (120 μ L). Purified by preparative LC-MS (H₂O/MeCN, 19:1-1:19, + 0.2% HCOOH). Yield: 5 mg (63%) as colorless oil. $[\alpha]_D^{20} +80.6$ (c 0.50, MeOH); ¹H NMR (500 MHz, CD₃OD): $\delta = 7.65$ (m, 1H, Ar-H), 7.58 (d, $J = 2.7$ Hz, 1H, Ar-H), 7.46 (d, $J = 8.9$ Hz, 1H, Ar-H), 7.39 (dd, $J = 2.7, 8.9$ Hz, 1H, Ar-H), 6.97 (m, 1H, Ar-H), 5.55 (d, $J = 1.5$ Hz, 1H, H-1), 4.11 (dd, $J = 1.8, 3.3$ Hz, 1H, H-2), 4.04 (br s, 2H, NHCH₂), 3.98 (dd, $J = 3.4, 9.5$ Hz, 1H, H-3), 3.81-3.70

(m, 3H, H-4, H-6a, H-6b), 3.65 (ddd, $J = 2.2, 5.6, 9.7$ Hz, 1H, H-5), 2.29 ppm (s, 3H, CH₃); ¹³C NMR (125 MHz, CD₃OD): $\delta = 173.48, 168.24$ (2 CO), 151.62, 136.58, 125.81, 123.06, 122.85, 120.72, 120.39, 119.40 (10C, Ar-C), 101.10 (C-1), 76.07 (C-5), 72.38 (C-3), 71.81 (C-2), 68.23 (C-4), 62.69 (C-6), 41.49 (NHCH₂), 11.74 ppm (CH₃); HRMS: m/z : Calcd for C₂₀H₂₃ClN₂NaO₉ [M+Na]⁺: 493.0990, found: 493.0990.

(1-[3-Chloro-4-(α -D-mannopyranosyloxy)phenyl]-4-methyl-1H-pyrrole-3-

carboxamido)-propanoic acid (25g). Prepared according to general procedure C from **24c** (9 mg, 0.017 mmol) with 1 M aq NaOH (1 mL) in MeOH (1 mL). The mixture was acidified with an excess of AcOH (120 μ L). Purified by preparative LC-MS (H₂O/MeCN, 19:1-1:19, + 0.2% HCOOH). Yield: 5 mg (63%) as colorless oil. $[\alpha]_D^{20} +84.8$ (c 0.50, MeOH); ¹H NMR (500 MHz, CD₃OD): $\delta = 7.58$ (d, $J = 2.4$ Hz, 1H, Ar-H), 7.56 (d, $J = 2.7$ Hz, 1H, Ar-H), 7.46 (d, $J = 9.0$ Hz, 1H, Ar-H), 7.38 (dd, $J = 2.7, 8.9$ Hz, 1H, Ar-H), 6.95 (m, 1H, Ar-H), 5.54 (d, $J = 1.5$ Hz, 1H, H-1), 4.11 (dd, $J = 1.8, 3.3$ Hz, 1H, H-2), 3.97 (dd, $J = 3.4, 9.5$ Hz, 1H, H-3), 3.81-3.70 (m, 3H, H-4, H-6a, H-6b), 3.64 (ddd, $J = 2.3, 5.6, 9.7$ Hz, 1H, H-5), 3.58 (t, $J = 6.7$ Hz, 2H, NHCH₂), 2.61 (t, $J = 6.7$ Hz, 2H, CH₂CO), 2.28 ppm (s, 3H, CH₃); ¹³C NMR (125 MHz, CD₃OD): $\delta = 175.25$ (CH₂CO), 168.07 (CONH), 151.58, 136.59, 125.80, 122.98, 122.83, 122.54, 121.21, 120.66, 120.32, 119.39 (10C, Ar-C), 101.10 (C-1), 76.07 (C-5), 72.38 (C-3), 71.81 (C-2), 68.23 (C-4), 62.69 (C-6), 36.43 (2C, CH₂CO, NHCH₂), 11.74 ppm (CH₃); HRMS: m/z : Calcd for C₂₁H₂₅ClN₂NaO₉ [M+Na]⁺: 507.1146, found: 507.1145.

3'-Chloro-N-(2-hydroxyethyl)-4'-(α -D-mannopyranosyloxy)biphenyl-3-carboxamide

(27i). Prepared according to general procedure D from **26**^[34] (30 mg, 0.073 mmol) and ethanolamine (9 μ L, 0.146 mmol, 2.0 eq) with TEA (31 μ L, 0.219 mmol, 3.0 eq) and COMU (63 mg, 0.146 mmol, 2.0 eq) in DMF (2 mL). Purified by preparative LC-MS (H₂O/MeCN, 19:1-1:19, + 0.2% HCOOH). Yield: 24 mg (73%) as colorless oil. $[\alpha]_D^{20} +77.9$ (c 1.20, MeOH); ¹H NMR (500 MHz, CD₃OD): $\delta = 8.06$ (t, $J = 1.5$ Hz, 1H, Ar-H), 7.81 (m, 1H, Ar-H), 7.75-7.73 (m, 2H, Ar-H), 7.58 (dd, $J = 2.3, 8.6$ Hz, 1H, Ar-H), 7.52 (t, $J = 7.8$ Hz, 1H, Ar-H), 7.45 (d, $J = 8.6$ Hz, 1H, Ar-H), 5.60 (d, $J = 1.5$ Hz, 1H, H-1), 4.12 (dd, $J = 1.8, 3.3$ Hz, 1H, H-2), 4.01 (dd, $J = 3.4, 9.5$ Hz, 1H, H-3), 3.81-3.71 (m, 5H, H-4, H-6a, H-6b, CH₂O), 3.66 (ddd, $J = 2.3, 5.3, 9.7$ Hz, 1H, H-5), 3.54 ppm (t, $J = 5.8$ Hz 2H, NHCH₂); ¹³C NMR (125 MHz, CD₃OD): $\delta = 170.29$ (CONH), 152.98, 140.92, 136.77, 136.32, 130.75, 130.24, 129.63, 127.60, 127.35, 126.57, 125.33, 118.66 (12C, Ar-C), 100.76 (C-1), 75.97 (C-

5), 72.40 (C-3), 71.85 (C-2), 68.22 (C-4), 62.65 (C-6), 61.62 (CH₂O), 43.63 ppm (NHCH₂); HRMS: *m/z*: Calcd for C₂₁H₂₄ClNNaO₈ [M+Na]⁺: 476.1088, found: 476.1088.

[3'-Chloro-4'-(α-D-mannopyranosyloxy)biphenyl-3-yl](3-hydroxyazetidin-1-

yl)methanone (27j). Prepared according to general procedure D from **26**^[34] (20 mg, 0.049 mmol) and 3-hydroxyazetidine hydrochloride (11 mg, 0.098 mmol, 2.0 eq) with TEA (20 μL, 0.147 mmol, 3.0 eq) and COMU (42 mg, 0.098 mmol, 2.0 eq) in DMF (2 mL). Purified by preparative LC-MS (H₂O/MeCN, 19:1-1:19, + 0.2% HCOOH). Yield: 19 mg (83%) as colorless oil. [α]_D²⁰ +74.9 (*c* 0.95, MeOH); ¹H NMR (500 MHz, CD₃OD): δ = 7.82 (m, 1H, Ar-H), 7.73 (m, 1H, Ar-H), 7.68 (d, *J* = 2.2 Hz, 1H, Ar-H), 7.59 (m, 1H, Ar-H), 7.56-7.51 (m, 2H, Ar-H), 7.46 (d, *J* = 7.7 Hz, 1H, Ar-H), 5.60 (d, *J* = 1.5 Hz, 1H, H-1), 4.63 (tt, *J* = 1.5 Hz, 1H, OCH), 4.59 (m, 1H, CH₂N), 4.42 (dd, *J* = 7.2, 10.2 Hz, 1H, CH₂N), 4.16 (dd, *J* = 3.4, 9.1 Hz, 1H, CH₂N), 4.12 (dd, *J* = 1.8, 3.3 Hz, 1H, H-2), 4.02-3.96 (m, 2H, H-3, CH₂N), 3.81-3.71 (m, 3H, H-4, H-6a, H-6b), 3.66 ppm (ddd, *J* = 2.3, 5.4, 9.7 Hz, 1H, H-5); ¹³C NMR (125 MHz, CD₃OD): δ = 172.11 (CONH), 153.06, 141.13, 136.63, 134.98, 130.57, 130.29, 129.60, 127.68, 127.63, 127.07, 125.37, 118.72 (12 C, Ar-C), 100.77 (C-1), 75.99 (C-5), 72.40 (C-3), 71.84 (C-2), 68.22 (C-4), 64.15 (CH₂N), 62.66 (C-6), 62.28 (OCH), 59.77 ppm (CH₂N); HRMS: *m/z*: Calcd for C₂₂H₂₄ClNNaO₈ [M+Na]⁺: 488.1088, found: 488.1088.

3'-Chloro-4'-(α-D-mannopyranosyloxy)-N-(pyridine-4-yl)biphenyl-3-carboxamide

(27k). Prepared according to general procedure D from **26**^[34] (37 mg, 0.090 mmol) and 4-aminopyridine (17 mg, 0.180 mmol, 2.0 eq) with TEA (33 μL, 0.270 mmol, 3.0 eq) and COMU (79 mg, 0.180 mmol, 2.0 eq) in DMF (2 mL). Purified by preparative LC-MS (H₂O/MeCN, 19:1-1:19, + 0.2% HCOOH). Yield: 24 mg (55%) as colorless oil. [α]_D²⁰ +62.4 (*c* 1.00, MeOH); ¹H NMR (500 MHz, CD₃OD): δ = 8.48 (br s, 2H, Ar-H), 8.16 (m, 1H, Ar-H), 7.92 (br d, *J* = 6.2 Hz, 3H, Ar-H), 7.83 (br d, *J* = 7.9 Hz, 1H, Ar-H), 7.76 (d, *J* = 2.2 Hz, 1H, Ar-H), 7.61-7.58 (m, 2H, Ar-H), 7.47 (d, *J* = 8.6 Hz, 1H, Ar-H), 5.61 (d, *J* = 1.3 Hz, 1H, H-1), 4.13 (dd, *J* = 1.8, 3.2 Hz, 1H, H-2), 4.01 (dd, *J* = 3.4, 9.5 Hz, 1H, H-3), 3.81-3.72 (m, 3H, H-4, H-6a, H-6b), 3.66 ppm (ddd, *J* = 2.3, 5.4, 9.6 Hz, 1H, H-5); ¹³C NMR (125 MHz, CD₃OD): δ = 168.97 (CONH), 153.09, 149.89, 149.21, 141.16, 136.51, 136.09, 131.66, 130.45, 129.70, 127.92, 127.67, 127.05, 125.39, 118.68, 115.98 (17C, Ar-C), 100.75 (C-1), 76.00 (C-5), 72.41 (C-3), 71.85 (C-2), 68.23 (C-4), 62.67 ppm (C-6); HRMS: *m/z*: Calcd for C₂₄H₂₄ClN₂O₇ [M+H]⁺: 487.1272, found: 487.1272.

3'-Chloro-4'-(α -D-mannopyranosyloxy)-N-(pyridine-4-ylmethyl)biphenyl-3-

carboxamide (27l). Prepared according to general procedure D from **26**^[34] (33 mg, 0.080 mmol) and 4-(aminomethyl)pyridine (16 μ L, 0.161 mmol, 2.0 eq) with DIPEA (41 μ L, 0.240 mmol, 3.0 eq) and COMU (71 mg, 0.161 mmol, 2.0 eq) in DMF (2 mL). Purified by MPLC on silica gel (DCM/MeOH, 9:1) followed by preparative LC-MS (H₂O/MeCN, 19:1-1:19, + 0.2% HCOOH). Yield: 25 mg (63%) as colorless oil. $[\alpha]_D^{20} +71.9$ (*c* 1.01, MeOH); ¹H NMR (500 MHz, CD₃OD): δ = 8.50 (br s, 2H, Ar-H), 8.11 (m, 1H, Ar-H), 7.86 (br d, *J* = 7.8 Hz, 1H, Ar-H), 7.78 (br d, *J* = 8.0 Hz, 1H, Ar-H), 7.74 (d, *J* = 2.2 Hz, 1H, Ar-H), 7.59-7.54 (m, 2H, Ar-H), 7.47-7.43 (m, 3H, Ar-H), 5.60 (d, *J* = 1.4 Hz, 1H, H-1), 4.65 (s, 2H, NHCH₂), 4.12 (dd, *J* = 1.8, 3.3 Hz, 1H, H-2), 4.01 (dd, *J* = 3.4, 9.5 Hz, 1H, H-3), 3.81-3.71 (m, 3H, H-4, H-6a, H-6b), 3.66 ppm (ddd, *J* = 2.3, 5.4, 9.7 Hz, 1H, H-5); ¹³C NMR (125 MHz, CD₃OD): δ = 170.10 (CONH), 153.04, 151.04, 150.08, 141.10, 136.67, 135.80, 131.11, 130.40, 129.66, 127.62, 127.42, 126.64, 125.36, 124.02, 118.68 (17C, Ar-C), 100.77 (C-1), 76.00 (C-5), 72.40 (C-3), 71.85 (C-2), 68.23 (C-4), 62.66 (C-6), 43.56 ppm (NHCH₂); HRMS: *m/z*: Calcd for C₂₅H₂₆ClN₂O₇ [M+H]⁺: 501.1429, found: 501.1524.

Competitive cell-free binding assay**Reagents**

Bacto-Yeast extract, Bacto-Agar, and Bacto-Tryptone were purchased from Becton Dickinson (Basel, Switzerland). Isopropyl 1-thio- β -D-galactopyranoside (IPTG) was obtained from Applichem (Darmstadt, Germany). Polymyxin B sulfate, Hepes (4-(2-hydroxyethyl)-piperazine-1-ethanesulfonic acid), oxalic acid, MgCl₂, CaCl₂, NaH₂PO₄, imidazole were from Fluka (Buchs, Switzerland). Ampicillin, bovine serum albumin (BSA) and ethylenediaminetetraacetic acid (EDTA), amino acids and BME vitamin mix were obtained from Sigma (Buchs, Switzerland). *n*-Heptyl α -D-mannopyranoside (**28**) was synthesized as previously described^[40]. The biotinylated polyacrylamide (PAA) glycopolymer Man α 1-3(Man α 1-6)Man β 1-4GlcNAc β 1-4GlcNAc β -PAA-biotin (TM-PAA) containing 20 mol% sugar residues and 5 mol% biotin was purchased from Lectinity (Moscow, Russia). MaxiSorp 96-well microtiter plates were from Nunc (Roskilde, Denmark).

Cloning of FimH-CRD wild type and R98A mutant

FimH-CRD construct linked to the thrombin cleavage site (Th), and a 6His-tag (6His) was generated as described previously.^[35] The R98A mutation was inserted by overlap extension PCR method^[41] using the wild type (*wt*) encoding plasmid as template. The correctness of the construct was confirmed by DNA sequencing (Microsynth, Balgach, Switzerland). The wild type and R98A proteins were expressed in the protease-deficient *E. coli* strain HM 125^[42] and purified by affinity chromatography on a Ni-NTA column as reported.^[35] The purity of the proteins was verified by SDS–PAGE analysis, and the amount was determined by HPLC using BSA as standard.^[43] The exact molecular mass was determined by LC-MS.

Competitive binding assay

To evaluate the affinity of the proteins a competitive binding assay described previously was applied.^[35] Microtiter plates (F96 MaxiSorp, Nunc) were coated with 100 μ L/well of a 10 μ g/mL solution of FimH-CRD in 20 mM HEPES, 150 mM NaCl and 1 mM CaCl₂, pH 7.4 (assay buffer) overnight at 4 °C. The coating solution was discarded and the wells were blocked with 150 μ L/well of 3% BSA in assay buffer for 2 h at 4 °C. After three washing steps with assay buffer (150 μ L/well), a serial dilution of the test compound (50 μ L/well) in assay buffer containing 5% DMSO and streptavidin-peroxidase coupled TM-PAA polymer (50 μ L/well of a 0.5 μ g/mL solution) were added. The plates were incubated for 3 h at 25 °C and 350 rpm and then carefully washed four times with 150 μ L/well assay buffer. After the addition of 100 μ L/well of ABTS-substrate, the colorimetric reaction was allowed to develop for 4 min, then stopped by the addition of 2% aqueous oxalic acid before the optical density (OD) was measured at 415 nm on a microplate-reader (Spectramax 190, Molecular Devices, California, USA). The IC₅₀ values of the compounds tested in duplicates were calculated with prism software (GraphPad Software, Inc., La Jolla, USA). The IC₅₀ defines the molar concentration of the test compound that reduces the maximal specific binding of TM-PAA polymer to FimH-CRD by 50%. The relative IC₅₀ (rIC₅₀) is the ratio of the IC₅₀ of the test compound to the IC₅₀ of *n*-heptyl α -D-mannopynoside (**28**).

Pharmacokinetic Assays

Aqueous solubility

Solubility was determined in a 96-well format using the μ SOL Explorer solubility analyzer (pIon, version 3.4.0.5). For each compound, measurements were performed in triplicate at pH 7.4 (for compounds **27k** and **27l** solubility at pH 3.0 was measured additionally). Six wells of a deep well plate, i.e. three wells per pH value, were filled with 300 μ L of PRISMA HT universal buffer adjusted to pH 3.0 or 7.4 by adding the requested amount of NaOH (0.5 M). Aliquots (3 μ L) of a compound stock solution (40-100 mM in DMSO) were added and thoroughly mixed. The final sample concentration was 0.4-1.0 mM, the residual DMSO concentration was 1.0% (v/v) in the buffer solutions. After 15 h, the solutions were filtrated (0.2 μ m 96-well filter plates) using a vacuum to collect manifold (Whatman Ltd., Maidstone, UK) to remove any precipitates. Equal amounts of filtrate and 1-propanol were mixed and transferred to a 96-well plate for UV/Vis detection (190 to 500 nm, SpectraMax 190, Molecular Devices, Silicon Valley, CA, USA). The amount of material dissolved was calculated by comparison with UV/Vis spectra obtained from reference samples, which were prepared by dissolving compound stock solution in a 1:1 mixture of buffer and 1-propanol (final concentrations 0.067-0.167 mM).

log $D_{7.4}$ determination

The in silico prediction tool ALOGPS^[44] was used to estimate the log P values of the compounds. Depending on these values, the compounds were classified into three categories: hydrophilic compounds (log P below zero), moderately lipophilic compounds (log P between zero and one) and lipophilic compounds (log P above one). For each category, two different ratios (volume of 1-octanol to volume of buffer) were defined as experimental parameters (Table 4).

Table 4. Compound classification based on estimated log P values.

compound type	log P	ratios (1-octanol: buffer)
hydrophilic	< 0	30:140, 40:130
moderately lipophilic	0 - 1	70:110, 110:70
lipophilic	> 1	3:180, 4:180

Equal amounts of phosphate buffer (0.1 M, pH 7.4) and 1-octanol were mixed and shaken vigorously for 5 min to saturate the phases. The mixture was left until separation of the two phases occurred, and the buffer was retrieved. Stock solutions of the test compounds were diluted with buffer to a concentration of 1 μ M. For each compound, six determinations, *i.e.* three determinations per 1-octanol:buffer ratio, were performed in different wells of a 96-well plate. The respective volumes of buffer containing analyte (1 μ M) were pipetted to the wells and covered by saturated 1-octanol according to the chosen volume ratio. The plate was sealed with aluminium foil, shaken (1350 rpm, 25 °C, 2 h) on a Heidolph Titramax 1000 plate-shaker (Heidolph Instruments GmbH & Co. KG, Schwabach, Germany) and centrifuged (2000 rpm, 25 °C, 5 min, 5804 R Eppendorf centrifuge, Hamburg, Germany). The aqueous phase was transferred to a 96-well plate for analysis by liquid chromatography-mass spectrometry (LC-MS, see below).

The $\log D_{7.4}$ coefficients were calculated from the 1-octanol:buffer ratio (o:b), the initial concentration of the analyte in buffer (1 μ M), and the concentration of the analyte in buffer (c_B) with Equation 1:

$$\log D_{7.4} = \log \left(\frac{1\mu\text{M} - c_B}{c_B} \times \frac{1}{o:b} \right) \quad (\text{eq. 1})$$

The average of the three $\log D_{7.4}$ values per 1-octanol:buffer ratio was calculated. If the two means obtained for a compound did not differ by more than 0.1 units, the results were accepted.

Parallel artificial membrane permeability assay (PAMPA)

Effective permeability ($\log P_e$) was determined in a 96-well format with the PAMPA permeability assay.^[38] For each compound, measurements were performed in quadruplicate at pH 7.4 (for compounds **27k** and **27l** permeability at pH 5.0 was measured additionally). For this purpose, wells of a deep-well plate were filled with 650 μ L System Solution. Samples (150 μ L) were withdrawn from each well to determine the blank spectra by UV-spectroscopy (190 to 500 nm, SpectraMax 190). Then, analyte dissolved in DMSO (10 mM) was added to the remaining System Solution to yield 50 μ M solutions. To exclude precipitation, the optical density was measured at 650 nm, with 0.01 being the threshold value. Solutions exceeding this threshold were filtrated. Afterwards, samples (150 μ L) were withdrawn to determine the reference spectra. Further 200 μ L was transferred to each well of the donor plate of the PAMPA sandwich (pIon, P/N 110 163). The filter membranes at the bottom of the acceptor

plate were infused with 5 μ L of GIT-0 Lipid Solution and 200 μ L of Acceptor Sink Buffer was filled into each acceptor well. The sandwich was assembled, placed in the GutBox™, and left undisturbed for 16 h. Then, it was disassembled and samples (150 μ L) were transferred from each donor and acceptor well to UV-plates. Quantification was done by UV/Vis-spectroscopy. Effective permeability ($\log P_e$) was calculated from the compound flux deduced from the UV/Vis spectra, the filter area, and the initial sample concentration in the donor well with the aid of the PAMPA Explorer Software (pIon, version 3.5).

LC-MS measurements

Analyses were performed using a 1100/1200 Series HPLC System coupled to a 6410 Triple Quadrupole mass detector (Agilent Technologies, Inc., Santa Clara, CA, USA) equipped with electrospray ionization. The system was controlled with the Agilent MassHunter Workstation Data Acquisition software (version B.01.04). The column used was an Atlantis® T3 C18 column (2.1 x 50 mm) with a 3 μ m-particle size (Waters Corp., Milford, MA, USA). The mobile phases (A, water; B, MeCN) contained 0.1% formic acid (v/v) and were delivered at 0.6 ml/min. The gradient was ramped from 95% A/5% B to 5% A/95% B over 1 min, and then hold at 5% A/95% B for 0.1 min. The system was then brought back to 95% A/5% B, resulting in a total duration of 4 min. MS parameters such as fragmentor voltage, collision energy, polarity were optimized individually for each drug, and the molecular ion was followed for each compound in the multiple reaction monitoring mode. The concentrations of the analytes were quantified by the Agilent Mass Hunter Quantitative Analysis software (version B.01.04 and B.03.01).

Supporting Information

NMR spectra and HPLC traces to document purity of the test compounds.

References

- [1] Foxman, B.; Barlow, R.; D'Arcy, H.; Gillespie, B.; Sobel, J. D. Urinary tract infection: Self reported incidence and associated costs. *Ann. Epidemiol.* **2000**, *10*, 509-515.
- [2] Roland, A. The etiology of urinary tract infection: Traditional and emerging

- p pathogens.
- Am. J. Med.*
- 2002**
- ,
- 113 (Suppl 1A)*
- , 14S-19S.
- [3] Cegelski, L.; Marshall, G. R.; Eldridge, G. R.; Hultgren, S. J. The biology and future prospects of antivirulence therapies. *Nat. Rev. Microbiol.* **2008**, *6*, 17-27.
 - [4] Wiles, T. J.; Kulesus, R. R.; Mulvey, M. A. Origins and virulence mechanisms of uropathogenic *Escherichia coli*. *Exp. Mol. Pathol.* **2008**, *85*, 11-19.
 - [5] Sanchez, G. V.; Master, R. N.; Karlowsky, J. A.; Bordon, J. M. In vitro antimicrobial resistance of urinary *Escherichia coli* isolates among U.S. outpatients from 2000 to 2010. *Antimicrob. Agents Chemother.* **2012**, *56*, 2181-2183.
 - [6] Mulvey, M. A.; Schilling, J. D.; Martinez, J. J.; Hultgren, S. J. Bad bugs and beleaguered bladders: interplay between uropathogenic *Escherichia coli* and innate host defenses. *Proc. Natl. Acad. Sci. U.S.A.* **2000**, *97*, 8829-8835.
 - [7] Schilling, J. D.; Mulvey, M. A.; Hultgren, S. J. Structure and function of *Escherichia coli* type 1 pili: new insight into the pathogenesis of urinary tract infections. *J. Infect. Dis.* **2001**, *183 (Suppl 1)*, S36-S40.
 - [8] Pak, J.; Pu, Y.; Zhang, Z.-T.; Hasty, D.L.; Wu, X.-R. Tamm-Horsfall protein binds to type 1 fimbriated *Escherichia coli* and prevents *E. coli* from binding to uroplakin Ia and Ib receptors. *J. Biol. Chem.* **2001**, *276*, 9924-9930.
 - [9] Firon, N.; Ofek, I.; Sharon, N. Interaction of mannose-containing oligosaccharides with the fimbrial lectin of *Escherichia coli*. *Biochem. Biophys. Res. Commun.* **1982**, *105*, 1426-1432.
 - [10] Firon, N.; Ofek, I.; Sharon, N. Carbohydrate specificity of the surface lectins of *Escherichia coli*, *Klebsiella pneumoniae*, and *Salmonella typhimurium*. *Carbohydr. Res.* **1983**, *120*, 235-249.
 - [11] Firon, N.; Ashkenazi, S.; Mirelman, D.; Ofek, I.; Sharon, N. Aromatic alpha-glycosides of mannose are powerful inhibitors of the adherence of type 1 fimbriated *Escherichia coli* to yeast and intestinal epithelial cells. *Infect. Immun.* **1987**, *55*, 472-476.
 - [12] Bouckaert, J.; Berglund, J.; Schembri, M.; Genst, E. D.; Cools, L.; Wuhler, M.; Hung, C. S.; Pinkner, J.; Slättergard, R.; Zavialov, A.; Choudhury, D.; Langermann, S.; Hultgren, S. J.; Wyns, L.; Klemm, P.; Oscarson, S.; Knight, S. D.; Greve, H. D. Receptor binding studies disclose a novel class of high-affinity inhibitors of the *Escherichia coli* FimH adhesin. *Mol. Microbiol.* **2005**, *55*, 441– 455.
 - [13] Wellens, A.; Garofalo, C.; Nguyen, H.; Van Gerven, N.; Slättegård, R.; Hernalsteens,

- J. P.; Wyns, L.; Oscarson, S.; De Greve, H.; Hultgren, S.; Bouckaert, J. Intervening with urinary tract infections using anti-adhesives based on the crystal structure of the FimH-oligomannose-3 complex. *PLoS One* **2008**, *3*, e2040.
- [14] Wellens, A.; Lahmann, M.; Touaibia, M.; Vaucher, J.; Oscarson, S.; Roy, R.; Remaut, H.; Bouckaert, J. The tyrosine gate as a potential entropic lever in the receptor-binding site of the bacterial adhesin FimH. *Biochemistry* **2012**, *51*, 4790–4799.
- [15] Sperling, O.; Fuchs, A.; Lindhorst, T. K. Evaluation of the carbohydrate recognition domain of the bacterial adhesin FimH: Design, synthesis and binding properties of mannoside ligands. *Org. Biomol. Chem.* **2006**, *4*, 3913–3922.
- [16] Han, Z.; Pinkner, J. S.; Ford, B.; Obermann, R.; Nolan, W.; Wildman, S. A.; Hobbs, D.; Ellenberger, T.; Cusumano, C. K.; Hultgren, S. J.; Janetka, J. W. Structure-based drug design and optimization of mannoside bacterial FimH antagonists. *J. Med. Chem.* **2010**, *53*, 4779–4792.
- [17] Klein, T.; Abgottspon, D.; Wittwer, M.; Rabbani, S.; Herold, J.; Jiang, X.; Kleeb, S.; Lüthi, C.; Scharenberg, M.; Bezençon, J.; Gubler, E.; Pang, L.; Smieško, M.; Cutting, B.; Schwardt, O.; Ernst, B. FimH antagonists for the oral treatment of urinary tract infections: from design and synthesis to in vitro and in vivo evaluation. *J. Med. Chem.* **2010**, *53*, 8627–8641.
- [18] Cusumano, C. K.; Pinkner, J. S.; Han, Z.; Greene, S. E.; Ford, B. A.; Crowley, J. R.; Henderson, J. P.; Janetka, J. W.; Hultgren, S. J. Treatment and prevention of urinary tract infection with orally active FimH inhibitors. *Sci. Transl. Med.* **2011**, *3*, 109ra115.
- [19] Han, Z.; Pinkner, J. S.; Ford, B.; Chorell, E.; Crowley, J. M.; Cusumano, C. K.; Campbell, S.; Henderson, J. P.; Hultgren, S. J.; Janetka, J. W. Lead optimization studies on FimH antagonists: discovery of potent and orally bioavailable ortho-substituted biphenyl mannosides. *J. Med. Chem.* **2012**, *55*, 3945–3959.
- [20] Pang, L.; Kleeb, S.; Lemme, K.; Rabbani, S.; Scharenberg, M.; Zalewski, A.; Schädler, F.; Schwardt, O.; Ernst, B. FimH antagonists: structure-activity and structure-property relationships for biphenyl α -D-mannopyranosides. *ChemMedChem* **2012**, *7*, 1404–1422.
- [21] Jiang, X.; Abgottspon, D.; Kleeb, S.; Rabbani, S.; Scharenberg, M.; Wittwer, M.; Haug, M.; Schwardt, O.; Ernst, B. Antiadhesion therapy for urinary tract infections –

- A balanced PK/PD profile proved to be key for success. *J. Med. Chem.* **2012**, *55*, 4700–4713.
- [22] Schwardt, O.; Rabbani, S.; Hartmann, M.; Abgottspon, D.; Wittwer, M.; Kleeb, S.; Zalewski, A.; Smieško, M.; Cutting, B.; Ernst, B. Design, synthesis and biological evaluation of mannosyl triazoles as FimH antagonists. *Bioorg. Med. Chem.* **2011**, *19*, 6454–6473.
- [23] Kleeb, S.; Pang, L.; Mayer, K.; Eris, D.; Sigl, A.; Preston, R. C.; Zihlmann, P.; Sharpe, T.; Roman, P. J.; Abgottspon, D.; Hutter, A.; Scharenberg, M.; Jiang, X.; Navarra, G.; Rabbani, S.; Smieško, M.; Lüdin, N.; Bezençon, J.; Schwardt, O.; Maier, T. Ernst, B. FimH antagonists: bioisosteres to improve the in vitro and in vivo PK/PD profile. *J. Med. Chem.* **2015**, *58*, 2221–2239.
- [24] Lindhorst, T. K.; Kieburg, C.; Krallmann-Wenzel, U. Inhibition of the type 1 fimbriae-mediated adhesion of *Escherichia coli* to erythrocytes by multiantennary D-mannosyl clusters: the effect of multivalency. *Glycoconjugate J.* **1998**, *15*, 605–613.
- [25] Nagahori, N.; Lee, R. T.; Nishimura, S.-L.; Pagé, S.; Roy, R.; Lee, Y. C. Inhibition of adhesion of type 1 fimbriated *Escherichia coli* to highly mannosylated ligands. *ChemBioChem* **2002**, *3*, 836–844.
- [26] Appeldoorn, C. C. M.; Joosten, J. A. F.; Maate, F. A.; Dobrindt, U.; Hacker, J.; Liskamp, R. M. J.; Khan, A. S.; Pieters, R. J. Novel multivalent mannose compounds and their inhibition of the adhesion of type 1 fimbriated uropathogenic *E. coli*. *Tetrahedron: Asymmetry* **2005**, *16*, 361–372.
- [27] Patel, A.; Lindhorst, T. K. A modular approach for the synthesis of oligosaccharide mimetics. *Carbohydr. Res.* **2006**, *341*, 1657–1668.
- [28] Touaibia, M.; Wellens, A.; Shiao, T. C.; Wang, Q.; Sirois, S.; Bouckaert, J.; Roy, R. Mannosylated G(0) dendrimers with nanomolar affinities to *Escherichia coli* FimH. *ChemMedChem* **2007**, *2*, 1190–1201.
- [29] Durka, M.; Buffet, K.; Iehl, J.; Holler, M.; Nierengarten, J.-F.; Taganna, J.; Bouckaert, J.; Vincent, S. P. The functional valency of dodecamannosylated fullerenes with *Escherichia coli* FimH—towards novel bacterial antiadhesives. *Chem. Commun.* **2011**, *47*, 1321–1323.
- [30] Bouckaert, J.; Li, Z.; Xavier, C.; Almant, M.; Caveliers, V.; Lahoutte, T.; Weeks, S. D.; Kovensky, J.; Gouin, S. G. Heptyl α -D-mannosides grafted on a β -cyclodextrin

- core to interfere with Escherichia coli adhesion: an in vivo multivalent effect. *Chem. Eur. J.* **2013**, *19*, 7847–7855.
- [31] (a) Eid, S.; Zalewski, A.; Smieško, M.; Ernst, B.; Vedani, A. A molecular-modeling toolbox aimed at bridging the gap between medicinal chemistry and computational sciences. *Int. J. Mol. Sci.* **2013**, *14*, 684–700; (b) Desmond Molecular Dynamics System, version 3.1, D. E. Shaw Research, New York, NY, 2012; (c) Maesetro-Desmond Interoperability Tools, version 3.1, Schrödinger, New York, NY, 2012; (d) Bowers, K. J.; Chow, E.; Xu, H.; Dror, R. O.; Eastwood, M. P.; Gregersen, B. A.; Klepeis, J. L.; Kolossvary, I.; Moraes, M. A.; Sacerdoti, F. D.; Salmon, J. K.; Shan, Y.; Shaw, D. E. Proceedings of the ACM/IEEE Conference on Supercomputing (SC06). "Scalable Algorithms for Molecular Dynamics Simulations on Commodity Clusters"; Tampa, Florida, November 11-17, 2006; (e) Maestro, version 9.3, Schrödinger, LLC, New York, NY, 2012.
- [32] Miyaoura, N.; Suzuki, A. Palladium-catalyzed cross-coupling reactions of organoboron compounds. *Chem. Rev.* **1995**, *95*, 2457-2483.
- [33] Antilla, J. C.; Baskin, J. M.; Barder, T. E.; Buchwald, S. L. Copper-diamine-catalyzed *N*-arylation of pyrroles, pyrazoles, indazoles, imidazoles, and triazoles. *J. Org. Chem.* **2004**, *69*, 5578-5587.
- [34] Pang, L. (2014). Antagonizing the Adhesion of Type 1 Fimbriae-Mediated Escherichia coli – A Novel Therapy for Urinary Tract Infections (Doctoral dissertation). University of Basel: Switzerland.
- [35] Rabbani, S.; Jiang, X.; Schwardt, O.; Ernst, B. Expression of the carbohydrate recognition domain of FimH and development of a competitive binding assay. *Anal. Biochem.* **2010**, *407*, 188-195.
- [36] Avdeef, A. In *Pharmacokinetic Optimization in Drug Research; Biological, Physicochemical and Computational Strategies*; Testa, B., van de Waterbeemd, H., Folkers, G., Guy, R., Eds.; Helvetica Chimica Acta: Zurich, **2001**; pp 305-326.
- [37] Dearden, J. C.; Bresnen, G. M. The measurement of partition coefficients. *QSAR Comb. Sci.* **1988**, *7*, 133-144.
- [38] Kansy, M.; Senner, F.; Gubernator, K. Physicochemical high throughput screening: parallel artificial membrane permeation assay in the description of passive absorption processes. *J. Med. Chem.* **1998**, *41*, 1007-1010.

- [39] Avdeef, A.; Bendels, S.; Di, L.; Faller, B.; Kansy, M.; Sugano, K.; Yamauchi, Y. PAMPA – critical factors for better predictions of absorption. *J. Pharm. Sci.* **2007**, *96*, 2893-2909.
- [40] Oscarson, S.; Tiden, A. K. Syntheses of the octyl and tetradecyl glycosides of 3,6-di-*O*- α -D-mannopyranosyl- α -D-mannopyranose and of 3,4-di-*O*- α -D-mannopyranosyl- α -D-mannopyranose. A new way for 2,4-di-*O*-protection of mannopyranosides. *Carbohydr. Res.* **1993**, *247*, 323–328.
- [41] Ling, M. M.; Robinson, B. H. Approaches to DNA mutagenesis: an overview. *Anal. Biochem.* **1997**, *254*, 157-178.
- [42] Meerman, H. J.; Georgiou, G. Construction and characterization of a set of E. coli strains deficient in all known loci affecting the proteolytic stability of secreted recombinant proteins. *Biotechnology* **1994**, *12*, 1107–1110.
- [43] Bitsch, F.; Aichholz, R.; Kallen, J.; Geisse, S.; Fournier, B.; Schlaeppli, J. M. Identification of natural ligands of retinoic acid receptor-related orphan receptor alpha ligand-binding domain expressed in Sf9 cells--a mass spectrometry approach. *Anal. Biochem.* **2003**, *323*, 139-149.
- [44] (a) VCCLAB, Virtual Computational Chemistry Laboratory, 2005, <http://www.vcclab.org> (accessed April 8, 2013); (b) Tetko, I. V.; Gasteiger, J.; Todeschini, R.; Mauri, A.; Livingstone, D.; Ertl, P.; Palyulin, V. A.; Radchenko, E. V.; Zefirov, N. S.; Makarenko, A. S.; Tanchuk, V. Y.; Prokopenko, V. V. Virtual computational chemistry laboratory-design and description. *J. Comput. Aided Mol. Des.* **2005**, *19*, 453-463.
- [45] Ohura, K.; Nozawa, T.; Murakami, K.; Imai, T. Evaluation of transport mechanism of prodrugs and parent drugs formed by intracellular metabolism in Caco-2 cells with modified carboxylesterase activity: temocapril as a model case. *J. Pharm. Sci.* **2011**, *100*, 3985-3994.
- [46] Hubatsch, I.; Ragnarsson, E. G. E.; Artursson, P. Determination of drug permeability and prediction of drug absorption in Caco-2 monolayers. *Nat. Protoc.* **2007**, *2*, 2111-2119.

2.4 Paper 4: 2-C-Branched Mannosides as a Novel Family of FimH Antagonists – Synthesis and Biological Evaluation

This chapter describes the exploration of an unoccupied cavity located in the vicinity of the carbohydrate recognition domain of FimH with the derivative of *n*-heptyl α -D-mannosides bearing various functional equatorial groups introduced in the 2-C position. To reveal a thermodynamic fingerprint of new FimH antagonists, ITC experiments with selected mannose-modified compounds were performed.

Contribution to the project:

Wojciech Schönemann designed and, together with the master student Marcel Lindegger, synthesized all new FimH antagonists reported in this chapter. Furthermore, he was responsible for writing of the entire chapter. Dr. Pascal Zihlmann performed ITC measurements of selected antagonists.

This paper was published in the *Perspectives in Science*.

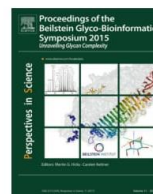
Schönemann, W.; Lindegger, M.; Rabbani, S.; Zihlmann, P.; Schwardt, O.; Ernst, B. 2-C-Branched mannosides as a novel family of FimH antagonists – Synthesis and biological evaluation. *Perspectives in Science* **2017**, *11*, 53-61.



Available online at www.sciencedirect.com

ScienceDirect

journal homepage: www.elsevier.com/pisc



2-C-Branched mannosides as a novel family of FimH antagonists—Synthesis and biological evaluation[☆]



Wojciech Schönemann, Marcel Lindegger, Said Rabbani, Pascal Zihlmann, Oliver Schwardt, Beat Ernst^{*}

Institute of Molecular Pharmacy, Pharmacenter, University of Basel, Klingelbergstrasse 50, CH-4056 Basel, Switzerland

Received 5 July 2016; accepted 9 September 2016
Available online 20 October 2016

KEYWORDS

Urinary tract infections;
Uropathogenic *Escherichia coli*;
FimH antagonists;
Carbohydrate-recognition domain;
2-C-Branched carbohydrates

Summary Urinary tract infections (UTIs), which are among the most prevalent bacterial infections worldwide, are mainly attributed to uropathogenic *Escherichia coli* (UPEC). Because of frequent antibiotic treatment, antimicrobial resistance constitutes an increasing therapeutic problem. Antagonists of the mannose-specific bacterial lectin FimH, a key protein mediating the adhesion of UPEC to human bladder cells, would offer an alternative anti-adhesive treatment strategy. In general, FimH antagonists consist of a mannose moiety and a wide range of lipophilic aglycones. Modifications of the mannose core led to a distinct drop in affinity. A visual inspection of the crystal structure of FimH revealed a previously unexplored cavity surrounded by Ile113, Phe142 and Asp140, which could be reached by functional groups in the equatorial 2-position of the mannose. Here, we describe the synthesis of 2-C-branched mannosides and evaluation of their pharmacodynamic properties. ITC experiments with the selected antagonists revealed a drastic enthalpy loss for all 2-C-branched antagonists, which, however, is partially compensated by an entropy gain. This supports the hypothesis that the target cavity is too small to accommodate 2-C-substituents.

© 2016 Published by Elsevier GmbH. This is an open access article under the CC BY license (<http://creativecommons.org/licenses/by/4.0/>).

Abbreviations: UPEC, uropathogenic *Escherichia coli*; UTI, urinary tract infection; CRD, carbohydrate-recognition domain; IC₅₀, half maximal inhibitory concentration; ITC, isothermal titration calorimetry; K_D, dissociation constant.

[☆] This is an open-access article distributed under the terms of the Creative Commons Attribution License, which permits unrestricted use, distribution, and reproduction in any medium, provided the original author and source are credited. This article is part of a special issue entitled Proceedings of the Beilstein Glyco-Bioinformatics Symposium 2015 with copyright © 2017 Beilstein-Institut. Published by Elsevier GmbH. All rights reserved.

^{*} Corresponding author. Fax: +41 61 267 15 52.

E-mail address: beat.ernst@unibas.ch (B. Ernst).

<http://dx.doi.org/10.1016/j.pisc.2016.10.002>

2213-0209/© 2016 Published by Elsevier GmbH. This is an open access article under the CC BY license (<http://creativecommons.org/licenses/by/4.0/>).

Introduction

Urinary tract infections (UTIs) are among the most prevalent bacterial infections affecting millions of people (Foxman et al., 2000). They are mainly associated with uropathogenic *Escherichia coli* (UPEC) (Roland, 2002). Currently, the first-line treatment involves antibiotics (Hooton et al., 2004; Fihn, 2003) which can induce resistance, especially when frequently applied (Sanchez et al., 2012). Therefore, novel and efficient non-antibiotic approaches are urgently needed.

In the first step of the infection cycle, UPEC attach to urothelial cells of the host by means of the bacterial adhesin called FimH, which is located at the tip of the approximately 300 bacterial type 1 pili (Mulvey et al., 2000; Schilling et al., 2001). This allows UPEC to evade elimination from the host organism by the bulk flow of the urine. FimH is composed of a lectin domain (FimH_L) containing a carbohydrate recognition domain (CRD) and a pilin domain (FimH_P) regulating the switch between the high and low affinity states of the CRD (Le Trong et al., 2010).

More than thirty years ago, Firon et al. (1982, 1983, 1987) reported on aryl α -D-mannosides abolishing FimH-mediated aggregation of UPEC with mannan-containing yeast cells (*Saccharomyces cerevisiae*) in *in vitro* assays. Over the course of the last few years, a range of highly potent monovalent antagonists consisting of a mannose moiety and a lipophilic aglycone was reported (Bouckaert et al., 2005; Sperling et al., 2006; Han et al., 2010; Klein et al., 2010; Cusumano et al., 2011; Han et al., 2012; Pang et al., 2012; Jiang et al., 2012; Schwardt et al., 2011; Kleeb et al., 2015; Brument et al., 2013; Jarvis et al., 2016; Chalopin et al., 2016). The various aglycones provide hydrophobic contacts or π - π stacking interactions to amino acids forming the entrance to the mannose binding pocket. This entrance called 'tyrosine gate' is composed of two tyrosines and one isoleucine. However, the pharmacokinetic properties, e.g., solubility and/or permeability, of most of the reported FimH antagonists are not suitable for an oral application. For physicochemical and pharmacokinetic reasons, the numerous reported multivalent FimH antagonists (Lindhorst et al., 1998; Nagahori et al., 2002; Appeldoorn et al., 2005; Patel and Lindhorst, 2006; Touaibia et al., 2007; Durka et al., 2011; Bouckaert et al., 2013) are rather suited for the therapy of *E. coli* induced colitis ulcerosa, a form of inflammatory bowel disease (Barnich et al., 2007; Carvalho et al., 2009).

When interacting with FimH, the mannose moiety establishes a perfect hydrogen bond network (Hung et al., 2002). Since every hydroxyl group of mannose is part of this network, the removal/replacement of individual various hydroxyl groups or the replacement of the whole mannose moiety by other hexoses (e.g., glucose, galactose, fructose) resulted in a significant loss of affinity (Bouckaert et al., 2005; Han et al., 2010; Old, 1972; Fiege et al., 2015). Moreover, recently reported 1-C-branched mannose derivatives bearing additional equatorial groups at the anomeric carbon also showed reduced activity compared to methyl α -D-mannoside (Gloe et al., 2015). In contrast, when the anomeric oxygen was replaced by carbon or nitrogen,

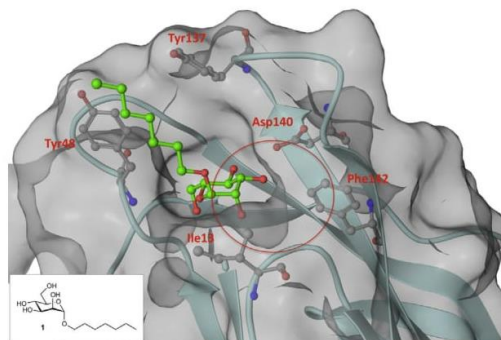


Figure 1 The crystal structure of FimH_LD co-crystallized with *n*-heptyl α -D-mannopyranoside (1, PDB ID: 4BUQ) (Fiege et al., 2015). A mainly hydrophobic cavity formed by Ile13, Phe142 and Asp140 is located next to the entrance of the mannose binding site and can be reached by equatorial substituents in the 2-position of the mannose moiety.

nanomolar affinity could still be reached (Schwardt et al., 2011; Brument et al., 2013; Chalopin et al., 2016).

A visual inspection of the crystal structure of FimH_LD co-crystallized with *n*-heptyl α -D-mannoside (1, PDB ID: 4BUQ) (Fiege et al., 2015) revealed a previously unexplored hydrophobic cavity formed by Ile13, Phe142 and Asp140, which is located close to the entrance to the mannose-binding pocket (Fig. 1). By extending the 2-position of the mannose moiety with equatorial substituents (\rightarrow derivatives 2a–k, Fig. 2), an interaction with the hydrophobic cavity should become possible.

An adaption of the synthetic pathway of previously reported 2-C-branched mannose derivatives, in which the 2-position is modified at an early stage, lead to rather laborious approaches (Mitchell et al., 2007). We therefore planned a more convergent synthesis with a more flexible introduction of aglycones as well as equatorial substituents in the 2-position.

Result and discussion

The synthetic route to 2-C-branched FimH antagonists fulfils two requirements: The facile introduction of various aglycones as well as various equatorial C-substituents in the 2-C-position of the mannose moiety.

Synthesis

The synthesis of the 2-C-branched mannoside donor 5 is depicted in Scheme 1. The 2-C-modified D-mannofuranose 3 was synthesized according to a literature procedure starting from commercially available D-mannose (Witczak et al., 1984). Selective benzylation of the hydroxymethyl group using dibutyltin oxide (Malleron and David, 1998) followed by cleavage of the acetonides under acidic conditions yielded the 2-C-branched D-mannopyranose 4 (Waschke et al., 2011). For its perbenzylation with benzoyl chloride in presence of a catalytic amount of 4-dimethylamino-pyridine (DMAP) in dry pyridine, elevated temperature

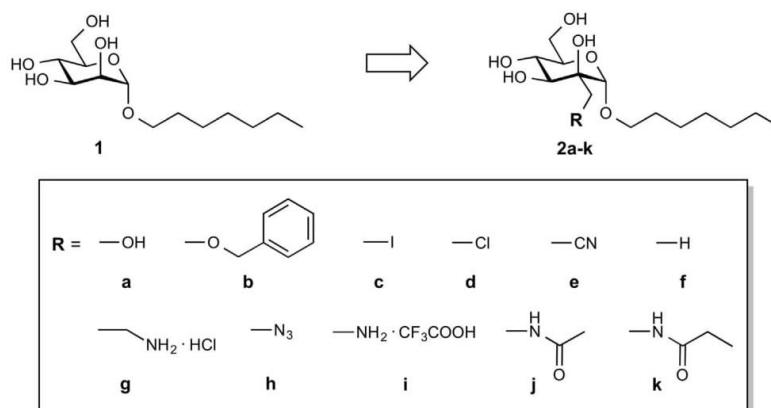


Figure 2 Modifications of the mannose moiety of *n*-heptyl α -D-mannopyranoside (**1**) by equatorial substituents in the 2-position.

(110–120 °C) had to be applied. Subsequently, the glycosyl donor **5** was obtained by reaction with thiophenol using $\text{BF}_3 \cdot \text{Et}_2\text{O}$ as a promoter. To couple donor **5** with 1-heptanol, different promoters were tested. Whereas with NIS/TMSOTf or NIS/TfOH donor **5** was only partially consumed after 24 h, it reacted within minutes in the presence of commercially available *p*-nitrobenzenesulfonyl chloride ($p\text{-NO}_2\text{PhSOCl}$) accompanied by silver triflate (AgOTf) (Crich et al., 2008). Apart from the desired α -anomeric mannoside **6** (32%), the 2-OH deprotected α -anomer **7** (32%) and the 2-OH deprotected β -anomer **8** (5%) were obtained as well. As silver triflate-mediated glycosylation has been reported to lead to partial transesterification affecting acetyl groups at the 2-O-position, low stereoselectivity of the glycosylation reaction was not unexpected (Ziegler et al., 1990; Nukada et al., 1999; Murakami et al., 2007).

To functionalize the equatorial substituent in the 2-C-position, **6** was debenzoylated by catalytic hydrogenolysis to afford the primary alcohol **9**. However, attempts to mesylate its primary hydroxyl group failed. Since we attributed the low reactivity of the hydroxyl group in **9** to steric hindrance, we switched to mannoside **7** with an unprotected axial hydroxyl group in the 2-position.

Indeed, after hydrogenolysis of **7** (\rightarrow **11**), we were able to selectively mesylate the primary hydroxyl groups (\rightarrow **12**). However, displacement of the mesylate by fluoride using KF in aprotic solvent in presence of crown ether at elevated temperature afforded epoxide **14** instead of the desired fluoride **13**. Under these reaction conditions, the strongly basic fluoride is obviously deprotonating the axial hydroxyl group followed by conversion of mesylate **12** into the epoxide **14** by an intramolecular $\text{S}_\text{N}2$ mechanism. With an excess of LiCl , epoxide **14** could be opened, leading to the chloride **15** in 41% yield. By acting as Lewis acid, the large excess of lithium ions can facilitate opening of the epoxide. Apart from the epoxide route, substituents can be introduced directly by nucleophilic substitution (see Scheme 2). However, prevalence of one mechanism over the other may depend on the nucleophile, i.e., its nucleophilicity and basicity as well as temperature and concentration.

The synthesis of a series of 2-C-branched FimH antagonists is depicted in Scheme 2. Debzoylation of **6** under Zemplén conditions (\rightarrow **2b**) followed by $\text{Pd}(\text{OH})_2$ -catalyzed hydrogenolysis afforded test compound **2a**. The configuration at the anomeric carbon of deprotected derivative **2a** ($^1J_{\text{H,C}} = 169 \text{ Hz}$) was unambiguously confirmed by the ^{13}C – ^1H coupling constant of the anomeric nuclei using uncoupled ^{13}C NMR. In general, the coupling constant for the equatorial anomeric proton amounts to $\sim 170 \text{ Hz}$, while a value of $\sim 160 \text{ Hz}$ is indicative for an anomeric proton in axial orientation (Bubb, 2003).

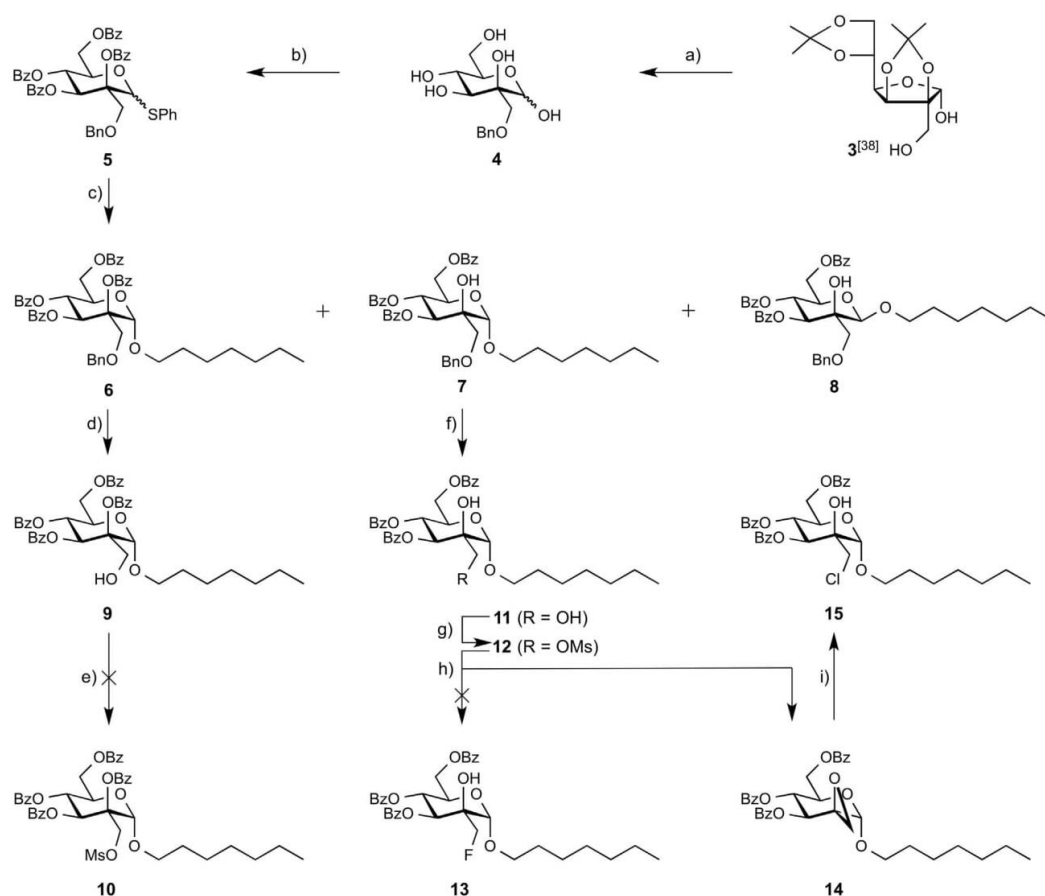
Upon mesylation of **11**, chloride was introduced using LiCl followed by deprotection of the intermediate with sodium methoxide to afford derivative **2d**. Direct introduction of chloride starting from mesylate was faster and gave a higher yield than the already discussed opening of epoxide **14**. Since only traces of epoxide were observed by TLC control, $\text{S}_\text{N}2$ reaction seems to be the prevailing mechanism in this particular case. However, more basic nucleophiles may lead to different results.

Using an identical synthetic approach, iodide **2c**, cyanide **2e** and azide **2h** were obtained with NaI , KCN and NaN_3 as nucleophiles. Hydrogenation of iodide **2c**, cyanide **2e** and azide **2h** in presence of $\text{Pd}(\text{OH})_2$ on carbon yielded the methyl derivative **2f** and amine derivatives **2g** and **2i**, respectively. In addition, when **2h** was hydrogenated and subsequently acylated with acetyl chloride or propionyl chloride followed by deacetylation under Zemplén conditions, amides **2j** and **2k** were obtained.

To evaluate the β -anomeric derivative as well in the biological assay, β -mannoside **8** was debenzoylated (\rightarrow **16b**, Scheme 3) followed by hydrogenolysis to yield **16a** ($^1J_{\text{H,C}} = 159 \text{ Hz}$).

Affinity and thermodynamic profile

The affinities of the 2-C-branched mannosides were determined in a cell-free competitive binding assay (Table 1) (Rabbani et al., 2010). The assay uses FimH_{LD} -Th-His₆ (Th: thrombin cleavage site) as a target protein and a

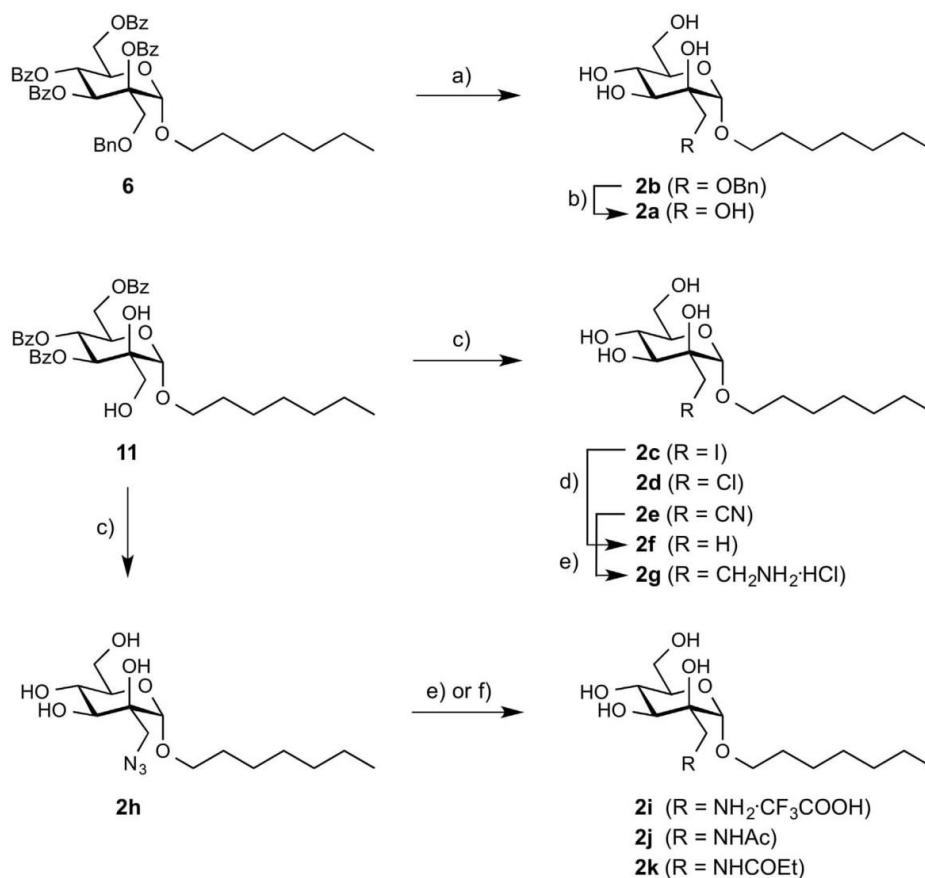


Scheme 1 (a) i. BnBr, Bu₂SnO, TBAB, toluene, 120 °C → 80 °C, 24 h; ii. Amberlyst-15 (H⁺), EtOH, H₂O, 50 °C, 43 h, 90%; (b) i. BzCl, DMAP, pyridine, 120 °C, 48 h; ii. PhSH, BF₃·Et₂O, DCM, 0 °C → rt, 24 h, 42%; (c) 1-heptanol, *p*-NO₂PhSCl, AgOTf, DCM, 4 Å MS, 0 °C → rt, 5 h, 32% for **6**, 32% for **7**, 5% for **8**; (d) Pd(OH)₂/C, H₂, EtOH, AcOH, rt, 22 h, 86%; (e) MsCl, TEA, DCM, 0 °C → 65 °C, 7 h, 0%; (f) Pd(OH)₂/C, H₂, EtOH, rt, 5 h, 93%; (g) MsCl, TEA, DCM, 0 °C → rt, 6 h, 86%; (h) KF, Kryptofix 2.2.2, DMSO, 100 °C, 2 h, 85%; (i) LiCl, DMF, 90 °C, 7 h, 41%.

biotinylated polyacrylamide glycopolymer as competitor. Conjugation of biotin with streptavidin-horseradish peroxidase allows quantification of the bound polymer and therefore the determination of the IC₅₀. The activity of all antagonists was measured twice in duplicates. The antagonist *n*-heptyl α-D-mannopyranoside (**1**) was used as a reference compound and tested in parallel to ensure comparability. The affinities are referred to the activity of **1** as rIC₅₀.

In addition to the competitive binding assay, ITC experiments were performed with mannosides **1**, **2a** and **2f** to reveal a thermodynamic fingerprint of mannose-modified FimH antagonists (Table 2). ITC enables direct measurement of the dissociation constant (*K*_D) and the change in enthalpy (ΔH°), which are further used to calculate the changes in free energy (ΔG°) and entropy (ΔS°) (Chen and Wadsö, 1982; Freire et al., 1990).

Unfortunately, all 2-C modifications proved to be detrimental to the affinity. Already the smallest substituent, a methyl group (→ **2f**), resulted in a 2.8-fold higher IC₅₀ value. A comparable 4.1-fold drop in activity was observed in ITC. This finding might be explained by an unexpected unfavourable steric clash of Ile13 and/or Phe142 with the methyl group already too big to fit to the targeted cavity. This hypothesis is supported by the considerably improved entropy term ($-T\Delta\Delta S^\circ -17.2$ kJ/mol) compared to the reference **1**, indicating an increased conformational flexibility of the ligand. The resulting disruption of the hydrogen bond network within the pocket is also reflected by a substantial decline of enthalpy ($\Delta\Delta H^\circ +20.6$ kJ/mol). A further reduction in affinity to the micromolar level for larger substituents, e.g., iodomethyl and chloromethyl (→ **2c** and **2d**, Table 1) is in full agreement with this argumentation.

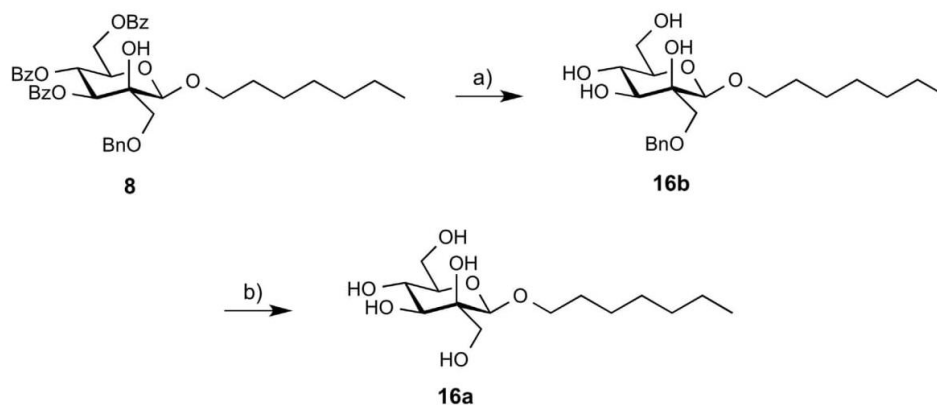


Scheme 2 (a) MeONa/MeOH, rt, 4 h, 85%; (b) Pd(OH)₂/C, H₂, EtOH, rt, 6 h, 75%; (c) i. MsCl, TEA, DCM, 0 °C → rt, 1.5–6 h; ii. NaI, LiCl, KCN or NaN₃, DMF or DMSO, 70–100 °C, 3–64 h; iii. MeONa/MeOH, rt, 1–6 h, 39% for **2c**, 38% for **2d**, 11% for **2e**, 73% for **2h**; (d) Pd(OH)₂/C, H₂, EtOH, TEA, rt, 44 h, 91%; (e) i. Pd(OH)₂/C, H₂, MeOH or EtOH, rt, 3–11 h; ii. 0.1% TFA or 0.01 M HCl, H₂O, MeOH, 76% for **2g**, 86% for **2i**; (f) i. Pd(OH)₂/C, H₂, EtOH, rt, 7 h; ii. AcCl or CH₃CH₂COCl, pyridine, DCM, rt, 2.5–5.5 h; iii. MeONa/MeOH, rt, 1.5–4 h, 20% for **2j**, 38% for **2k**.

Unexpectedly, the benzyloxymethyl group in **2b**, despite its bulkiness, only slightly reduced the activity compared to the methyl substituent (→**2f**). Furthermore, **2b** performed better compared to the halogens **2c** and **2d**. This may result from a smaller van der Waals radius of oxygen compared to chloride or iodide. Moreover, a solvent exposed phenyl ring can be involved in non-specific hydrophobic interactions with the surface of the protein, attenuating the negative effect of the size of the 2-C-branch.

The antagonists bearing hydrogen bond donating groups, such as a hydroxyl group (→**2a**), an amine (→**2i**) or an amide (→**2j** and **2k**), were among the most active derivatives. The hydroxymethyl group (→**2a**) led to roughly a 5-fold drop in affinity in both, competitive binding assay and ITC. Compared to the methyl group (→**2f**), this substituent was expected to disrupt the hydrogen bond network even further due to its larger size and to cause additional

enthalpy costs due to a desolvation penalty related to the hydroxyl group. However, the enthalpy loss in this case was smaller ($\Delta\Delta H'_{2a-2f} = 6.1$ kJ/mol) implying additional beneficial interactions formed by **2a**. As a consequence, the entropy gain was limited ($-T\Delta\Delta S' = 10.4$ kJ/mol) compared to **2f**. However, this beneficial effect was almost compensated by a loss in entropy. Furthermore, the structurally similar aminomethyl derivative **2i** was the most active compound within the series with only 2.1-fold lower affinity compared to reference **1**. Presumably, the hydroxymethyl (→**2a**) and aminomethyl (→**2i**) groups are involved in electrostatic interactions with a hydrogen bond acceptor, i.e., Asp140 or the backbone amide of Ile13. The improved affinity of **2i** may result from the fact that the ammonium group in **2i** can form a slightly stronger interaction (Lopes Jesus and Redinha, 2011). Finally, when we incorporated a longer linker between the nitrogen and the sugar moiety (→**2g**)

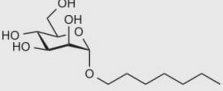
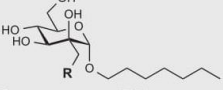
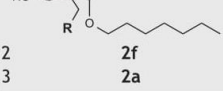


Scheme 3 (a) MeONa/MeOH, rt, 2 h, 68%; (b) Pd(OH)₂/C, H₂, EtOH, rt, 3 h, 93%.

Table 1 Affinity of FimH antagonists. The rIC₅₀ values were calculated by dividing the IC₅₀ of the compound of interest by the IC₅₀ of the reference compound *n*-heptyl α-D-mannopyranoside (**1**). rIC₅₀ values below 1.0 are obtained for antagonists more active than reference compound **1**, whereas rIC₅₀ above 1.0 are obtained for antagonists less active than reference compound **1**.

Entry	Compound	R	IC ₅₀ [nM]	rIC ₅₀
1	1		48.9–65.2	1
2	2a	–OH	311.0	4.9
3	2b		340.9	5.4
4	2c	–I	>2000	38.9
5	2d	–Cl	>2000	304
6	2e	–CN	522.3	9.7
7	2f	–H	181.2	2.8
8	2g	–CH ₂ NH ₂ ·HCl	>2000	37.1
9	2h	–N ₃	437.0	6.9
10	2i	–NH ₂ ·CF ₃ COOH	135.0	2.1
11	2j		182.5	3.4
12	2k		295.2	5.5
13	16a	–OH	446.4	7.0
14	16b		4400	69.4

Table 2 Thermodynamic profile of FimH antagonists in binding to FimH_{LD}-Th-His₆ at 25 °C and pH 7.4.

Entry	Compound	R	K _D [nM]	ΔG° [kJ/mol]	ΔH° [kJ/mol]	−TΔS° [kJ/mol]
1			28.9	−43.0	−50.3	7.3
2		−H	118.6	−39.5	−29.7	−9.9
3		−OH	154.0	−38.9	−35.8	−3.1

the affinity was lowered to the micromolar level. Similarly to the aminomethyl derivative **2i**, the amide **2j** had one of the best affinities in the series. However, elongation of the aliphatic chain attached to the amide (\rightarrow **2k**) again resulted in reduction of potency.

Quite surprisingly, the β -anomeric derivative **16a** (Table 1, entry 13) performed only slightly worse than its α -anomeric analogue **2a**. However, when a benzyloxymethyl group was introduced (\rightarrow **16b**, entry 14) the affinity was almost 13-fold lower than for its α -anomeric counterpart **2b**, according to docking studies (data not shown) due to a steric clash with Ile13.

Conclusions

A new family of mannose-based FimH antagonists equipped with equatorial substituents at the 2-position of the sugar moiety was designed and synthesized to target a cavity located close to the entrance of FimH-CRD. Only when the axial 2-hydroxyl group was unprotected (\rightarrow **11**), the otherwise unsuccessful substitution at the equatorial 2-position of the mannose moiety could be performed, leading to the test compounds **2c–k**. In one case, the intermediate epoxide **14** could be isolated, indicating two possible reaction pathways; one via direct S_N2-substitution and one via the epoxide **14**. The resulting epoxide intermediate could be opened, however, affording only a moderate yield.

The activities of the 2-C-branched FimH antagonists were evaluated in a cell-free competitive binding assay and compared to the reference compound *n*-heptyl α -D-mannopyranoside (**1**). None of the modifications proved to be advantageous for binding to FimH-CRD. The loss of affinity is probably related to steric hindrance as it was already observed upon introduction of the smallest substituent, a methyl group (\rightarrow **2f**). With hydrogen bond donating substituents (\rightarrow **2a**, **2i–k**), affinity could be partially regained. Unexpectedly, the β -anomer **16a** performed only slightly worse than its α -anomeric counterpart **2a**. However, as already experienced in the α -series, a larger benzyloxymethyl substituent (\rightarrow **16b**) severely compromised affinity.

Finally, ITC experiments with the selected antagonists **1**, **2a** and **2f** revealed a drastic enthalpy loss for

the 2-C-branched antagonists, which, however, is partially compensated by an entropy gain. This supports the hypothesis that the target cavity is too small to accommodate 2-C-substituents. However, with larger, hydrogen bond donating substituents the enthalpy loss could be substantially reduced.

Acknowledgement

Financial support for PZ from the Swiss National Science Foundation (200020_146202) is gratefully acknowledged.

Appendix A. Supplementary data

Supplementary data associated with this article can be found, in the online version, at <http://dx.doi.org/10.1016/j.pisc.2016.10.002>.

References

- Appeldoorn, C.C.M., Joosten, J.A.F., el Maate, F.A., Dobrindt, U., Hacker, J., Liskamp, R.M.J., Khan, A.S., Pieters, R.J., 2005. Novel multivalent mannose compounds and their inhibition of the adhesion of type 1 fimbriated uropathogenic *E. coli*. *Tetrahedron: Asymmetry* 16, 361–372, <http://dx.doi.org/10.1016/j.tetasy.2004.11.014>.
- Barnich, N., Carvalho, F.A., Glasser, A.-L., Darcha, C., Jantscheff, P., Allez, M., Peeters, H., Bommelaer, G., Desreumaux, P., Colombel, J.-F., Darfeuille-Michaud, A., 2007. CEACAM6 acts as a receptor for adherent-invasive *E. coli*, supporting ileal mucosa colonization in Crohn disease. *J. Clin. Invest.* 117, 1566–1574, <http://dx.doi.org/10.1172/jci30504>.
- Bouckaert, J., Berglund, J., Schembri, M., De Genst, E., Cools, L., Wuhrer, M., Hung, C.-S., Pinkner, J., Slättergard, R., Zavialov, A., Choudhury, D., Langermann, S., Hultgren, S.J., Wyns, L., Klemm, P., Oscarson, S., Knight, S.D., Greve, H.D., 2005. Receptor binding studies disclose a novel class of high-affinity inhibitors of the *Escherichia coli* FimH adhesin. *Mol. Microbiol.* 55, 441–455, <http://dx.doi.org/10.1111/j.1365-2958.2004.04415.x>.
- Bouckaert, J., Li, Z., Xavier, C., Almant, M., Caveliers, V., Lahoutte, T., Weeks, S.D., Kovensky, J., Gouin, S.G., 2013. Heptyl α -D-mannosides grafted on a β -cyclodextrin core to interfere with *Escherichia coli* adhesion: an

- in vivo multivalent effect. *Chem. Eur. J.* 19, 7847–7855, <http://dx.doi.org/10.1002/chem.201204015>.
- Brument, S., Sivignon, A., Dumych, T.I., Moreau, N., Roos, G., Guérardel, Y., Chalopin, T., Deniaud, D., Bilyy, R.O., Darfeuille-Michaud, A., Bouckaert, J., Gouin, S.G., 2013. Thiazolylaminomannosides as potent antiadhesives of type 1 pilated *Escherichia coli* isolated from Crohn's disease patients. *J. Med. Chem.* 56, 5395–5406, <http://dx.doi.org/10.1021/jm400723n>.
- Bubb, W.A., 2003. NMR spectroscopy in the study of carbohydrates: characterizing the structural complexity. *Concepts Magn. Reson. A* 19A, 1–19, <http://dx.doi.org/10.1002/cmr.a.10080>.
- Carvalho, F.A., Barnich, N., Sivignon, A., Darcha, C., Chan, C.H.F., Stanners, C.P., Darfeuille-Michaud, A., 2009. Crohn's disease adherent-invasive *Escherichia coli* colonize and induce strong gut inflammation in transgenic mice expressing human CEACAM. *J. Exp. Med.* 206, 2179–2189, <http://dx.doi.org/10.1084/jem.20090741>.
- Chalopin, T., Alvarez Dorta, D., Sivignon, A., Caudan, M., Dumych, T.I., Bilyy, R.O., Deniaud, D., Barnich, N., Bouckaert, J., Gouin, S.G., 2016. Second generation of thiazolylmannosides, FimH antagonists for *E. coli*-induced Crohn's disease. *Org. Biomol. Chem.* 14, 3913–3925, <http://dx.doi.org/10.1039/c6ob00424e>.
- Chen, A.-t., Wadsö, I., 1982. Simultaneous determination of ΔG , ΔH and ΔS by an automatic microcalorimetric titration technique. Application to protein ligand binding. *J. Biochem. Biophys. Methods* 6, 307–316, [http://dx.doi.org/10.1016/0165-022X\(82\)90012-4](http://dx.doi.org/10.1016/0165-022X(82)90012-4).
- Crich, D., Cai, F., Yang, F., 2008. A stable, commercially available sulfonyl chloride for the activation of thioglycosides in conjunction with silver trifluoromethanesulfonate. *Carbohydr. Res.* 343, 1858–1862, <http://dx.doi.org/10.1016/j.carres.2008.03.002>.
- Cusumano, C.K., Pinkner, J.S., Han, Z., Greene, S.E., Ford, B.A., Crowley, J.R., Henderson, J.P., Janetka, J.W., Hultgren, S.J., 2011. Treatment and prevention of urinary tract infection with orally active FimH inhibitors. *Sci. Transl. Med.* 3, 109ra115, <http://dx.doi.org/10.1126/scitranslmed.3003021>.
- Durka, M., Buffet, K., Iehl, J., Holler, M., Nierengarten, J.-F., Taganna, J., Bouckaert, J., Vincent, S.P., 2011. The functional valency of dodecamannosylated fullerenes with *Escherichia coli* FimH—towards novel bacterial antiadhesives. *Chem. Commun.* 47, 1321–1323, <http://dx.doi.org/10.1039/c0cc04468g>.
- Fiege, B., Rabbani, S., Preston, R.C., Jakob, R.P., Zihlmann, P., Schwardt, O., Jiang, X., Maier, T., Ernst, B., 2015. The tyrosine gate of the bacterial lectin FimH: a conformational analysis by NMR spectroscopy and X-ray crystallography. *ChemBioChem* 16, 1235–1246, <http://dx.doi.org/10.1002/cbic.201402714>.
- Fihn, S.D., 2003. Acute uncomplicated urinary tract infection in women. *N. Engl. J. Med.* 349, 259–266, <http://dx.doi.org/10.1056/nejmcp030027>.
- Firon, N., Ofek, I., Sharon, N., 1982. Interaction of mannose-containing oligosaccharides with the fimbrial lectin of *Escherichia coli*. *Biochem. Biophys. Res. Commun.* 105, 1426–1432, [http://dx.doi.org/10.1016/0006-291x\(82\)90947-0](http://dx.doi.org/10.1016/0006-291x(82)90947-0).
- Firon, N., Ofek, I., Sharon, N., 1983. Carbohydrate specificity of the surface lectins of *Escherichia coli*, *Klebsiella pneumoniae*, and *Salmonella typhimurium*. *Carbohydr. Res.* 120, 235–249, [http://dx.doi.org/10.1016/0008-6215\(83\)88019-7](http://dx.doi.org/10.1016/0008-6215(83)88019-7).
- Firon, N., Ashkenazi, S., Mirelman, D., Ofek, I., Sharon, N., 1987. Aromatic α -glycosides of mannose are powerful inhibitors of the adherence of type 1 fimbriated *Escherichia coli* to yeast and intestinal epithelial cells. *Infect. Immun.* 55, 472–476.
- Foxman, B., Barlow, R., D'Arcy, H., Gillespie, B., Sobel, J.D., 2000. Urinary tract infection: self reported incidence and associated costs. *Ann. Epidemiol.* 10, 509–515, [http://dx.doi.org/10.1016/s1047-2797\(00\)00072-7](http://dx.doi.org/10.1016/s1047-2797(00)00072-7).
- Freire, E., Mayorga, O.L., Straume, M., 1990. Isothermal titration calorimetry. *Anal. Chem.* 62, 950A–959A, <http://dx.doi.org/10.1021/ac00217a002>.
- Gloe, T.-E., Stamer, I., Hojnik, C., Wrodnigg, T.M., Lindhorst, T.K., 2015. Are D-manno-configured Amadori products ligands of the bacterial lectin FimH? *Beilstein J. Org. Chem.* 11, 1096–1104, <http://dx.doi.org/10.3762/bjoc.11.123>.
- Han, Z., Pinkner, J.S., Ford, B., Obermann, R., Nolan, W., Wildman, S.A., Hobbs, D., Ellenberger, T., Cusumano, C.K., Hultgren, S.J., Janetka, J.W., 2010. Structure-based drug design and optimization of mannose bacterial FimH antagonists. *J. Med. Chem.* 53, 4779–4792, <http://dx.doi.org/10.1021/jm100438s>.
- Han, Z., Pinkner, J.S., Ford, B., Chorell, E., Crowley, J.M., Cusumano, C.K., Campbell, S., Henderson, J.P., Hultgren, S.J., Janetka, J.W., 2012. Lead optimization studies on FimH antagonists: discovery of potent and orally bioavailable ortho-substituted biphenyl mannosides. *J. Med. Chem.* 55, 3945–3959, <http://dx.doi.org/10.1021/jm300165m>.
- Hooton, T.M., Besser, R., Foxman, B., Fritsche, T.R., Nicolle, L.E., 2004. Acute uncomplicated cystitis in an era of increasing antibiotic resistance: a proposed approach to empirical therapy. *Clin. Infect. Dis.* 39, 75–80, <http://dx.doi.org/10.1086/422145>.
- Hung, C.-S., Bouckaert, J., Hung, D., Pinkner, J., Widberg, C., DeFusco, A., Auguste, C.G., Strouse, R., Langermann, S., Waksman, G., Hultgren, S.J., 2002. Structural basis of tropism of *Escherichia coli* to the bladder during urinary tract infection. *Mol. Microbiol.* 44, 903–915, <http://dx.doi.org/10.1046/j.1365-2958.2002.02915.x>.
- Jarvis, C., Han, Z., Kalas, V., Klein, R., Pinkner, J.S., Ford, B., Binkley, J., Cusumano, C.K., Cusumano, Z., Mydock-McGrane, L., Hultgren, S.J., Janetka, J.W., 2016. Antivirulence isoquinolone mannosides: optimization of the biaryl aglycone for FimH lectin binding affinity and efficacy in the treatment of chronic UTI. *ChemMedChem* 11, 367–373, <http://dx.doi.org/10.1002/cmdc.201600045>.
- Jiang, X., Abgottspon, D., Kleeb, S., Rabbani, S., Scharenberg, M., Wittwer, M., Haug, M., Schwardt, O., Ernst, B., 2012. Antiadhesion therapy for urinary tract infections—a balanced PK/PD profile proved to be key for success. *J. Med. Chem.* 55, 4700–4713, <http://dx.doi.org/10.1021/jm300192x>.
- Kleeb, S., Pang, L., Mayer, K., Eris, D., Sigl, A., Preston, R.C., Zihlmann, P., Sharpe, T., Jakob, R.P., Abgottspon, D., Hutter, A.S., Scharenberg, M., Jiang, X., Navarra, G., Rabbani, S., Smieško, M., Lüdin, N., Bezençon, J., Schwardt, O., Maier, T., Ernst, B., 2015. FimH antagonists: bioisosteres to improve the in vitro and in vivo PK/PD profile. *J. Med. Chem.* 58, 2221–2239, <http://dx.doi.org/10.1021/jm501524q>.
- Klein, T., Abgottspon, D., Wittwer, M., Rabbani, S., Herold, J., Jiang, X., Kleeb, S., Lüthi, C., Scharenberg, M., Bezençon, J., Gubler, E., Pang, L., Smieško, M., Cutting, B., Schwardt, O., Ernst, B., 2010. FimH antagonists for the oral treatment of urinary tract infections: from design and synthesis to in vitro and in vivo evaluation. *J. Med. Chem.* 53, 8627–8641, <http://dx.doi.org/10.1021/jm101011y>.
- Le Trong, I., Aprikian, P., Kidd, B.A., Forero-Shelton, M., Tchesnokova, V., Rajagopal, P., Rodriguez, V., Interlandi, G., Klevit, R., Vogel, V., Stenkamp, R.E., Sokurenko, E.V., Thomas, W.E., 2010. Structural basis for mechanical force regulation of the adhesin FimH via finger trap-like β sheet twisting. *Cell* 141, 645–655, <http://dx.doi.org/10.1016/j.cell.2010.03.038>.
- Lindhorst, T.K., Kieburg, C., Krallmann-Wenzel, U., 1998. Inhibition of the type 1 fimbriae-mediated adhesion of *Escherichia coli* to erythrocytes by multiantennary D-mannosyl clusters: the effect of multivalency. *Glycoconj. J.* 15, 605–613, <http://dx.doi.org/10.1023/a:1006920027641>.
- Lopes Jesus, A.J., Redinha, J.S., 2011. Charge-assisted intramolecular hydrogen bonds in disubstituted cyclohex-

- ane derivatives. *J. Phys. Chem. A* 115, 14069–14077, <http://dx.doi.org/10.1021/jp206193a>.
- Malleron, A., David, S., 1998. A preparation of protected 2-deoxy-2-hydroxymethyl-D-mannose and -D-glucose derivatives not involving organometallic reagents. *Carbohydr. Res.* 308, 93–98, [http://dx.doi.org/10.1016/S0008-6215\(98\)00080-9](http://dx.doi.org/10.1016/S0008-6215(98)00080-9).
- Mitchell, D.A., Jones, N.A., Hunter, S.J., Cook, J.M.D., Jenkinson, S.F., Wormald, M.R., Dwek, R.A., Fleet, G.W.J., 2007. Synthesis of 2-C-branched derivatives of D-mannose: 2-C-aminomethyl-D-mannose binds to the human C-type lectin DC-SIGN with affinity greater than an order of magnitude compared to that of D-mannose. *Tetrahedron: Asymmetry* 18, 1502–1510, <http://dx.doi.org/10.1016/j.tetasy.2007.06.003>.
- Mulvey, M.A., Schilling, J.D., Martinez, J.J., Hultgren, S.J., 2000. Bad bugs and beleaguered bladders: interplay between uropathogenic *Escherichia coli* and innate host defenses. *Proc. Natl. Acad. Sci. U. S. A.* 97, 8829–8835, <http://dx.doi.org/10.1073/pnas.97.16.8829>.
- Murakami, T., Hirono, R., Sato, Y., Furusawa, K., 2007. Efficient synthesis of ω -mercaptoalkyl 1,2-*trans*-glycosides from sugar peracetates. *Carbohydr. Res.* 342, 1009–1020, <http://dx.doi.org/10.1016/j.carres.2007.02.024>.
- Nagahori, N., Lee, R.T., Nishimura, S.-L., Pagé, D., Roy, R., Lee, Y.C., 2002. Inhibition of adhesion of type 1 fimbriated *Escherichia coli* to highly mannosylated ligands. *ChemBioChem* 3, 836–844, [http://dx.doi.org/10.1002/1439-7633\(20020902\)3:9<836::aid-cbic836>3.0.co;2-2](http://dx.doi.org/10.1002/1439-7633(20020902)3:9<836::aid-cbic836>3.0.co;2-2).
- Nukada, T., Berces, A., Whitfield, D.M., 1999. Acyl transfer as a problematic side reaction in polymer-supported oligosaccharide synthesis. *J. Org. Chem.* 64, 9030–9045, <http://dx.doi.org/10.1021/jo990712b>.
- Old, D.C., 1972. Inhibition of the interaction between fimbrial haemagglutinins and erythrocytes by D-mannose and other carbohydrates. *J. Gen. Microbiol.* 71, 149–157, <http://dx.doi.org/10.1099/00221287-71-1-149>.
- Pang, L., Kleeb, S., Lemme, K., Rabbani, S., Scharenberg, M., Zalewski, A., Schädler, F., Schwardt, O., Ernst, B., 2012. FimH antagonists: structure-activity and structure-property relationships for biphenyl α -D-mannopyranosides. *ChemMedChem* 7, 1404–1422, <http://dx.doi.org/10.1002/cmdc.201200125>.
- Patel, A., Lindhorst, T.K., 2006. A modular approach for the synthesis of oligosaccharide mimetics. *Carbohydr. Res.* 341, 1657–1668, <http://dx.doi.org/10.1016/j.carres.2006.01.024>.
- Rabbani, S., Jiang, X., Schwardt, O., Ernst, B., 2010. Expression of the carbohydrate recognition domain of FimH and development of a competitive binding assay. *Anal. Biochem.* 407, 188–195, <http://dx.doi.org/10.1016/j.ab.2010.08.007>.
- Roland, A., 2002. The etiology of urinary tract infection: traditional and emerging pathogens. *Am. J. Med.* 113 (Suppl. 1A), 14S–19S, [http://dx.doi.org/10.1016/S0002-9343\(02\)01055-0](http://dx.doi.org/10.1016/S0002-9343(02)01055-0).
- Sanchez, G.V., Master, R.N., Karlowsky, J.A., Bordon, J.M., 2012. *In vitro* antimicrobial resistance of urinary *Escherichia coli* isolates among U.S. outpatients from 2000 to 2010. *Antimicrob. Agents Chemother.* 56, 2181–2183, <http://dx.doi.org/10.1128/aac.06060-11>.
- Schilling, J.D., Mulvey, M.A., Hultgren, S.J., 2001. Structure and function of *Escherichia coli* type 1 pili: new insight into the pathogenesis of urinary tract infections. *J. Infect. Dis.* 183 (Suppl. 1), S36–S40, <http://dx.doi.org/10.1086/318855>.
- Schwardt, O., Rabbani, S., Hartmann, M., Abgottspon, D., Wittwer, M., Kleeb, S., Zalewski, A., Smieško, M., Cutting, B., Ernst, B., 2011. Design, synthesis and biological evaluation of mannosyl triazoles as FimH antagonists. *Bioorg. Med. Chem.* 19, 6454–6473, <http://dx.doi.org/10.1016/j.bmc.2011.08.057>.
- Sperling, O., Fuchs, A., Lindhorst, T.K., 2006. Evaluation of the carbohydrate recognition domain of the bacterial adhesin FimH: design, synthesis and binding properties of mannoside ligands. *Org. Biomol. Chem.* 4, 3913–3922, <http://dx.doi.org/10.1039/b610745a>.
- Touaibia, M., Wellens, A., Shiao, T.C., Wang, Q., Sirois, S., Bouckaert, J., Roy, R., 2007. Mannosylated G(0) dendrimers with nanomolar affinities to *Escherichia coli* FimH. *ChemMedChem* 2, 1190–1201, <http://dx.doi.org/10.1002/cmdc.200700063>.
- Waschke, D., Thimm, J., Thiem, J., 2011. Highly efficient synthesis of ketoheptoses. *Org. Lett.* 13, 3628–3631, <http://dx.doi.org/10.1021/ol2012764>.
- Witczak, Z.J., Whistler, R.L., Daniel, J.R., 1984. Synthesis of 3-C-(hydroxymethyl)erythritol and 3-C-methylerythritol. *Carbohydr. Res.* 133, 235–245, [http://dx.doi.org/10.1016/0008-6215\(84\)85201-5](http://dx.doi.org/10.1016/0008-6215(84)85201-5).
- Ziegler, T., Kováč, P., Glaudemans, C.P.J., 1990. Transesterification during glycosylation promoted by silver trifluoromethanesulfonate. *Eur. J. Org. Chem.*, 613–615, <http://dx.doi.org/10.1002/jlac.1990199001115>.

3. Summary and outlook

The first objective of the present thesis was to optimize physicochemical and pharmacokinetic properties of two FimH antagonists by a prodrug approach in order to achieve oral bioavailability. The first one was a highly active derivative of the biphenyl α -D-mannopyranosides containing a carboxylic acid in *para*-position (\rightarrow **1**) of the terminal phenyl ring. Numerous promoieties were introduced masking the polar character of carboxylic acid. Since aliphatic esters resulted in too low solubility, promoieties functionalized with oxygenated or nitrogenated substituents were studied. This led to prodrugs with moderate to high solubility and permeability, undergoing quick hydrolysis by esterases upon absorption.

The second prodrug approach started from the methylsulfone bioisostere (\rightarrow **2**) of carboxylic acid derivative **3** (Figure 1). This time, promoieties were introduced at the C-6 hydroxyl group of the mannose moiety. It could be demonstrated that acylation of only one hydroxyl group of the mannose promoiety was sufficient to improve lipophilicity and permeability into the required range for good absorption.

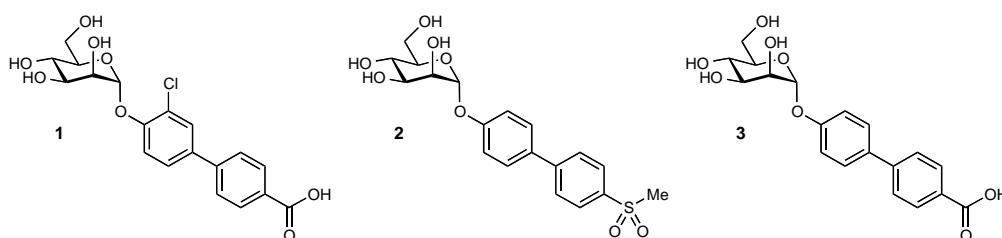


Figure 1. Chemical structure of FimH antagonists used as a basis for the study of ester prodrug derivatives.

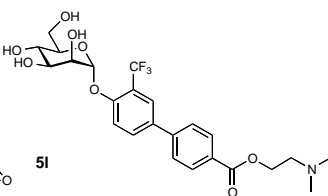
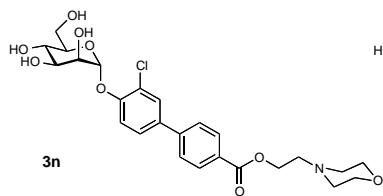
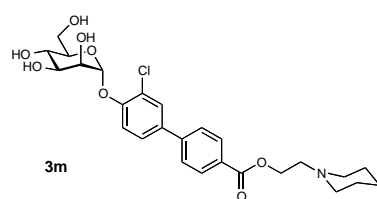
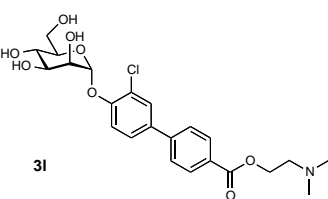
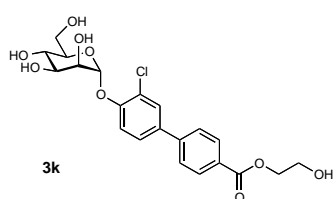
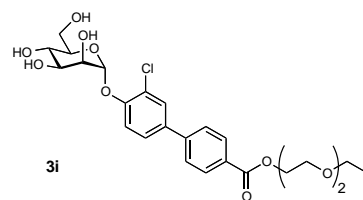
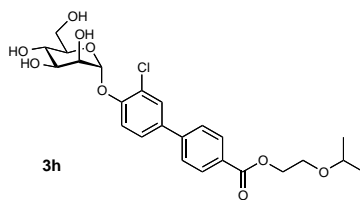
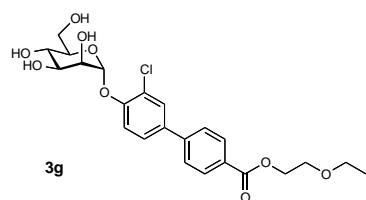
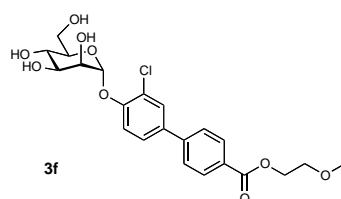
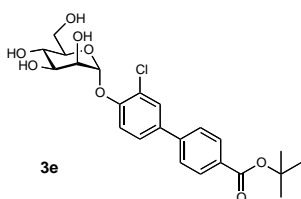
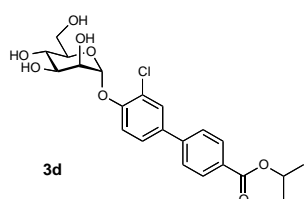
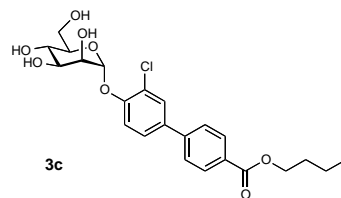
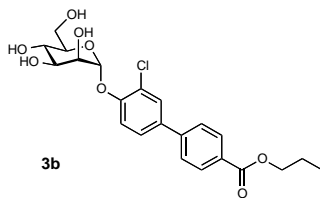
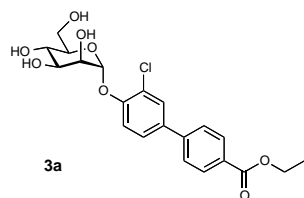
In the second part of this thesis new and unexplored regions of the FimH lectin were studied with the aim to identify FimH antagonists with further improved affinities. First, for establishing a stable interaction with Arg98, a library of compounds with elongated substituents attached to the terminal phenyl or pyrrole ring of the biaryl aglycone was synthesized. Competitive binding assays with wild type FimH and the R98A mutant however, revealed equal affinities for both proteins, indicating that this approach failed. Based on additional information, which we plan to obtain from co-

crystallized representative of this approach with the FimH lectin domain, improved antagonists may be designed.

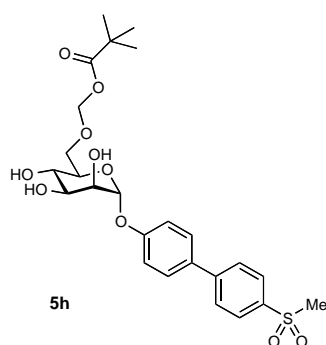
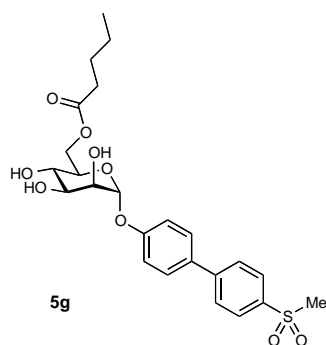
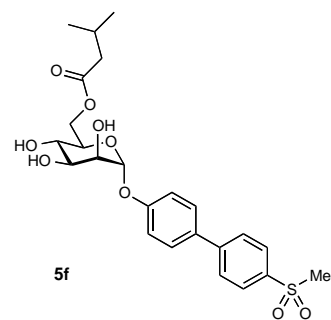
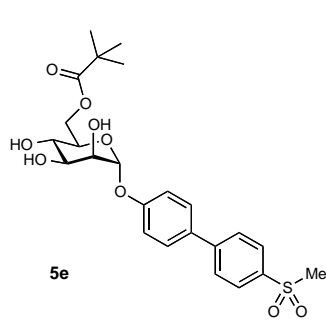
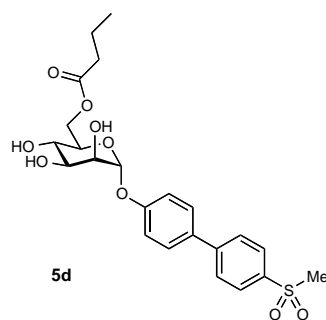
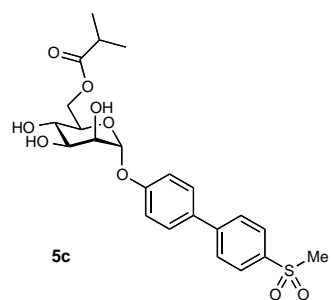
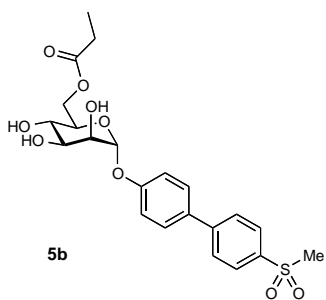
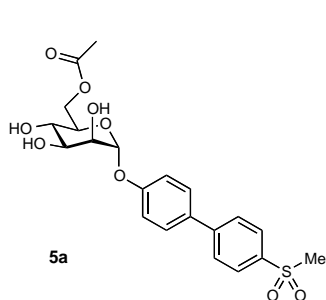
In a second approach, another region of the FimH lectin was explored with the goal to identify a new class of antagonists targeting a cavity located in the close proximity to the binding pocket. In order to capitalize on additional ligand-lectin contacts, 2-*C*-branched α -D-mannosides were synthesized. However, no significant improvement in affinity was observed. Noteworthy is the fact that the α - and β -anomeric 2-*C*-hydroxymethyl derivatives had very similar affinities. Also in this case, crystal structures would help to understand why promising docking results did not materialize in improved affinities for 2-*C*-branched α -D-mannosides.

4. Formula Index

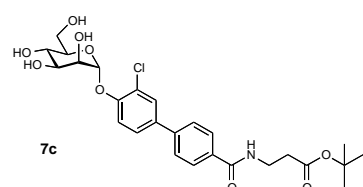
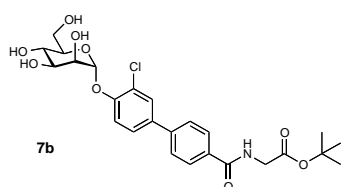
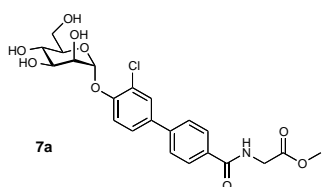
Manuscript 1:

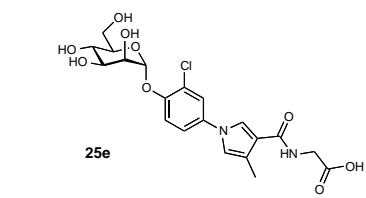
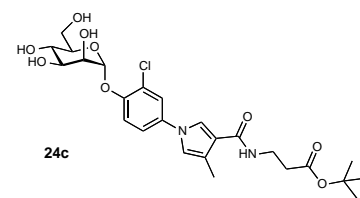
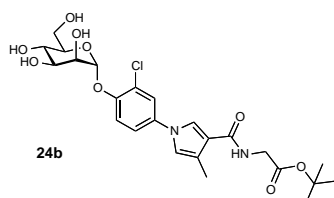
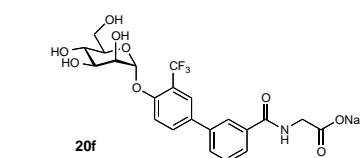
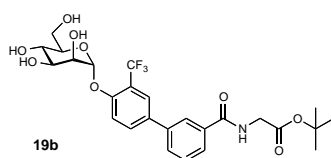
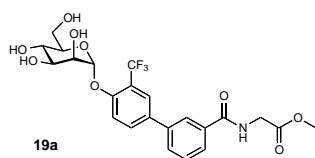
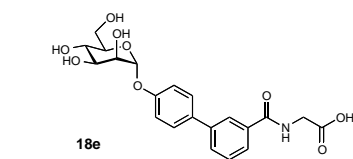
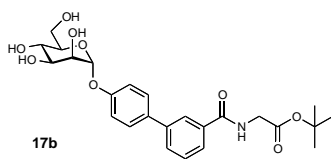
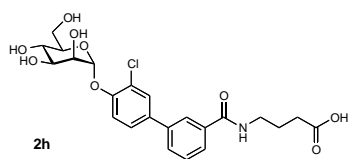
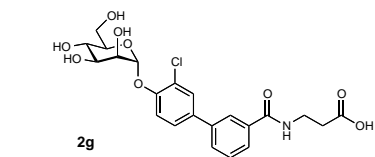
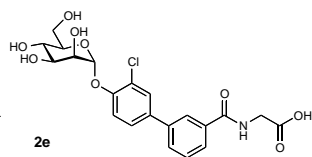
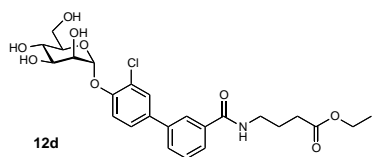
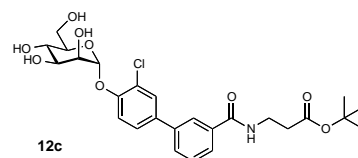
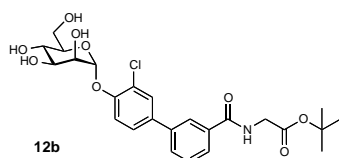
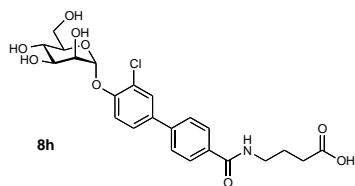
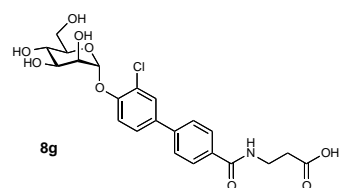
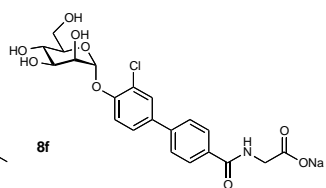
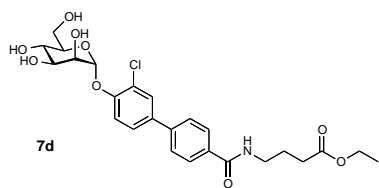


Paper 2:

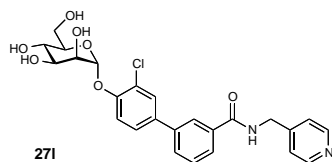
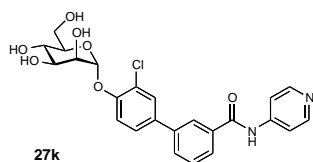
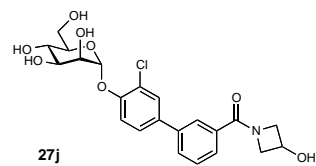
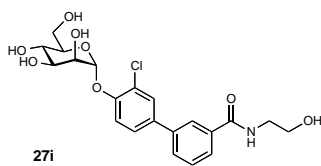
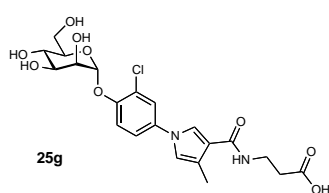


Chapter 3:

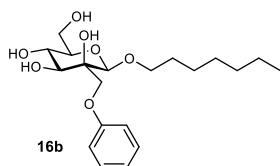
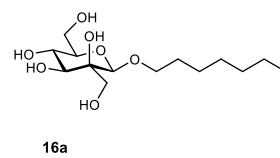
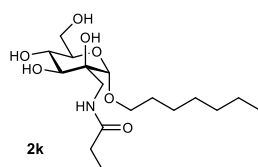
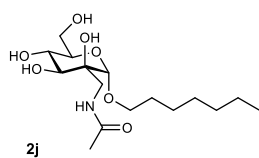
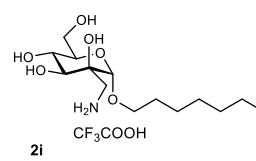
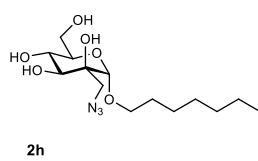
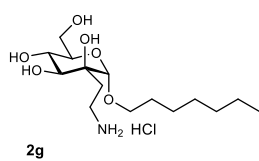
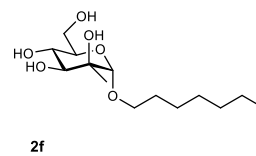
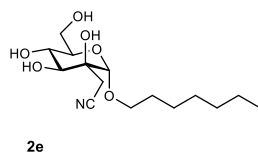
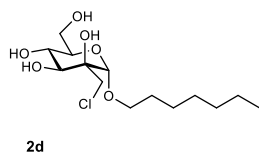
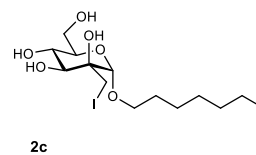
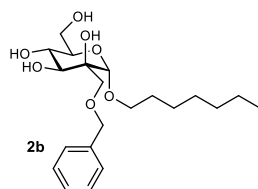
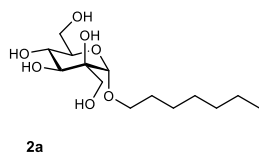


Chapter 3 (continued):

Chapter 3 (continued):



Paper 4:



Name: **Wojciech Schönemann**
 Address: Breisacherstrasse 22
 CH-4057 Basel, Switzerland
 Mobile phone: +48 (0)7 93 43 90 88
 E-mail: wojciechschonemann@gmail.com
 Date of birth: 22 July 1985
 Nationality: Polish
 Marital status: single



Education

01.2011-present **University of Basel, Institute of Molecular Pharmacy, Ph.D. candidate**

06.2009 **French-Polish Double Master Diploma in Chemistry**,
 obtained at the Jagiellonian University (Poland) and the University of Orléans (France)

Title of the thesis: New methods for the synthesis and crystallographic investigation of 1-C-alkyl-iminosugars in the D-gluco and L-ido series

2008 – 2009 **University of Orléans**, Institute of Organic and Analytical Chemistry

2004 – 2009 **Jagiellonian University**, Faculty of Chemistry
Specialization: biological chemistry

2000 – 2004 **8th Stanisław Wyspiański High School in Krakow**
Profile: mathematics, chemistry and computer science

Work experience

09.2009 – 03.2010 Institute of Organic and Analytical Chemistry – junior research fellow

07.2009 – 08.2009 Institute of Organic and Analytical Chemistry – trainee

04.2007 – 06.2007 PLIVA Pharmaceuticals Company, Krakow, Poland – trainee

Teaching experience

2015 Supervisor of a master thesis: “*Synthesis and Biological Evaluation of a New Class of FimH Antagonists*”, University of Basel

2013 Supervisor of a master thesis: “*Synthesis and Characterization of Pharmacodynamic and Pharmacokinetic Properties of New FimH Antagonists*”, University of Basel

2012	Supervisor of a master thesis: “ <i>Synthesis and Pharmacokinetic Characterisation of FimH Antagonist Prodrugs</i> ”, University of Basel
2011-2013	Supervisor in the practical course on solid-phase peptide synthesis, University of Basel

Activities

7-11.09.2014	XXIII International Symposium on Medicinal Chemistry in Lisbon – participant (poster)
10.02.2014	Annual Research Meeting, University of Basel – participant (poster)
06.09.2013	The Swiss Chemical Society Fall Meeting – participant (poster)
04.2013 – 12.2014	Swiss Chemical Society - member
11-19.10.2012	10 th Swiss Course on Medicinal Chemistry, Leysin, Switzerland
02-05.12.2007	International Conference on Chemistry at the Service of Society “Why Chemistry ?!” – participant (2 posters)
12.2007–21.2008	Students’ Section of Polish Chemical Society - member
01 – 08.06.2007	II nd Krakow - Jena Student Chemistry Workshop, Jena, Germany – participant
2004 - 2009	Chemistry Student Society of Jagiellonian University – member

Publications

1. Schönemann, W.; Gallienne, E.; Ikeda, K.; Asano, N.; Nakagawa, S.; Kato, A.; Adachi, I.; Górecki, M.; Frelek, J.; Martin, O.R. *Chem Med Chem.* **2013**, *11*, 1896. (**back cover**)
2. Schönemann, W.; Gallienne, E.; Compain, P.; Ikeda, K.; Asano, N.; Martin, O.R. *Bioorg. Med. Chem.* **2010**, *18*, 2645. (**front cover**)

Language & technical skills

Polish:	mother tongue
English:	very good
Computer skills:	MestReNova, SciFinder, Chem Draw, Microsoft Windows, Microsoft Office (Excel, PowerPoint, Word)